# LEACHING OF SULPHIDE MINERALS CONTAINING COPPER AND SILVER

by

Michael James Sheridan, B.Sc.(Eng), A.R.S.M.

A thesis submitted for the degree of Doctor of Philosophy of the University of London and for the Diploma of Imperial College.

Metallurgy Department,
Royal School of Mines,
Imperial College,
London, S.W.7.

JANUARY, 1975

ABSTRACT.

Three sulphidic materials were synthesised from the elements. These were a silver-doped bornite, containing 1.20 wt. % Ag, stromeyerite, of formula $Cu_{1.07}Ag_{0.93}S$, and a mixed sulphide material containing bornite, α-chalcopyrite and stromeyerite.

Samples of the three synthetic materials, in particulate form, were leached in acidified ferric sulphate solutions at temperatures ranging from 30° to 90°C. The effects of temperature, $Fe^{3+}$ concentration, particle size, sample weight, stirring speed and chloride ion on the copper and silver dissolutions were studied. Leaching with hydrogen peroxide and manganese dioxide were also used on the stromeyerite. Finally, the leaching characteristics of mixtures of separate particles of bornite, α-chalcopyrite and stromeyerite were studied.

The solid phases and residues were studied by X-ray diffraction, electron probe microanalysis and microscopic examination.

The presence of silver as an isomorphous constituent had little effect on the dissolution characteristics of bornite. Stromeyerite dissolved in two distinct stages. The first, in which 50% of the Cu was dissolved, was extremely fast and involved solid state transformations resulting in the formation of a mixture of silver sulphide and covellite, CuS, which dissolved very slowly.

Copper dissolved from the mixed sulphide material much faster than was expected, the constituent phases apparently having the same dissolution mechanism as the pure materials. Electrochemical and mineralogical factors were considered to explain the faster copper dissolution.

In all cases, the dissolution of silver from the three synthetic materials was extremely small, except when sufficient chloride ion was present to form the complex $AgCl_3^{2-}$.

CONTENTS

## INTRODUCTION

Leaching is an important step in any hydrometallurgical process for the recovery of one or more metals from an ore. It involves the treatment of the ore with a solvent to produce an aqueous solution containing the required metal(s). This solution is subsequently purified and concentrated prior to recovery of the metal(s).

A number of leaching techniques are in operation[1,2]. These include in situ or in place leaching, often involving the fracturing of the ore body by explosives [3], heap or dump leaching, percolation or vat leaching and agitation leaching.

Although theoretical and practical studies have been carried out recently on heap and dump leaching[4,5,6], and nuclear chemical mining [7], most of the information on the dissolution behaviour of minerals has come from laboratory investigations using rotating discs or agitated suspensions of particles of pure minerals. The use of synthetic minerals has been found more effective than using specific natural ores for determining the mechanisms which are operative during leaching. The principal reason for this is that the presence of other minerals in the ore, or impurities in the lattices of the minerals, might strongly influence the dissolution process [8]. This is especially so since many minerals have been found to have dissolution mechanisms involving solid

state transformations [9-12], or electrochemical dissolution mechanisms involving the electronic conduction properties of semiconducting minerals [13,14].

The present work is an attempt to discover the precise nature of the effect of impurities on the leaching of sulphide minerals especially with regard to the solid-state transformations that occur as the dissolution proceeds. The copper-iron-sulphur system was chosen because a number of investigations have recently been completed into the kinetics and mechanisms of the reactions involved in the dissolution of chalcopyrite[12] and bornite[11].

Bornite was chosen to be the host mineral of the impurity because it has two well-defined leaching stages, a solid-state transformation from $Cu_5FeS_4$ to $Cu_3FeS_4$, followed by a complete breakdown of the structure to give elemental sulphur. The impurity element chosen was silver since there are a number of chemical similarities between copper and silver, and it is known that silver is a common constituent of many sulphides[15,16] and that it probably substitutes for copper in the lattices of copper sulphides in which it is sometimes preferentially concentrated[17]. In addition, it is a valuable constituent of any ore and any information regarding its behaviour during leaching would be of some importance.

A bornite containing a known amount of

silver was synthesised and leached in acidic ferric sulphate solutions. Ferric sulphate was used because it is the most used commercial leaching agent for copper minerals[18]. Attempts to synthesise a bornite containing larger amounts of silver resulted in the formation of a mixed sulphide material containing bornite, chalcopyrite and stromeyerite, a silver-copper sulphide. A leaching study was carried out on this material and from the known dissolution kinetics of chalcopyrite, bornite and stromeyerite, the extent to which electrochemical (galvanic) mechanisms play a part in the dissolution was investigated.

SECTION I

## LITERATURE SURVEY

### 1.1. Leaching of Silver and Its Minerals.

#### 1.1.1. Previous Work on the Leaching of Silver.

The conventional method of treating silver ores is by cyanidation. Thorough studies have been made of the dissolution of silver and silver sulphide in cyanide solutions using rotating discs and other methods, and the kinetics and mechanisms are well understood[19].

However very few investigations have been carried out on the behaviour of silver and its minerals in other solvents. Much of the literature on the leaching of ores or concentrates containing silver is concerned with the possibility of using reactions to treat the ores on a commercial scale, in which case the chemistry and reaction kinetics of the minerals present are not treated fully, or only the leaching behaviour of the major constituents of the ores have been studied in detail.

It has been known for many years that silver dissolves in solutions of ferric sulphate, brine, sodium thiosulphate and ferric chloride. The solutions and mixtures thereof form the basis of many early patents for the extraction of silver from its ores[20-26]. For instance, David[21] used a solution of $FeCl_3$, NaCl, HCl and $Na_2SO_4$ to extract the metals from copper and silver bearing material,

while Joseph[22] used an aqueous solution containing NaCl, nitric acid and aqua ammonia.

In a process for treating the sulphide ores of Pb, Ag and Cu, Christensen[26] found that a hot solution of one or more of the common chlorides, containing a small amount of ferric chloride, dissolved galena, agentite and chalcocite, the ferric chloride acting to give soluble chlorides and free sulphur e.g.:

$Ag_2S + 2FeCl_3 = 2AgCl + S + 2FeCl_2$ (1.1.1)

Sodium, calcium, magnesium, ferrous iron, potassium, ammonium and manganese chloride solutions, containing ferric chloride, rapidly dissolved the minerals whereas zinc chloride was much less active due to the limited solubility of Ag, Pb and Cu chlorides in this solution. Ferric chloride was the least suitable of the chlorides to be used as the concentrated solution owing to the slight solubility of the Ag and Pb chlorides.

Extractions of 95 - 98% of the silver occurring as sulphide were obtained in 15 - 30 minutes. Christensen noted that silver in galena was brought into solution just as rapidly as the galena, whereas silver in chalcopyrite or pyrite, upon which the chloride solutions did not act, was recovered with these minerals in the residue.

Two processes patented at this time used the electrolysis of an NaCl solution as a means of dissolving silver bearing ores. Slater[23] used a solution of NaCl and $FeCl_2$.

The latter was oxidised to $FeCl_3$ in the electrolysis and with the free HClO that was also formed dissolved ores containing copper and silver. Reyes[24] electroly sed a solution of sodium chloride containing a silver and gold bearing ore in a finely divided state. The electric current was sufficient to produce nascent chlorine and soluble chlorides of silver and gold which were precipitated in a metallic state upon contact with metal or carbon electrodes.

One process for a lead-silver ore[27] consisted of a chloridising roast followed by leaching with a saturated brine solution. By using an acidified brine solution and additions of 2 - 7% salt to the mast feed, the extraction of silver was raised to 80 - 90%. A similar treatment was described by Jones[28] for a cupreous pyrite containing a small amount of silver and gold.

The first systematic work on the leaching of silver sulphide was undertaken by Cooke[29] to test some of the hypotheses of the secondary enrichment of ores. In leaching studies with ferric sulphate and dilute sulphuric acid, 1 gram samples, either -40 mesh or -80 + 100 mesh, were placed in a sealed flask containing 200 mls of solution and kept in a dark room at room temperature for a period of 1 to 3 months. The contents were shaken daily and the solutions analysed after removal of the solid residue by filtration. The solutions contained 35 grams ferric sulphate per litre and approximately

F/20 sulphuric acid, and exerted a powerful solvent action on all the minerals tested except argentite, $Ag_2S$. The results for the natural minerals were well substantiated by repeating the experiments with chemically pure artificial minerals.

The action on argentite was more powerful the more ferric sulphate was present. This was explained by assuming that sulphuric acid was the active agent producing $H_2S$ by the reaction:

$$Ag_2S + H_2SO_4 = Ag_2SO_4 + H_2S \quad (1.1.2).$$

Due to the very low solubility product of the sulphide (section 4.3) this reaction stops unless the $H_2S$ is removed. This was suggested to be the main function of the ferric sulphate:

$$Fe_2(SO_4)_3 + H_2S = 2FeSO_4 + H_2SO_4 + S \quad (1.1.3)$$

For the double compounds of silver with antimony and arsenic, silver was found to be the less soluble constituent. Pyrargite ($Ag_3SbS_3$) turned black within a very few days, an effect which was thought to be due to the accumulation of silver sulphide on its surface as antimony was leached out. However the author did not confirm this by analysis.

In 1928 Head and Miller[30] carried out an investigation on the metal losses occurring in the treatment of oxidised lead and silver ores. They determined that much of the losses were due to the lead and silver being present as plumbojarosite and argento-

jarosite, respectively, of general formula $RO.\ 3\ Fe_2O_3.\ 4SO_3.\ 6H_2O$ where R = Pb or $Ag_2$, both of which seemed to be relatively common minerals in the oxidised ores.

Leaching experiments were carried out on pure argentojarosite using various solvents such as sodium thiosulphate, ammonium acetate, sodium hydroxide, potassium cyanide, and brine solutions containing various additives such as ferric chloride, bromine, hydrochloric acid and sulphuric acid. The tests were made at room temperature in test tubes which were agitated intermittently for 24 hours. The percentage of silver removed in each instance was relatively low (between 4 and 11%). It was assumed that the silver combined as argentojarosite had not been affected. Tests on roasting of the argentojarosite followed by cyanide leaching showed that 65 - 80% of the silver could be rendered soluble by roasting at a temperature of 800 - 850°C for 1½ hours due to the silver in many of the particles being reduced to the metallic state.

Brine leaching tests using various amounts of sulphuric acid per ton of solution were made with samples of a mixed argentojarosite - plumbojarosite ore. The silver extractions were always less than 5% even after chloridising roasts, whereas the lead extractions increased from 20% to 46%. A cyanide leach of the calcine gave a 39% extraction of the silver.

The use of saturated brine for the extraction of silver in mixed ores is old, although the silver was always converted to a soluble form, such as silver chloride by roasting the ore with salt. An investigation on the leaching of unroasted minerals of silver was carried out by Bradford[31] using a brine solution containing ferric chloride acting on a mixed lead-silver ore.

Following this Oldright[32] conducted a number of experiments on the leaching of silver in unroasted concentrator tailings with ferric chloride in saturated brine. The silver content was so small (2.92 oz/ton) that time was not spent in identifying the silver minerals.

Five leaching tests were made at 60°C using 1 litre of solution to 250 grams of ore. The results showed that over 80% of the silver in the unroasted tailings was extracted by leaching for 2 hours with a warm brine solution containing a ferric salt.

Traill et al[33] described tests made on high grade chalcopyrite flotation concentrates containing pyrite, pyrrhotite, sphalerite and small quantities of silver and gold (11.22 and 0.80ozs/ton respectively), which showed the amenability of the ore to ferric-ferrous liquors leaching for the extraction of the base metals and the concentration of the precious metal values.

After roasting with sulphur in non-

oxidising conditions for 3 hours at 725°C and leaching with a ferric-ferrous chloride liquor containing 77 grams/litre ferric ion and 71 grams/litre ferrous ion at 90 - 95°C for 5½ hours, 85% and 90% of the gold remained in the leach residues in two separate tests. However the silver was apparently quite soluble since 91.4% and 87.0% dissolved in the two separate tests and was recovered with the copper by precipitation.

Direct leaching using the same charge of ore and leaching liquor showed only a slight variation from the combined roasting and leaching experiments.

Although Downie[34] described a process in 1937 for the recovery of pure silver from silver sulphide precipitates by boiling with sulphuric acid, most of the subsequent work on the leaching of silver from ores, not amenable to cyanidation, has dealt with the use of ferric salts.

A British patent[35] describes a process for the extraction of Pb, Hg or Ag from sulphide ores using a dilute aqueous solution of a ferric salt, whose negative radical is capable of forming a readily soluble salt with the metal to be extracted. Ferric nitrate, acetate or borate were preferred, in a neutral or slightly acid solution at a low temperature and low concentration to prevent dissolution of other sulphides. However the patent does not give any details of experimental work on silver ores.

Lee and Muir[36] determined that the use of ferric sulphate in conjunction with the maintenance of a balance between ferric and ferrous ion concentration by oxidising agents increased the silver extraction from ores and concentrates. They describe a process which comprises the roasting of the ore or concentrate to a calcine and delivering this to a neutral or acid leach circuit in which a balance of ferric ion concentration over ferrous ion concentration, favourable to the solution of metallic silver, is maintained by the use of suitable oxidising agents such as potassium permanganate or manganses dioxide. The prior heat treatment plus the oxidising agents control the concentration of such constituents as ferrous sulphate, lower oxides of iron and copper, and metallic copper, which are detrimental to the dissolution of Ag from materials soluble to neutral or acidified solutions.

In tests to show the feasibility of this process, a material consisting of 1650 oz. Ag/ton, 20% Cu, 11% Pb, 12% Fe, 25%S and 18% Sb was roasted initially at 400 - 450°C and then at 600°C. The calcine, with silver now present as sulphate and the associated constituents in their higher oxide forms was leached at 40 - 60°C in three stages, an initial Ag leach, a neutralization leach and a final acid leach. In two separate tests, typical consumptions of oxidising agents were 10lbs. of $MnO_2$ and 4 lbs of $KMnO_4$ per ton of material, and 4 lbs $MnO_2$ and 2lbs $KMnO_4$ per ton of material respectively. The discrepancy was thought to be due to the former material

being exposed to less suitable roasting conditions.

By this method 96% of the Ag was extracted compared to nearly 70% with no control of the $Fe^{3+}/Fe^{2+}$ ratio. The silver was recovered as metallic sponge by precipitation on an electro-positive metal or as metallic silver by electrodeposition.

A detailed investigation of the dissolution kinetics of pure silver in solutions of ferric sulphate, ferric nitrate, ferric perchlorate and ceric sulphate was carried out by Salzberg, King and co-workers[37,38,39]. A pure silver cylinder of approximately 1.5cm diameter and 2 cm long was rotated in 500 mls of solution and its dissolution measured by weighing the silver cylinders before and after each run. The rate was studied as a function of (a) concentration of ions involved, (b) concentration of the acid, (c) speed of stirring, (d) temperature and (e) the E.M.F. of the silver-silver ion, and ferric-ferrous ion cell. Some of their results are shown in Fig.1.

It had been known for some time that whereas metals down to copper in the E.M.F. series dissolve in ferric salt solutions at the maximum diffusion controlled rates, silver dissolves much more slowly and the dissolution rates decrease with time far faster than is to be expected from known values of the equilibrium constant for the reaction:

$$Ag + Fe^{3+} = Ag^{+} + Fe^{2+} \quad (1.1.4).$$

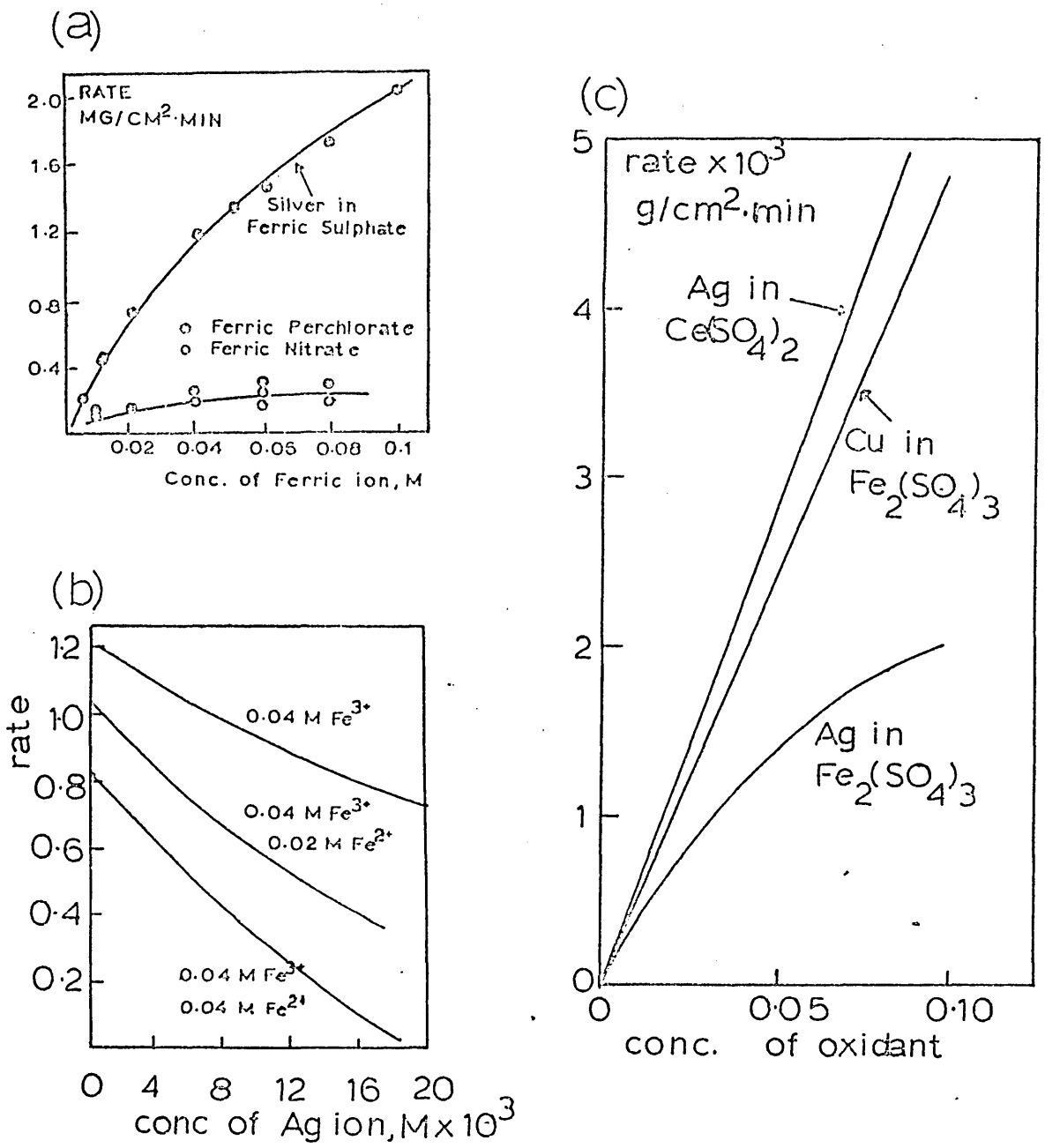


FIGURE 1 : (a) Dissolution rate of silver in ferric sulphate, ferric perchlorate, and ferric nitrate as a function of ferric ion concentration. Salzberg and King[37].

(b) The effect of silver sulphate on the dissolution rate of silver in ferric sulphate. Salzberg and King[37].

(c) Rate versus concentration of oxidant , in g-ion/litre, for Ag in ceric sulphate solutions compared with diffusion control (Cu in ferric sulphate) and desorption control (Ag in ferric sulphate). Salzberg, Knoetgen, and Molless[39].

Comparison with the dissolution of copper under similar conditions[37] showed that in very dilute ferric sulphate, silver dissolves at a rate approaching that of diffusion control, and that another factor is of increasing importance at higher concentrations (Fig. 1(a)).

In considering the curvature of the plot of rate versus ferric ion concentration, the strong inhibiting effect of ferrous and silver ions (fig.1(b)) and the lack of proportionality of this effect to the product of the ion concentrations, Salzberg and King concluded that all these ions are adsorbed on the silver surface and thus influence the rate. An equation was derived, on the basis of a number of assumptions, describing all features of the observed rates, including the effects of adsorption and of the reverse reaction.

This equation, of the form:

$$R, \text{ rate, } = \frac{K_1 C_3 - K_2 C_1 C_2}{1 + K_3 C_3 + K_4 C_1 + K_5 C_1^{\,2} + K_6 C_2 + K_7 C_2^{2} - K_8 C_1 C_2} \qquad (1.1.5)$$

Where $C_1$, $C_2$ and $C_3$ are the concentrations of the ions $Ag^{+}$, $Fe^{2+}$ and $Fe^{3+}$ respectively, gave excellent agreement with the experimental data with the exception of a few scattered points.

The assumptions in the derivation were that the forward rate is proportional to the amount of ferric ion adsorbed, the reverse reaction occurs when a free ferrous ion collides with an adsorbed silver ion, or vice

versa, and that the surface area covered by adsorbed ferric ions is small compared to the area covered by ferrous and silver ions, when these ions are present in appreciable concentrations.

It was postulated that the lower rates for nitrate and perchlorate solutions (Fig. 1(a)) could be explained by the formation of a sulphato-ferric ion. If it is assumed that the entire silver surface acquires a positive change from adsorbed ions as soon as dissolution begins, this ion, of negative or reduced positive change would be adsorbed and react more readily than a triply positive (hydrated) ferric ion.

In a later paper, King and Lang[38] investigated further with ferric perchlorate solutions. The same experimental conditions were used, and the same variables considered as with ferric sulphate solutions. Two factors were concluded to be responsible for the difference in dissolution rates :

(a) silver perchlorate is more strongly adsorbed on silver than silver sulphate is, and,

(b) a sulphato-ferric complex ion reacts more rapidly than the normal hydrated ferric ion.

Evidence for a sulphato-ferric complex was obtained by spectrophotometric measurements on solutions of perchlorate and sulphate and mixtures of the two. Replacing perchlorate by sulphate increased the adsorption over

the whole range shown and eliminated the transmission maximum of 260 mμ. A new ionic species was evidently present and the low concentrations used suggest that this was the ion $FeSO_4^+$, probably in hydrated form.

The rate equation (1.1.5) was applied to solutions of ferric perchlorate alone and with additions of silver and ferrous perchlorate and gave good agreement with the experimental data. The following assumptions were made :

(1) Ferric ion is not adsorbed but reacts when it encounters a bare silver atom;
(2) the back reaction may occur when a silver atom strikes an adsorbed ferrous ion, or vice versa; and
(3) silver and ferrous ions formed by the reaction are not desorbed instantly.

In contrast to the dissolution in ferric sulphate and perchlorate, Salzberg, Knoetgen and Molless[39] have found that the dissolution of silver in ceric sulphate is diffusion controlled. These results seem to corroborate the idea that a large difference in oxidation potential between the metal and solution facilitates diffusion control, while a small difference results in desorption control. Salzberg el al[39] suggest that this is due to the potential difference being a measure of the heat of the reaction, a high oxidation potential implying a large heat of reaction. In a system such as ceric sulphate/silver, where the potential difference is large (0.75 volts), the heat of reaction is large enough to supply sufficient energy for

immediate desorption of the ions produced in the reaction, which then becomes diffusion controlled. Whereas in a system such as ferric sulphate/silver where the potential difference is only 0.050 volts, the heat of reaction is only slight and the metal ions do not leave the surface immediately, giving rise to desorption control

The kinetics of solution of pure silver has also been studied in nitric acid. Kaiser [40] has studied the dissolution in 3-5.5M $HNO_3$ containing 2.3 - 3.6 x $10^{-3}$M $HNO_2$ by measuring the current-voltage curves with rotating disc electrodes. The solution rate was found to depend on the cathodic potential current. This was explained by assuming a diffusion layer model for the dissolution.

The oxidation and dissolution of pure silver sulphide, in solutions other than cyanide, has also received some attention. Sato [41] developed an electrochemical method for the identification of the first-step oxidation or reduction reactions of sulphide minerals. This was based on the assumption that the electrode potential of a sulphide mineral in an oxidising or reducing solution is controlled by the first step of its consecutive oxidation or reduction reactions.

The sulphides of copper, lead, silver, iron and zinc were studied. The results indicated that the direct oxidation of a simple sulphide mineral at low temperatures is a process in which the metal atoms move into

the surrounding solution to become aqueous cations, accompanied by a step-wise decrease in the metal-sulphur ratio of the remaining solid phase. In the case of reduction, sulphur atoms move into the solution to become aqueous sulphide ion, with a step wise increase in the metal to sulphur ratio of the remaining solid phase. The path of the step-wise oxidation is not necessarily the same as that of the reduction.

Thus, the results of the electrode potential measurements with argentite in solutions containing sulphide ion species ($S^{2-}$, $HS^-$ and $H_2S$) indicated that the sulphide is reduced according to the following electrode reaction:

$$2Ag + S^{2-} = Ag_2S + 2e \quad (1.1.6).$$

In weakly basic solutions the potential is controlled by the equation

$$2Ag + HS^- = Ag_2S + H^+ + 2e \quad (1.1.7)$$

and in acid solutions by

$$2Ag + H_2S = Ag_2S + 2H^+ + 2e \quad (1.1.8)$$

The measurements of the electrode potential values for argentite in $Ag^+$ ion solutions were made only in acid conditions and suggested that the oxidation reaction at the silver sulphide electrode is

$$Ag = Ag^+ + e \quad (1.1.9)$$

owing to the free migration of silver atoms within the sulphide crystal. However this reaction requires no involvement of sulphur which is known to have an effect on the electrode potential of $Ag_2S$. Hence the more likely reaction was thought to be:

$$Ag_2S = AgS + Ag^+ + e \quad (1.1.10)$$

AgS is unknown in nature but has been prepared artifically[41]. Sato noted that this mechanism of oxidation was very similar to that of chalcocite.

Azerbaeva and Tseft (1964)[42] studied the behaviour of synthetic pure silver sulphide, selenide and telluride in common leaching agents such as ferric chloride, cupric chloride and ferric sulphate. The solvents used were solutions of ferric chloride ($Fe^{3+}$ 100 gms/litre, $Fe^{2+}$ 50 grams/litre), ferric sulphate ($Fe^{3+}$ 68 gm/litre), and cupric chloride ($Cu^{2+}$ 50 g/litre). The cupric chloride solution was saturated with sodium chloride in order to retain in solution the cuprous chloride formed during the process. The variables studied were the influence of temperature, amount of solvent, and duration of leaching, on the degree of decomposition of the silver compounds.

The leaching studies on silver sulphide were performed at the boiling point for two hours, with double the theoretical amount of reactant. The results (see table) show that silver is extracted more completely by a

mixture of ferrous and ferric chloride than by ferric sulphate. However, almost complete (over 90%) decomposition of silver sulphide occured only in the presence of sodium or ammonium chloride. Preliminary experiments showed that silver sulphide, selenide and telluride did not decompose in aqueous solutions of ammonia, ammonium chloride and sodium chloride. Therefore addition of these compounds to other solvents was thought to merely raise the solubility of the silver chloride, formed on the surface of the compounds, by reactions such as:

$$Ag_2S + 2Fe(aq)^{3+} + 2Cl^-(aq) = 2AgCl + 2Fe^{2+} + S^o \quad (1.1.11)$$

$$Ag_2S + 2Cu^{2+}(aq) + 6Cl^-(aq) = 2AgCl + 2CuCl_2^-(aq) + S^o \quad (1.1.12)$$

It was noted that ammonium chloride was a more active solvent than sodium chloride:

| Reactant | % Silver in sulphide converted to sulphate/chloride. |
|---|---|
| $Fe_2(SO_4)_3$ | 43 |
| $CuCl_2$ + NaCl (to saturation) | 91 |
| $FeCl_3$ + $FeCl_2$ | 79 |
| $FeCl_3$ + $FeCl_2$ + NaCl | 93.2 |
| $FeCl_3$ + $FeCl_2$ + $NH_4Cl$ (to saturation) | 100. |

Silver telluride and selenide were both decomposed more easily. The decompositon increased with rise in temperature, increase in the amount of solvent and an increase in the leaching time. All three compounds

investigated were found to be almost completely decomposed by ferric and cupric chloride solutions at the boiling point with a twofold excess of reactant in the presence of sodium or ammonium chloride.

A mixture of ferrous and ferric chloride has been used in a process for leaching complex sulphide ores containing silver which is dissolved and subsequently obtained as a byproduct precipitate[43]. Ablanov[44] has used a similar solution, containing 50 gm/litre divalent and 100 gm/litre trivalent iron, in a number of leaching experiments on concentrates containing various mixtures of pyrite, chalcopyrite, bornite, covellite and small amounts of sphalerite and galena. The concentrates were leached at boiling point temperature for two hours. Again the silver present (not stated in what form) is dissolved and was recovered from the solution by precipitation on a copper-filter.

When oxidised sulphide ores containing gold and silver are leached with ammonia in the presence of oxygen at around 180°C, the gold and silver are partially dissolved as ammines. Sobol et al[45] leached concentrates containing 6.8-813 g/ton Au and up to 1675 g/ton of Ag, with aqueous $NH_4OH$ in an autoclave with an oxygen partial pressure of 10 - 15 atmospheres and a total pressure of 30 - 35 atmospheres. The oxygen was added continuously and the leaching continued until the theoretical amount of oxygen required for the oxidation of the sulphide and such elements as Fe, As,

Sb and Se was absorbed. At 180°C, complete oxidation of a concentrate containing 18% sulphur required 2 hours. The concentration of gold in the solution was between 3 - 84 mg/l and that of silver was from 100 - 760 mg/l.

Kakovskii and co-workers have carried out several investigations on the leaching of silver sulphide and other silver minerals in various solvents using the rotating disc method.(46).

In the only paper found in this literature survey on the kinetics of stromeyerite leaching, Potashnikov et al(47) studied its dissolution in aqueous nitric acid solutions. The rate was independent of the speed of the rotating disc and the effect of the $HNO_3$ concentration (C) followed the expression $V = 4.5 \times 10^{-11} C^2$ where V is in moles $Cm^{-2}Sec^{-1}$. The dissolution rate coefficient in 2.0, 3.0, 4.0 and 5.0 M $HNO_3$ was found to be 5.2,4.2, 4.2 and 4.6 respectively, the arrhenius equation being $\log K = -4.315 (1.8 \times 10^3/T)$. The activation energy when the dissolution of Copper and Silver proceeds separately is approximately 5Kcal/mole; if the dissolution is combined (both metals), the rate constant increased two fold at 25°C.

Kakovskii(48) also studied the leaching of rotating discs of synthetic silver chloride (the mineral cerargyrite) in aqueous solutions of ammonia, and sodium thiosulphate solutions. The effects of rotational speed, solvent concentration, temperature and pH were studied.

With experimental conditions of 0.1 mole/litre thiosulphate, 0.154 moles/litre ammonia and a temperature of 25°C, the rates of dissolution were proportional to the square root of the number of revolutions per minute of the discs. This suggests that the dissolution is controlled by diffusion of the reagents towards the disc surface for both $NH_3$ and sodium thiosulphate leaching. Experiments at constant rotational speed but varying solvent concentrations show that both reactions are first order with respect to $NH_3$ and sodium thiosulphate.

The experimental activation energies were 5.03 for the thiosulphate leaching and 5.48 Kcal./mole for the $NH_3$ leaching, values that are normally associated with kinetically controlled reactions in the absence of proof of diffusion control. Kakovskii explained these apparent discrepancies. In the case of thiosulphate leaching, there is a stagewise reaction (to produce $AgS_2O_3^-$ and $Ag(S_2O_3)_2^{3-}$ complexes) and the incomplete dissociation of the $Na_2S_2O_3^-$ ion, both of which are stimulated by an increase in temperature and result in an experimental activation energy above that expected for a diffusion controlled process. In the case of the ammonia leaching, there is an excess of ammonia, the bulk of which is not utilized in the leaching reaction, resulting in an experimental rate constant much lower than the theoretical value, because in the theoretical calculations it is assumed that all the ammonia fed to the disc surfaces reacts completely.

Varying the pH from 4.6 to 12.1 showed the rate of solution of AgCl in aqueous solutions of thiosulphate falls both in acid and alkaline media although the dissolution is only slightly pH dependent. Comparisons with the rate of dissolution by cyanide solutions, show that dissolution in thiosulphate or ammonia compare favourably, the rate of dissolution by $Na_2S_2O_3$ being slightly greater. Factors for accelerating the process are vigorous stirring, an increase in the concentration of the complexing agent, and an increase in temperature.

An electro-oxidation technique was used by Scheiner et al in investigations on the extraction of silver from silver mill tailings [49] and from refractory ores [50]. The process involves passing current through a brine pulp to generate chlorine at the anode and base at the cathode. The chlorine and base combine to form hypochlorite which then oxidizes the carbonaceous and sulphide portions of the ore. The process had been used in the pretreatment of carbonaceous gold ores and sulphide mercury ores and subsequent investigation indicated that the process could be successfully applied to other sulphide and refractory minerals with the metal values dissolving as chloro-complexes.

Electro-oxidation on silver tailings at 30°C with an electrolyte concentration of 20wt.% sodium chloride showed an improvement in silver extraction of from 6% to 25% over cyanidation treatment [49]. It was thought

that oxidation in the presence of chloride ion had converted silver minerals to silver chloride which was soluble in the brine solution as the tetrachloro complex:

$$Ag_2S + 4OCl^- = 2AgCl + SO_4^{2-} + 2Cl^- \qquad (1.1.13)$$

$$AgCl + 3Cl^- = AgCl_4^{3-} \qquad (1.1.14)$$

Scheiner et al[50] conducted acid chloride leaching as well as electroxidation experiments on refractory ores containing silver which were not readily amenable to cyanidation due to the presence of manganese minerals and various oxidized and reduced iron minerals. These studies resulted in the development of a sulphur dioxide (sulphurous acid) - sodium chloride leaching sequence which extracted 80 - 85% of the silver from this type of ore. This was an increase of 9 to 61% silver extraction over that obtained by conventional cyanidation techniques.

Silver minerals of four distinct groups were identified in the ores by microscopic and electron probe examination :

(1) Silver sulphide.
(2) Agentojarosite.
(3) Silver contained in the iron oxides and
(4) In manganese carbonate - oxide minerals.

The electro-oxidation experiments were conducted using a 20% sodium chloride solution and a pulp density of 35%. The cell consisted of three carbon electrodes suspended in the pulp with the current density held constant at 0.5 amp per $in^2$. With a high grade

concentrate containing 35% Iron, 0.75% manganese and 50oz of silver per ton, the silver extraction was only 34% even though 192 kilowatt-hours per ton of material was used.

Only minor amounts of manganese and iron dissolved during the treatment. Cyanidation of the electrolyzed tails did not increase silver extraction. The results indicated that silver minerals, other than sulphides, were not altered sufficiently by electro-oxidation to allow the silver to react with chloride or cyanide ions.

Since a strong and reducing acid such as sulphurous acid (sulphur dioxide + water) dissolves both Mn(IV) and Mn(II) minerals as well as the oxide iron minerals, Scheiner et al conducted a series of sulphurous acid leaching experiments to determine the effect of iron and manganese removal on the silver extraction. The ore was leached using an aqueous solution of 6% $H_2SO_3$ as the source of sulphur dioxide. The iron and manganese dissolved during the acid treatment as chloride complex salts, liberating the silver. The results (Fig. 2(a)) showed that the manganese minerals consume essentially all of the initial $SO_2$ added to the system, the iron extraction was nil and the silver extraction remained constant at the 35% level obtained by direct cyanidation of the untreated ore. The iron and silver codissolved with increasing addition of sulphur dioxide until silver extraction levelled off at 86%. There was no difference

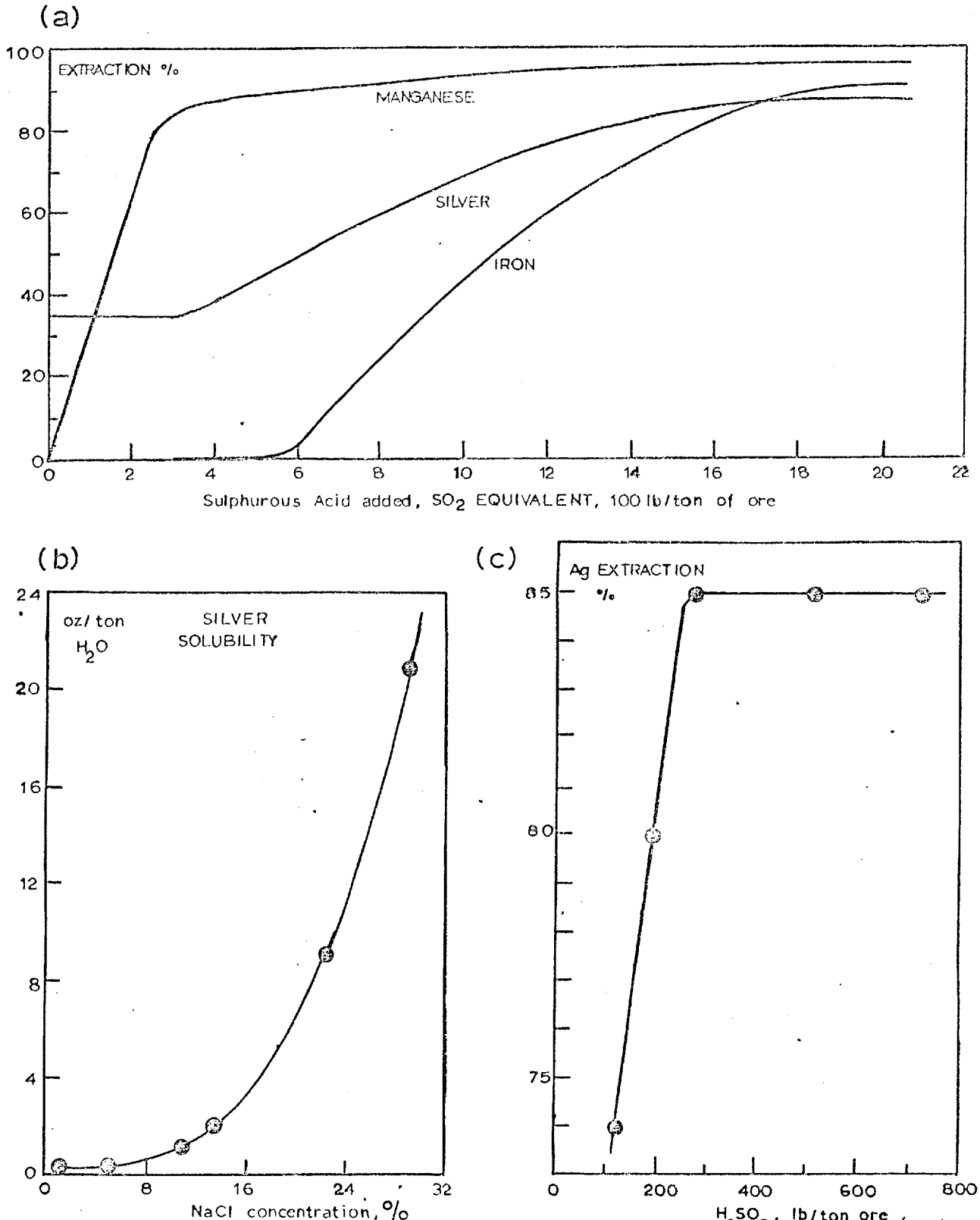


FIGURE 2 : Extraction of silver from refractory ores. Schoiner et al (50).

(a) Effect of $SO_2$ treatment on metal extraction from refractory ores.

(b) Effect of salt concentration on the solubility of silver.

(c) Effect of $H_2SO_3$ addition on silver extraction by a sulphurous acid - 20% sodium chloride solution.

in silver extraction when a 12% $SO_2$ - air mixture was bubbled into the ore slurry instead of adding $H_2SO_3$.

Analysis of the tails showed that the silver remaining was in the form of the agentojarosite $Ag_2Fe_6(OH)_{12}(SO_4)_4$ mineral. Additional treatment of the tails with 3N NCl, $H_2SO_4$ or $HNO_3$ followed by cyanidation increased the total silver extraction to 95% due to the agentojarosite being destroyed by the strong acid.

Subsequent experiments were carried out on low grade refractory silver ores (2.7 - 5.9 oz/ton) using a sulphurous acid - sodium chloride leach solution, containing 20 per cent sodium chloride to ensure the solubility of the silver chloride, (fig. 2(b)). The results in figure 2(c) shows that silver extraction increased rapidly up to a maximum of 85% with increased additions of $H_2SO_3$ and then remained constant. Once again the levelling off of silver extraction was attributed to the presence of agentojarosite mineral from which the leaching solution could not liberate and dissolve the silver.

The silver extraction for this leaching system was essentially independent of particle size, since the iron and manganese minerals containing the silver were also dissolved, whereas the silver extraction increased by 19% and 23% respectively, for electro-oxidation and cyanidation after decreasing the particle aize from -20 to -200 mesh since this liberated

and exposed more of the silver minerals to the extractant.

A similar leach system substituting $H_2SO_4$ for the $SO_2$ in the sodium chloride leach solution gave similar silver extractions except when the ores contained substantial amounts of manganese. In this case the silver extraction decreased due to a large amount of the silver being present in the manganese minerals.

One source of silver is the anode sludges produced in the electrolytic refining of copper. In a process patented by Dutko[51], the sludges are roasted to produce soluble sulphates of Cu, Zn, Ni and 60 to 70% of the Ag. After leaching, the silver is isolated by cementation. The remaining 30% of the Ag, together with the remaining Au, Pb and Sb, is obtained by leaching with a 0.1 to 0.5% cyanide solution, followed by precipitation with Zn powder.

Another hydrometallurgical process for the treatment of these sludges was patented by Hoffmann andErnst in 1971[52]. The sludge, containing Ag, Se, Te, Pb, Sb, Sn, As, Bi, Zn, Cu, Ni, Fe, Au and Pt, is diluted to a thin paste by adding aqueous HCl (up to 12N) and chlorine introduced to convert the metals to their corresponding chlorides. The filter cake from this mixture is washed with acidified hot $H_2O$ (pH3) to remove $PbCl_2$ and slurried in $NH_4OH$ (2 - 12N) for one hour to separate the silver as the soluble complex $Ag(NH_3)Cl$. This is decomposed at 100° and the pure AgCl recovered is converted to AgOH

by an aqueous hot NaOH solution with subsequent reduction to silver by addition of dextrose. The resultant Ag powder is then melted and Ag ingots are recovered. The dried powder contained 99.999% Ag and the recovery yield was 97.2% based on the Ag content of the sludge.

The treatment of mixed sulphide ores containing silver has been the subject of several patents recently. Posel[53] treated sulphide ores and concentrates containing Cu, Ag and Ni by leaching with nitric acid at 115° - 125°C and greater than 50 psig pressure under an oxidising atmosphere. The metals were recovered in high yield.

A process for the electrolytic recovery and separation of lead, silver and zinc from mixed sulphide ores was patented by Gordy[54]. An aqueous slurry containing 60 wt. % powdered ore is treated in an electrolytic cell for a few hours with a direct current of 2.8 - 5 volts and 30 - 100 amps/sq.feet of anode area, with HCl as the electrolyte ( 3 - 6 moles/litre concentration) and 0.1 - 0.6 moles/litre CuCl to form a soluble chlorocuprous complex. The electric current acting on the ore with the $(CuCl_2 + H)^-$ complex ion converts PbS to $PbCl_2$ and $PbSO_4$ and $Ag_2S$ to AgCl precipitates, while Cu, Fe, and Zn all dissolve as ions. After electrolysis and filtration the solids are washed with $NH_4OH$, cyanide or thiosulphate solution to extract the respective soluble silver complex.

Stenger and Kramer[55] described a process for the in situ leaching of noble metal values from ores involving a feed of chlorinated brine into a subterranean strature. They found that the initial brine oxidation potential should be about 800 to 1200 millivolts, with the loaded brine, after contact with the ore, having a residual oxidation potential of about 200 millivolts and preferably at least 500 mV. These potentials were produced by introducing chlorine or alkali metal hypochlorite (NaOCl) into the brine, from 5 to about 3000 ppM of 'dissolved' chlorine being sufficient.

The brine temperature is important. Above 60°C the solubility of chlorine in brine is impaired and below 10°C there is a limitation on the solubility of the silver values. The brines used should be preferably saturated with respect to the inorganic salt component ($NaCl$ or $CaCl_2$.) but dilute brines containing as little as 10% $NaCl$ or $CaCl_2$ can be used but with a much lower leaching rate. Mixtures of these salts, such as are present in naturally occurring brines could also be used.

Investigations showed that these solutions could be used on ores containing $AgCl$, $Ag_2S$, $Ag_2CO_3$, Au and AuTe, the noble metal values being recovered by precipitation with hydrogen sulphide or a water-soluble sulphide, after removal of any Pb, Cu, or Zn present. The depleted brine is then recycled after aeration to reduce the $H_2S$ content and after contacting with chlorine to raise the oxidation potential.

A number of other papers, although primarily concerned with the dissolution of some other metal, have mentioned the behaviour of the silver present as ores or concentrates are leached. In the recovery of Cu, Fe, and S from chalcopyrite concentrates using a ferric chloride leach, Haver and Wong [103] noted that considerable proportions of silver dissolved in the ferric chloride e.g., 60.6% of the silver dissolved during a leach at 106° for 2 hours, from an ore containing 0.86oz/ton silver.

In the Cymet process [100], which involves the electro-oxidation of sulphide to sulphur at an anode, with the consequent solution of metal ions and the reduction of these ions at a cathode, recovery of silver into the copper was 96% from a chalcopyrite ore containing 2oz/ton silver. The yield of recovery was influenced by the form of occurrence but no poor silver recovery was encounted in tests.

Finally, Prater et al [109] leached copper concentrates (60% chalcopyrite, 10% bornite), which contained 3.5 oz of Silver per ton, with nitric acid. Higher silver extractions were obtained with higher nitric acid concentrations e.g., 63% $HNO_3$ concentration gave 66.2% Ag extraction while 13% $HNO_3$ concentration gave 17.8% Ag extraction.

1.1.2 The Equilibrium reaction : $Fe^{3+} + Ag = Ag^{+} + Fe^{2+}$

From the preceding section it can be seen that the ratio $Fe^{3+}/Fe^{2+}$ plays an important role in the leaching of silver minerals by

solutions containing ferric salts, due to the equilibrium:

$$Ag + Fe^{3+} = Ag^{+} + Fe^{2+} \quad (1.1.14)$$

This reaction is also one of the most important as regards the geochemistry of silver in near surface processes,[15]. The $Fe^{2+}/Fe^{3+}$ content of soil solutions is one of the factors that influence the mobility and fixation of silver in soils and the above reaction is one of the mechanisms for the precipitation of native silver from downward migrating solutions resulting in secondary enrichment of silver deposits.

Stokes[56] first demonstrated the reversibility of the reaction in 1906 in experiments on the behaviour of hot ascending solutions. A simple apparatus was devised, in the lower, warmest part of which the reaction between the metal and ferric sulphate solution was brought about, while in the upper, cooler, portion the reaction was reversed, with deposition of metal.

It is one of the comparatively few reactions in which at equilibrium the concentration of reactants and products can be determined by ordinary methods of chemical analysis. Noyes and Brann[57] studied the reaction between metallic Silver and ferric nitrate solutions:

$$Ag + Fe(NO_3)_3 = AgNO_3 + Fe(NO_3)_2 \quad (1.1.15)$$

The analyses were all made volumetrically

using permanganate ion for the ferrous ion and potassium thiocyanate for the silver ion. The amount of ferric nitrate in the equilibrium mixtures was determined by the difference between the amount of total iron at the start and the amount of ferrous ion found.

Values of the equilibrium constant were calculated from the concentrations of the three salts at equilibrium expressed in formula weights per litre:

$$\text{Equilibrium, const, } K = \frac{(Fe(NO_3)_2)\ x(AgNO_3)}{(Fe(NO_3)_3)} \quad (1.1.16)$$

The effect of nitric acid on the constant was quite marked up to 0.02N but a further increase in the acid concentration had no appreciable effect. The value of the constant varied considerably with the salt concentration, being considerably larger in the dilute solutions than in the more concentrated ones. Noyes and Brann plotted the values against the total nitrate concentration and by a straight line extrapolation to zero concentration obtained a value of 0.128 for the equilibrium constant at 25°C for the ion reaction. However their points were widely scattered so that the extrapolation was somewhat uncertain.

Both Cooke[29] and Tananaeff[58] studied the equilibrium using sulphate solutions. The equilibrium constant was calculated using the equation $K = C_1 . C_2 / C_3$ where $C_1$ and $C_2$ are the $Ag^+$ and $Fe^{2+}$ equilibrium concentrations and $C_3$ is the $Fe^{3+}$ concentration. Cooke

obtained an average value of approximately 0.006 and noted an hydrolysis effect at very dilute concentrations. Tananaeff conducted experiments at $0^{\circ}$, $25^{\circ}$ and $45^{\circ}$ in air, a $CO_2$ atmosphere and a nitrogen atmosphere. The average values obtained were:

$$K(0^{\circ}) = 0.0019, K(25^{\circ}) = 0.0060, K(45^{\circ}) = 0.0110.$$

Shaw and Hyde[59] measured the equilibrium constant analytically and electrometrically in nitrate solutions. Analyses were carried out in the usual way and for the electrometric work the following cell was used.

$$Ag,\ AgNO_3,\ KNO_3\,(sat),\ Fe(NO_3)_2,\ Fe(NO_3)_3,\ Pt.$$

The equilibrium constant decreased with increase inionic strength. To obtain a true equilibrium constant the values were plotted against ionic strength and extrapolated to zero ionic strength. This gave a value of 0.130, in satisfactory agreement with the value of 0.114 obtained from the electrometric measurements.

However, King[60] called attention to the errors involved in this method of extrapolating to zero concentration. The value of the constant as determined by Noyes and Brann, and Shaw and Hyde, was:

$$K = (Fe^{2+})\ (Ag^{+})/(Fe^{3+}) \qquad (1.1.17)$$

While the true constant (or K extrapolated to $\mu = 0$) is given by:

$$Ko = \frac{CAg^{+} C Fe^{2+}}{C Fe^{3+}} \cdot \frac{fAg^{+} f Fe^{2+}}{f Fe^{3+}} = \frac{K f_1 f_2}{f_3} \qquad (1.1.18)$$

Where $f_{1,2,3}$ represent the activity coefficients of the ions. Considering very low ionic strengths, King used the Debye Huckel expression for f, namely

$$- \log f(\text{ion}) = 0{:}5 z^2 \sqrt{\mu} \text{ (at } 25^{\circ}C) \qquad (1.1.19)$$

to obtain the equation,

$$\log K = \log Ko - 2\sqrt{\mu} \qquad (1.1.20)$$

Thus, if log K is plotted against $\sqrt{\mu}$, at sufficiently low ionic strengths the plot should approach a straight line with the slope -2, the intercept being log Ko.

Using the values of K obtained by Noyes and Brann, and Shaw and Hyde, King discovered that these values were too far removed from $\mu = 0$ to give any idea of the correct extrapolation, but suggested that Ko would not be less than 0.178.

Schumb and Sweetser[61] attempted to obtain a more accurate value of the equilibrium constant by studying the reaction over a wider range of concentration to lessen the amount of extrapolation necessary. Perchlorates were used in this work in preference to the nitrates because a higher concentration of perchloric than of Nitric Acid could be used without attacking the powdered silver. The equilibrium mixtures were analyzed

potentiometrically for ferrous ion and silver ion using a bright platinum gauze electrode and a saturated calomel electrode, the ferric ion concentration being determined as the difference between the total iron in solution and the ferrous ion.

Two series of experiments were carried out at 25°C with a different constant ratio of perchloric acid to ferric perchlorate in each series. The equilibrium constant was calculated in terms of concentrations from the expression

$$K = (Fe^{2+})\,(Ag^{+})\,/(Fe^{3+}) \qquad (1.1.17)$$

When K was plotted against total perchlorate solution or $\mu$, the ionic strength, a smooth curve for each series was obtained. However a plot of $\log K + 2.02\mu^{\frac{1}{2}}$ against $\mu$ gave curves much more suitable for extrapolation. The curves for the two series were very nearly superimposable.

The equations of the curves for the two series were calculated separately by the method of least squares. These gave K the values 0.539 and 0.523 at zero ionic strength. If the two series are averaged the equation for the resulting curve is found to be:

$$\text{Log } K + 2.02\mu^{\frac{1}{2}} = -0.275 + 1.645\mu - 0.316\mu^{2} \qquad (1.1.21)$$

This gives K the value 0.531, which was taken to be the true value of the equilibrium constant at 25°C.

Although this value is higher than previously accepted values, there is evidence to support it. Thus, Bray and Hershey[62] developed a method for calculating the amount of hydrolysis in a solution of ferric ion, and with the aid of this hydrolysis correction they recalculated the data of Noyes and Brann and concluded that K should have the value 0.363, instead of 0.128, which agrees more closely with Schumb and Sweetser's value.

1.1.3 Complex Formation between Silver and Chloride ions

It has long been known that silver is fairly soluble in concentrated solutions of various chlorides and many leaching processes have used brine solutions and other chloride solutions for the dissolution of silver ores (section 1.1.1). The solubility of the silver increases with chloride concentration due to the formation of a number of complex ions. The species which have been identified in these solutions are: $AgCl(aq)$, $AgCl_2^{2-}$, $AgCl_3^{2-}$, $AgCl_4^{3-}$, $Ag_2Cl^{+}$ and $Ag_3Cl^{3+}$.

The stability constants of these ions have been calculated in a large number of investigations from both solubility and potentiometric measurements. Values of these constants have been tabulated for the following equilibria[63]:

| | | |
|---|---|---|
| $Ag^+ + Cl^- = AgCl$ , | Stepwise constant | K1 |
| $AgCl + Cl^- = AgCl_2^-$ , | '' '' | K2 |
| $AgCl_2^- + Cl^- = AgCl_3^{2-}$ , | '' '' | K3 |
| $AgCl_3^{2-} + Cl^- = AgCl_4^{3-}$ , | '' '' | K4 |
| $Ag^+ + 2Cl^- = AgCl_2^-$ , | Cumulative constant | $\beta 2$ |
| $Ag^+ + 3Cl^- = AgCl_3^{2-}$ , | '' '' | $\beta 3$ |
| $Ag^+ + 4Cl^- = AgCl_4^{3-}$ , | '' '' | $\beta 4$ |
| $2Ag^+ + Cl^- = Ag_2Cl^+$ , | '' '' | $\beta 12$ |
| $3Ag^+ + Cl^- = Ag_3Cl^{2+}$ , | '' '' | $\beta 13$ |
| $AgCl(S) = AgCl(aq)$ , | Solubility constant | $Ks_1$ |
| $AgCl(S) + Cl^- = AgCl_2^-$ , | '' '' | $Ks_2$ |
| $AgCl(S) + 2Cl^- = AgCl_3^{2-}$ , | '' '' | $Ks_3$ |
| $AgCl(S) + 3Cl^- = AgCl_4^{3-}$ , | '' '' | $Ks_4$ |
| $AgCl(S) + Ag^+ = Ag_2Cl^+$ , | '' '' | $Ks_{12}$ |

Bodlander and Eberlein[64] first postulated the existence of a complex ion, $AgCl_4^{3-}$, and calculated its complexity constant $\beta_4$ from the solubility of silver chloride in 4M potassium chloride using data from Hellwig.[65]. Forbes[66] measured the solubility of silver chloride in various chloride solutions and found that the solubility was proportional to integral powers of the chloride concentration in well defined concentration intervals suggesting the possible formation of complex ions of silver chloride molecules with chlorine ions. The complex $AgCl_3^{2-}$ fitted the data for solutions with a chloride concentration below 1.5N while the complex $AgCl_4^{3-}$ was suggested at concentrations above 2.5N. In the case of potassium and ammonium chlorides, a third ion was suspected from the data for solutions above 3.0 normal. No evidence of the ion $AgCl_2^-$ was found in this work but a later investigation[67] on solutions less than normal

in chloride suggested that this ion might predominate at lower concentrations

These finds were confirmed by Pinkus and co-workers[68] in work on the solubility of silver chloride in solutions of sodium chloride, potassium chloride, Lithium chloride and hydrochloric acid, varying in concentration from 0.001 to 0.1molar. The solubility decreased with increase in chloride concentration to a minimum at 0.0025 M chloride ion, corresponding to a silver chloride concentration of $2.5 \times 10^{-7}$ moles/litre for KCl and $2.97 \times 10^{-7}$ for NaCl solutions. Later measurements[69] gave the minimum solubility at 0.003M chloride ion as $3.63 \times 10^{-7}$ moles of AgCl per litre in the presence of KCl and NaCl, $4.17 \times 10^{-7}$ in the presence of LiCl and $4.47 \times 10^{-7}$ in hydrochloric acid.

Subsequently the solubility increased rapidly with increase in chloride concentration indicating the formation of stable soluble complexes of the form $Ag_M Cl^-_{M+1}$. The degree of complexity, that is the fraction of silver chloride present as a complex, was calculated to be practically 100% at chloride concentrations greater than 0.05 moles/litre.

From the solubility of silver chloride in 5M to 12.5M hydrogen chloride, Erber and Schuhly[70] calculated a complexity constant for the complex $AgCl_n^{1-n}$ and concluded that n = 4 was more probable than n = 2 or 3.

Garret et al[71] obtained the character

of the ionic species in potassium chloride solutions at 25°C by a graphical method (section 6.1.5). This indicated that the chief reaction in the concentration range studied (up to 0.9 moles KCl per 1000 gms $H_2O$) was represented by:

$$AgCl(S) + 2Cl^- = AgCl_3^{2-} \qquad (1.1.22)$$

with a solubility constant ($K_{S_3}$) of $1.3 \times 10^{-4}$. Garret considered all the silver chloride to be in the form of the complex $AgCl_3^{2-}$ above 0.1 molar KCl but did not eliminate the possibility of the complex $AgCl_2^-$ being present at lower concentrations.

Barney et al[72] determined the composition and instability constant of the complex present at very low chloride concentrations from an accurate determination of the minimum solubility and the corresponding anion concentration. A radiochemical technique using $^{110}Ag$ was used to determine the solubility of silver in the concentration range $10^{-6}$-$10^{-7}$ moles/litre. The minimum occurred at $(Ag^+) = 1.55 \times 10^{-7}$ moles/litre and $(Cl^-) = 1.50 \times 10^{-3}$ moles/litre, from which the calculated number of $Cl^-$ ions coordinated to a single $Ag^+$ is 2.14 indicating that the predominate species in this concentration range is $AgCl_2^-$.

A similar radioassay technique was used By Jonte and Martin[73] to determine the concentration of silver in chloride solutions at concentrations less than 0.1 molar, for the temperatures of 15, 25 and 35°C. At 25°C a minimum of solubility was found at a silver

Concentration of about $5 \times 10^{-7}$M for a chloride activity of $2 \times 10^{-3}$. The data was interpreted in terms of equilibrium involving the undissociated species AgCl(aq) and the complex ion $AgCl_2^-$.

Leden[74] determined the solubility of silver chloride at 25°C in sodium chloride solutions containing sodium perchlorate to an ionic strength of 5M by electroanalyses and potentiometric titrations. From potentiometric measurements in solutions not saturated with sodium chloride it was concluded that silver compounds other than the complex ions $AgCl_3^{2-}$ and $AgCl_4^{3-}$ can only exist in minute amounts in solutions containing more than 1M chloride. In a solution of 5M NaCl about 1/3 to $\frac{1}{2}$ of the silver is thus to be found as $AgCl_4^{3-}$ and the rest as $AgCl_3^{2-}$, and in 1M NaCl 80 to 90% of the total silver is found as $AgCl_3^{2-}$.

At lower concentrations Berne and Leden[75] identified the complexes AgCl(aq) and $AgCl_2^-$. The solubility of silver chloride in sodium chloride at 25°C was determined by a radioassay technique at ionic strengths of 0.2 and 5M obtained by additions of sodium perchlorate. The stability constants of these complexes were determined at zero ionic strength.

Leiser[76] determined the species present at 18°C when silver chloride dissolved in sodium chloride solutions up to 2 molar, using radiochemical measurements.

The concentration ranges over which they are the dominant species were determined as : $10^{-4}$-$10^{-2}$ M for AgCl(aq), $10^{-2}$ - 0.2M for $AgCl_2^-$ and > 0.2 M NaCl/litre for $AgCl_3^{2-}$.

Chateau and Hervier[77] measured the solubility of silver chloride in solutions of potassium chloride at 25°C and confirmed the existence of the two complexes $AgCl_2^-$, and $AgCl_4^{3-}$ but found no evidence for the ion $AgCl_3^{2-}$. For potassium chloride concentrations between 0.1 and 0.5M they determined that the dominant species was $AgCl_2^-$ while for concentrations greater than 1.5M, $AgCl_4^{3-}$ predominates. Between 0.5M and 1.5M, it was concluded that the complex of $AgCl_3^{2-}$ was not formed and that the complexes, $AgCl_2^-$ and $AgCl_4^{3-}$ coexisted.

Marcus[78] used an anion exchange resin for the sorption of metal - anion complexes from aqueous solutions of the metal at different anion concentrations. Experiments with silver chloride were carried out in the concentration ranges of 0.00 2-12M hydrochloric acid and $1.5 \times 10^{-6}$ M to $4.6 \times 10^{-3}$M silver, the distribution of silver between the resin and the solution being measured by the aid of $^{110}Ag$ tracer. The complex formation constants were in reasonable agreement with those found by other methods. The predominant complex was found to be $AgCl_3^{2-}$ with the formation of $AgCl_4^{3-}$ taking place only at high chloride ion activities.

The solubility of AgCl in water and aqueous solutions of sodium chloride with

concentrations from $2.10^{-5}$ to 4.0 M at 18° was also studied by Mironov[79] by means of the radioactive isotope $^{110}Ag$. The data agreed with previous work within experimental errors. A minimum of solubility was obtained at $3 \times 10^{-3}$ M sodium chloride concentration corresponding to a silver chloride solubility of $2.97. 10^{-7}$ moles/litre. The stability constants of the ions of the form $AgCl_n^{1-n}$ were determined for $n = 1,2,3,4$.

Rasse[80] demonstrated the solubility of AgCl in HCl solutions, showing a decrease to a minimum of $10^{-7}$ moles/litre at $10^{-3}$ moles/litre $Cl^-$ and then an increase to $1.7. 10^{-5}$ moles/l in N HCl. The author explained this increase as due to the formation of the complex $AgCl_2^-$.

Ciantelli[81] attributed the increased solubility of AgCl in NaCl and $NaClO_4$ solutions, having a constant ionic strength and a chloride ion concentration varying between 0.5 and 5M, to the formation of three complexes, $AgCl_2^-$, $AgCl_3^{2-}$ and $AgCl_4^{3-}$. The fraction of the silver occurring in the form of one of these complexes was plotted against the chloride concentration, for each complex (see Fig. 4(a) ). Above 1M chloride concentration, the amount of $AgCl_2^-$ is small. In a 5M chloride ion solution, 60 - 70% of the dissolved silver was calculated to be present as $AgCl_4^{3-}$ and the rest as $AgCl_3^{2-}$.

Figure 3. compares the solubility data from a number of investigations at chloride

concentrations below 1M, and Figure 4 (b) compares data at higher chloride concentrations.

As well as ions of the form $AgCln^{1-n}$ there are cations formed by silver chloride. Among those identified or postulated are $AgCl^+$, $Ag_2Cl^+$ and $Ag_3Cl^{2+}$. Pinkus, Frederic and Schepmans[83] interpreted work on the solubility of silver chloride in silver nitrate solutions of concentration from $5.10^{-6}$ to 2 Molar in terms of a complex being formed, either $Ag_3Cl_2^+$ or $Ag_2Cl^+$.

Berne and Leden[75] also studied silver chloride in silver nitrate solutions and showed the dissolution to be by reactions of the form:

$$mAgCl(S) + nAg^+ = Ag_{m+n}Cl_m^{n+} \quad (1.1.23)$$

The strength of these complexes was found to be of the same order of magnitude as of the complexes $AgCln^{1-n}$. If $Ag^+$ is $< 0.3M$, $Ag^+$, AgCl and $Ag_2Cl^+$ were found to dominate completely in the silver nitrate solutions. Leiser[84] determined the solubilities of silver halides in silver nitrate solutions at concentrations up to 2M at 20°C. A radiochemical technique was used and from the solubility curves the dissociation constants and concentrations ranges of the complexes were found. The predominant complexes for silver chloride were:

| | | |
|---|---|---|
| AgCl (aq) | from $10^{-4}$ -$10^{-2}$ | mole $AgNO_3$ /litre |
| $Ag_2Cl^+$ | from $2.10^{-2}$-0.1 | " " " |
| $Ag_3Cl^{2+}$ | above 0.2 | " " " |

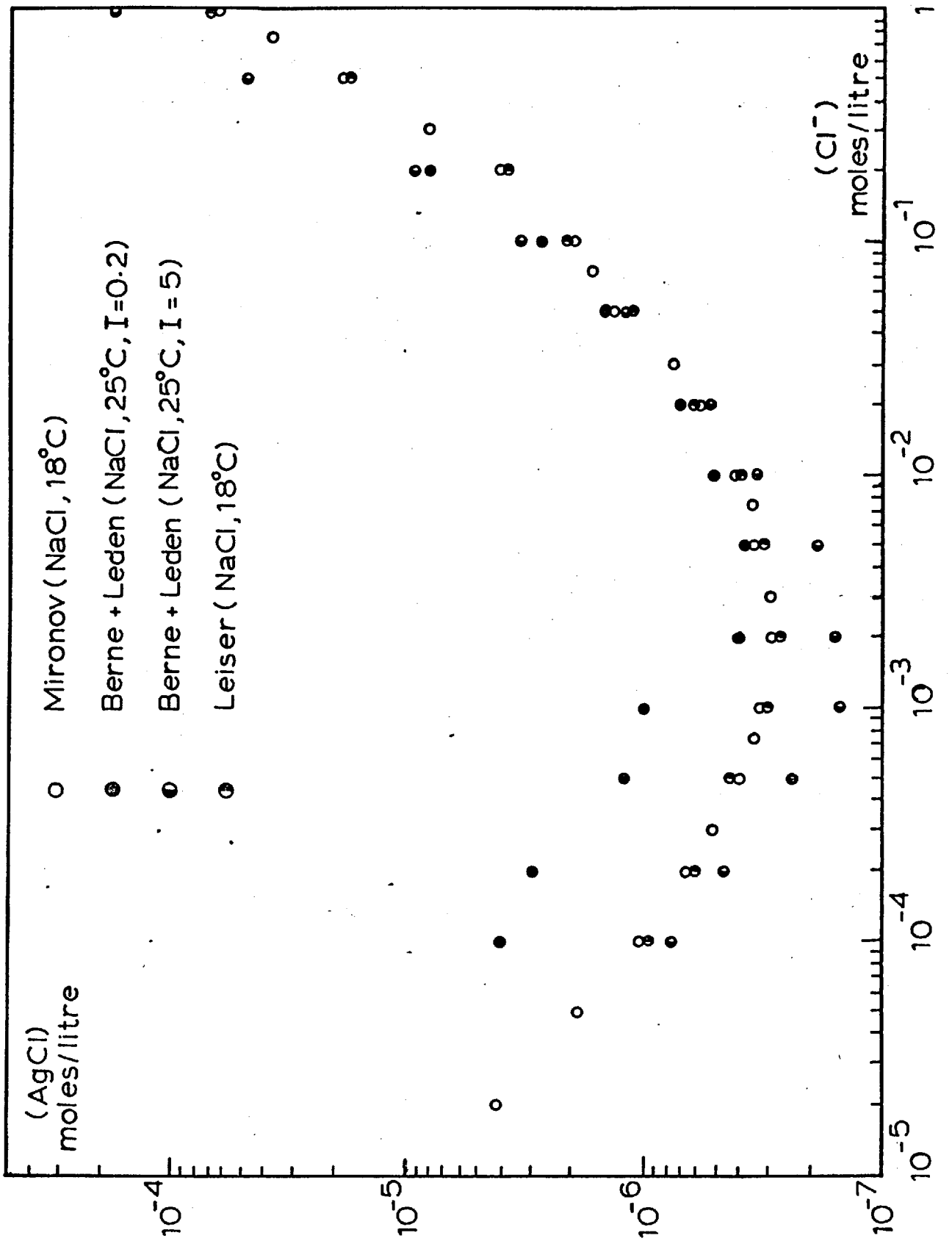


FIGURE 3 : Effect of chloride ion on the solubility of silver chloride at $Cl^-$ concentrations less than 1 Molar. Mironov[79], Berne and Leden[75], and Leiser[76].

(a)

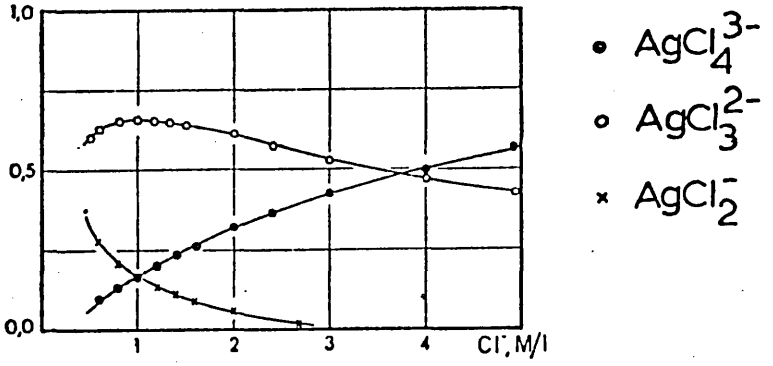


(b)

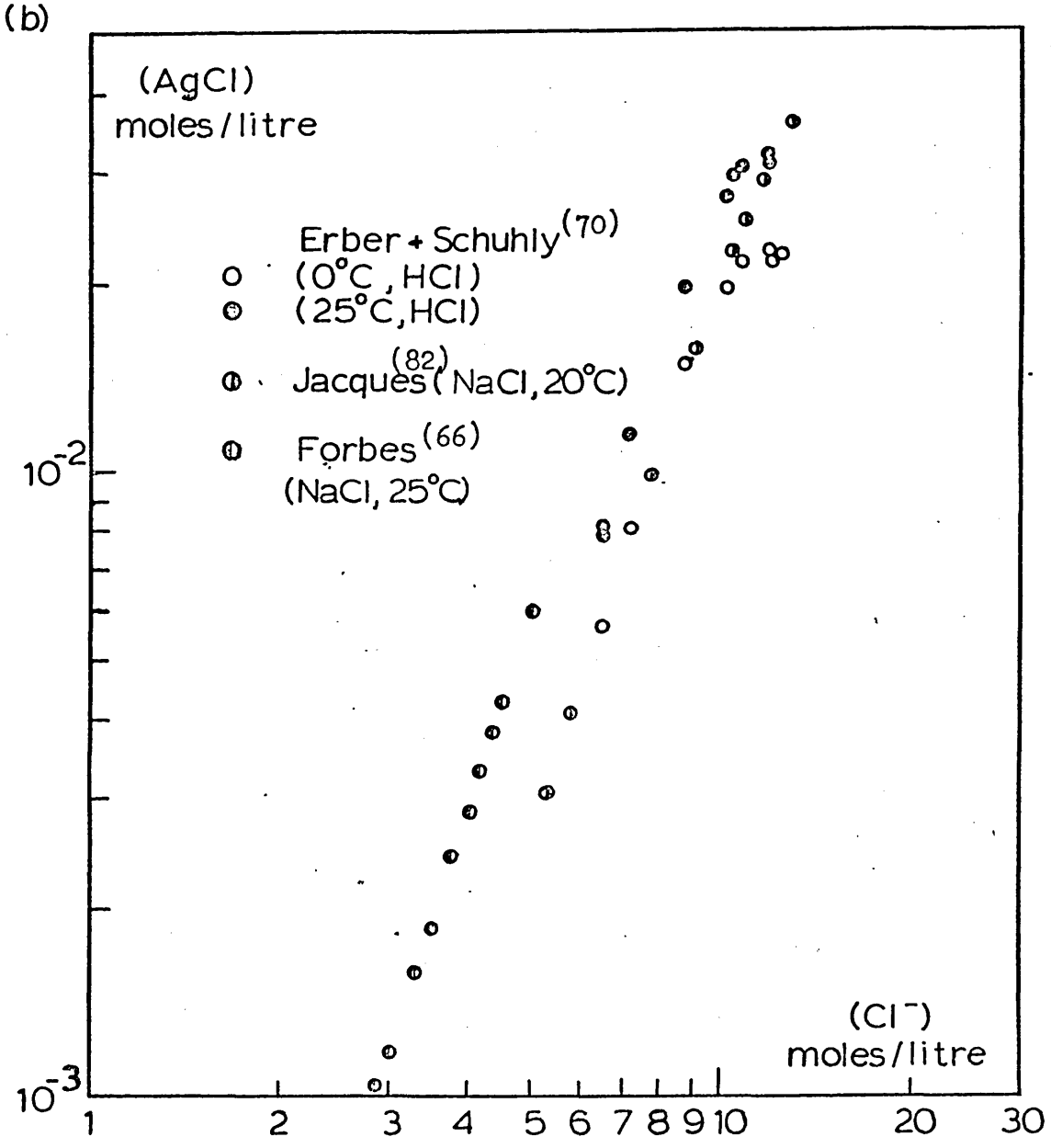


FIGURE 4 : (a) Fraction of silver occurring as the various complexes, as a function of chloride concentration. Ciantelli (81).

(b) Effect of chloride concentration on the solubility of AgCl at $Cl^-$ concentrations greater than 1 Molar.

## 1.2 Leaching of copper minerals.

The dissolution of the sulphide minerals of copper has been the subject of many investigations. The behaviour of covellite, chalcocite, chalcopyrite and bornite has been studied in solutions containing sulphuric acid, ferric sulphate, ferric chloride, nitric acid, cyanide salts and perchloric acid as well as in bacterial, electrochemical and high pressure leaching systems. These have been fully reviewed in recent publications[18,85-90].

In this survey a brief review will be given of work concerning the two most important copper-iron sulphides which are relevant to the present study.

### 1.2.1. Leaching of Bornite; $Cu_5FeS_4$ :

Most of the studies on the leaching of bornite are concerned with the dissolution of the mineral in acidified ferric sulphate solutions. Sullivan[91] noted that the dissolution occurred in two stages. In the early part of tests on a natural crushed bornite the copper was dissolved whereas the iron and sulphur were not attacked. However as the tests progressed the iron and sulphur were both attacked appreciably.

The dissolution rate was virtually independent of the strength of ferric sulphate if enough reagent was present and independent of the acid strength. However an increase in temperature markedly affected the dissolution rate.

Sullivan considered the dissolution to be due to three reactions based on a representation of Bornite as $2Cu_2S.CuS.FeS$. :-

$$Cu_2S + Fe_2(SO_4)_3 = CuSO_4 + 2FeSO_4 + CuS \quad (1.2.1)$$
$$CuS + Fe_2(SO_4)_3 = CuSO_4 + 2FeSO_4 + S \quad (1.2.2)$$
$$FeS + Fe_2(SO_4)_3 = 3FeSO_4 + S \quad (1.2.3)$$

giving an overall reaction, with a final product of elemental sulphur, as follows:-

$$Cu_5FeS_4 + 6Fe_2(SO_4)_3 = 5\ CuSO_4 + 4S \quad (1.2.4)$$

Uchida et al[92] found that concentrations of ferric ion greater than 0.5 g/l did not improve the rate of leaching whereas Kopylov and Orlov[93] found an increase of $Fe^{3+}$ (as ferric sulphate) concentration from 9 to 35 g/l increased the rate. However the factor which most affected the leaching rate was the temperature. Kopylov and Orlov determined the activation energy as $5.5 \pm 1.4$ Kcal per mole which indicated a process controlled by diffusion.

These authors[93] were the first to notice the formation of a new solid phase after the first few minutes of dissolution. From X-ray diffraction patterns they concluded that this phase was chalcopyrite and with this discovery as a basis discussed the mechanism of dissolution of bornite by writing the formula as $2Cu_2S.CuFeS_2$. As with that of Sullivan, this representation is structurally invalid and it was not until the work of Dutrizac et al that a more correct dissolution mechanism for bornite

was proposed.

Dutrizac et al[94] studied the dissolution of bornite by rotating sintered discs of synthetic mineral in acidified ferric sulphate solutions. In tests made above 40°C a partially leached disc showed three distinct layers, the residual unreacted bornite, a material with an X-ray pattern very similar to bornite whose lattice spacings gradually decreased with increasing distance from the normal bornite and finally a yellow layer identified by X-ray diffraction analysis as a mixture of chalcopyrite and sulphur.

Electron microprobe analyses indicated that the S/Fe ratio remained fixed at 4 across both the bornite and the nonstoichiometric bornite and that the Cu/S and Cu/Fe ratios dropped steadily. Hence it was proposed that at temperatures above 40°C dissolution occurred with the formation of a non-stoichiometric bornite:

$$Cu_5FeS_4 + x\,Fe_2(SO_4)_3 = Cu_{5-x}FeS_4 + x\,CuSO_4 + 2x\,FeSO_4 \qquad (1.2.5)$$

which on further dissolution gave chalcopyrite and elemental sulphur:

$$Cu_{5-x}FeS_4 + (4-x)Fe_2(SO_4)_3 = CuFeS_2 + (4-x)\,CuSO_4 + (8-2x)FeSO_4 + 2\,S^o \qquad (1.2.6)$$

The chalcopyrite then dissolved at a much slower rate:

$$CuFeS_2 + 2Fe_2(SO_4)_3 = CuSO_4 + 5FeSO_4 + 2S^\circ \quad (1.2.7)$$

At temperatures below 25°C only reaction (1.2.5) was observed with x having a maximum value of 1.2, representing 25% copper dissolution. No iron or sulphur dissolved during the formation of this non-stoichiometric bornite. A natural bornite dissolved in an identical manner (Fig 5 (a)).

The dissolution rate depended on the ferric ion concentration for ferric ion strengths of less than about 0.06 M but was independent of higher concentrations (Fig. 5(b)). An average activation energy of 5.7 ± 1.3 Kcal per mole was obtained for the dissolution.

Dutrizac and MacDonald[95] also leached a crushed bornite ore in columns, with acidified ferric sulphate solution, to determine the controlling factors in percolation leaching. X-ray diffraction analysis of the reacted bornite indicated the same reaction products as for the rotating disc experiments. Hence it was assumed that the bornite ore dissolved according to the same reactions previously reported i.e., equations (1.2.5), (1.2.6) and (1.2.7).

In the percolation leaching tests, the dissolution occurred in two stages, a rapid linear stage and a slow non-linear stage. The initial step is largely controlled by the bulk delivery of the oxidant to the ore. The rate depends directly on the ferric ion concentration below about 0.1M $Fe^{3+}$, but is

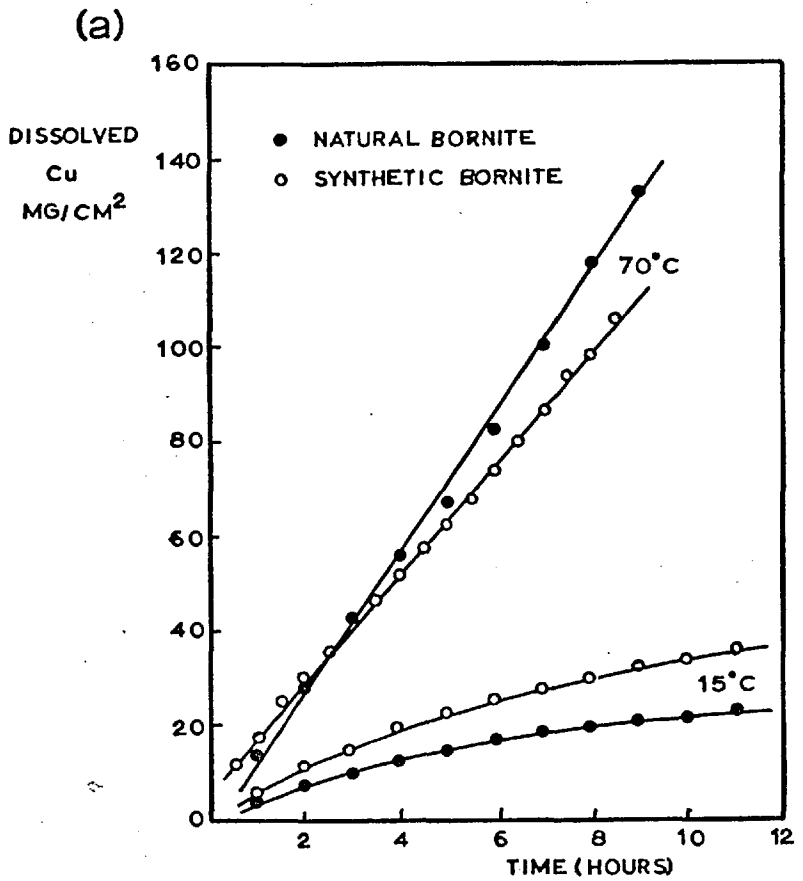


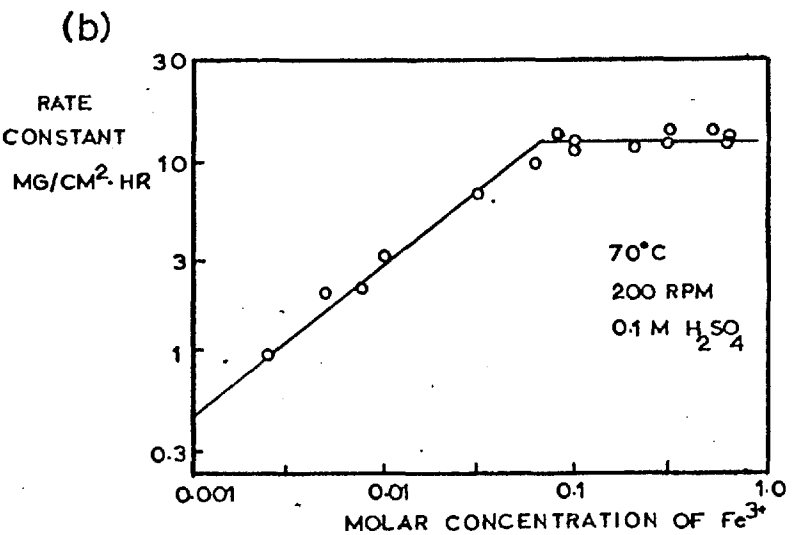


FIGURE 5 : (a) Comparison of the leaching rates of natural and synthetic Bornite. Dutrizac et al(94).

(b) Effect of Ferric ion concentration on the rate of synthetic Bornite dissolution. Dutrizac et al(94).

relatively insensitive to higher concentrations. The second leaching stage is controlled by chemical and physical factors and, unlike the first stage, it is temperature dependent. The upper limit for rapid copper conversion was assumed to be set by the conversion of bornite to slowly dissolving chalcopyrite.

An investigation by Ugarte[11], however, showed that the solid phase formed after the first stage of leaching bornite was Idaite ($Cu_3FeS_4$) and not chalcopyrite as reported in the previous studies. Ugarte studied the leaching of bornite in particulate form in ferric sulphate solutions between the temperatures of 15 and 90°C. The effects of changing particle size, sample weight, stirring speed, sulphuric acid concentration and ferric ion concentration were broadly in agreement with those found by other workers. His results can be summarised:-

(1) At temperatures above 40°C, the dissolution rate was characterized by a first stage of fast dissolution of copper (until 40% of the copper had dissolved) and a second stage of slow dissolution which was sensitive to temperature (Figure 6). An activation energy of 2.1 $\pm$ 0.1 Kcal/mole was obtained for the first part of the reaction. Below 40°C, the first part of the reaction can be separated into two sections; one section extending up to about 27% of the copper dissolved

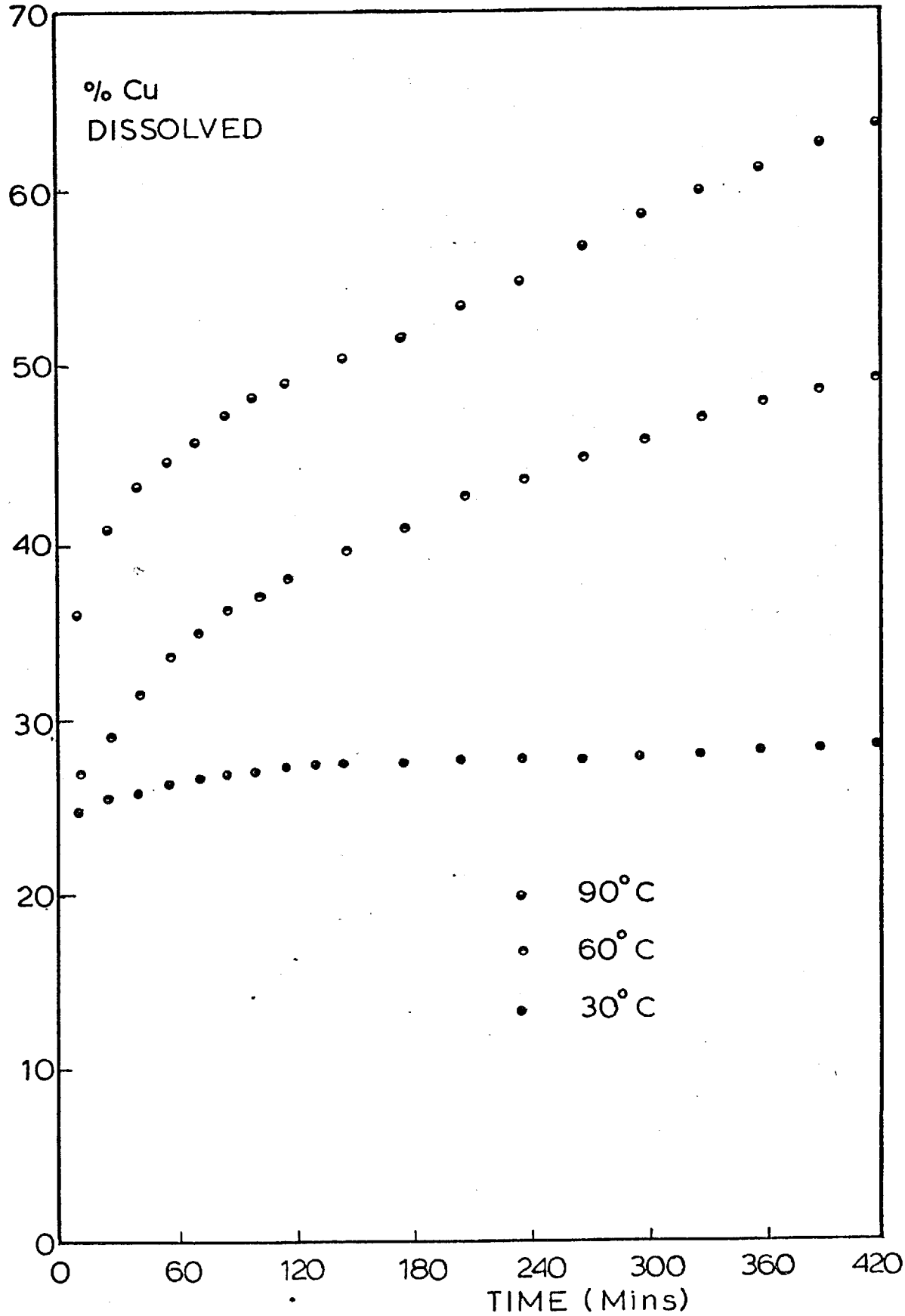


FIGURE 6 : Effect of Temperature on the rate of leaching synthetic Bornite. Ugarte[11].

and a much slower section from this point to a maximum of 40% of the copper dissolved (see 30°C curve in Figure 6).

(2) A reduction in particle size increased the rate of the first part of the reaction but the second part was unaffected by any variation;

(3) When a sufficient stirring speed was used, the dissolution rate was unaffected by any variation of the stirrer speed;

(4) At 30°C, concentrations of $Fe^{3+}$ ion higher than 0.03M did not increase the amount of copper dissolved, while the reaction at 90°C was dependent on $Fe^{3+}$ concentration up to 0.065M. Figure 7 shows that at higher concentrations, the rate became independent of $Fe^{3+}$ ion concentration;

(5) Acid concentration had no effect on the rate of leaching, its presence being necessary, however, to prevent the hydrolysis and precipitation of ferric ions;

and finally,

(6) The sample weight had no effect on the rate of dissolution per unit mass.

The two dissolution stages above 40°C were considered to be the formation of the phase idaite by the fast reaction:

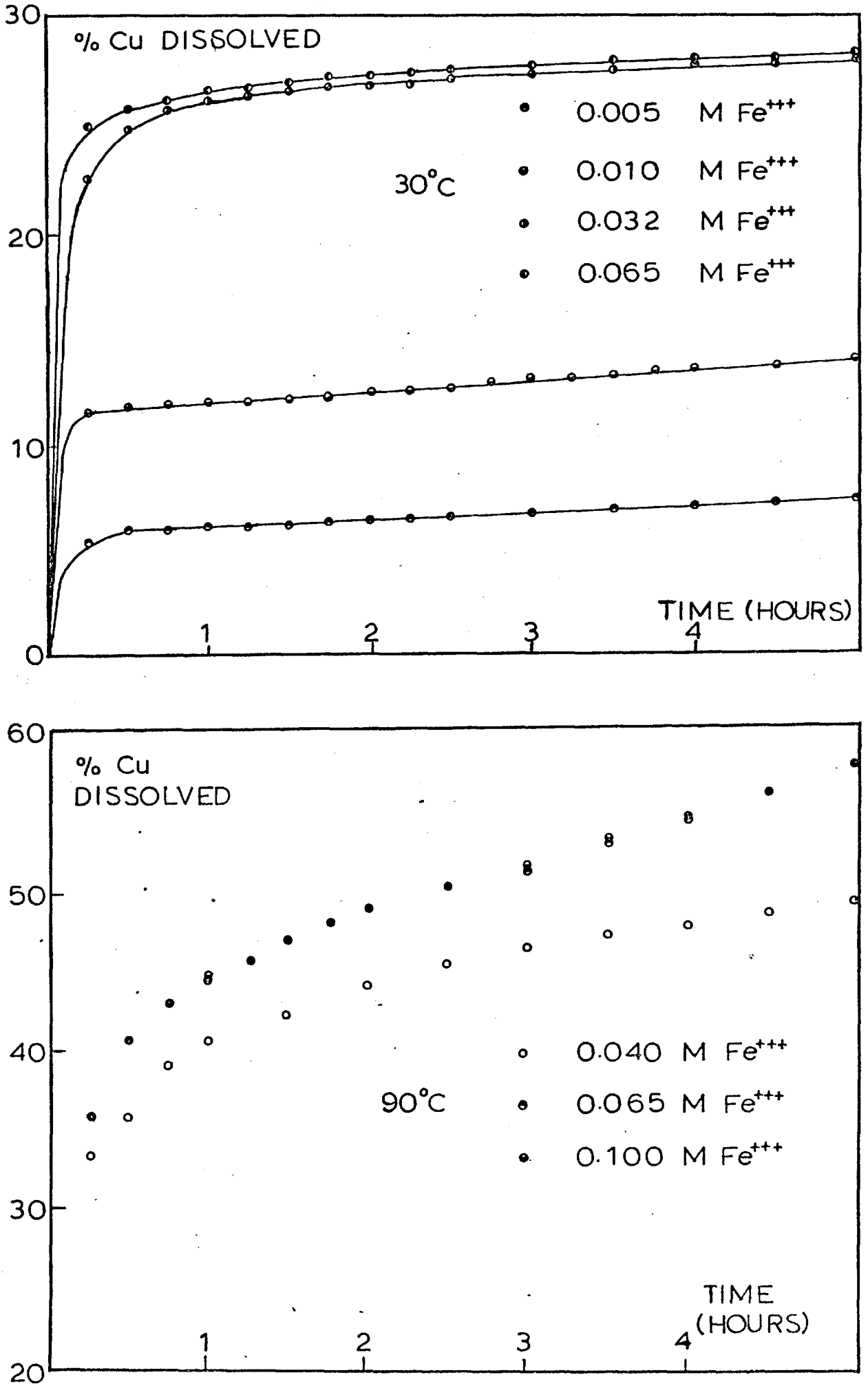


FIGURE 7 : Effect of Ferric ion concentration on the rate of leaching Bornite at (a) 30°C, and (b) 90°C. Ugarte[11].

$$Cu_5FeS_4 + 2Fe_2(SO_4)_3 = Cu_3FeS_4 + 2CuSO_4 + 4FeSO_4 \quad (1.2.8)$$

followed by the slow dissolution of this phase to give elemental sulphur:

$$Cu_3FeS_4 + 4Fe_2(SO_4)_3 = 3CuSO_4 + 9FeSO_4 + 4S \quad (1.2.9)$$

Below 40°C, reaction (1.2.8) proceeded in two steps. A fast reaction to give a non-stoichiometric bornite:

$$Cu_5FeS_4 + x\,Fe_2(SO_4)_3 = Cu_{5-x}FeS_4 + x\,CuSO_4 + 2x\,FeSO_4 \quad (1.2.10)$$

where x had a maximum value of 1.35, and a much slower reaction to give idaite:

$$Cu_{5-x}FeS_4 + (2-x)\,Fe_2(SO_4)_3 = Cu_3FeS_4 + (2-x)CuSO_4 + (4-2x)FeSO_4 \quad (1.2.11)$$

X-ray diffraction analysis, electron microprobe analyses and reflectivity measurements proved conclusively that the solid phase formed after the first stage of leaching was Idaite. The discrepancy with previous work was explained by the fact that previous workers had only used X-ray diffraction analysis to identify this phase, and the X-ray diffraction pattern of idaite is almost identical to that of chalcopyrite. It is only by electron probe microanalysis and reflectivity measurements that a definite distinction can be made between the two minerals.

The dissolution mechanism and accompanying

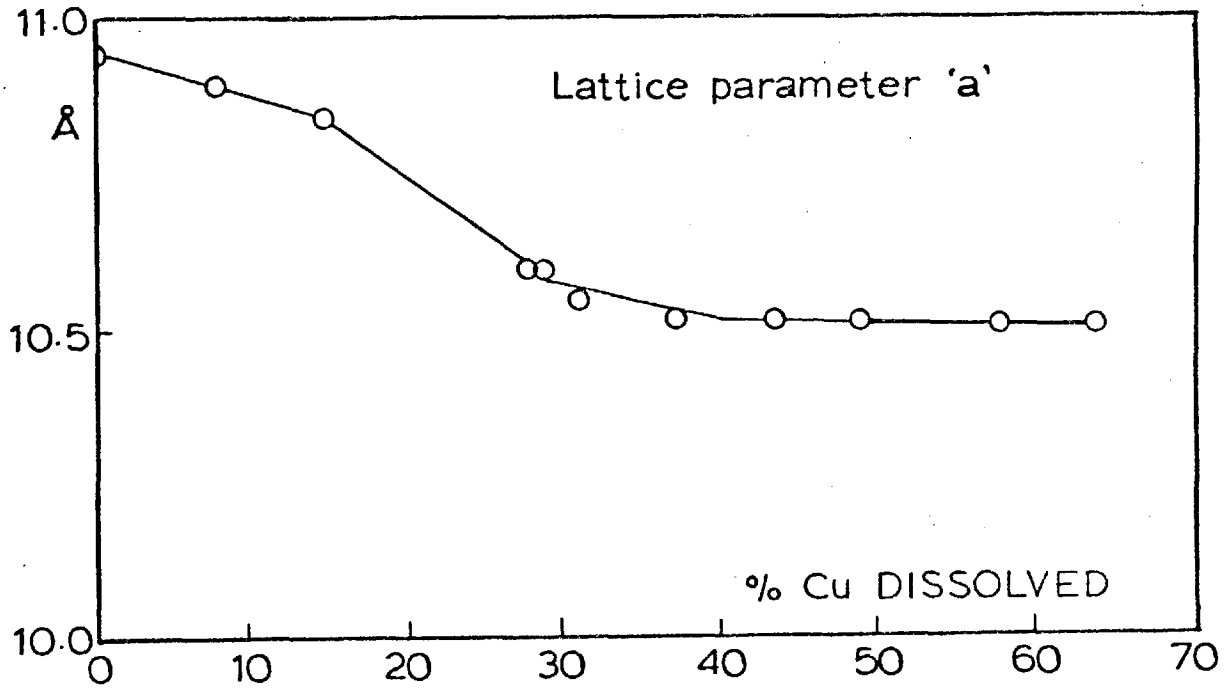


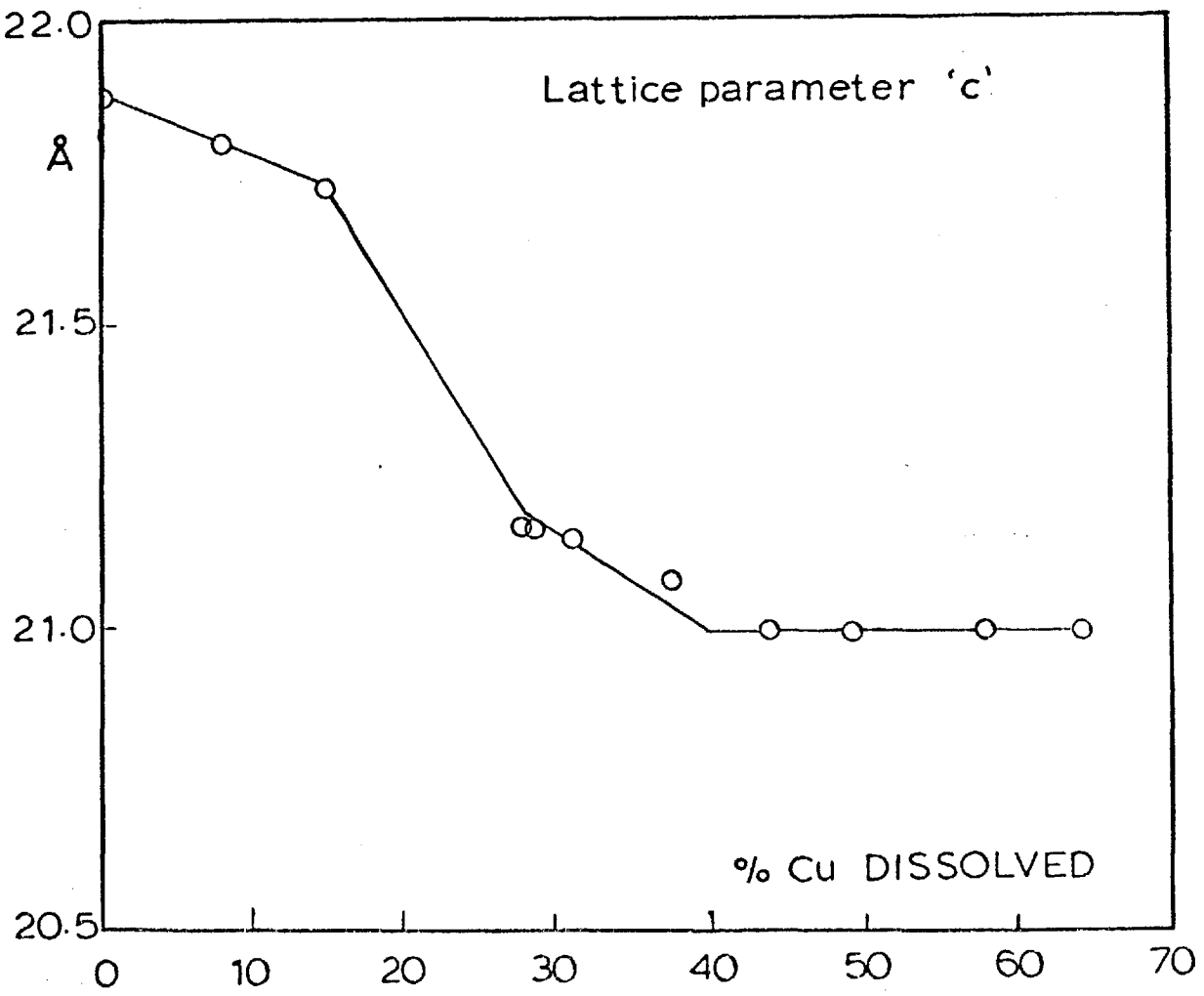


FIGURE 8 : Variation of lattice parameters of Bornite as copper is dissolved. Ugarte[11].

structural change can be explained from the crystal structure of bornite. Copper ions occur in two types of lattice position. Two - fifths of them lie in parallel planes and have been described as ionically bound. These are able to diffuse rapidly in the solid, and so can quickly be dissolved out, giving a continuous change in the lattice parameters due to the contraction of the bornite unit cell, (Figure 8) and leaving a material of composition $Cu_3FeS_4$. This does not change on leaching but breaks down by a chemical reaction to give elemental sulphur with copper and iron ions transferring to the solution.

Lowe[96] concluded that this solid stage transformation of bornite to idaite was only one of several processes controlling the reaction rate at various stages of dissolution of bornite. He conducted leaching experiments on mounted single specimens of copper and copper iron sulphide minerals using ferric sulphate solutions in an agitation cell having a nitrogen atmosphere. The rate equations obtained for each mineral were compared to theoretical equations determined for various rate - controlling processes.

This showed that the mechanism for ferric sulphate leaching of bornite was complex, the dissolution being controlled, at different stages, by ferric sulphate diffusion, step A below, a possible solid state diffusion of cuprous ions within the sulphide (as proposed by Ugarte), step B, and chemisorption reactions with the metal sulphide, step C :

(A) $\boxed{Fe_2(SO_4)_3}$ d=d $\xrightarrow{K_2}$ $\boxed{Fe(SO_4)_3}$ d=o (1.2.12)

(B) $Cu_5FeS_4 \rightleftharpoons Cu_3FeS_4^{2-} + 2\boxed{Cu^+}$ d=d

$\boxed{2Cu^+}$ d=d $\xrightarrow{K_2}$ $\boxed{2Cu^+}$ d=o

$Cu_3FeS_4^{2-} + \boxed{2Cu^+}$ d=o + $2Fe_2(SO_4)_3$

$\rightleftharpoons Cu_3FeS_4 + 2CuSO_4 + 4FeSO_4$ (1.2.13)

(C) MS + $\boxed{Fe_2(SO_4)_3}$ d=o $\rightleftharpoons$ $\boxed{MS...Fe_2(SO_4)_3}$ c

$\boxed{MS...Fe_2(SO_4)_3}$ c $\rightleftharpoons$ $\boxed{MS...Fe_2(SO_4)_3}^*$ c

$\boxed{MS...Fe_2(SO_4)_3}^*$ c $\xrightarrow{K_{2\,3}}$ $\boxed{MSO_4...S....2FeSO_4}$ c

$\boxed{MSO_4...S...2FeSO_4}$ c $\rightleftharpoons MSO_4 + S + 2FeSO_4$

(1.2.14)

Groves and Smith[97] have studied the reaction of bornite with chlorine in an aqueous system. Size fractions of bornite ( -100 + 325 mesh) were leached using a downward percolation method using sodium hypochlorite as the source of chlorine. The postulated reaction was:

$Cu_5FeS_4 + 18.5Cl_2 + 16H_2O \longrightarrow 5Cu^{2+} + Fe^{3+} + 4SO_4^{2-} + 32H^+ + 37Cl^-$ (1.2.17)

with a chlorine requirement of 3.70 moles/mole Cu. The leaching tests showed that the chlorine requirement approached the theoretical value as 100% copper extraction was approached.

However the leaching reactions were complex since the ratio of dissolved copper to iron after 1 hour was 9.04, compared to the expected 5.00 for the molecular formula of bornite ($Cu_5FeS_4$). Microscopic examination of piece of leached bornite revealed a surface coating of elemental sulphur and a zone of altered material from the surface inwards which was thought to be a form of nonstoichiometric copper-deficient bornite.

Recently Peters and Loewen[88] have leached copper minerals in perchloric acid solutions using moderate pressures of oxygen and have obtained a different solid state transformation product from Bornite. Bornite was leached in 1 M acid at 125°C and a pressure of 95 psig oxygen for 30 minutes and for 6 hours. X-ray diffraction patterns of the residues indicated that both chalcocite and covellite were present with no evidence of any residual bornite left after 30 minutes of leaching. Two transformation reactions were proposed:

$$Cu_5FeS_4 + 4H^+ + O_2 = 4CuS + Cu^{2+} + Fe^{2+} + 2H_2O \quad (1.2.18)$$

$$Cu_5FeS_4 + 2H^+ + \tfrac{1}{2}O_2 = Cu_2S + 3CuS + Fe^{2+} + H_2O \quad (1.2.19)$$

These results were thought to be consistent with the thermal behaviour of Bornite. When bornite is heated in the temperature range 80° to 150°C, digenite is rapidly formed but decomposes below 105°C to give chalcoite and covellite.

1.2.2. Leaching of Chalcopyrite, $CuFeS_2$:

Chalcopyrite is the most abdundant of the

copper-iron sulphides and also the most difficult to leach by conventional hydrometallurgical techniques. For these reasons a large body of work has been amassed over the years on the dissolution of chalcopyrite in many different solvents and on methods of improving its dissolution rate in these solvents.

The leaching studies can be placed in five main groupings:

(1) Bacterial leaching;
(2) Leaching at high pressures and temperatures, usually in the presence of oxygen, using either acidic or ammoniacal solutions;
(3) Leaching at atmospheric pressure using aqueous solutions of chlorine, ferric salts and cyanide salts, as well as nitric, sulphuric and hydrochloric acids;
(4) Leaching of the chalcopyrite after 'activation' of the ore or concentrate. The 'activation' usually involves an oxidative roast, or reaction at high temperature with copper, sulphur, hydrogen or iron, or thorough grinding. This produces an ore more amenable to conventional leaching agents;
(5) Electrochemical dissolution by the application of an electrical current to a cell in which one of the electrodes is made of chalcopyrite (usually the anode).

The various alternatives for the treatment

of chalcopyrite have been extensively reviewed by Ferreira[12], Dutrizac and Macdonald[18], Dasher[85], Roman and Benner[86], Wadsworth[87], Subramanian and Jennings[89], and Paynter[98]. Corrans et al[99], and Tuovinen[206] have discussed the practical and theoretical aspects of bacterial leaching and Kruesi et al[100] describe an electrochemical process for converting chalcopyrite concentrates to pure copper. However since the present work is concerned with the direct leaching of sulphide minerals in acidic solutions, only the studies that can be placed in group (3) will be discussed in the following survey.

Jackson and Stickland,[101] and Groves and Smith[97], have studied the dissolution of chalcopyrite in aqueous chlorine solutions. Jackson and Stickland found the reaction rate to be controlled by mass transport, the ore becoming coated with a layer of a sulphur - sulphur monochloride mixture. Groves and Smith used sodium hypochlorite as the source of chlorine and found the reaction to be:

$$CuFeS_2 + 8.5Cl_2 + 8H_2O \longrightarrow Cu^{2+} + Fe^{3+} + 2SO_4^{2-} + 16H^+ + 17Cl^- \quad (1.2.20)$$

The sulphate to copper ratios were less than the theoretical value of 2.0, varying from 0.92 to 1.88 due to the formation of elemental sulphur.

Klets and Liopo[102] leached a chalcopyrite sample with a ferric chloride solution and assumed the reactions taking place to be:

$$CuFeS_2 + 4FeCl_3 = CuCl_2 + 5FeCl_2 + 2S^o \quad (1.2.21)$$

$$8S + 6H_2O = H_2S_3O_6 + 5H_2S \quad (1.2.22)$$

$$CuCl_2 + H_2S = CuS + 2HCl \quad (1.2.23)$$

$$CuCl_2 + FeCl_2 + 2H_2S = (CuS.FeS) + 4HCl \quad (1.2.24)$$

More recently Haver and Wong[103] leached a chalcopyrite concentrate in a ferric chloride solution containing 212 g $Fe^{3+}$/litre and found that the optimum conditions for the reaction were a high temperature (106°C), and a fine grind (nearly 100% - 325 mesh) and a $FeCl_3/CuFeS_2$ weight ratio of 2.7. Most of the copper was in solution as $Cu^+$ indicating the reaction to be:

$$CuFeS_2 + 3FeCl_3 \longrightarrow CuCl + 4FeCl_2 + 2S^o \quad (1.2.25)$$

Ermilov et al[104] considered the reaction to be:

$$CuFeS_2 + 4FeCl_3 = CuCl_2 + 5FeCl_2 + 2S \quad (1.2.26)$$

The rate was first order with respect to the $FeCl_3$ concentration and the parobolic reaction rate was thought to be due the progressive thickening of the sulphur layer on the particles surface.

Ferric chloride is known to be a better oxidising agent for copper sulphides than ferric sulphate. Uchida et al[92] found that copper in chalcopyrite was hardly extracted by leaching with dilute ferric sulphate solutions. In comparable experiments with a leaching solution of 0.01N sulphuric acid and 0.4M $Fe^{3+}$, 40% of the copper from bornite

was leached out in two weeks compared with only 4 - 5% of the copper from chalcopyrite.

In 1969, Dutrizac et al[105] conducted a thorough study into the kinetics of dissolution of synthetic chalcopyrite in acidic ferric sulphate solutions using rotating discs of the mineral. The stoichiometry of the reaction was determined as

$$CuFeS_2 + 2Fe_2(SO_4)_3 = CuSO_4 + 5FeSO_4 + 2S^o \quad (1.2.27)$$

In a solution containing 0.11 M $Fe^{3+}$ and 0.1M $H_2SO_4$ at 70°C, both the synthetic chalcopyrite and a natural chalcopyrite gave a linear relationship between the dissolved copper and the square root of time, indicating that the dissolution kinetics were parabolic (Fig.9(a)). The difference in magnitude of the leaching rates was thought to be due to the larger true area of the synthetic material and the presence of impurities in the natural chalcopyrite.

An increase in temperature in the range 50 to 94°C resulted in a faster dissolution rate with parabolic kinetics being observed over the whole temperature range. The insensitivity of the rate to the acid concentration and the speed of rotation of the disc, together with a calculated activation energy of 17±3 kcal/mole, led the authors to postulate that the rate was controlled by a diffusion process.

The dependence of the leaching rate on the ferric ion concentration below 0.01 molar (Fig. 9(b)) led to the conclusion that below 0.01M $Fe^{3+}$ the rate controlling step was the

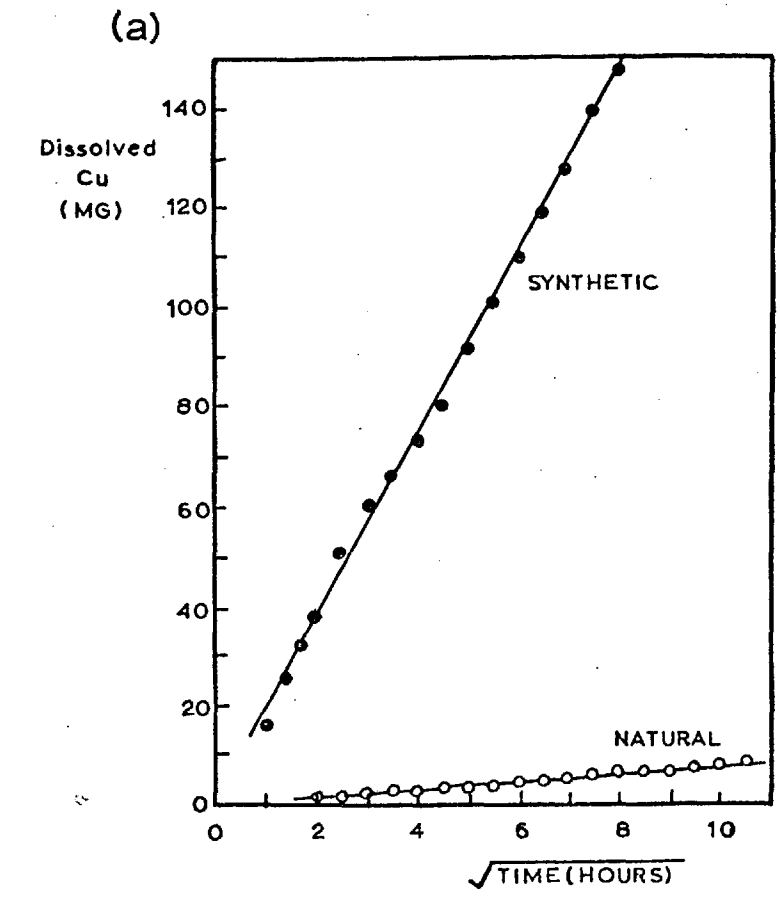


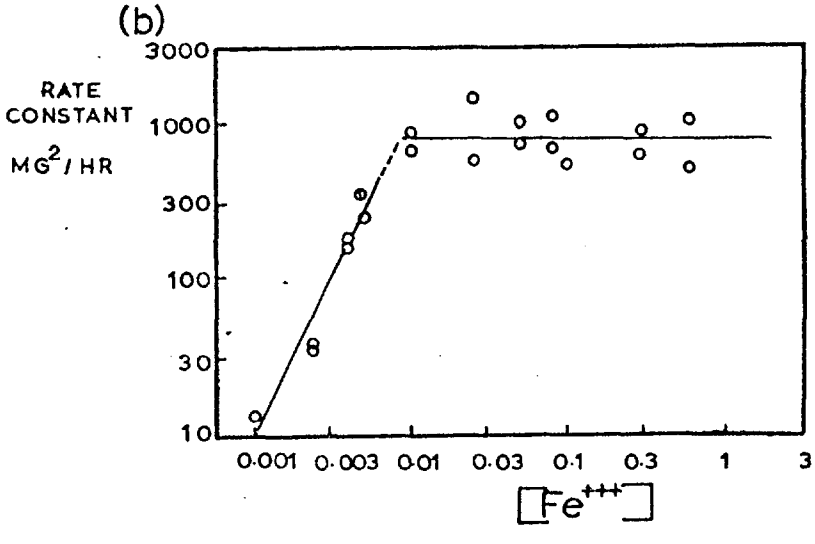


FIGURE 9(a)Dissolution of synthetic and natural Chalcopyrite discs at 70°C and 250 rpm in 0.11M $Fe^{3+}$ and 0.1M $H_2SO_4$ solution. Dutrizac et al[105].

(b)Effect of Ferric ion concentration on the rate of copper leaching from synthetic Chalcopyrite at 80°C, 250 rpm, in 0.1M $H_2SO_4$ solutions. Dutrizac et al[105].

inward diffusion of $Fe^{3+}$ through a layer of sulphur. Experiments using variable amounts of ferrous sulphate in the solutions suggested that above 0.01M$Fe^{3+}$ the rate controlling step is the outward diffusion of ferrous ion through the sulphur layer.

Lowe[96] leached ground and sized samples of chalcopyrite with ferric sulphate solutions in a continuous flow reaction cell under a nitrogen atmosphere. The stoichiometry of the reaction was as in equation (1.2.27). From the rate equations the dominant dissolution mechanism was suggested to be surface-reaction controlled chemisorption (as in mechanism C, equation 1.2.14).

Ferreira[12] synthesised two forms of chalcopyrite, a cubic β-form of composition $CuFeS_{1.83}$, and an α form, apparently tetragonal, with a composition of $Cu_{1.12}Fe_{1.09}S_2$, having about 10.7% excess Cu and 8.3% excess iron over the stoichiometric $CuFeS_2$. Crushed samples of these materials were leached in acidic ferric sulphate solutions, hydrogen peroxide and hydrochloric acid.

In acidic ferric sulphate solutions, the dissolution of β-chalcopyrite was significantly affected by temperature (Fig. 10(a)). The leaching reaction was characterised by three stages. The first stage of the reaction, in which about 17.5% of the copper and a small amount of iron was removed, was sensitive to temperature and very inaccurate approximations gave $7 \pm 3$ kcal.mole$^{-1}$ for the apparent

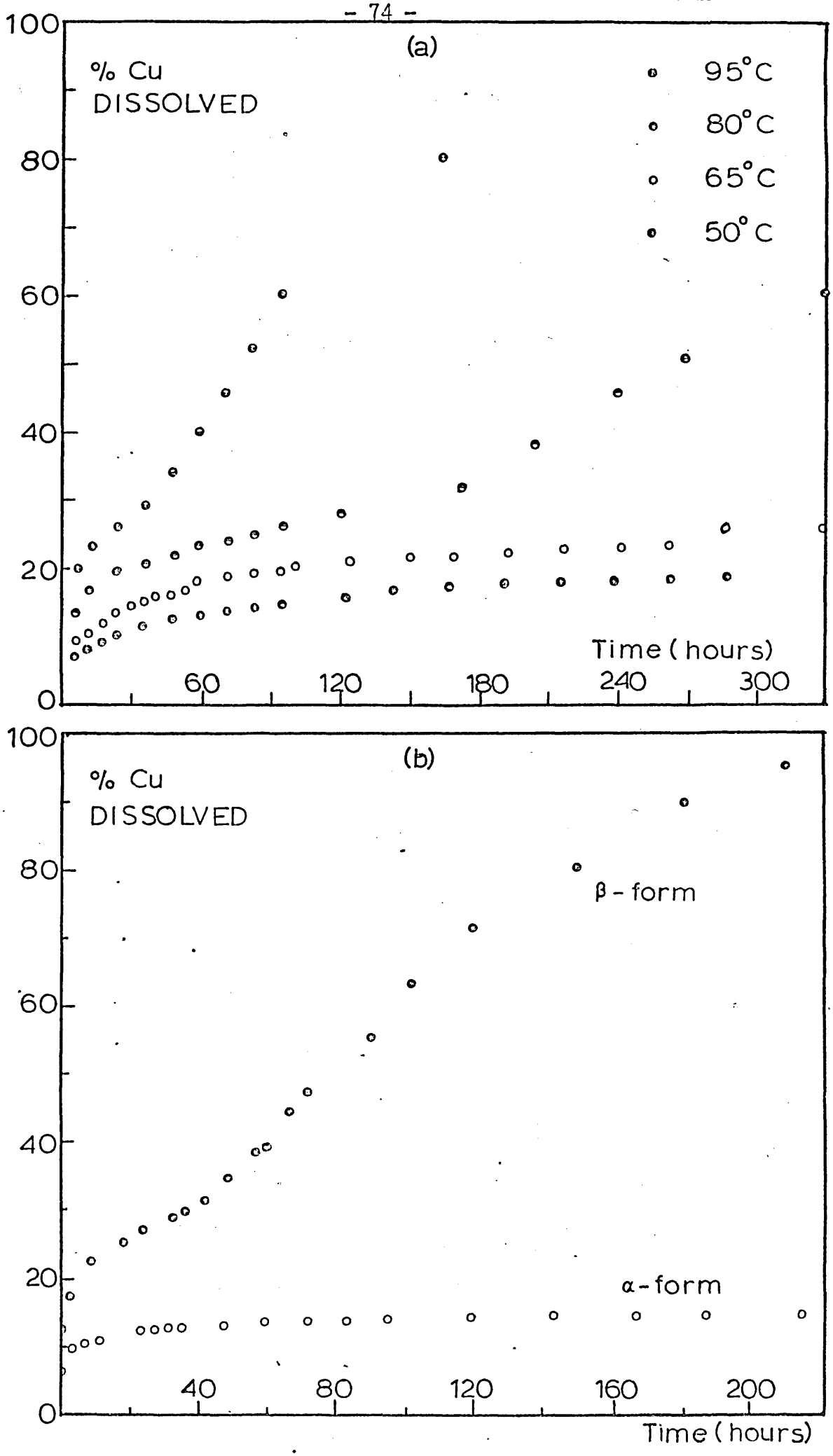


FIGURE 10 : (a) Effect of Temperature on the rate of leaching of β - Chalcopyrite, (b) Comparison of the leaching rate of a stable sample of α-chalcopyrite with a sample of β-chalcopyrite. Ferreira (12).

activation energy. The rate of copper dissolution was increased by a reduction in particle size but was unaffected by increasing the ferric ion concentration from 0.01 to 0.03 M The amount of copper dissolved was proportional to the initial weight and the final metal to sulphur ratio in the solid residue was 2 : 2 compared with the initial 2 : 1.83.

The rate of the reaction seemed to be controlled mainly by the diffusion of copper atoms to the solid-liquid interface with a resultant contraction in the unit cell, shown by the variation in the d-spacings of the solid residues as the copper was removed (Fig. 11).

Rate curves for the second stage of the reaction (20% to 30 - 35%) approached linearity. The Arrhenius plot for the activation energy gave two distinct lines which indicated that a homogeneous reaction was favoured at high temperatures (above 65°C) and a heterogeneous reaction at low temperatures, the respective values for the activation energies being 20 kcal/mole and 1.5 kcal/mole.

Figure 11 shows that an abrupt collapse of the β-structure occurred in this stage with the d-spacings becoming much smaller than was found for later samples. 'Recovery' was not complete until 31.5% of the copper was removed and at this point the solid had d-spacings corresponding very closely to those of α-chalcopyrite, and had a composition of $CuFe_{1.2}S_{2.3}$

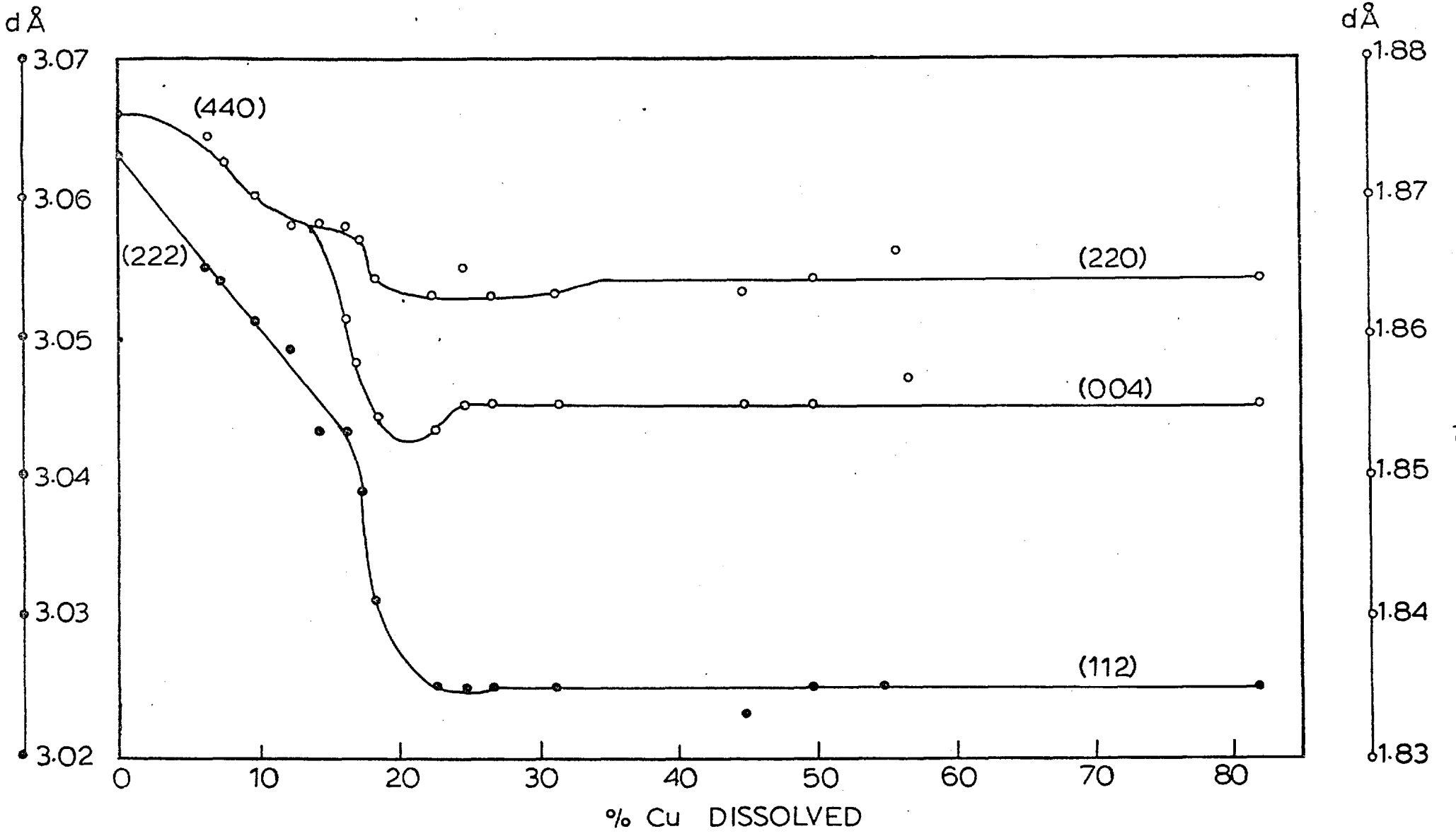


FIGURE 11 : Variation of the d-spacings with percentage of copper removed from β- chalcopyrite. Ferriera[12].

The third stage (>35% copper removed) was the chemical reaction of $CuFe_{1.2}S_{2.3}$ to produce elemental sulphur, which coated the residue, reducing the rate of reaction which was linear until about 60% of the copper was removed. The residues with above 35% of the copper removed showed no appreciable variation of the d-spacing values. No rate curves were determined below 80°C since the reaction proceeded very slowly.

From these results Ferreira devised a mechanism for the dissolution in terms of charge balance by considering the oxidation states for the elements in $CuFeS_{1.83}$ to be:

$Cu^{+}\ Fe^{2+}_{0.34}\ Fe^{3+}_{0.66}\ S^{2-}_{1.83}$ i.e., 34% of the iron is in the form, $Fe^{2+}$.

In the first and second stage of leaching about 34% of the copper was removed, and Ferreira considered that an electron transfer occurs within the solid, to keep charge neutrality, in the form of the ferrous iron being oxidized to ferric iron. Since 19% of the iron and 15% of the sulphur was also removed, this led to a final theoretical composition for the solid at the end of the second stage of leaching of $Cu^{+}\ Fe^{3+}_{1.227}\ S^{2-}_{2.3405}$.

This agreed well with the composition $CuFe_{1.2}S_{2.3}$ found by analysis of the solid residues.

Hence Ferreira expressed the two initial stages of β-chalcopyrite leaching by the

equation:

$$2.30\ CuFeS_{1.83} + 0.574Fe_2(SO_4)_3 = 0.47\ CuSO_4 + 1.252FeSO_4 + 1.83CuFe_{1.2}S_{2.3} \quad (1.2.28)$$

and the third stage by:

$$CuFe_{1.2}S_{2.3} + 2.2Fe_2(SO_4)_3 = CuSO_4 + 5.6FeSO_4 + 2.3S^o \quad (1.2.29)$$

The leaching experiments on the α-chalcopyrite ($Cu_{1.12}Fe_{1.09}S_2$) with acidic ferric sulphate solutions showed that the rate of copper removal was slower than that of β-chalcopyrite under identical conditions (Fig. 10 (b)). The storage time of the α-chalcopyrite affected the leaching rate apparently due to the diffusion of the excess copper over the stoichiometric (10.7%) to the surface of the synthetic material.

A leaching experiment conducted after 14 months of storage showed that 11 - 12% of the copper was easily removed and subsequently the behaviour of the near to stoichiometric solid was very similar to natural chalcopyrite, dissolving by the reaction:

$$CuFeS_2 + 2Fe_2(SO_4)_3 = CuSO_4 + 5FeSO_4 + 2S \quad (1.2.27)$$

with no change in composition or lattice parameters.

Increasing the ferric ion from 0.01M to 0.1M did not affect the initial removal of the

excess copper, thus supporting the diffusion mechanism. Firm conclusions could not be drawn for the subsequent reaction because of the greater hydrolysis of the iron at the higher concentration.

Ferreira noted that although the residues of β-chalcopyrite after 30 - 35% of copper dissolution had a structure very similar to the α-form, the leaching rates in $Fe^{3+}$ were quite different, the residues from β-chalcopyrite leaching much faster. This led Ferreira to conclude that the relative proportions of the elements in the lattice structure seem to play a more important role than the structure itself.

On leaching the α-chalcopyrite with $10^{-1}$N hydrochloric acid at 80°C, Ferreira found the rate of copper dissolution to be much faster than when using acidic ferric sulphate solutions at 95°C. This was thought to be due to the formation of the $CuCl_2^-$ complex. The effect of chloride ion on the dissolution rate was shown by adding 0.1 mole of NaCl to the ferric sulphate leaching run. Figure 12 shows the immediate increase in the dissolution rate.

Dutrizac et al[106], using acid solutions containing 0.1M $Fe^{3+}$ and 6 gm/litre NaCl at 80°C on rotating discs of synthetic and natural chalcopyrites, found the presence of NaCl increased the copper extractions by factors ranging from 1.6 to over ten times. However in column leaching studies the same authors

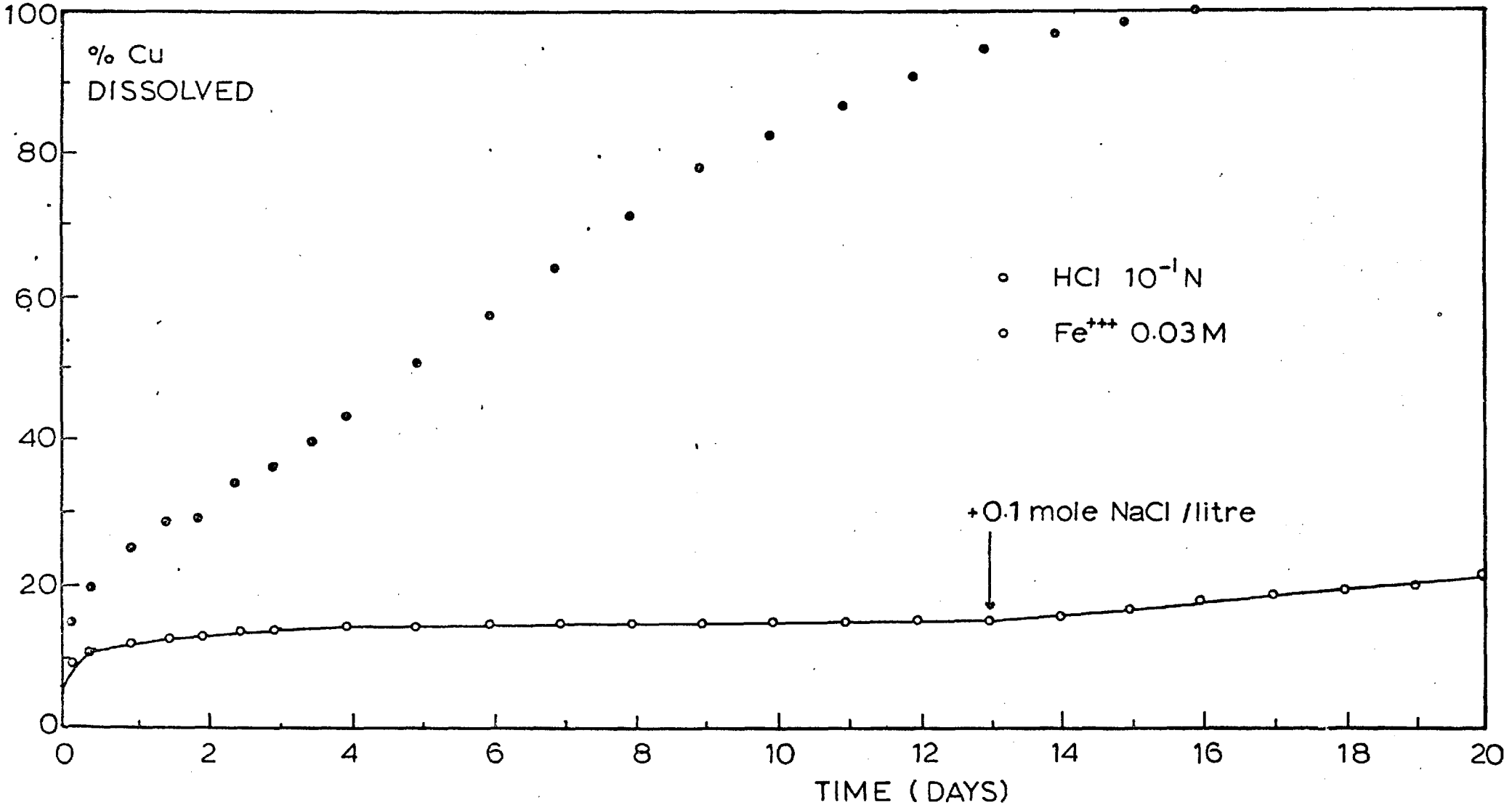


FIGURE 12 : Effect of chloride ion on the rate of leaching of α-chalcopyrite. Ferreira[12].

found that the NaCl accelerated the dissolution only at temperatures above 50°C, and had an inhibiting effect at lower temperatures.

Munoz-Ribadeneira and Gomberg[107] have considered the use of a sodium chloride-sulphuric acid leach solution, in conjunction with fracturing an underground ore body by nuclear explosives and recovering the copper by 'in situ' leaching. The data indicated an appreciable dissolution of the copper in a reasonable leaching time. The dissolution rate was found to be first order with respect to the copper concentration and proportional to the one third power of the chloride ion concentration in the range 0.05N to 1N.

Baur, Gibbs and Wadsworth[108] studied the leaching kinetics of the initial stage of chalcopyrite dissolution in sulphuric acid solutions using radiochemical techniques. The amount of copper dissolved increased with increasing strength of the sulphuric acid solution in the pH ranges 4.60 to 0.28. The rate curves showed an initial period of fast dissolution lasting a few minutes, then a 'plateau' region lasting up to ten minutes and thirdly a second period of lesser rate than the first.

The rate of the initial copper extraction followed first order kinetics, and the rate of the third stage was also approximately linear at room temperature. Both rates were essentially independent of pH between 1 and 2.5.

The removal of oxide layers could account for the first order kinetics of the initial dissolution stage, if the layers are thin. However Baur et al found that iron was dissolved at a much faster rate than copper, which led them to suggest that the first order kinetics could be explained by the saturation of the lattice with vacancies due to the formation of iron depleted surface layers by the overall reaction:

$$4Fe^{3+}\ (\text{lattice}) + CuFeS_2 \longrightarrow 4\ Fe^{3+}_{\square}\ (\text{vacancy}) + 12\ \oplus\ (+\text{ve electron hole}) + 5Fe^{2+} + Cu^{2+} + 2S^{\circ} \qquad (1.2.30)$$

At room temperature a relatively large increase in the amount of copper dissolved for a small initial increase in the amount of oxidant added was characteristic of this type of oxidation when the oxidant was ferric ion or dichromate ion. Hexavalent chromium additions in the range 0 to 0.0103 moles $Cr^{6+}$ produced a more striking effect than did ferric ion in the range 0 to 0.69 molar. Addition of hydrogen peroxide also produced a dramatic increase in the amount of copper dissolved but gaseous oxygen additions at room temperature did not produce any measurable increase in the range 0-0.84 atmospheres partial pressure of $O_2$.

Figure 13(a) shows the results obtained with oxygen at various temperatures at a pH of 1.25. The rate of the initial dissolution process increased with temperature giving an experimental activation energy of approximately

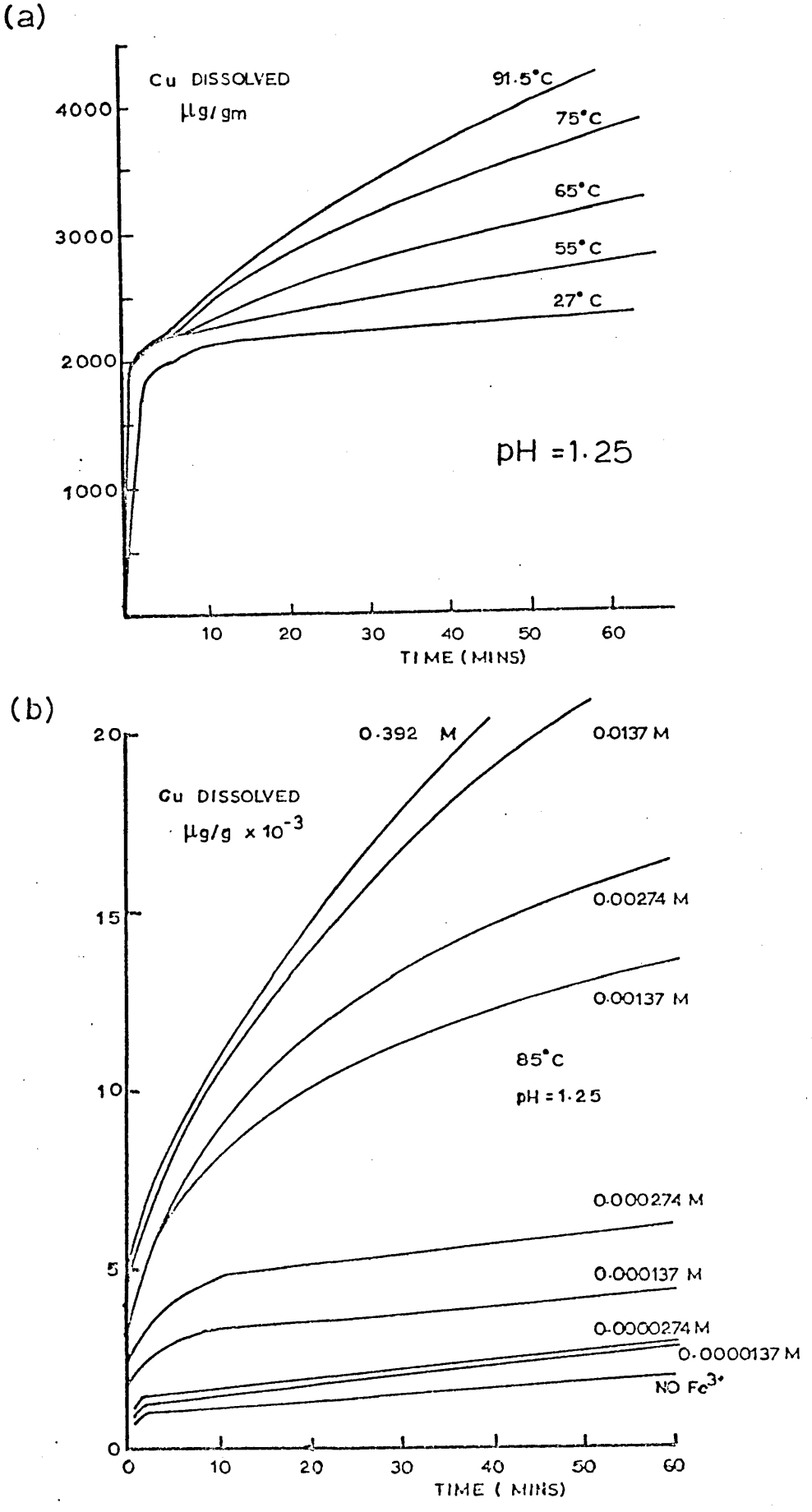


FIGURE 13 : (a) Effect of Temperature on dissolution of 10µm Chalcopyrite. Oxygen purged. Baur et al[108].

(b) Effect of ferric sulphate concentration on rate of dissolution of $CuFeS_2$ at 85°C and pH 1.25. Baur et al[108].

4.8 kcal/mole. The second rate process, beyond the plateau value is clearly not linear and the rate was found to increase with increasing oxygen partial pressure. Baur suggested that this process followed mixed surface plus transport kinetics, a combination of diffusion of oxygen through a deposited sulphur film and a surface reaction at the chalcopyrite-sulphur interface:

$$O_2 + 4H^+ + 4e^- = 2H_2O \qquad (1.2.31)$$

The activation energies were 12.5 kcal/mole for the linear process and 10.2 kcal/mole for the diffusion process. The effect on the leaching rate of additions of ferric sulphate to the sulphuric acid solution at 85°C and pH1.25 are shown in Figure 13 (b). The results for 0.392M ferric sulphate fitted a parabolic equation but lower concentrations fell off at longer periods of time due to depletion of ferric sulphate in the solution.

The authors concluded that the rate of dissolution was dependent on the diffusion of ferric ion through a deposited sulphur film, resulting from the anodic dissolution of chalcopyrite according to the reaction

$$CuFeS_2 \rightleftharpoons Cu^{2+} + Fe^{2+} + 2S^o + 4e^- \qquad (1.2.32)$$

With consumption of ferric ion by the balancing cathodic reaction:

$$4Fe^{3+} + 4e^- = 4Fe^{2+} \qquad (1.2.33)$$

The parabolic rate constant for this process increased with $Fe^{3+}$ concentration at low concentrations and then levelled off above 0.01 molar due to the formation of strong sulphate complexes of the form $FeSO_4^+$ and $Fe(SO_4)_2^-$. The activation energy for the ferric ion diffusion was about 20 kcal/mole in fair agreement with the value of 17 kcal/mole obtained by Dutrizac et al.

From the results of this study it appears that transport through a layer of sulphur (and possibly basic iron sulphate) is rate controlling and not charge transfer processes in the surface reaction. This was confirmed by Baur et al who measured the potential of a piece of chalcopyrite against a standard calomel electrode as the chalcopyrite dissolved and showed that the electrode potential changed markedly during the dissolution, but did not seem to effect the leaching rate.

Recently Prater et al[109], and Habashi[110], have used nitric acid as a leachant for chalcopyrite. Prater et al investigated the most effective conditions for the dissolution of a chalcopyrite concentrate with the conversion of sulphur to the elemental form and the precipitation of iron as hydrogen jarosite. Their reaction may be summarised:

$$6CuFeS_2 + 10HNO_3 + 10H_2SO_4 = 6\,CuSO_4 + 10NO + 12S^o + 3Fe_2O_3.4SO_3.9H_2O + 6H_2O \quad (1.2.34)$$

Increased temperature, addition of $H_2SO_4$ and higher nitric acid concentrations increased markedly the rate of copper extraction but decreased the elemental sulphur yield due to oxidation to the sulphate form.

Jarosite precipitation was optimized by a high pH, high temperature, high percent solids and reasonably high sulphate concentrations. Initially the pH rose due to the reaction:

$$6CuFeS_2 + 22HNO_3 + 9H_2SO_4 = 6CuSO_4 + 3Fe_2(SO_4)_3 + 22NO + 6S^o + 20H_2O \quad (1.2.35)$$

This rise is halted briefly by the hydrolysis of iron:

$$6Fe^{3+} + 4SO_4^{2-} + 14H_2O = 3Fe_2O_3 .4SO_3 .9H_2O + 10H^+ \quad (1.2.36)$$

Excessively high $HNO_3$ concentrations increased the reagent consumption due to the production of $NO_2$ gas instead of NO, and increased $S^o$ oxidation. Decreasing the concentration from 50 to 20% cut $HNO_3$ consumption in half while doubling the yield of $S^o$.

Habashi represented the dissolution of chalcopyrite by nitric acid by the equation:

$$3CuFeS_2 + 20HNO_3 = 3Cu(NO_3)_2 + 3Fe(NO_3)_3 + 10H_2O + 6S^o + 5NO \quad (1.2.37)$$

with oxidation of the elemental sulphur to sulphate:

$$2HNO_3 + S \longrightarrow H_2SO_4 + 2NO \quad (1.2.38)$$

Copper recovery increased with increasing time, acid concentration and temperature. With dilute acid (7.5% $HNO_3$) the elemental sulphur recovery increased with increasing time and temperature up to 100°C, but with more concentrated acid (60% $HNO_3$) the amount of sulphur initially formed decreased with increasing time and temperature. Even under the most favourable conditions, however, the recovery of elemental sulphur did not exceed 50%.

The dissolution of iron followed that of copper although 80 - 95% could be precipitated as an oxide by leaching under pressure at 110°C, or leaching at ambient pressure with sufficient acid for the reaction to occur as follows:

$$6CuFeS_2 + 22HNO_3 = 6Cu(NO_3)_2 + 3Fe_2O_3 + 12S^o + 10NO + 11H_2O. \quad (1.2.39)$$

## 1.3. Effect of the Presence of Impurities on the Leaching of Sulphides.

It is obvious that many physical and mineralogical factors will play an important part in the leaching behaviour of a particular mineral. Among the factors that Prosser[8] considered may have an effect on the chemical reactions of minerals were crystal structure, texture, surface orientation, polycrystallinity, porosity, inclusions, dislocations, impurities, and non-stoichiometry. Other authors have shown the important effects of point defects[111], cold work and alloying additions[112], non-stoichiometry[113], impurity ions[114] and light intensity[115] on the dissolution of minerals either due to catalytic activity or a change in the solid-state electronic properties of the semiconductor minerals. Gerlach et al[116] have demonstrated that there is a direct connection between the leaching behaviour of a mineral and the atom spacings in the solid matter lattice, while Warren and Roach[117] have explained the 'accelerated' type of leaching often found with goethite and hematite as due to the anisotropic dissolution of the minerals, the basal, or near basal, plane having been shown to be the most rapidly leached.

Despite the fact that the presence of impurities may have a marked influence on the dissolution of a particular mineral, most leaching studies have used either concentrates or samples containing various amounts of other minerals. To gain a better understanding of the dissolution mechanisms operative during leaching, pure, synthetic, minerals have often been used (section 1.2).

It is only recently that attempts have been made to study the effects produced by the presence of other minerals on the leaching behaviour of certain minerals, and to what extent electrochemical (galvanic) mechanisms can explain the observations.[13]

It was first suggested in 1830 by Fox[118] that certain ores might act like metals in galvanic combinations. Skey[119] first called attention to the accelerating or retarding effect of one sulphide mineral on another in chemical changes, when the two are in contact. Gottschalk and Buehler[120] experimentally demonstrated that the rate of oxidation of sulphides increased when dissimilar ones were mixed, showing similar cathodic-anodic relationships

as in the corrosion of metals. Finding a close relationship between the electrode potentials and the relative rates of oxidation of sulphide minerals, they arranged the minerals according to their measured electrode potentials in a series analgous to the electrochemical series of metals, thus providing a link between the electrode potentials and the oxidation reactions of sulphide minerals.

A feature of this and subsequent series (reviewed by Wright[13]) is the noble behaviour of pyrite ($FeS_2$). Gottshalk and Buehler[120] noted that the presence of pyrite accelerated the dissolution of both galena and sphalerite provided that the sulphides were in electrical contact, while, more recently, Majima[121] has shown that its presence also accelerates the dissolution of chalcopyrite in aerated $H_2SO_4$ solutions at room temperature. This is of importance in hydrometallurgical processes since pyrite is a very common gangue material in most ores.

A galvanic (or electrochemical) mechanism requires that the different sulphides be in good electrical contact. This condition is

only partially satisfied when diluted slurried ores are used since the particles touch at just a few contact points which must be frequently broken by the agitation of the medium. Dutrizac et al[122] mixed pure synthetic bornite and chalcopyrite with predetermined amounts of a second sulphide phase and pressed the mixes into pellets to ensure good contact between the grains. The pellets were formed into sintered discs and leached by rotating the discs at 200 rpm in acidified ferric sulphate solutions containing 0.1M $Fe^{3+}$ and 0.1M $H_2SO_4$ at 70°C and 15°C.

It was shown that addition of relatively large amounts of $Cu_{1.8}S$ or $FeS_2$ (up to 10% for the $Cu_{1.8}S$ and 25% for $FeS_2$) had no significant effect on the rate of copper extraction from the bornite at 70°C, but chalcopyrite additions of up to 25% decreased the rate slightly. (Fig 14(a)). This was thought to be in accordance with control of bornite dissolution by mass transport across a liquid boundary layer adjacent to the disc. Addition of inert material would reduce the active disc area and thus decrease the dissolution rate slightly. $CuFeS_2$ can be considered inert since it dissolves so

(a)

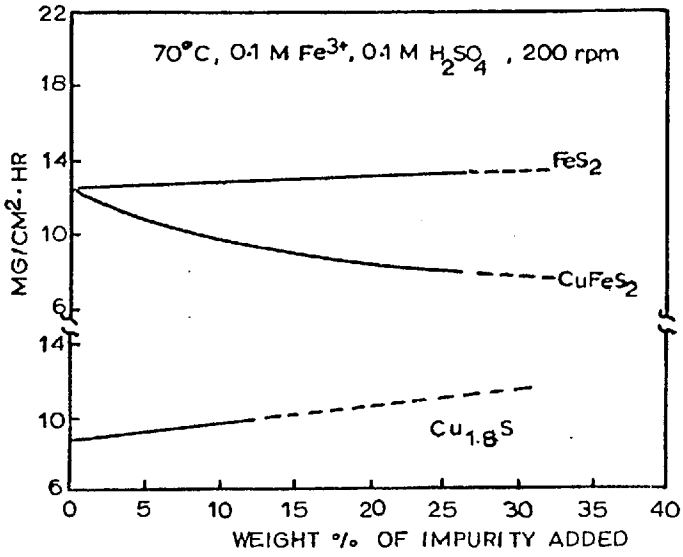


(b)

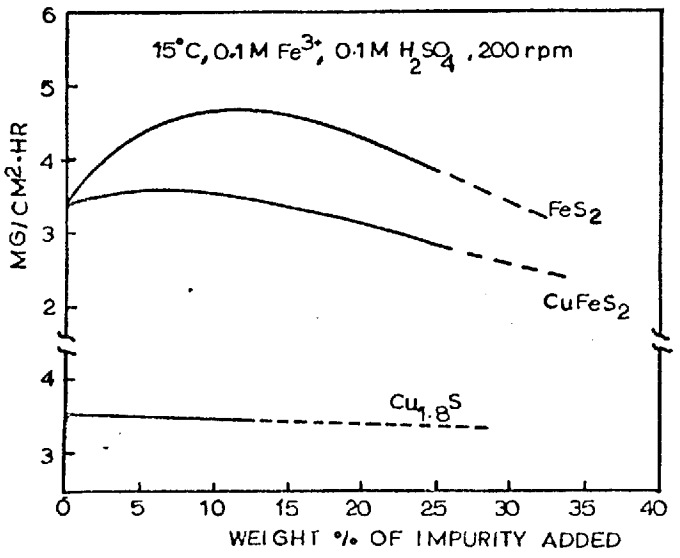


FIGURE 14 : The effect of $FeS_2$ , $CuFeS_2$ , and $Cu_{1.8}S$ additions on the bornite dissolution rate at (a) 70°C, (b) 15°C. Dutrizac et al[122].

slowly and the $FeS_2$ is inert with respect to copper dissolution, while $Cu_{1.8}S$ dissolves as rapidly as $Cu_5FeS_4$ and obviously is not inert.

At 15°C, none of the impurities, $Cu_{1.8}S$, $CuFeS_2$ and $FeS_2$, had a major effect on the dissolution rate (Fig. 14(b)). For volume percentages of up to 25%, the $Cu_{1.8}S$ and $CuFeS_2$ had almost no effect, while $FeS_2$ appeared to increase the rate of copper extraction. This accelerating effect was thought to be due to the pyrite assisting the mass transfer of the reagents to the bornite surface, although the fact that the rest potential of pyrite is positive with respect to bornite suggests that pyrite would also encourage the bornite dissolution if the rate were controlled by a galvanic process.

Dutrizac et al[123] have also considered the effects of bornite, cubanite, galena, molybdenite, sphalerite, stibnite and barite on the dissolution rate of chalcopyrite using the same experimental techniques as above. The leaching tests were carried out in 0.1M-$Fe^{3+}$, 0.1M$H_2SO_4$ solutions at 80°C at a disc speed of 200 rpm. Preliminary experiments

showed that none of the added sulphides exerted a significant effect on the rate of $CuFeS_2$ dissolution when not in contact with it.

In separate slurry leaching experiments using a ground chalcopyrite ore, it was also determined that the presence of 50 mg/l of any one of Se, Te, As, Sb, Bi or Mo in the initial leaching solution had no significant effect on the dissolution of the chalcopyrite.

Experiments using various amounts of barite (natural $BaSO_4$) were undertaken to show the effect of an inert filler on the dissolution rate of a chalcopyrite disc. The addition of barite caused the $CuFeS_2$ dissolution rate to decrease slightly, this decrease being simply explained by the reduction of the area of $CuFeS_2$ available for leaching. Figure 15 shows the effect of the inert filler as well as the effect of the presence of other sulphide impurities.

Bornite in contact with the chalcopyrite produced a substantial increase in the total amount of dissolved copper but the presence of cubanite ($CuFe_2S_3$) had little net effect

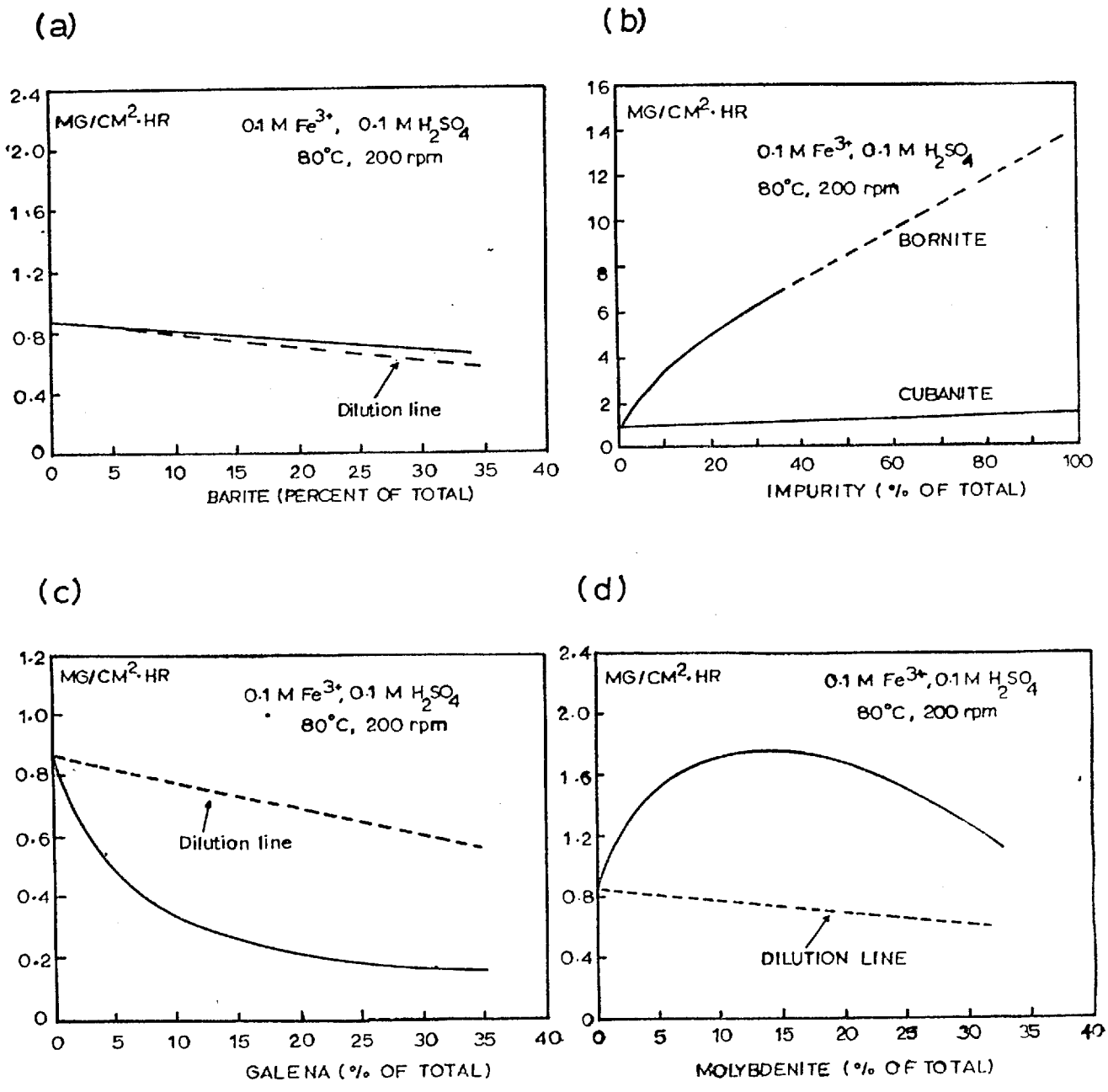


FIGURE 15 : Effect of impurity additions on the rate of chalcopyrite dissolution : (a) Barite,

(b) Bornite and Cabanite,

(c) Galena,

(d) Molybdenite. Dutrizac et al[123].

(Fig 15(b)). The chalcopyrite-bornite mixtures appeared to dissolve slightly more rapidly than the weighted sum of the dissolution rates of the pure sulphides while the chalcopyrite - cubanite mixtures behaved almost additively.

Sulphides other than those of copper exhibited both accelerating and inhibiting effects on the rate of dissolution of chalcopyrite. The presence of pyrite accelerated the dissolution by a factor of three. These observations were explained by a galvanic mechanism by assuming that the surface of the pyrite is kinetically favourable for the reduction of ferric ion to the ferrous state:

$$4Fe^{3+} + 4e^{-} = 4Fe^{2+} \qquad (1.3.1)$$

with the reaction at the chalcopyrite as follows:

$$CuFeS_2 \longrightarrow Cu^{2+} + Fe^{2+} + S^{o} + 4e^{-} \qquad (1.3.2)$$

The flow of electrons is completed through the sulphides. All compositions studied contained discrete grains of pyrite and clearly there is the good electrical contact between the phases necessary for a galvanic corrosion mechanism.

The effect of galena (PbS) was also consistent with a galvanic mechanism (Fig 15(c)). The potentials of galena and chalcopyrite indicate that the chalcopyrite should be cathodically protected and the galena anodically dissolved. This was borne out by the pellet containing 25% galena dissolving only about $^1/_3$ as rapidly as would be expected if the galena were just an inert impurity, and by the observation that the galena grains were heavily coated with lead sulphate which is formed during the dissolution of lead in sulphate solutions.

The results obtained for $ZnS$-$CuFeS_2$ were erratic and depended on the iron contant of the sphalerite. The presence of high iron sphalerite slightly retarded the chalcopyrite dissolution rate but small amounts (10%) of low - iron sphalerite have a slight beneficial effect on the dissolution rate. These results seemed to be generally consistent with a galvanic mechanism for dissolution if one took into account the change in potential of the sphalerite with change in iron content.

Whenstibnite ($Sb_2S_3$) and chalcopyrite

were sintered the sulphides reacted to form pyrite and tetrahedrite ($Cu_{12}Sb_4S_{13}$). The increased dissolution was explained by the presence of the noble sulphide, pyrite, and the fact that tetrahedrite appeared to dissolve more rapidly than chalcopyrite. Finally, the results obtained with molybdenite were unexpected (Fig. 15(d)). According to the potentials the molybdenite should have greatly suppressed the chalcopyrite dissolution rate. In fact, the rate increased. In the presence of 10%$MoS_2$, the rate was about twice that which would be expected if the molybdenite were just an inert filler. It was concluded that either the molybdenite - chalcopyrite mixtures do not follow the galvanic mechanism during dissolution or that the reported rest potential for molybdenite is in error.

Other work on the leaching of sulphides with solid additives, both sulphidic and non-sulphidic, has been reported in Japan. Kunieda et al[124] have studied the hydrometallurgical oxidation of ZnS in aqueous solutions of $H_2SO_4$ in the presence of CuS, $PbO_2$. The main dissolution reaction of ZnS in the acid solution was a type of $H_2S$ evolution. The dissolution was

accelerated and elemental sulphur produced when CuS, $PbO_2$ or graphite was added to the ZnS. As these additives have a higher potential than ZnS, the following galvanic reaction was thought to be wholly or partly incorporated in the dissolution of the zinc sulphide:

The anodic reaction

$$ZnS = Zn^{2+} + S^{o} + 2e. \qquad (1.3.3.)$$

and the cathodic reaction

$$2H^{+} + \tfrac{1}{2}O_2 + 2e = H_2O \qquad (1.3.4)$$

Iwai [125] studied the interaction of sulphide particles of ZnS and PbS suspended in dilute $H_2SO_4$ solutions. The experiments were carried out at 25 - 70°C, pH 0.5-2, 0.2-0.5M sulphide, air pressure of 1 - 2 l/min and an agitation speed of 600 rpm. The main dissolution reaction of both the ZnS and PbS was $H_2S$ formation. However for ZnS and PbS suspensions the reaction occurred in two stages : in the early stages of dissolution the ZnS dissolves and the acid dissolution of the coexisting PbS is repressed. After some time the dissolution of ZnS is repressed and the dissolution of PbS begins. The repression of the ZnS dissolution was explained by

the formation of sulphur layers on the ZnS particle surface.

In their work on the initial-stage sulphuric acid leaching kinetics of chalcopyrite which has already been described (see section 1.2.2), Baur et al[108] considered the effect of metallic additions on the dissolution mechanisms of chalcopyrite and the importance of cathodic reactions of sulphide minerals. Half-gram samples of three finely divided metal powders (silver, copper and iron), were added to $\frac{1}{2}$ gram samples of chalcopyrite in the usual experimental procedure. The results obtained were explained in terms of the standard electrode potentials of the metals.

$$Ag^{+} + e^{-} = Ag^{o} \qquad E^{o} = 0.799V$$
$$Cu^{2+} + 2e = Cu^{o} \qquad E^{o} = 0.340V$$
$$Fe^{2+} + 2e = Fe^{o} \qquad E^{o} = 0.409V$$

The silver couple is more positive, copper somewhat less positive and iron much less positive than chalcopyrite, whose best value was found to be 0.462 volts.

At 27°C, and a pH of 1.25, the presence

of silver metal produced practically no increase in the amount of copper dissolved. This was as expected because the couple $Ag^{o}/CuFeS_2$ does not increase the anodic voltage sufficiently for the discharge of oxygen by the oxidation of water and the consequent increase in oxygen concentration on the mineral surface which would result in an increased dissolution rate.

Metallic iron additions produced a decrease in copper concentration for about 10 minutes followed by a rapid increase after about 30 minutes. This was explained as due to the cathodic dissolution of the chalcopyrite instead of the usual anodic dissolution (see equations 1.2.32 and 1.3.2). The iron has a lower potential than chalcopyrite producing, on contact, a negative overpotential causing the reaction:

$$2CuFeS_2 + 2e^- = Cu_2S + 2Fe^{2+} + 3S^{2-} \quad (1.3.5)$$

In the presence of $H^+$, the $S^{2-}$ reacts thus:

$$3S^{2-} + 6H^+ = 3H_2S \quad (1.3.6)$$

The anodic reaction is

$$Fe^{o} = Fe^{2+} + 2e^- \quad (1.3.7).$$

giving the overall reaction

$$2CuFeS_2 + 6H^+ + Fe^{o} = Cu_2S + 3H_2S + 3Fe^{2+} \quad (1.3.8)$$

which is favoured thermodynamically.

The initial copper concentration probably results from the usual anodic dissolution of $CuFeS_2$ (equations 1.2.32 and 1.3.2.). The decrease in copper results from reaction with $H_2S$ to form covellite CuS, and from cementation on the metallic iron. The $Cu_2S$ formed in reaction (1.3.8) seemed to dissolve in the usual manner to produce CuS and copper in solution; which was precipitated as CuS until the $H_2S$ concentration was low enough to allow copper ion build up in the solution.

The copper metal addition increased the dissolution markedly. Neglecting the exchange reaction between lattice and solution copper ions, Baur et al cnnsidered the reactions:

$$H_2S + Cu^0 = Cu_2S + 2H^+ + 2e^- \quad \text{(anodic)} \quad (1.3.9).$$

$$2CuFeS_2 + 2e^- + 6H^+ = Cu_2S + 2Fe^{2+} + 3H_2S \quad (1.3.10)$$

(cathodic)

The immediate release of copper to solution indicates that the anodic reaction of $Cu_2S$ and copper is rapid enough in the presence of oxygen to suppress the formation of $H_2S$. The $Cu_2S$ formed will, in the presence

of oxygen, be converted to CuS giving an overall reaction:

$$2CuFeS_2 + 6Cu^{o} + 3O_2 + 12H^{+}$$
$$= Fe^{2+} + 4\ CuS + 4Cu^{2+} + 6H_2O \quad (1.3.11)$$

The CuS formed would continue to react, forming $Cu^{2+}$ and elemental sulphur. A determination of the parbolic rate constant indicated that the overall kinetics are controlled by the anodic dissolution of $Cu_2S$.

This work illustrated the possible usefulness of a two stage reaction in which $CuFeS_2$ is converted cathodically to $Cu_2S$ using metals with more negative potentials, followed by the anodic dissolution of the $Cu_2S$ formed, using an appropriate oxidant.

## 1.4. Crystal Structures.

### 1.4.1. Silver sulphide:

Silver sulphide is the most common sulphide of silver that occurs in nature. It is known to exist in three modifications between room temperature and its melting point, a low temperature monoclinic form ($Ag_2$SIII, β-$Ag_2$S), an intermediate form with a body centred cubic structure ($Ag_2$SII, α-$Ag_2$S) and a high temperature form, apparently with a face-centred cubic structure ($Ag_2$SI). Two polymorphs of $Ag_2$S composition have been described as distinct mineral species. Argentite commonly occurs with external cubic morphology and displays characteristic twinning in polished sections. Acanthite has a monoclinic structure and morphology and is usually untwinned in polished sections.

It is now known that the cubic structure is never retained at room temperature, and these specimens are actually acanthite ($Ag_2$SIII, β-$Ag_2$S) pseudomorphic after argentite ($Ag_2$SII, α-$Ag_2$S).

Ramsdell[126], Emmons et al[127], Schneiderhöhn[128] and Palacios and Silva[129]

were amongst the early workers who first studied the crystal structures of naturally occurring silver sulphides. Despite its externally cubic morphology, Ramsdell found that samples of argentite did not give the X-ray pattern expected of a cubic structure but gave a pattern identical to that of acanthite which was at that time considered to be orthorhombic, Ramsdell concluded that argentite must have a high temperature cubic form which is unstable at lower temperatures and undergoes molecular readjustment to become a pseudomorph of acanthite.

Evidence for this conclusion was given by Emmons et al who obtained X-ray patterns at high temperatures. Above 180°C the stable form of silver sulphide was found to be isometric with a body-centred cubic space lattice. From this they concluded that all silver sulphide at ordinary temperature has the same space lattice as acanthite and is probably orthorhombic, the externally isometric natural crystals of silver sulphide (agentite) being formed at temperatures above 180°C and becoming acanthite paramorphs at lower temperatures.

This conclusion was supported by optical work of Schneiderhohn who compared the behaviour of argentite with that of chalcocite:

β-Argentite (orthorhombic) $\underset{\leftarrow}{\overset{179^{\circ}C}{\rightleftharpoons}}$ α-$Ag_2S$ (isometric)

β-Chalcocite (orthorhombic) $\underset{\leftarrow}{\overset{91^{\circ}C}{\rightleftharpoons}}$ α-$Cu_2S$ (isometric)

Palacios and Silva (1931) made both powder photographs and spectro graphic measurements from the face of an argentite crystal. From the latter they obtained a 'split' reflection, the two parts corresponding to interplanar spacings of 2.45 and 2.39 Å respectively. They correlated the first value with a cubic lattice, and assumed that the second pertained to the orthorhombic modification. Identical X-ray power photographs were obtained from argentite, acanthite and artificial material, and indicated a mixture of cubic and orthorhombic crystals below 180°C, but above this transition point only the cubic form was evident. Thus according to their interpretations of the data, both the high and the low temperature modifications are present in all samples of silver sulphide at room temperature, the unit cell dimensions of the cubic form being a = b = c = 4.90 Å and those of the apparently orthorhombic being a = 4.77, b = 6.92, c=6.88Å.

An X-ray investigation by Ramsdell[130] indicated that the low temperature form of silver sulphide (acanthite) is in actual fact monoclinic. The previous assignment of acanthite to the orthorhombic and cubic systems on the basis of morphology and X-ray data, were both explained by the pseudo-orthorhombic and pseudo-cubic character of the actual monoclinic cell. The close correspondence of the interfacial angles with those of systems with higher symmetry (i.e., cubic form) is due to the cell dimensions, and the occurrence of crystals with apparent orthorhombic symmetry is due both to cell dimensions and to the effect of polysynthetic twinning.

The X-ray investigation using Weissenberg (CuKα radiation), Laue and Powder techniques, gave the following data for the monoclinic cell:

$a = 9.47\text{Å}$ $b = 6.92\text{Å}$ $c = 8.28\text{Å}$

$a : b : c = 1.368 : 1 : 1.96$

$c \sin\beta = 6.86$; $\beta = 124^{\circ}$.

Probable space group B21/c ($C_{2h}^{5}$)

The cell volume was calculated to be $449.8\text{Å}^3$ with eight $Ag_2S$ moles per unit cell.

On this basis the calculated density was 7.27 compared to literature values of 7.22. Polysynthetic twinning //e to the 001 plane was observed on all crystals.

Kracek,[131] in studying the phase relations in the sulphur-silver system, studied the transition in silver sulphide from room temperature to the melting point at 838 ± 2°C. There are two transitions, each of which occurs at variable temperatures over a limited range of composition. The mean temperatures for the lower transition $Ag_2$ SIII (monoclinic) $\leftrightharpoons$ $Ag_2$ S-II (body-centred cubic) are 177.8°C in sulphur rich and 176.3°C for silver rich preparations; for the upper transition $Ag_2$ SII $\rightleftharpoons$ $Ag_2$ SI they are, respectively, 622°C and 586°C. This incorporation of limited excess of sulphur or silver ions in the respective lattices was thought to be due to the semi-conducting properties of the substance and the inherently disordered lattice structures, especially that of the $Ag_2$ SII modification.

The structure of this $Ag_2$ SII modification (agentite, $\alpha$-$Ag_2$ S) was determined by Rahlfs[132] from four lines on a powder photograph taken

at 250°C. It was described as a body-centred cubic structure in which the sulphur atoms occupy the corners and centre (000; $\frac{1}{2}\frac{1}{2}\frac{1}{2}$) of a 4.88 Å cubic cell, and in which the silver atoms are statistically distributed in 42 possible positions. (Figure 16(a)). Hence the structure is, according to this view, ordered with respect to sulphur ions, and disordered with respect to silver.

Djurle (133) in an X-ray study of the Ag - Cu - S system considered the phases occurring at the composition $Ag_2S$. The two transition temperatures for $Ag_2S$ were found to be in complete agreement with the work of Kracek, and all three phases $Ag_2S$III, $Ag_2S$II, $Ag_2S$I were identified using Guinier and high temperature X-ray cameras. The $Ag_2S$III phase (acanthite, $\beta$-$Ag_2S$) gave a monoclinic unit cell with the following lattice parameters:

$a = 9.531$, $b = 6.925$; $C = 8.278$Å($\pm 0.005$Å)

and $\beta = 123 \pm 0.10°$, in good agreement with the values of Ramsdell.

The $Ag_2S$II phase (agentite, $\alpha Ag_2S$) had a body centred cubic structure in accord with the work of Rahlfs. The cell edge was determined

(a)

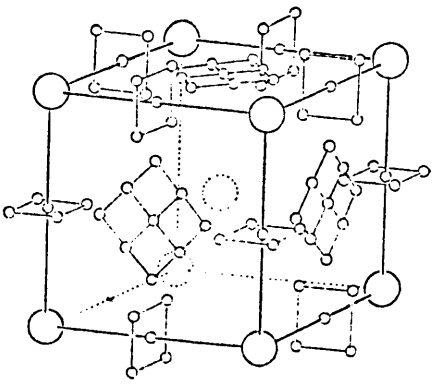

(b)

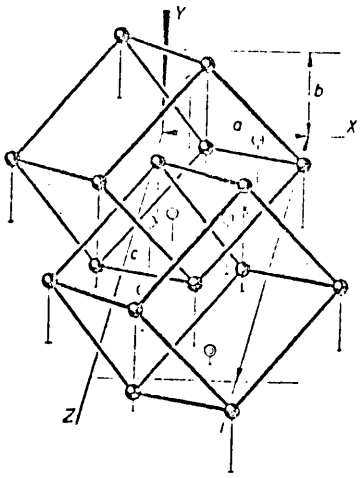


(c)

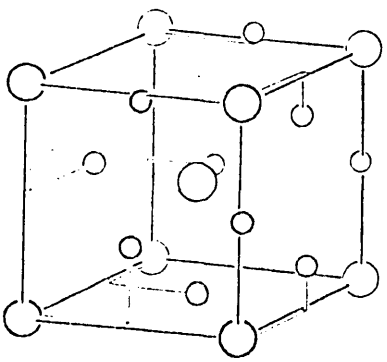

FIGURE 16 : (a) Structure of $\alpha$-$Ag_2S$ (large circles, sulphur atoms). Rahlfs[132].

(b) Structure of acanthite ($\beta$- $Ag_2S$). Projection inclined 20° to 'b' axis. Dark circles represent sulphur atoms, light circles silver atoms. Fruch[135].

(c) Structure of the $\beta$-form according to a unit cell of the $\alpha$-form (large circles, sulphur atoms). Sadanaga and Sueno[137].

at various temperatures:

at 189°C = a = 4.870 )
300°C = a = 4.890 ) ± 0.008Å.
500°C = a = 4.926 )

which were in good agreement with the value of 4.88Å at 250°C given by Rahlfs.

A powder photograph of the $Ag_2$ SI modification was taken at 600°C. Only one line of the pattern could be seen due to the very high background blackening. But since all the other high temperature phases of the Ag-Cu-S system were face-centred cubic with /220/ as their strongest diffraction line, and with regard to the suspected isomorphism of the highest temperature modifications, the one line for the $Ag_2$ SI phase was indexed as /220/ of a face-centred cubic lattice, with the cube edge a = 6.269 ± 0.020Å.

Frueh (134) obtained three lines of d-spacings 3.17Å, 2.24Å and 1.819Å from the X-ray diffraction of a $Ag_2$ SI sample using a high temperature powder camera at 650°C. These can be indexed either as the (100), (110) and (111) planes of a simple cubic cell of a=3.17Å, or as the (200), (220) and (222) planes of

a face centred cubic cell of a = 6.34Å. However, allowing but one formula weight of $Ag_2S$ per unit cell, the calculated density of 12.84 makes the simple cubic cell unlikely. On the other hand, the face-centred cubic cell of 6.34Å edge could contain 4 formula weights and have a density of 6.42, which is a little less than the measured density of the room temperature form (7.2). Hence this seems to confirm Djurle's assumption that the $Ag_2S$ I form is face-centred cubic.

Frueh [135] redetermined the cell constants of the $Ag_2S$ III modification ($\beta$-$Ag_2S$) after adopting a primitive cell related to Ramsdell's cell by $\frac{1}{2}0\frac{1}{2}$ /010/$\frac{1}{2}0\frac{1}{2}$. The constants were obtained for a sample of naturally occurring acanthite by the Buerger precession technique using MoK$\alpha$ radiation. The space group of a single crystal of $\beta$-$Ag_2S$ was found to be monclinic $P2_1/n$; the cell constants were determined as a = 4.23, b = 6.91Å, C = 7.87Å, $\beta$ = 99° 35'. There are 4 ($Ag_2S$) per unit cell which has a volume of 226.8Å.

The structure of acanthite was described by Frueh with the sulphur atoms arranged in a

slightly distorted body-centred cubic array (Figure 16(b)) with one of the twofold axes of the cube parallel to $[0\bar{1}0]$, the $2_1$ axis of the monoclinic space group. The faces of this sulphur cube lie in the (103), (121), $(\bar{1}21)$ planes and the average cell edge length is 4.86Å. One of the Ag atoms lies either a little above or a little below the plane, and is triangularly coordinated to three sulphurs at 2.50Å, 2.61Å and 2.69Å respectively. The other Ag atom lies half way between the planes, and links them together by having one close sulphur in the plane above and one in the plane below at 2.49Å and 2.52Å.

Other interatomic distances were found to be:

| Atom | Neighbour | Distance |
|---|---|---|
| $Ag_1$ | $Ag_1$ | 3.41; 3.56; 3.57 |
| | $Ag_{11}$ | 3.04; 3.12; 3.14; 3.19 |
| | S | 2.49; 2.52; 3.07 |
| $Ag_{11}$ | $Ag_{11}$ | 3.15; 3.73. |
| | S | 2.50; 2.61; 2.69 |
| S | S | 4.08; 4.09; 4.15; 4.19 |

Thus according to Frueh acanthite has in common with the high temperature form agentite

($\alpha$ - $Ag_2S$, $Ag_2S$ II) a body centred cubic arrangement of the sulphur atoms, although the arrangement of the silver atoms in the two polymorphs is quite different.

Bragg and Claringbull[136], using the work of Frueh, have attempted to explain the confusion arising from the apparent cubic form of $Ag_2S$, argentite, which exists at room temperature. On cooling, any one of the six $[\bar{1}10]$ axes of the high temperature form may become the $[\bar{1}10]$ axis of the acanthite structure. Hence the high temperature crystal is converted into an aggregate of twinned crystals of low-temperature form with the same approximate body centred cubic sulphur structure in common orientation in all the twin domains, thus retaining the original cubic morphology. It is these apparent cubic crystals that have been named argentite by mineralogists.

Sadanaga and Sueno[137] conducted an X-ray study on the $\alpha$ - $\beta$ transition of $Ag_2S$ to follow the progress of twin formation. A refinement of the structure of the low temperature form was first carried out. This gave lattice constants of a = 4.231, b = 6.93, c = 9.526 and $\beta = 125^{\circ}29'$

with a space lattice group of $P2_1/C$ instead of $P2_1/n$, determined by Frueh, due to a change of the c-axis to the $[\bar{1}01]$ direction of his axial setting so as to facilitate the correlation of the structure with that of $Ag_2$ SII form in the subsequent study of the transition (Figure 16(c)). In other respects the two $Ag_2$ SIII structures are essentially the same.

The interatomic distances can be compared with those of Frueh[135]:

| | | | | | |
|---|---|---|---|---|---|
| $Ag_1$ - | $Ag_1$ | 3.35 | 3.58 | 3.58 | |
| | $Ag_{11}$ | 3.08 | 3.11 | 3.11 | 3.20 |
| | S | 2.47 | 2.51 | 3.47 | 3.83; |
| $Ag_{11}$ - | $Ag_{11}$ | 3.12 | 3.73 | | |
| - | S | 2.56 | 2.54 | 2.70 | 2.99 |
| S - | S | 4.13 | 4.14 | 4.15 | 4.23 |

From this structure and heat treatments of specimens, the authors followed the progress of twin formation in the transition $Ag_2$ SIII $\longrightarrow$ $Ag_2$ SII. It appears that as the temperature rises, the $Ag_2$ SIII structure makes the first approach to the $Ag_2$ SII form by giving itself more marked cubicity through the change in the $\beta$-angle; at the next step simulates the symmetry of the high temperature form in short ranges in

the crystal by twinning; and finally, at the transition temperature, rearranges into parallel orientation the twin individuals which have been deranged by rotations, perhaps by the function of active grain boundaries.

This progression of twin formation with increasing temperature prior to the inversion temperature is confirmed by work of Taylor[138], who observed twinning in an $Ag_2S$ sample on heating well below 177°C. This twinning was preserved upon subsequent cooling of temperature. Twinning occurred at 156 ± 2, 168 ± 3°C, the latter sample having a very similar appearance to a sample heated above the inversion temperature at 185 ± 2°C. However no twinning was observed at 140°C after heating for 1 month.

The results cast doubt on the use of the presence of twinning in $Ag_2S$ as an accurate temperature indicator in geological processes.

1.4.2. Stromeyerite

Three sulphides of silver and copper are known to exist, stromeyerite $Cu_{1+x}Ag_{1-x}S$, jalpaite $Cu_{0.45}Ag_{1.55}S$, and mckinstryite $Cu_{0.8}Ag_{1.2}S$. Stromeyerite has long been recognised as a

distinct mineral species but it is only recently that jalpaite and mckinstryite have been conclusively identified in nature.

At first it was thought that stromeyerite was a compound with a definite 1 : 1 ratio between silver and cuprous sulphide. Schwartz [139] prepared stromeyerite synthetically by compressing these proportions of powdered $Ag_2S$ and $Cu_2S$ and subjecting the compressed pellets to subsequent heat treatment. It was found that stromeyerite can be quickly and easily made by temperatures as low as 75°C. The synthetic stromeyerite when made at temperatures above 100°C showed the bladed or 'oleander leaf' structure observed by many authors in natural ores [166]. Schwartz showed that this bladed structure is due to an inversion in crystal structure at 93°C. Specimens of natural stromeyerite and that formed at low temperature also showed the structure on exposure to the heat of illumination by arc light under the microscope (see section 5.4).

However, with the theoretical proportions for a 1 : 1 mixture of $Ag_2S$ and $Cu_2S$ (60.89 and 39.11 wt.% respectively), Schwartz found that silver was present as an additional phase

in many instances.

Suhr[140] used single crystals of stromeyerite to obtain crystal data by the Weissenberg and Precession techniques with Cu radiation. The unit cell was determined to be orthorhombic with the cell constants a = 4.06Å, b = 6.66 Å and c = 7.99Å giving a cell volume of 215.5Å$^3$ containing 4 CuAgS. The space group symmetry was determined as either $Cmc2_1$ - ($C_{2V}^{12}$) or Cmcm($D_{2n}^{17}$).

In experiments on the $Ag_2S$-$Cu_2S$ system Suhr prepared samples containing various proportions of $Ag_2S$ and $Cu_2S$ by com pressing the mixtures into pellets and heating at various temperatures for various lengths of time. Suhr noted that in samples prepared for the atomic proportions Ag : Cu : S of 1 : 1 : 1, a trace of jalpaite , $Ag_3CuS_2$ detectable by X-ray diffraction, appeared with the stromeyerite. When atomic proportions Ag : Cu : S of 0.9 : 1 · 1 : 1 was used, a diffraction pattern of stromeyerite alone was produced. It was suggested that stromeyerite was either a defect structure with a deficiency of silver atoms (holes substituted for silver), or a structure in which some copper atoms occupy silver positions.

The possibility of a defect structure with up to 0.1 of the Ag atoms missing was suggested by Frueh[141]. This work confirmed the unit cell dimensions and space group reported by Suhr, using single crystals of stromeyerite and the Buerger precession technique with Mo radiation. The unit cell contains $Ag_4$ $Cu_4$ $S_4$ with each element occupying four-fold special positions. The Ag is at 000; $00\frac{1}{2}$, $\frac{1}{2}\frac{1}{2}0$ and $\frac{1}{2}\frac{1}{2}\frac{1}{2}$. The Cu and S atoms are at $0y\frac{1}{4}$, $0\bar{y}\frac{3}{4}$, $\frac{1}{2}\frac{1}{2}+y\frac{1}{4}$, and $\frac{1}{2}\frac{1}{2}-y\frac{3}{4}$, where the y parameter for Cu is 0.46 and for S is 0.80.

The structure (Fig 17 (a)) is essentially made up of zig-zag chains of silver and sulphur atoms paralleling the c-axis. The planes parallel to (001) are composed of layers of loosely packed face-centred silver atoms alternating with layers of triangularly coordinated sulphur and copper atoms. The silver-sulphur distance in the chain is 2.40Å which is identical to that found in similar silver-sulphur chains in proustite ($Ag_3AsS_3$) and pyrargyrite ($Ag_3SbS_3$). The silver-sulphur-silver bond angle is about 113° and the sulphur-silver-sulphur bond angle is 180°. In the copper-sulphur layers each copper atom has two sulphur atoms

(a)

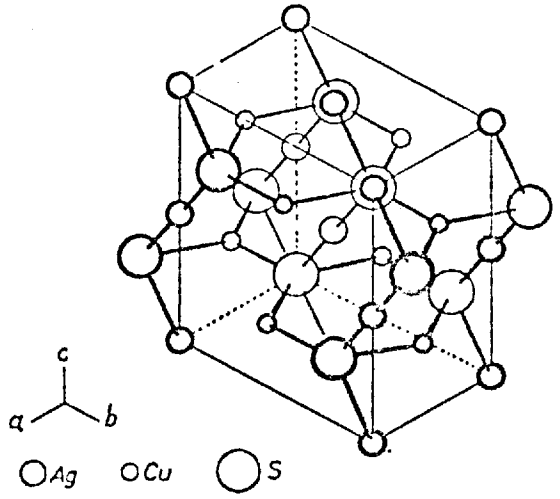


(b)

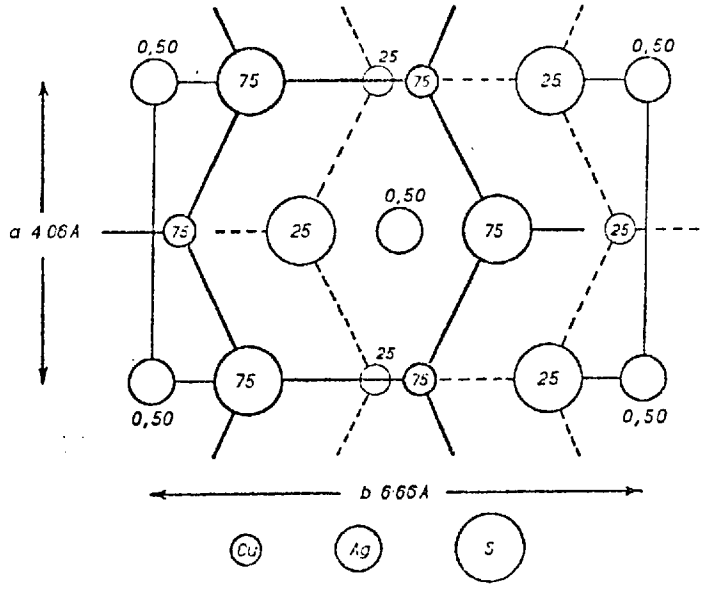


(c)

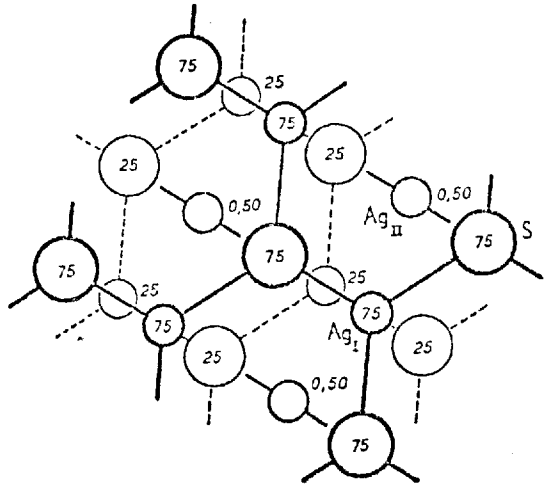


FIGURE 17 : (a) The structure of stromeyerite. Frueh[141].
(b) The structure of stromeyerite projected on (001), the 'c' axis. Bragg and Claringbull[136].
(c) The structure of acanthite projected on (010), the 'b' axis. Bragg and Claringbull[136].

at 2.29Å and one sulphur atom at 2.26Å. This planar copper-sulphur layer is much like that in covellite where the sulphur copper distance is 2.20.

Frueh obtained evidence for a defect structure for stromeyerite, in agreement with the experimental findings of Schwartz and Suhr , by a limited application of the electronic theories of the metallic state to stromeyerite. If stoichiometric (CuAgS), stromeyerite would have eight valence electrons for every three atoms, or an $^{e}/_{a}$ ratio of 2.66. This does not exactly fill any of the principal Brillouin zones and it seems likely that the principal zone, which determines the valence band, will be filled to capacity and the excess electrons of the stoichometric compound must be accommodated in the conduction band at a higher energy level.

Frueh suggested that it may involve less of a total energy gain to omit electron-contributing atoms from the structure rather than to accommodate these extra electrons at the higher energy level. For the structure of stromeyerite the removal of a silver atom would involve less

bond breaking and consequent energy gain than if a copper or sulphur atom were removed (two bonds compared to three and five bonds respectively). The removal of 0.1 of the silver atoms would reduce the $^{e}/_{a}$ ratio to 2.63 enabling all the electrons to be accommodated within the principal zone. Hence Frueh suggested a more accurate formula for stromeyerite of $Ag_{1-x}CuS$ where x has some value between 0 and 0.1.

In a later work, Frueh[142] proposed that the presence of an impurity atom in a vacant site in the structure of a non-stoichiometric compound may relieve, to some degree, the local strain in the structure caused by the vacancy, and thus make this impure compound the one of lower energy. The electrons of this impurity atom would probably lie in an impurity level somewhere between the top of the valence band and the bottom of the conduction band. From the structure of stromeyerite it is evident that the copper positions are quite distinct from the silver positions, both in co-ordination number and in bond lengths. Therefore the copper can be considered as an impurity when it proxies for silver in the

structure. From these considerations Frueh therefore proposed that the non-stoichiometric composition $Ag_{0.93}Cu_{1.07}S$, as found by Djurle[133], was the stable one; because when the impurity copper atoms, whose electrons lie in an impurity level below the conduction band, are substituted for the silver atoms, less energy is involved than the energy necessary to lift the electrons of the silver atoms from the valence band to the conduction band.

In an X-ray study of the Ag-Cu-S system Djurle[133] found three modifications at the composition $Ag_{0.93}Cu_{1.07}S$. The examination revealed two transition temperatures, the lower one at 90°C (compared to 93°C - Schwartz) and the upper one at about 180°C. The Guinier photograph taken at room temperature gave an orthorhombic cell with cell constants of a = 4.066 ± 0.002Å, b = 6.628 ± 0.003Å, c = 7.972 ± 0.004Å - which can be compared with those of Suhr.

The modification above 90°C was indexed hexagonally, giving a unit cell content of $2Ag_{.93}Cu_{1.07}S$ and the dimensions:

at 100°C a = 4.138±0.004Å ) c/a = 1.983
c = 7.105±0.007Å )
and
at 152°C a = 4.158±0.004Å ) c/a = 1.963
c = 7.068±0.007Å )

The high temperature modification was considered to have a face-centred cubic unit cell with a cell content of $4Ag_{0.93}Cu_{1.07}S$ and the following cell constant:

at 196°C a = 5.961 )
300°C a = 5.973 ) ± 0.009Å
500°C a = 5.993 )

The study of Skinner[143] was in complete agreement with Djurle's observations on the stable phases, with stromeyerite being more copper-rich than CuAgS but retaining the 2 : 1 metal/sulphur ratio. He found that a stoichiometric stromeyerite CuAgS could be produced by annealing a charge of this composition at temperatures below 93.3°C. Evidence was also found to indicate that stromeyerite had a measurable composition range, extending from CuAgS towards $Cu_2S$ but not significantly towards $Ag_2S$, and enclosing the compositions $Cu_{1.10}Ag_{0.9}S$ and $Cu_{1.07}Cu_{0.93}S$ proposed by Suhr and Djurle, respectively. Hence Skinner considered a more correct representation of the composition would

be $Cu_{1+x}Ag_{1-x}S$ where $0 \leqslant x \leqslant 0.1$.

Bragg and Claringbull[136] have compared the structure of stromeyerite with that of acanthite. The similarity may be seen by projecting the stromeyerite along the C axis as in Fig. 17(b) and projecting the acanthite structure along the b axis as in Fig.17(c). The layers of sulphur and copper atoms, with each copper lying between three sulphur atoms at an average distance of 2.28Å, are very similar to the sulphur-silver layers in acanthite, and these layers are linked together by silver atoms (with a silver-sulphur distance of 2.40Å) halfway between them, again in much the same way as in acanthite. The numbers in the structure refer to heights of atoms above the face of the unit cell along the axis of projection in hundredths of the projected unit cell edge.

1.4.3 Jalpaite - The formula for Jalpaite has been written in various ways and its existence as a distinct mineral species has, at times, been discredited. However recent work has verified its existence in nature with the formula $Ag_{3.0}Cu_{1.0}S_{2.0}$.[144]

Despite earlier descriptions of the mineral by many authors, the work of Schwartz[139] on the relations of the mineralsargentite, stromeyerite and chalcocite tended to throw doubt on the existence of jalpaite as a distinct mineral. Mixtures of the approximate composition attributed to jalpaite ($Ag_2S$ = 83.37%; $Cu_2S$ = 17.63%) were heated at various temperatures but none of these specimens revealed a compound or mineral species distinct fromargentite and stromeyerite. Schwartz's observations would suggest that many so called jalpaites are solid solutions of $Cu_2S$ and $Ag_2S$.

However in his investigation of the $Ag_2S$ - $Cu_2S$ system using the chemically pure elements, Suhr[140] identified a distinct phase at $Ag_{7.5}Cu_{2.5}S_{5.0}$, corresponding to the mineral Jalpaite, and Djurle[133] identified by X-ray diffraction a definite ternary phase of composition $Ag_{1.55}Cu_{0.45}S$ which he assumed to correspond to the mineral Jalpaite.

The phase had two transition temperatures, a lower one at 112°C and the upper one at 290-310°C. The low temperature modification is tetragonal with a body centred unit cell with

the dimensions, at room temperature of:

$a = 8.673 \pm 0.004$Å, $C = 11.756 \pm 0.006$Å

$c/a = 1.355$.

At 105°C, the values become:

$a = 8.725 \pm 0.009$Å, $c = 11.74 \pm 0.01$Å

The density, calculated from the cell constants, assuming 16 $Ag_{1.55}Cu_{0.45}S$ per unit cell was $6.8 g/cm^3$ in good agreement with the measured density of $6.9 g/cm^3$.

At 112°C the phase transforms into a body-centred cubic lattice with a cell constant that varies with temperature as follows:

at 116°C a = 4.825 )
152°C a = 4.836 ) ± 0.005Å
300°C a = 4.870 )

The cell volume is $1/8$ of that of modification III indicating $2Ag_{1.55}Cu_{0.45}S$ as the cell contents.

For the high temperature modification only two lines of the X-ray pattern could be discerned due to the high background blackening. These two lines were given indeces consistent with a face centred cubic lattice, since all the other high temperature modifications in the Ag - Cu - S system could be indexed on this

basis.

The cube edge at three different temperatures were as follows:

$300^{\circ}C$ a = 6.110 )
$400^{\circ}C$ a = 6.123 ) ± 0.006Å
$500^{\circ}C$ a = 6.140 )

A cell content of $4Ag_{1.55}Cu_{0.45}S$ is consistent with these cell constants.

Skinner[143] also established the existence of jalpaite having a composition of $Ag_{1.55}Cu_{0.45}S$. The Jalpaite inverted at $117^{\circ}C$ to a bcc phase identical with argentite, an observation in fair agreement with the $112^{\circ}C$ observed by Djurle.

Grybeck and Finney[144] reported on new occurrences of jalpaite in natural ores and undertook extensive studies of the physical, chemical and structural properties of the mineral. The specimens were analysed for silver and copper by wet chemistry. Within the accuracy of the analyses, there seems to be little doubt that the jalpaite corresponds to the composition $Ag_3CuS_2$. The discrepancy between these analyses and the $Ag_{1.55}Cu_{0.45}S$ of Skinner

and Djurle cannot be fully explained but it was suggested that it could be due to a solid solution field tending towards copper deficiency from the 'ideal' formula $Ag_3CuS_2$, similar to the silver deficiency indicated for stromeyerite ($Ag_{1-x}Cu_{1+x}S$) (section 1.4.2).

Crystal fragments were used to determine the unit cell using data from precession and X-ray powder photographs. The jalpaite was found to be tetragonal, space group $I4_1/amd$ with $a = 8.633$ and $c = 11.743$Å. The unit cell contains eight $Ag_3CuS_2$ giving a calculated density of 6.827 compared to the observed value of 6.820. This single crystal investigation confirmed the tetragonal system and unit cell dimensions originally presented by Djurle. The X-ray powder patterns of the natural jalpaite were essentially the same as Djurle's synthetic $Ag_{3.1}Cu_{0.9}S_{2.0}$.

At the moment no data is available on the distribution of the silver and copper in the jalpaite structure for comparison with the other Ag-Cu-S minerals.

1.4.4. McKinstryite:

This is the most recent of the silver-copper-sulphides to be identified in nature. The existence of a new compound between acanthite and stromeyerite was first recorded in the work of Suhr (140). Djurle(133) found a stable phase of composition $Ag_{1.2}Cu_{0.8}S$ which he denoted as β. He observed two transition temperatures, one at 95 to 99°C and the upper one at 120 to 143°C. No indexing of the diffraction patterns of the lower temperature phases βIII and βII was attempted but the X-ray pattern of the high temperature phase βI was indexed as derived from a face-centred cubic lattice, in common with the other high temperature modifications in the Cu - Ag - S system. The edge of the unit cube was found to be:

at 151°C a = 5.999 )
300°C a = 6.015 ) ± 0.006Å
500°C a = 6.042 )

This is consistent with cell content of $4Ag_{1.2}Cu_{0.8}S$.

Skinner(143) identified a similar compound in his studies on the phase relations of the Cu - Ag - S system. He found that the compound $Ag_{1.2}Cu_{0.8}S$, broke down at 94.4°C, in fair

agreement with Djurle's observations, to a mixture of jalpaite plus a hexagonal close packed phase with a composition $(Cu_{0.96}Ag_{1.04})S$.

The compound was first identified as a mineral in 1966, and was named McKinstryite[145]. The formula indicated by analysis is slightly more copper rich than $Cu_{0.8}Ag_{1.2}S$, calculating to $Cu_{0.82}Ag_{1.18}S$, leading the authors to suggest that the formula should be written $Cu_{0.8+x}Ag_{1.2-x}S$, where $0 \leq x \leq 0.02$. X-ray diffraction patterns showed that the natural mineral was identical to Djurle's β-phase and to the phase identified by Skinner.

Single crystal X-ray diffraction studies by the Buerger precession method established that the symmetry of Mckinstryite is orthorhombic, space group Pnam or $Pna2_1$. The cell edges determined by this method were a = 13.99Å, b = 15.66Å and c = 7.80 Å. On refinement, using X-ray diffraction data measured against $CaF_2$ as an internal standard with a high angle goniometer, the cell constants were determined as a = 14.043 ± 0.005Å, b = 15.677 ± 0.006Å, c = 7.803 ± 0.005 Å.

The calculated cell occupancy was 32 formula units of $Cu_{0.82}$ $Ag_{1.18}S$ using a cell volume of $1717.8 \pm 0.8$Å$^3$, a molecular weight of 211.47 and a specific gravity of $6.61 \pm 0.03$.

The similarity of spacings and intensities between some of the strong lines for stromeyerite and mckinstryite led the authors to suspect that the two compounds might have certain structural elements in common. Stromeyerite, like mckinstryite, has an orthorhombic cell. According to Djurle[133] the dimensions of the stromeyerite cell are a = 4.066Å, b = 6.628Å and c = 7.972Å, space group Cmcm. The possibility of a structural relation between stromeyerite and mckinstryite is further supported by an apparent dimensional relationship between the two cells such that

a mckinstryite (14.0Å) ≃ $4d_{(110)}$ stromeyerite (13.9Å)

c mckinstryite (7.8Å) ≃ $d_{(130)}$ stromeyerite (7.8Å)

b mckinstryite (15.7Å) ≃ 2c stromeyerite (15.9Å).

The net defined by the (110), (130) and c of stromeyerite is very nearly orthogonal. The slight changes necessary to bring the stromeyerite and mckinstryite nets into orthogonal

register could probably be accounted for by very slight changes in the general atomic positions in the mckinstryite cell, relative to stromeyerite, and consequent to the compositional difference between them.

A further natural occurrence of mckinstryite was reported by Robinson and Morton[146]. Electron probe microanalyses revealed an average composition of $Cu_{0.72}Ag_{1.28}S_{0.91}$, silver rich domains existing within the mineral. This mckinstryite had less copper, an excess of silver and a deficiency in sulphur compared to that of Skinner et al.[145] The results suggested a generalised formula of $Cu_{0.8-x}Ag_{1.2+x}S_{1-y}$ where both x and y are relatively large. The silver attained values of as high as 1.38 formula units in some samples, but in some specimens of low silver, a formula of $Cu_{0.79}Ag_{1.21}S_{0.93}$ was obtained.

The orthorhombic unit cell parameters were determined as:

$a = 13.962 \pm 0.001$Å

$b = 15.675 \pm 0.002$Å

$c = 7.755 \pm 0.002$Å

This gave a cell volume of 1697.2 $\pm$0.3Å$^3$, which with a molecular weight of 212.8 (for $Cu_{0.772}Ag_{1.278}S_{0.906}$) and the observed density of 6.64 $\pm$ 0.04, gave a calculated cell occupancy of 31.9 $\pm$ 0.4 formula units in good agreement with Skinner et al, although the cell volumes are significantly different.

The authors considered the non-stoichiometry of the mckinstryite as either due to a deficiency of sulphur or an excess of silver ($Cu_{0.8}Ag_{1.41}S$). The specific gravity determinations suggest that the former case is most probable. The defect was presumed to be a type of Schottky defect whereby some of the anion sites in the lattice are vacant. Electrical neutrality must be maintained by a certain amount of metallic bonding probably taking place with the silver. However, as far as is known, no crystal-structure investigation has yet been performed on mckinstryite.

1.4.5. Structure of Bornite.

Morimoto and Kullerud[147] studied the polymorphism in bornite and confirmed the existence of two stable forms and one transitional metastable form. A non-quenchable

face-centred cubic form with a = 5.50 ± 0.01Å is stable above 228 ± 5°C. A metastable cubic form, with a = 10.94Å, appears on rapid cooling from above this temperature, but within days this inverts to the stable low temperature tetragonal polymorph with cell dimensions a = 10.94Å and c = 21.88Å.

According to Morimoto[148], the crystal structure of the high temperature form is essentially the antifluorite structure, only slightly more complicated. The sulphur atoms occupying the nodes of the cubic face-centred lattice with a = 5.50Å are cubically close packed. Each tetrahedron of sulphur atoms on the average contains 3/4 of a metal atom. This fractional atom is itself statistically distributed over 24 equivalent sites inside the sulphur tetrahedron. In the whole cell, six metal atoms are statistically distributed over 24 x 8 = 192 sites.

The metastable form is transitional between the high temperature form and the low temperature form. According to Morimoto the cubic arrangement of the metastable form is a result of the twinning of a large number of

small domains in eight different orientations. All the domains that have the same orientation constitute one crystal, even if they are not singly connected. Each such crystal has rhombohedral symmetry with $a_{rh.} = 6.70\text{Å}$ and $\alpha = 33^{\circ}32'$. These eight crystals are in twin relations.

The structure of the rhombohedral form can be derived from that of the high temperature form. The statistical distribution of 3/4 of the metal atom among 24 possible sites inside each sulphur tetrahedron changes to the statistical distribution of one metal atom among four possible sites. The structure can be described as a layer structure parallel to (0001), with two kinds of sulphur layers, $M_1$, $M_{11}$ and $M_{111}$*. The $S_1$ layers are sandwiched between the $M_{11}$ and $M_{111}$ layers, while the $S_{11}$ layers only have the $M_1$ layers on one side.

A study of the structure of the low temperature form of bornite based on the structure of the rhombohedral form determined by Morimoto was carried out by Manning[149] in a paper on the bonding properties of sulphur in bornite. By assuming that some of the M-$S_1$ bonds were ionic (non-coordinate), Manning concluded that

* $M_1$, $M_{11}$, and $M_{111}$ are the three kinds of metal layers.

the S atoms must be 4-coordinated i.e., tetrahedrally coordinated.

This fits into practice well since in the rhombohdral form the $M_1$-$S_1$ and the three $S_1$-$M_{111}$ are oriented tetrahedrally and the $S_{11}$ atoms are also tetrahedrally coordinated (to one $M_{111}$ and three $M_1$ atoms). In this theory the $M_{11}$ atoms are bound by electrostatic forces and this accounts for the high coordination number of both the $S_1$ and $S_{11}$ atoms (7 and 5-coordinate respectively).

Manning indicated that the bornite structure can be likened qualitatively to a sphalerite-type skeleton containing layers of ionically bound interstitial atoms. Taking the sphalerite-bornite analogy one step further, he said that the 'interstitial' ionic $M_{11}$ atoms in bornite would seem to be Cu(I) because the preferred coordination of Cu(I) is tetrahedral. The remaining Fe and Cu atoms are therefore distributed among the $M_1$ and $M_{111}$ sites.

Manning proposed to write the structure as: $(Cu_3FeS_4)^{2-}2Cu^+$.

Electrical measurements have shown that bornite has the properties of a semiconductor. Therefore $Cu^+$ must partake in the tetrahedral coordination of the sphalerite-type skeleton. The electronic configuration of the free S atom is $3s^2 3p^4$ so that two additional electrons can make up the four tetrahedrally oriented electron pairs. He said that the sphalerite type skeleton of bornite is therefore one of Cu(I) and Fe(III).

This sphalerite-type skeleton ($Cu_3FeS_4$) of bornite can be derived from the structure of chalcopyrite ($CuFeS_2$) by replacing four (0 $\frac{1}{2}$ 3/4) iron atoms with copper atoms.

1.4.6. The Structure of Chalcopyrite

The low temperature, α- form of Chalcopyrite has a complicated tetrahedral structure which is essentially a super lattice on that of zinc blende. The sulphur atoms occupy the same sites as in zinc blende while the copper + iron atoms are to be found on the former Zn sites, arranged in an orderly way. Thus each sulphur atom is surrounded by four metal atoms, two copper and two iron, at the corners of a nearly regular tetrahedron, while each metal

atom is similarly surrounded by four sulphur atoms.

Its unit cell is an elongated tetragonal prism containing four molecules, with dimensions, according to Pauling and Brockway [150], of a = 5.24Å and c = 10.30Å. The doubled c compared to the a axis is an expression of the way atoms alternate with one another in the metallic planes normal to this axis. A recent refinement of the crystal structure of chalcopyrite gave the following crystal data[151]

Formula : $CuFeS_2$

Space group : $I\bar{4}2d$ (No.122)

Cell dimensions: a = 5.289, c = 10.423

Interatomic distances:

Cu-S = 2.302, Fe-S = 2.257

These metal-sulphur distances are significantly closer than those reported previously e.g., from Pauling and Brockway: Cu-S = 2.32Å, Fe-S = 2.20Å. Stereochemical evidence also indicated that the structure exists in a strong covalently bonded configuration which has an effective ionic state between $Cu^{+}$ $Fe^{3+}S_2^{2-}$ and $Cu^{2+}Fe^{2+}S_2^{2-}$, in agreement with the suggestions of other workers[150, 152, 153] but at variance to Frueh's approach in terms of zone theory[154]. A unit cell model of the structure is shown in Figure 18.

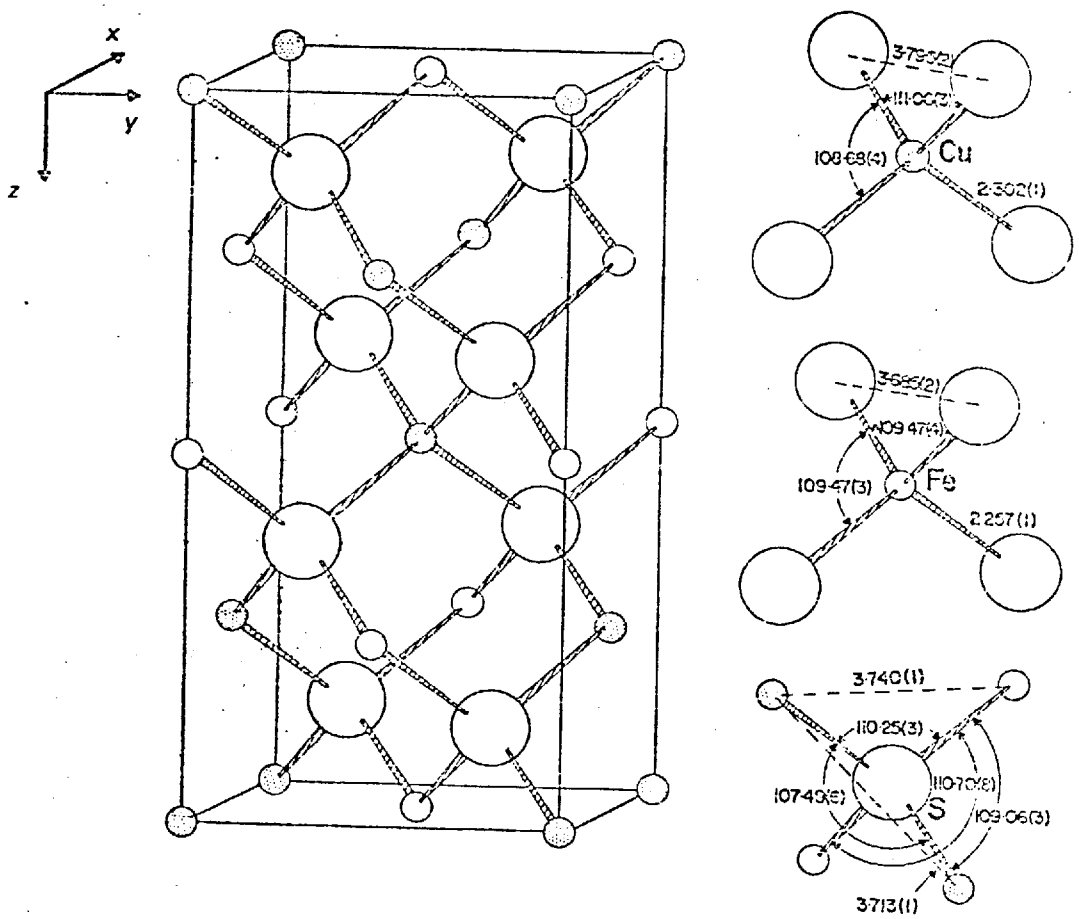


(a) (b)

FIGURE 18 : (a) Unit cell model showing crystal structure of Chalcopyrite. Hall and Stewart[151].

(b) Interatomic bond lengths and angles of each atom in Chalcopyrite. Hall and Stewart[151].

## 1.5. Phase Relations.

### 1.5.1. The Cu - Ag - S System.

The phase relations in the Cu - Ag - S system have been studied using synthetically prepared materials[133, 139, 140, 143] and by investigations into the mineralogy of naturally occurring silver deposits[155]. As mentioned earlier, Schwartz[139] synthesised stromeyerite from $Ag_2S$ and $Cu_2S$ but cast doubt on the existence of jalpaite Several experiments were made to determine what extent $Cu_2S$ and $Ag_2S$ are soluble in eachother. From the X-ray studies it seemed that considerable solubility occurs at both ends of the system $Cu_2S$ - $Ag_2S$. The general limits seem to be about 20 per cent $Cu_2S$ soluble in $Ag_2S$ and 15.per cent $Ag_2S$ soluble in $Cu_2S$, before a second phase, stromeyerite, appears.

Suhr[140] prepared samples with compositions from acanthite $Ag_2S$ to chalcocite $Cu_2S$ from the chemically pure elements by compressing mixtures into pellets and heating. The resulting X-ray diffraction data contradicted the findings of Schwartz in that no appreciable substitution for copper sulphide in silver sulphide or silver sulphide in

copper sulphide occurred. At the composition of $Ag_{95}Cu_5S_{50}$, jalpaite and a trace of free silver appear with acanthite, while at $Ag_5Cu_{95}S_{50}$ stromeyerite, copper and unidentified phase 'B' appeared with no chalcocite. Suhr also found that the stromeyerite and jalpaite have very limited solid solution fields. Two unknown compounds A and B were found. A copper-rich compound (B) between chalcocite and stromeyerite, and a silver rich compound (A), later assumed to be the same as Djurle's β-phase and called mckinstryite (section 1.4.4).

Djurle[133] identified three tenary phases $Ag_{1.55}Cu_{0.45}S$, $Ag_{1.2}Cu_{0.8}S$, and $Ag_{0.93}Cu_{1.07}S$, and indicated that the modifications above the highest transition temperatures (290-310°C, 120-143°C and 180°C respectively) all belong to a face centred cubic phase $(AgCu)_2S$. From the data obtained from many Guinier powder photographs Djurle constructed a phase diagram for room temperature (20°C).

Skinner[143] conducted the most extensive investigation into the Cu - Ag - S system and found his observations to be in complete agreement with those of Djurle. The phases

identified by Skinner at 25°C are listed below:

| Phase | formula | Crystallography |
|---|---|---|
| Covellite, cv | CuS | Hexagonal |
| Digenite, dg | $Cu_{1.8}S$ | Isometric |
| Djurleite, dj | $Cu_{1.96}S$ | Low symmetry |
| Chalcocite, cc | $Cu_2S$ | Orthorhom bic |
| Jalpaite, jp | $Cu_{0.45}Ag_{1.55}S$ | Tetragonal |
| Stromeyerite, strm. | $Cu_{1+x}Ag_{1-x}S$ | Orthorhombic |
| β-phase(mckinstryite), β | $Cu_{0.8}Ag_{1.2}S$ | Orthorhombic |
| Acanthite, ac | $Ag_2S$ | Monoclinic |

Skinner found that the solubility limit of $Ag_2S$ in chalcocite was 1.87 ± 0.37 mole% $Ag_2S$ at 63°C. The stable assemblages in the ternary system at room temperature are shown in Fig 19(b). Native silver is in equilibrium with chalcocite, stromeyerite, β(mckinstryite), jalpaite and acanthite. The two phase field Ag + chalcocite forbids the existence of Cu with stromeyerite, jalpaite, β(Mckinstryite), or acanthite. The join chalcocite-stromeyerite forbids the existence of either Cu or Ag with Djurleite, or covellite. In the sulphur rich assemblages, covellite coexists stably with digenite, stromeyerite, β(Mckinstryite), jalpaite

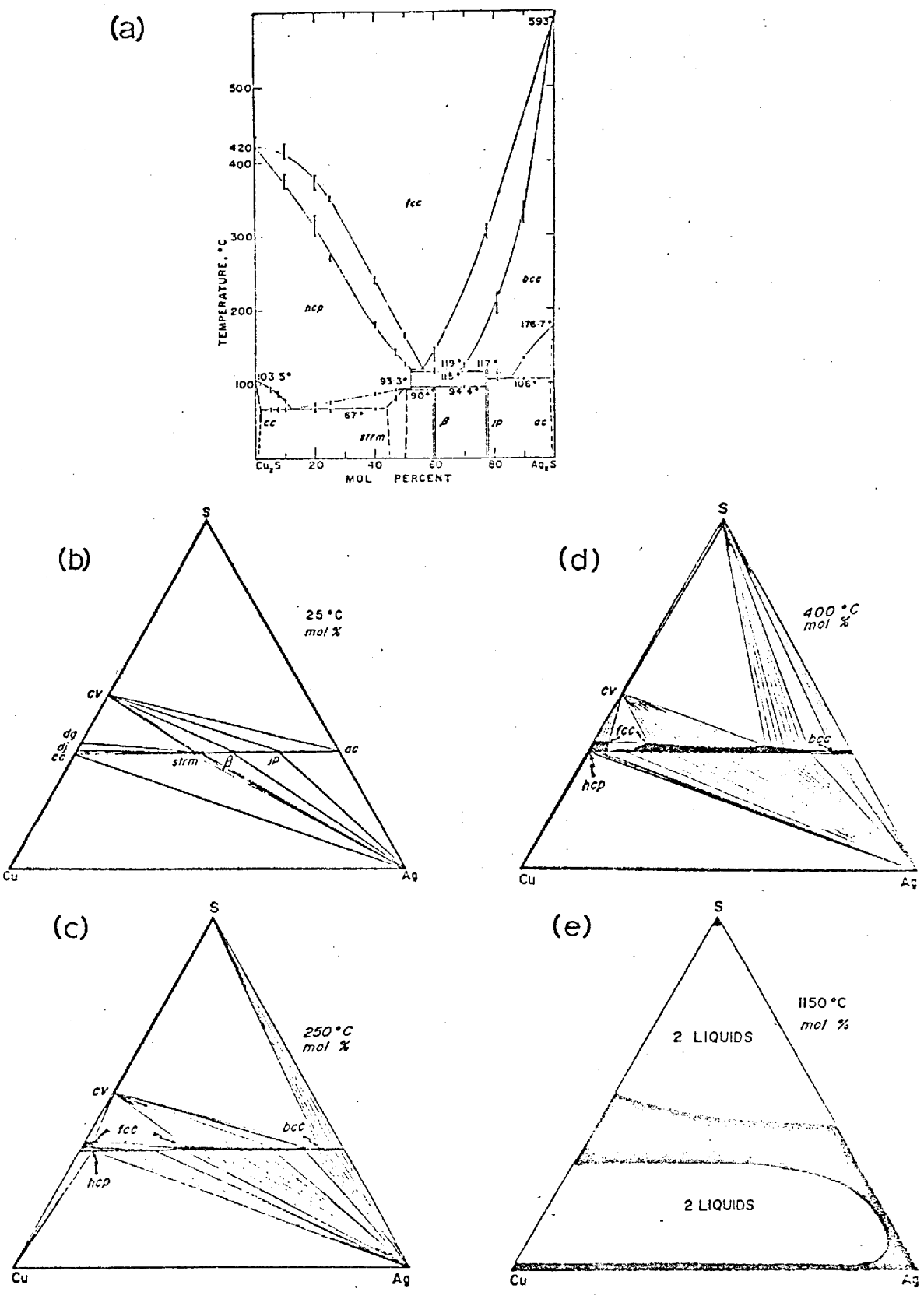


FIGURE 19 : (a) The binary system $Cu_2S$ - $Ag_2S$. Skinner[143].

(b) Cu - Ag - S system at 25°C. Djurle[133].

(c) Cu - Ag - S system at 250°C. Skinner[143].

(d) Cu - Ag - S system at 400°C. Skinner[143].

(e) Cu - Ag - S system at 1150°C. Skinner[143].

and acanthite. Native sulphur can coexist stably only with covellite or acanthite.

The only known ternary compounds of Cu, Ag and S lie along the composition join $Cu_2S$-$Ag_2S$ and a detailed examination by Skinner of this binary join elucidated many of the essential features of the ternary system at higher temperatures. No quenching procedure was discovered which allowed the retention of high temperature phases at room temperature, however it was possible to determine most of the essential phase relations by a careful, high temperature X-ray diffraction study and by examination of the distribution of low temperature breakdown products in quenched samples. The structural changes and inversion temperatures at the compositions of stromeyerite, jalpaite and mckinstryite have been reported in previous sections and Skinner interpreted the results by the phase diagram as shown in Fig 19(a) for the $Cu_2S$-$Ag_2S$ join.

The high temperature phase relations in the system Cu-Ag-S are dominated by the phase fields of three solid phases with extremely wide compositional ranges.

Each of these three phases is characterised by a distinctive kind of ordered sulphur lattice within which a disordered array of cations is distributed over a number of possible sites. There is a hexagonal close packed structure type (hcp) similar to that of high chalcocite, a face centred cubic structure type (fcc) similar to that of high digenite and a body-centred cubic structure type based on that of the $Ag_2S$II modification, $\alpha$-$Ag_2S$, of silver sulphide.

As the temperature is raised the general phase relations do not change markedly from those at 25°C. The h c p phase first appears at 67°C and following the breakdown of Djurleite at 93°C, the stromeyerite inversion at 93.3°C and the chalcocite inversion at 103.5°C, it exists as a broadfield form $Cu_2S$ to $Cu_{0.96}$-$Ag_{1.04}S$. The inversion of digenite to an f c c structure is completed at 83°C, and above the chalcocite inversion temperature a f c c field around the digenite composition is in equilibrium with the broad h c p field. A second f c c field appears at 119°C at a composition of 44 mol% $Cu_2S$ + 56 mol% $Ag_2S$ producing a stable assemblage of two f c c fields which

remains stable up to an unknown temperature above 420°C, at which the two f c c fields merge.

The disposition of the lines between the expanding h c p, f c c and covellite fields is shown in Fig 19(c) for 250°C. The tie lines retain the same general orientation as at room temperature, with Ag remaining in equilibrium with a h c p phase close to $Cu_2S$ in composition and covellite remaining in equilibrium with a b c c phase close to $Ag_2S$ in composition. Two fields for the f c c phase have developed, one around digenite composition and the others along the $Cu_2S$-$Ag_2S$ join, enclosing the compositions of both stromeyerite and β. At 325 ± 25°C the assemblage covellite + b c c phase becomes unstable and is replaced by the assemblage S + f c c phase. The composition field for the b c c phase continues to shrink with increasing temperature, as does the h c p phase field, while the two f c c phase fields increase rapidly in extent until at 400°C they are the dominant phases in the diagram as shown in Figure 19(d).

With further increase in temperature the

covellite + f c c phase shrinks rapidly, being replaced by f c c phase + S, until by 510°C, just above the covellite breakdown, only a small b c c field remains and liquid sulphur is in equilibrium with a broad band of f c c phases whose fields stretch from $Cu_2S$ to $Ag_2S$. After the inversion of b c c sulphur rich argentite at 622°C, a broad f c c field extends as a belt across the ternary diagram. Both Cu and Ag remain as stable solids.

The first appearance of a liquid phase other than sulphur is not known with certainty. The last f c c phases on the Ag-S sideline and Cu -S sideline disappear at 838°C and 1,129°C respectively, and a single homogenous liquid field exists along the Cu - Ag sideline above the melting point of Cu at 1083°C.

Along both the Ag - S and Cu - S sidelines, two regions of liquid immiscibility occur, the liquids having compositions close to S, to $Cu_2S$ or $Ag_2S$ and to Cu or Ag, respectively. Skinner considered the possible phase relations at 1150°C to be as in Figure 19 (e).

Rojkovic[155] has recently studied silver mineralization in a U - Ni - Co - Bi - Ag deposit using electron-probe microanalysis and microscopic techniques. The assemblages of the silver minerals were in good agreement with those found in laboratory studies. His measurements confirmed the composition of stromeyerite as $Cu_{1+x}Ag_{1-x}S$ and that of Mckinstryite as $Cu_{0.8+x}Ag_{1.2-x}S$.

Diez[156] studied the Cu - Ag - S system between 200 and 450°C and found four phases, other than the metallic phases and molten sulphur, which were derived from the following phases of the binary systems Ag - S and Cu - S : (1) cubic $Cu_2S$, with an f c c lattice of S ions; (2) hexagonal $Cu_2S$; (3) $Ag_2S$, with a b c c lattice of S ions; and (4) CuS, covellite. It can be seen that these findings are in complete agreement with Skinner's results.

1.5.2. The Cu - Fe - S system.

The phase relations in this ternary system have been studied in great detail from 1100°C to 25°C, but it still remains one of the most confusing systems and many

questions remain unanswered.

The tie lines between the stable phases at 700°C are shown in Fig. 20(b) and those at 25°C in Fig. 20(a). The first figure was taken from Yund and Kullerud[157] and the second from Barton and Skinner[158]. Assemblages consisting of two condensed phases are indicated by numeral '2', and the phases have been given the following abbreviations:

| Phase | Abbreviation | Composition | Crystallography |
|---|---|---|---|
| Chalcocite | cco | $Cu_2S$ | Orthorhombic |
| Djurleite | djur | $Cu_{1.96}S$ | Low symmetry |
| Digenite | dig | $Cu_{1.8}S$ | Isometric |
| Covellite | cov | CuS | Hexagonal |
| Pyrrhotite | po | FeS | Hexagonal |
| Bornite | bnt | $Cu_5FeS_4$ | Tetragonal |
| Bornite | bn | $Cu_5FeS_4$ | Isometric |
| Idaite | id | $Cu_{5.5}FeS_{6.5}$ | Hexagonal |
| Chalcopyrite | Cpt | $CuFeS_2$ | Tetragonal |
| Chalcopyrite | Cp | $CuFeS_2$(?) | Isometric |
| Cubanite | Cbt | $CuFe_2S_3$ | Tetragonal |

It should be noted that idaite in these diagrams has been given the formula $Cu_{5.5}FeS_{6.5}$ and not $Cu_3FeS_4$ as suggested by Sillitoe and Clarke[159], and Levy[160].

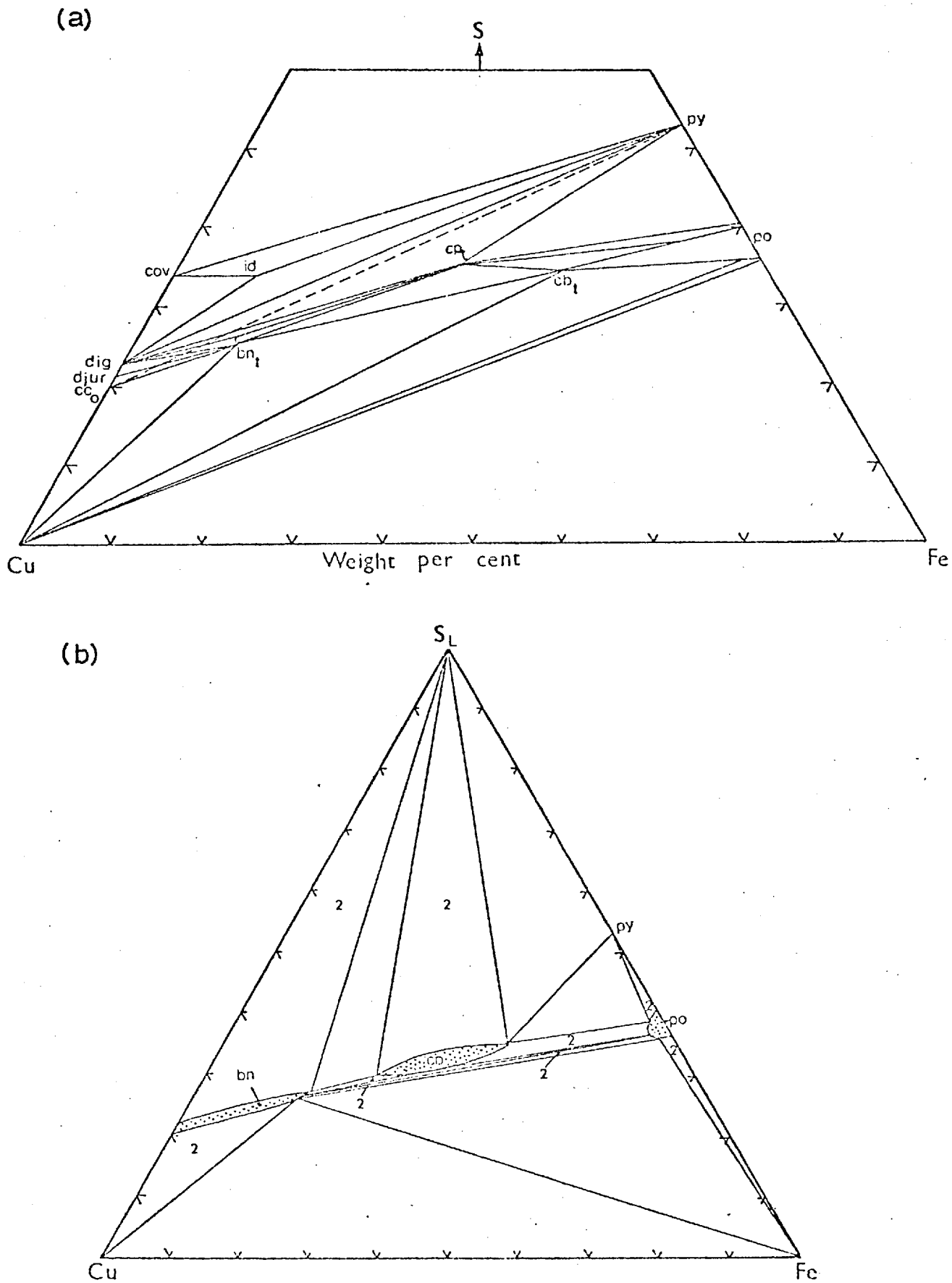


FIGURE 20 : (a) Phase relations in the Cu – Fe – S system at 25°C. Barton and Skinner[158].

(b) Phase relations in the Cu – Fe – S system at 700°C. Yund and Kullerud[157].

The main features of the Cu - Fe - S phase relations can be described in terms of the three principal solid-solution series, a pyrrhotite solid solution field, a chalcopyrite solid solution field and a bornite solid solution field (marked po, cp and bn in Fig. 20(b)).

The chalcopyrite solid solution field extends from a composition of $CuFe_2S_3$ (cubanite) to a composition with a Cu/Fe atomic ratio of almost 2/1. This solid solution field has a sphalerite type structure and occurs only at high temperatures (above 550°C). At lower temperatures the field separates into two roots, a chalcopyrite root with compounds having a sphalerite type structure and a cubanite root with compounds having a wurtzite-like structure.

The bornite solid solution field includes, above 290°C, chalcocite ($Cu_2S$) digenite ($Cu_{1.85}S$) and bornite ($Cu_5FeS_4$). At about 700°C, extensive solid solution of chalcopyrite ($CuFeS_2$) in bornite ($Cu_5FeS_2$) extends the bornite solid solution field to a Cu/Fe ratio of less than 3.

All three solid-solution fields have marked variations in their metal/sulphur ratios and copper/iron ratios. In ore deposits, none of the solid solution fields are quenched because they reequilibrate by exsolution and internal reactions to yield compositions consistent with much lower temperatures. This is consistent with the highly cation disordered structures in which the energy barriers are so small between the ordered and disordered forms, that the disordered states cannot be quenched.

More recently, Cabri[161] has studied the phase relations in the central portion of the Cu - Fe - S system at 100°C and 600°C and has shown that at low temperatures, the minerals chalcopyrite ($CuFeS_2$), cubanite ($CuFeS_3$), talnakhite ($Cu_9Fe_8S_{16}$), mooihoekite ($Cu_9Fe_9S_{16}$) and haycockite ($Cu_4Fe_5S_8$) are stable phases.

1.5.3. The Ag-Fe-S system

Taylor[162, 163] has studied the phase equilibria and mineral assemblages in the temperature ranges 150 - 700°C and 700°C - 1200°C. The ternary compounds of silver and

iron that have been identified are friesite ($Ag_2Fe_5S_8$), argyropyrite ($Ag_3Fe_7S_{11}$) and sternbergite ($AgFe_2S_3$), often known as argentopyrite and sometimes given the formula $AgFeS_2$ (182).

Taylor found that no ternary solid phases are encountered above 150°C.

1.5.4. The Ag - Cu - Fe - S system.

Only one paper has been found on this system. This was work conducted by Ludor (164) in 1924, who heated four different mixtures of Cu - Ag - Fe and S to their melting points, analysed the liquids, and then examined the solid phases formed on cooling. He concluded that molten mixtures in the system Ag - Cu - Fe - S almost invariably separate into two layers, the silver tending to concentrate in the lower layer and the iron in the upper. In the solid state, quaternary equilibrium seemed to exist between Ag, Cu, Fe and $Ag_2S$-$Cu_2S$ - FeS mixed crystals, and between Ag, Fe, FeS and $Ag_2S$-$Cu_2S$ - FeS mixed crystals. Ternary equilibrium existed between Ag, Cu and sulphide mixed crystals, and between Ag, FeS and sulphide mixed crystals; and

binary equilibrium between Ag and sulphide mixed crystals, and between Cu and sulphide mixed crystals.

No evidence has been found in the literature for a quaternary compound of Cu, Ag, Fe and S, although the four elements do exist together in sulphosalts[15] such as Tetrahedrite - tennantite $(Cu,Fe,Ag)_{12}(SbAs)_4S_{13}$ and Stylotypite $(Ag, Cu, Fe)_3SbS_3$.

## SECTION 2

## EXPERIMENTAL PROCEDURE.

### 2.1. Synthesis of Sulphides

The sulphides of copper, iron and silver and mixtures which were studied in the leaching experiments were all synthesised from the pure elements. The specifications of the materials are given in section 2.5.1. Before use, the iron sponge was reduced in a stream of hydrogen at 500°C.

The syntheses were carried out in vacuum at a temperature of 900°C in a two compartment silica vessel. The sulphur powder was placed in the smaller compartment and then the appropriate metals were introduced into the larger compartment. The separation of sulphur and metal was necessary to avoid the very fast, and possibly explosive reaction which might occur with direct contact between molten sulphur and the metals as the temperature increased.

The silica vessel was evacuated with an oil-diffusion pump and sealed with an oxygen torch. The system was then placed within the constant temperature zone of a horizontal

electric tube furnace designed to reach 1100°C. The heating was controlled by a transitol electronic controller and the temperature of the silica vessel checked with a 13% Pt - Pt/Rh thermocouple connected to a potentiometer.

A similar heating procedure was used for all the syntheses. The temperature was first increased to the range 550 - 600°C and kept at this temperature until all the sulphur had reacted with the metal in the vessel since exceedingly high pressures are exerted by pure sulphur vapour at higher temperatures (165). The end of this period was indicated by the silica vessel becoming clear of sulphur vapour. This usually took from three to four days.

Then the temperature was slowly increased to 900°C and kept there for several days, the length of time varying from synthesis to synthesis. The cooling procedures of the different syntheses were also slightly different.

Three separate syntheses were carried out using the above procedure with the starting amounts as shown below: (in grams)

| Element | | Charge A | Charge B | Charge C |
|---|---|---|---|---|
| Copper | (rod) | 52.7296 | 52.5728 | 20.8320 |
| Silver | (grain) | 1.0173 | 10.0064 | 30.7385 |
| Iron | (sponge) | 9.3744 | 10.2776 | - |
| Sulphur | (powder) | 21.5289 | 23.6032 | 9.8246 |

2.1.1. Charge A - Silver-doped Bornite.

Charge 'A' was used in an attempt to introduce silver as an isomorphous replacement for copper in the bornite lattice. The amounts of iron and sulphur required were calculated from the weights of copper and silver using the formula $(Cu,Ag)_5 FeS_4$ i.e., 50 mole % copper + silver, 10 mole % iron and 40 mole % sulphur.

The heating procedure was as described above and the silica vessel and its contents were kept at 900°C for ten days. The cooling procedure was identical to that used by Ugarte[11] in the preparation of pure synthetic bornite.

After the ten days at 900°C, the temperature was lowered slowly (approximately 0.5°C/minute) to 700°C, maintained at this for about 10 hours, then cooled to 200°C for a further six hours and finally cooled slowly to room

temperature. This procedure takes account of transformations occurring in the bornite structure as it is cooled, and ensures a homogeneous product.

The final product consisted of a single solid crystalline mass having the pinkish-brown to brown colour associated with the fresh fracture of naturally occurring bornite [166]. On opening the tube in air the crystals immediately changed to the violet and bluish colours normally associated with natural bornite surfaces.

On fracturing the solid mass, the pinkish-brown colour appears on the fracture surface but soon stains to the violet-bluish colour. Fracturing the solid also showed two holes left in place of the two copper rods which confirmed that the mechanism of formation of the sulphide phase was by diffusion of the metal to the sulphur gas - solid interface, as reported by King[9] for chalcocite, Ugarte[11] for bornite and Ferreira[12] for chalcopyrite.

To check the homogeneity of the material X-ray diffraction analysis and microscopic

examinations were carried out on a number of samples from different areas of the solid mass. The X-ray diffraction patterns had only the lines of tetragonal bornite in good agreement with the data of Ugarte and of the A.S.T.M. file (FigureC-1.1 and TableB-1.1). The microscopic examination did not reveal the presence of any other phase.

Atomic absorption analysis of solutions of the material in nitric acid gave an analysis in good agreement with the initial amounts of the elements used, which were Cu 62.29, Ag.1.20, Fe 11.07 and sulphur 25.43 weight per cent.

Finally the homogeneity of the material was checked by electron probe microanalysis. A number of samples of the material were mounted, polished and carbon coated before use. It at once became evident that the material was being damaged by 'normal' beam currents of 90-100nA at 25 KV. During this time the Ag count increased from a very low level to quite a high one, while the Cu count dropped by about a third. This occurred within about 10 - 15 seconds of the beam being focussed on the sample surface, and thus introduced serious errors in the spot

counts for these elements at fixed positions.

However, it was found that by reducing the current to 15nA only (still at 25 KV), this effect was almost eliminated as far as copper was concerned, but many of the measurements still showed a slight increase in Ag count during the one minute counting period resulting in silver contents higher than expected. The measurements were made using pure copper, silver and iron standards and a pure CdS standard for sulphur. After treatment of the counts for the corrections discussed in section 2.4.3, typical analyses were as follows:

| | Weight per cents (Atomic per cents in brackets) | | | |
|---|---|---|---|---|
| Sample | Cu | Ag | Fe | S |
| 1 | 62.3(50.4) | 2.9 (1.4) | 11.2(10.3) | 23.7(3.80) |
| 2 | 61.5(50.1) | 4.1 (2.0) | 11.1(10.3) | 23.3(37.7) |
| 3 | 62.8(50.5) | 2.0 (1.0) | 11.3(10.3) | 24.0(38.2) |
| Initial | 62.29(49.44) | 1.20(0.56) | 11.07(10.00) | 25.43(40.00) |

It should be noted that a low beam current reduces reproducibility appreciably and this, together with the beam current effect described above, probably accounts for the variation in the analyses.

Better checks for the homogeneity of the material were obtained by electron probe scans across the polished surface of the material. Reasonable traces for Cu, Fe and Ag were obtained on selected areas of the specimens. Typical traces are shown in Figure 27 which clearly shows the erratic behaviour of silver, due not only to the electron beam current effect but also the fact that the silver is present in only small quantities and a somewhat magnified scale had to be used for the trace.

Despite these problems with the electron probe microanalysis, it is evident that the results, together with the X-ray diffraction and microscopic observations, indicate that the synthetic material is a homogeneous bornite containing silver as an isomorphous constituent distributed homogeneously throughout the structure.

2.1.2. Charge 'B' - Mixed Sulphide Material.

Following the apparent success of incorporating 1.20 weight per cent of silver in the bornite lattice, a second synthesis was carried out using a much higher silver content. The amounts of iron and sulphur were again

calculated from the weights of copper and silver using the formula $(Cu, Ag)_5 FeS_4$. The contents of the charge for the synthesis gave the following weight per cents : Cu 54.50, Ag 10.37, Fe 10.65 and sulphur 24.47.

The preparation of the charge and the heating and cooling procedures were exactly as for charge 'A'. The final product was a single mass of blue-grey colour with a much finer crystallinity than the previous synthetic material. A fresh fracture had the same pinkish brown colour as the silver-doped bornite, charge 'A', and like the previous material it turned a bluish colour after a while. The fracture also showed the holes left by the diffusion of the copper rods but, in addition, it also showed a much greater porosity than was noticed for the previous synthetic material. Photographs of pieces of this material in Figure 21 illustrate these observations.

Analysis by atomic absorption of the solutions obtained by dissolving samples in nitric acid gave good agreement with the starting amounts of the elements. However, microscopic, X-ray diffraction and electron

(a)

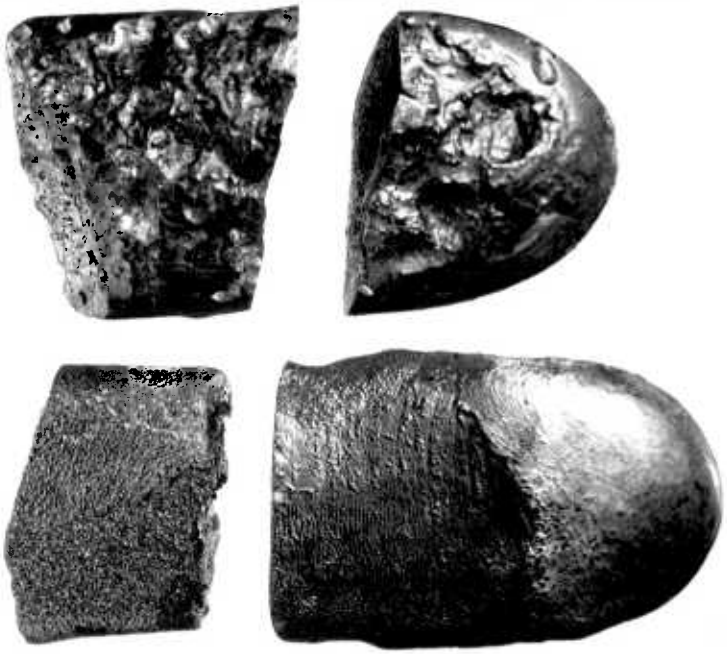

(b)

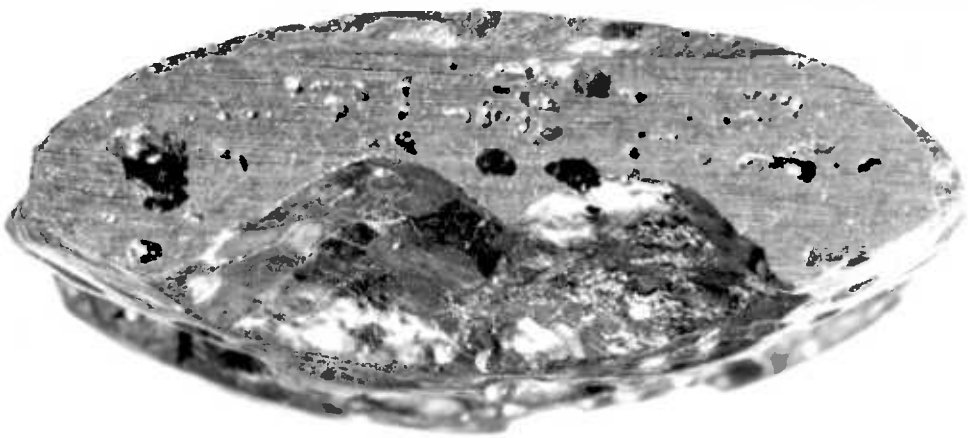

(c)

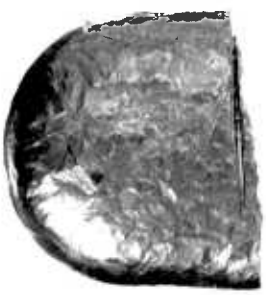

FIGURE 21 : (a) External appearance of synthesised Mixed Sulphide Material, upper and lower surfaces (approx. x2).
(b) Cross-sectional view of Mixed Sulphide Material (approx. x5).
(c) External appearance of synthetic Stromeyerite, upper and lower surfaces (approx. x2). 'Wire' silver in upper piece, upper left hand corner.

probe observations showed that the material was not the homogeneous solid it first appeared to be.

Three phases were visible on microscopic observation of polished samples. These were a yellow phase in the form of elongated, interconnnected grains, a light-coloured matrix which turned bluish violet on leaving the sample in air after polishing, and a bluish grey phase. The latter phase appeared in two forms, as a 'band' between the yellow phase and the matrix, and as very fine lamellae, with a definite orientation, in the matrix. On crushing the material to a particle size of -180 + 125 microns and examining the polished particles, it appears that there are no apparent preferential cracking directions in the solid (figure C-215). The fine lamellae of the blue grey phase appear throughout the matrix. Examination of a number of polished samples from different areas of the material showed that all three phases were distributed throughout the solid in approximately the same relative amounts.

The phases were identified by X-ray

diffraction. The X-ray pattern for the material could only be explained by a mixture of three sulphides, bornite, $Cu_5FeS_4$, chalcopyrite, $CuFeS_2$ and stromeyerite $Cu_{1.07}Ag_{0.93}S$. (Figure C-1.5 and Table B-3.1). The fact that the matrix turned bluish violet in air indicated that this was bornite, the yellow phase was obviously chalcopyrite and hence stromeyerite was the blue-grey phase. By assuming that all the silver had gone into the stromeyerite, the relative amounts of the sulphides were estimated from the initial amounts of the elements. This gave 70% bornite, 20% stromeyerite and 10% chalcopyrite, in fair agreement with visual estimates.

This identification of the constituents of the material was supported by the electron probe microanalysis. From observations, on an oscilloscope, of the back-scattered electron intensities it was demonstrated that the matrix phase consisted of a fine 'criss-cross' pattern of two atomic numbers, but which was too fine to sort out quantitatively, and that the yellow phase was surrounded by a phase of much higher atomic numbers than the rest of the sample.

Figure 59 (section 6.5) compares the electron probe traces for copper and sulphur, and iron and silver, across a sample of the material. The copper-sulphur trace shows three distinct regions. One has a high sulphur but low copper content; another has a low sulphur but high copper content; and the third seems to occur between the first two phases and has a slightly lower sulphur content. The iron-silver traces show that the silver and iron contents are opposed, i.e., areas of high silver have low iron contents, and vice versa. These observations are consistent with the material being a mixture of bornite, chalcopyrite and stromeyerite. The iron-silver traces also indicate that as well as surrounding areas of high iron content (chalcopyrite) the silver phase is present as a fine intergrowth throughout the material.

As with the previous synthetic material (Charge 'A'), this mixed sulphide material was damaged by beam currents of 100nA. Hence for quantitative measurements of the elements by spot counts at fixed positions, a 30nA beam current was used. This seemed to reduce the damage considerably. The standards used were

pure Cu, Fe and Ag and CdS for sulphur. Even after the corrections (section 2.4.3) however, the measurements must be considered as inaccurate for a number of reasons.

First of all the low beam current reduced reproducibility, as has already been mentioned; Secondly, the spot counts for a particular phase may be affected by 'pickup' from the surrounding phases, the effect depending on the relative sizes of the beam diameter and the grain of the phase being measured; and finally the results were affected by the method that had to be used for selecting the area required for measurement. This was done by first obtaining a back scattered electron intensity picture, selecting the area and then switching to the counting devices. This introduces an extra error due to defocussing, the error being greatest for the sulphur measurements.

The analyses obtained for the various phases were as follows:

| Phase | Weight per cent (Atomic per cent in brackets) Cu | Ag | Fe | S |
|---|---|---|---|---|
| Matrix (1) | 60.58 | 10.51 | 12.34 | 16.57 |
| | (53.30) | ( 5.45) | (12.35) | (28.50) |
| Matrix (2) | 64.35 | 6.63 | 12.56 | 16.46 |
| | (55.68) | ( 3.39) | (12.41) | (28.32) |
| Bornite | 63.33 | - | 11.12 | 25.55 |
| | (50.00) | - | (10.00) | (40.00) |
| 'Yellow (1) | 45.76 | 1.28 | 32.71 | 20.25 |
| | (36.54) | ( 0.61) | (30.05) | (32.40) |
| 'Yellow' (2) | 42.85 | 2.07 | 37.98 | 17.10 |
| | (35.36) | ( 1.00) | (35.66) | (27.97) |
| Chalcopyrite | 34.64 | - | 30.42 | 34.94 |
| | (25.00) | - | (25.00) | (50.00) |
| 'Silver' (1) | 30.18 | 57.18 | 1.30 | 11.34 |
| | (34.33) | (38.38) | ( 1.69) | (25.61) |
| 'Silver' (2) | 45.33 | 37.04 | 5.24 | 12.39 |
| | (46.41) | (22.34) | ( 6.10) | (25.14) |
| Stromeyerite | 33.93 | 50.06 | - | 16.00 |
| | (35.67) | 30.99) | - | (33.33) |

All the samples gave low sulphur contents which can be explained largely by the de-focussing effect. The high silver contents of the matrix are obviously due to the presence of

lamellae of stromeyerite in this phase, and the small percentages of iron in stromeyerite, and silver in the chalcopyrite can be explained by pickup from adjacent phases.

Although these results are not very helpful quantitatively, they do tend to confirm the conclusion based on the microscopic and X-ray diffraction analyses that this material 'B' is a bornite containing intergrowths of chalcopyrite and stromeyerite.

Since it was known that chalcopyrite, bornite and stromeyerite all enter into extensive solid solutions at high temperatures, experiments were carried out to determine whether the copper, silver, iron and sulphur formed a quenchable single homogeneous phase at higher temperatures. 5 gram charges of the mixed sulphide phase were sealed in a small evacuated silica vessel and heated in a small muffle furnace. The temperatures used were 700 and 900°C. After four days at these temperatures the silica vessels were quenched in a bucket of distilled water. Microscopic examination of polished samples from both quench products, however, showed the same phases present

as in the original material although the chalcopyrite was now present as very fine blades or lamellae obviously aligned along certain crystallographic planes (the (111) planes according to Edwards [167]) in a way similar to the stromeyerite in both the original material and the quench products.

2.1.3. Charge 'C' - Stromeyerite.

Since the leaching behaviour of pure bornite and chalcopyrite are already well known it was decided to synthesise a pure stromeyerite for leaching in order to explain the leaching behaviour of the mixed sulphide material 'B'. The amounts of copper, silver and sulphur were calculated from the formula $Cu_{1.07}Ag_{0.93}S$. The synthesis procedure was as before but after four days at 900°C, the power to the furnace was interupted and the silica vessel and its contents cooled overnight in the furnace to room temperature, causing the vessel to crack.

The appearance of the final product suggested that the charge had become molten and resolidified. Its colour was a steel grey with a metallic lustre, similar to natural occurrences of the stromeyerite mineral [166].

Photographs in Figure 21 show that the upper surface was smooth while the underside was very shiny and contained a large number of holes. On opening the silica tube no change in colour occurred and a fresh fracture face gave the same steel grey colour with no change on standing in air.

All over the outer surface of the synthesised product, both upper and underside surfaces, there appeared to be 'growths' of some sort. These were fine strands which appeared to have diffused out of the main mineral. One of these can be seen in the upper mineral piece in Figure 21(C). On X-ray analysis these strands were found to be pure silver and it is thought that they are similar to the 'wire' silver which forms on the surface of argentite after heating and cooling [168].

X-ray analysis of the main solid product showed that its diffraction lines agreed with those for $Cu_{1.07}Ag_{0.93}S$ (Table B-2.1). A sample of the sulphide was dissolved in concentrated nitric acid for analysis by atomic absorption. This gave good agreement with the expected composition required for stromeyerite:

Cu, 33.93; Ag, 50.06; S, 16.00 weight per cent.

Microscopic examination of polished samples indicated the phase to be homogeneous. However the surface was covered in an intricate mass of blades or lamellae, resembling oleander leaves in shape, which has been noticed in natural specimens [166]. Electron probe micro-analysis showed no significant variation in the composition across these lamellae (Figure 44). The traces seem to indicate some variation in composition but this can be explained by the use of a low beam current to avoid damage to the sample. No attempts were made to obtain quantitative measurements by spot-counts because of this damage.

It was concluded that the material was a homogeneous phase of stromeyerite with a composition of $Cu_{1.07}Ag_{0.93}S$.

## 2.2 Leaching Procedure

The leaching experiments were carried out at atmospheric pressure in the temperature range 30 to 90°C. The apparatus consisted of a 250 ml. reaction vessel connected by means of a metallic clip to a five neck lid. The general arrangement of the apparatus is shown in Figure 22.

The central neck of the lid held a two-bladed glass stirrer for agitation of the leaching system. This was connected through a mercury (or silicone oil) seal and a rubber joint to a RZR laboratory stirrer, the speed of which could be varied from 170 to 1700 rpm. In all the leaching runs the stirrer speed was set and checked during the run by stroboscopic means using a Dawe Transistor stroboflash Type 1209D.

In the other four necks of the lid were a condenser to avoid evaporation, a baffle to ensure a turbulent regime in the solution and to keep the particles in suspension, a thermometer to check the temperature of the solution and, in the fourth neck, a tube for direct sampling of the solution by means of a pipette. The neck used for sampling was that opposite to

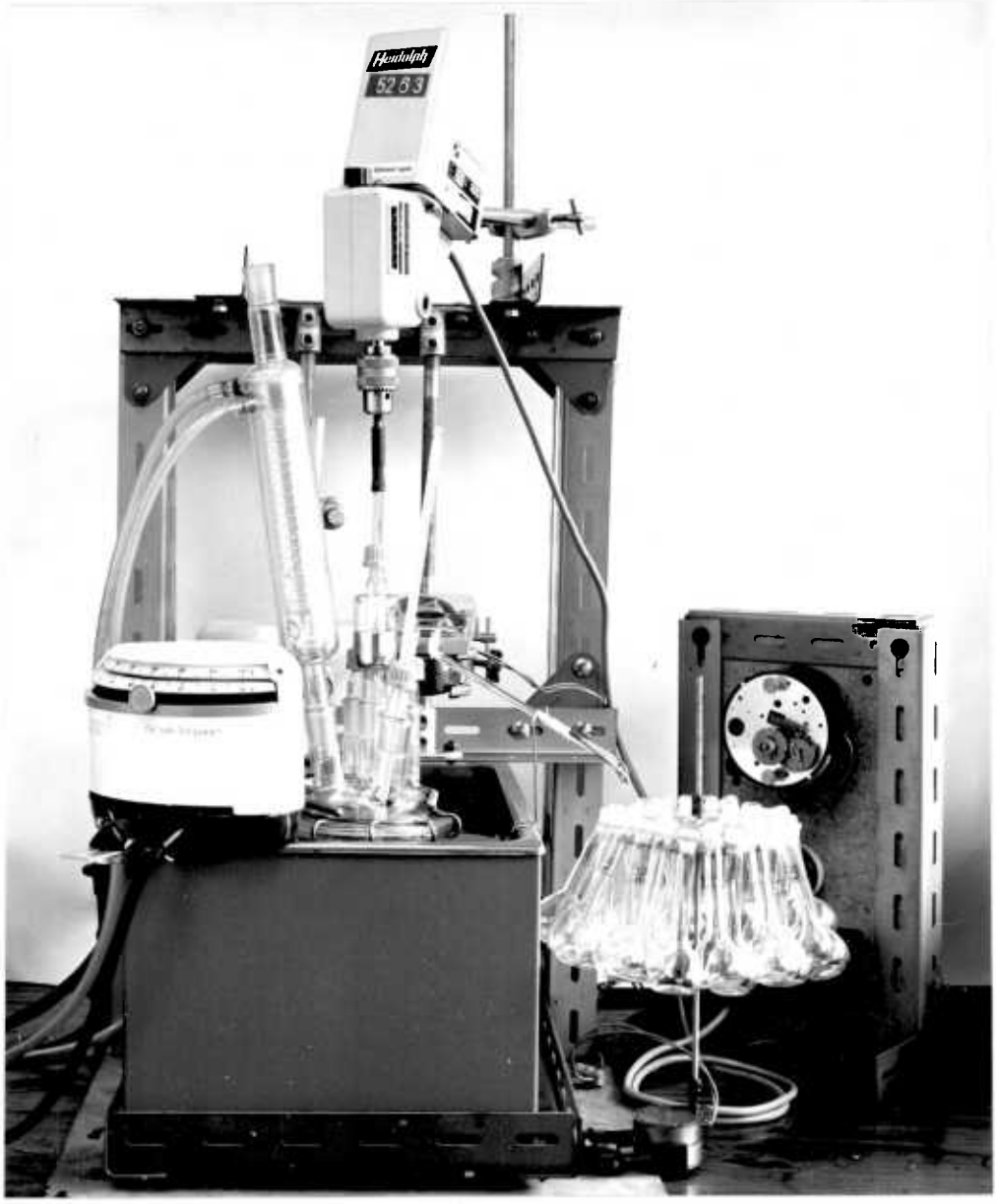


FIGURE 22 : The Leaching Apparatus. The set-up to the right of the oil bath could be used for automatic sampling of the leach solution.

the condenser.

This whole system was immersed in an oil-bath to the level of the vessel-lid joint. The bath capacity was 20 litres with internal measurements of 527 mm (length), 247 mm (width) and 202 mm (depth). The temperature of the oil was controlled by a Griffin Accurostat, a combination of a heater, pump and temperature sensor. The unit controlled temperatures in the range ambient to 95°C with a fluctuation, under optimum conditions, of 0.02 deg.C. The 1 KW tubular heater is protected by a liquid level cut-out device, and a safety overheat cut-out operates should the bath temperature rise 2 - 3 deg. C above the set point. Circulation of the bath liquid is given by a centrifugal pump with an output of 8 litres/minute.

Once the apparatus was assembled, 200 mls of the required leaching solution was introduced into the 250 ml reaction vessel through one of the necks. When the solution had reached thermal equilibrium with the thermostatically controlled oil-bath, the solid to be leached was added to the solution. The synthetic sulphide material had been crushed and sieved using 100 mm diameter

stainless steel sieves to obtain the required particle size range. This process was usually carried out only minutes before starting a leaching run, to avoid possible oxidation or other contamination of the particle surfaces.

The solid, usually 0.5 or 1 gram, was introduced into the system by means of a small funnel which was immediately rinsed with solution previously extracted from the reaction vessel to remove any adhering particles. Samples of the leaching liquor were extracted periodically using a 5 ml calibrated pipette. Prior to the sample-taking, the stirrer was switched off for a brief moment to allow the solid particles to settle so that none would be removed with the solution sample.

Whenever samples were taken the same volume of fresh leaching solution, kept at the temperature of the run, was injected into the reaction vessel to maintain a constant volume of solution. Calculations involving the determination of final concentrations took into account the dilution factors of the products.

In a certain number of the leaching

experiments samples of the solid particles were removed instead of samples of the solution. After allowing the particles to settle, small amounts were removed using a pipette with a wide orifice. These solid samples were used for X-ray diffraction, electron probe micro-analysis and microscopic examination.

At the end of the leaching run, the reaction vessel was removed from the oil bath and its contents filtered to separate the leaching solution and the final residue. The former was stored and the latter washed with distilled water and acetone and dried. With the residues that contained a considerable amount of elemental sulphur, it was found that identification of the other phases by microscopic techniques were made easier by removing this sulphur. Hence prior to the analysis of these residues, the elemental sulphur was dissolved in $CS_2$ using a Soxhlet extractor apparatus with single thickness 10 x 50 mm cellulose extraction thimbles for holding the residues.

The leaching apparatus was thoroughly washed after each experiment with a dilute solution of Decon 75 concentrate and rinsed with

distilled water and acetone.

Finally a few leaching experiments were carried out using samples of the synthetic stromeyerite mounted in Araldite resin. The purpose of this was to observe the effect of the leaching agent on one surface of the material. The same apparatus, described above for particulate leaching, was used. Solid slices of the sulphide material were obtained using an Anderman cutting bench. This had a diamond loaded slitting wheel driven by a 1/20th HP motor and cooled by a through flow of water.

These slices were placed in small Araldite mounts (approximately 1 cm diameter) with a certain length of polythene strip connected to the mount, by means of which the mount was 'dangled' through one of the necks in the reaction vessel lid with the polished sample surface in contact with the solution. After a certain length of time (up to 7 days) the samples were dissected at right angles to the leached surface and remounted and polished to show the extent of leaching into the solid slices of sulphide material. Microscopic and electron microprobe analyses were carried out on these mounted leached solids (sections 5.4 and 5.5).

2.3 Analysis of Solutions.

The solutions removed during the leaching runs and the final leach solutions were analysed for copper, silver, and sometimes iron, by atomic absorption spectrophotometry. The apparatus used was a single beam Perkin Elmer 290 B atomic absorption spectrophotometer with a graphical read-out on a Perkin Elmer model 56 pen recorder.

The wavelengths used were 324.7 nm for copper 248.3 nm for iron and 328.1 nm for silver. A multi-element Ag - Cu - Fe - Ni - Cr hollow cathode lamp was usually used for all analyses at an operating current of 10 MA. On a few occasions a copper single element lamp was used, with no significant difference, for the copper analyses.

Due to the closeness of the copper and silver wavelengths a spectral slit width of 0.2 nm was used with the multi element lamp to avoid interferences. An air-acetylene mixture was adjusted to obtain an oxidising (lean, blue) flame with a 2" burner.

Calibration curves of deflection versus

concentration were drawn, using standards prepared from 1000 ppm stock solutions. The same diluent was used for both the standard solutions and the aliquots of the leach liquor. These curves showed that the working ranges for Ag, Cu and Fe were linear up to 5 micrograms/ml and that the optimum conditions for the equipment used occurred in the working range 0 - 10 micrograms/ml for all three elements.

The leach liquor samples and final leach solutions were diluted to within this range using a Hook and Tucker variable diluter. With a sample volume range of from 0.05 to 1.0 mls and a maximum diluent volume of 10 mls, this enabled dilutions of up to 200 x to be used. The operation was always checked several times to ensure no errors occurred in the dilution.

The present work and previous work on the determination of silver and copper by atomic absorption spectrophotometry [169-172] indicate that none of the other ions existing in the solutions interfere with the analyses for these elements. The only interference was found in analysing for silver in solutions containing a very high chloride ion concentration. On

diluting with a 0.1M HCl solution, precipitation of some of the silver occurred in a few seconds. This was overcome by diluting with a solution of higher chloride concentration.

The leach solutions, not containing any ferric sulphate or sulphuric acid, were also analysed for a sulphate ion using a nephelometric technique. The experimental procedure described by Vogel [173] was rigidly adhered to. An 'EEL' Nephelometer head was used with readings of turbidity relative to a standard presented on the linear scale of an external 'EEL' Unigalvo, type 200.

The initial and final pH readings of the leach solutions were made using a Pye Model 78 pH meter connected to a Pye Ingold type 401 combined glass and reference electrode. The pH meter was also used for voltage measurements in an attempt to follow the change in the E.M.F. of the leach liquor in the reaction vessel as the leaching progressed. A calomel electrode and a platinum electrode were placed in contact with the solution through separate necks of the reaction vessel lid.

As will be reported later (section 3.1.2) these attempts although demonstrating the rapid formation of ferrous ions in the solution, were somewhat defeated by the formation of a jarosite precipitate, due to the presence of potassium ion from the calomel electrode, which had an inhibiting effect on the leaching reaction.

## 2.4. Analysis of Solids.

### 2.4.1. Atomic Absorption Analysis.

The equipment and conditions described in section 2.3. were also used for the analysis of copper, iron and silver in the leach residues and the original synthetic materials. A sample of the solid was attacked with sufficient hot concentrated nitric acid until complete dissolution of the solid had occurred. Usually 30 - 40 mls of the acid was required for a 0.05 gm sample. The dissolution was carried out in a Kjeldhal flask and the resultant solution was cooled and diluted with sulphuric acid (pH1) to within the range desired for direct determination by atomic absorption. A blank solution was also prepared for comparison.

### 2.4.2. Microscopic Analysis.

The leach residues and samples of the synthetically prepared materials were mounted in Araldite epoxy resin MY 753 using the Araldite hardner HY 951. The mounts were first ground on a Struers Lunn Minor grinding machine through a series of papers of standardised grits 220, 320, 400 and 600 and then polished on a Struers DP4 automatic polishing machine. 6 Micron and 1 micron DP cloths were used in turn using

Marcon diamond abrasive compound sprays with DP lubricant-red (oil base) for the 6 micron cloth and DP lubricant-blue (water soluble) for the 1 micron cloth. Great care had to be taken during the early grinding with residues that had been extensively leached otherwise the sample would 'disappear' due to the small size and brittleness of the particles.

Initial Microscopic observations of the polished samples were performed on a conventional reflected light microscope prior to photomicrography using a Reichert Universal camera microscope MeF. This is an inverted instrument fitted with a camera back and a Reichert Remiphot exposure meter. The microscope works with transmitted or reflected, normal or polarised light and is suitable for working from micro to oil immersion objectives.

Photomicrographs were taken on standard 5 x 4 plates and then printed. The colour photomicrographs were taken with a 35 mm Leica camera using Ektachrome High Speed Type B film (ASA 125) for slides which were then printed.

2.4.3. Electron Probe Microanalysis.

Electron probe microanalysis was performed on polished samples of the unleached synthetic materials and on the residues from the leach runs. Specimens for the Electron probe were prepared in exactly the same form as for a normal microscopic examination. In addition, the surfaces of the samples must be electrically conducting and to ensure this the samples were vacuum-sputtered with carbon.

The theory, development, and various experimental aspects of electron probe microanalysis have been discussed by many authors.[174,175] The main possible sources of error and its comparison with other techniques of local analysis have also been considered.[176]

In this study the instrument used was a JEOL model JXA -3A, made in 1967, fitted with scanning facilities. The probe diameter was approximately 1 micron and magnifications of from 300x to 2400x could be obtained. The apparatus gave a resolution of 1 micron for the electron images and a resolution of between 4 and 5 microns for the X-ray images. It could be used for the range of elements from sodium

to uranium (atomic numbers 11 to 92) and, under optimum conditions, gave an accuracy for quantitative analysis of ± 1% for amounts of elements greater than 10 weight per cent.

The instrument was used for quantititative measurements of Cu, Ag, Fe and sulphur at a number of fixed spots on the surface of samples. The intensities of the reflected X-rays were compared with similar reflections produced from pure standards. After adjustment for the background radiation, the 'raw count' data was processed by a computer program[177] which calculated the atomic and weight per cents after correcting for the following effects : (1) Absorption effect. (2) Atomic numbers effect; and (3) characteristic fluorescence factor.

The electron beam was also made to scan a preselected area of the sample while X-ray and backscattered electron data were monitored on an oscilloscope. In this way an area on the sample surface rather than a point could be studied. Electron Probe scans were recorded for Cu, Ag, Fe and sulphur across the various samples to find any inhomogeneity in the unleached materials and to show any change in the

distribution of the elements in the residues after leaching.

2.4.4. X-ray diffraction analysis.

The phases present in the unleached material and the leach residues were identified by the method of X-ray powder diffraction. The interplanar spacings (d - spacings) measured from the positions of the reflections on the X-ray powder photographs, together with the intensities of these reflections, were checked against the data given in the literature for known substances using the ASTM Powder Data file and an identification effected.

The camera used was a Multiple Guinier-De Wolff focussing camera.(178) This is of the type that uses X-rays from a focussing monochromator. A converging X-ray beam produced by reflecting the incident beam from a curved crystal monochromator, is transmitted through a specimen and the Guinier camera records the front reflection region of the spectrum.

The chief advantage of this type of camera is that the monochromator almost completely eliminates the white radiation in the beam,

with the result that X-ray patterns have a low background intensity. This allows very weak lines, such as superstructure lines, which would otherwise be masked by the background fog, to be observed. One disadvantage is that the camera only records the reflection range from $0^{o}$ to approximately $40^{o}$ of Bragg angle. However in the present work, this range was more than adequate for the identification of substances.

The camera was used in a horizontal position and was designed as a multiplecamera, consisting of four single camera units placed one above the other. Similarly four samples were mounted by means of sellotape one above the other in a cassette divided into four sections, with the obvious advantage that the four can be photographed at once. The samples were prepared by crushing a few milligrams of the material to a sieve size of less than 45 microns and dusting the powder directly on to the sellotape attached to the cassette. Photographs taken with no samples present showed that the sellotape gives several broad diffraction bands at the low angle end of the pattern. Their positions were noted so that they could be eliminated on measuring the patterns obtained with the samples.

In order to measure the X-ray patterns a reference line must be obtained on the film and the film itself must be calibrated to obtain a relationship between the distance from this reference line and the Bragg angle, $\theta$. The reference line was obtained by making an exposure of the primary X-ray beam at a low voltage ($\simeq$ 15 KV) and a low current by opening the beam trap for 4 to 5 seconds. Calibration was done by using NaCl as one of the samples in all of the films that were taken. By measuring the distance of the NaCl lines from the reference line and using the known Bragg angles for these reflections (Table B-5.8) a relationship between distance and $\theta$ was obtained and used in the measurement of the patterns of the other samples in that particular film.

The distances on the films were measured with a Hilger and Watts film measuring rule (1 vernier scale = 0.05 mm) and the $\theta$ values obtained were used to calculate the interplanar spacings (d) using Bragg's relation :

$$\lambda = 2d \sin \theta.$$

The wavelength ( $\lambda$ ) of the radiation used was either that of CuKα (1.5418Å) or that of CoKα (1.7902Å). With the copper-iron sulphides the CuKα radiation produced a very heavy background in the photographs due to the intense fluorescent radiation. Hence most samples were analysed using CoKα radiation, although for the copper-silver sulphides either of the radiations could be used with equally low background intensities.

At X-ray generator settings of 30KV and 20mA, the exposure times varied from 2 to 4 hours, the average being about $2\frac{1}{2}$ hours. 174mm x 46mm strips of Ilford Industrial G x-ray film were used and developed and fixed using conventional commercial reagents.

The intensities of the X-ray reflections were recorded from the films by a Joyce-Loeble automatic recording microdensitometer model MK111B. The relative intensities of the various reflections were estimated from the heights of the corresponding peaks on the recorded curves (typical traces are shown in Figures 57 and 58 in section 6.2).

## 2.5. Materials.

### 2.5.1. Elements for Synthesis of Sulphides.

Spectrographic examination of the elements used in the synthesis of the sulphides gave the following estimates for the amount of impurities present:

(a) Copper rod - Spectrographically Pure (Johnson Matthey) : Silver, 5 ppm; Lead, 3 ppm; Nickel, 1 ppm; Silicon, 1 ppm; Bismuth, Cadmium, Iron and Magnesium, each less than 1 ppm.

(b) Iron Sponge - Spectrographically Pure (Johnson Matthey) : Silicon, 3 ppm; Magnesium, 2 ppm; Manganese, 2 ppm; Nickel, 2 ppm; Copper and Silver, each less than 1 ppm.

(c) Silver grain - Spectographically Pure (Johnson Matthey) : Iron, 1 ppm; Cadmium, Copper and Magnesium, each less than 1 ppm.

(d) Sulphur powder - Spectographically Pure (Johnson Matthey) : Aluminium, 0.5 ppm; Sodium, 0.2 ppm; Zinc, 0.2 ppm; Barium, 0.1 ppm; Nickel, 0.1 ppm; Copper, 0.05 ppm; Titanium, 0.05 ppm; Magnesium, 0.03 ppm; Manganese,

0.03 ppm; Silver, 0.03 ppm; Boron, 0.01 ppm; Calcium, Iron and Silicon, each less than 1 ppm.

2.5.2 Leaching agents.

The leaching experiments were carried out using solutions of ferric sulphate, ferric chloride, sodium chloride and hydrogen peroxide. One experiment was done with a suspension of Manganese dioxide in dilute sulphuric acid.

The leaching solutions were prepared by dissolving the necessary amount of reagent for the concentration required in either dilute sulphuric or hydrochloric acid. Sulphuric acid with a pH of 1 was used for the ferric sulphate and hydrogen peroxide solutions, while 0.1M HCl was used for the chloride solutions. The acidic solutions were required to maintain the ferric ions in solution, avoiding the hydrolysis and subsequent precipitation of iron.

All of these reagents are commercially available and their specifications are listed below.

(a) Ferric Sulphate $Fe_2(SO_4)_3 . 9H_2O$.
General Purpose reagent (Hopkin and Williams).

Assay: 97% minimum $Fe_2(SO_4)_3 \cdot 9H_2O$

Maximum limits of impurities : Chloride(Cl), 0.04%; Nitrate ($NO_3$), 0.003%; Ferrous Iron (Fe), 0.028%.

(b) Ferric Chloride $FeCl_3 \cdot 6H_2O$

Analytical Reagent (Hopkin and Williams)

$FeCl_3 \cdot 6H_2O$ not less than 98.0%

Maximum limits of impurities, in weight per cents, :

| | |
|---|---|
| Insoluble matter | 0.003 |
| Free Acid (HCl) | 0.5 |
| Free Chlorine (Cl) | 0.001 |
| Nitrogen compounds ($NO_3$) | 0.002 |
| Phosphate ($PO_4$) | 0.001 |
| Sulphate ($SO_4$) | 0.005 |
| Arsenic (As) | 0.0001 |
| Calcium group + Mg | 0.05 |
| Copper (Cu) | 0.0025 |
| Ferrous Iron (Fe) | 0.015 |
| Lead (Pb) | 0.005 |
| Manganese (Mn) | 0.08 |
| Potassium (k) | 0.01 |
| Sodium (Na) | 0.03 |
| Zinc (Zn) | 0.01 |

(c) Sodium Chloride NaCl

Analytical reagent (BDH Chemicals)

Minimum Assay : 99.9% NaCl after ignition.

Maximum limits of impurities, in weight per cents, :

| | |
|---|---|
| Insoluble matter | 0.003 |
| Calcium group + Mg | 0.004 |
| Free Acid (HCl) | 0.0018 |
| Heavy Metals (Pb) | 0.0005 |
| Free Alkali | 0.05mlsN/l |
| Ammonium ($NH_4$) | 0.0005 |
| Bromide and Iodide (Br) | 0.005 |
| Barium (Ba) | 0.001 |
| Ferrocyanide ($Fe(CN)_6$) | 0.0001 |
| Arsenic (As) | 0.00004 |
| Nitrate ($NO_3$) | 0.0005 |
| Phosphate ($PO_4$) | 0.005 |
| Sulphate ($SO_4$) | 0.002 |
| Potassium (K) | 0.01 |
| Iron (Fe) | 0.0003 |

(d) Hydrogen Peroxide $H_2O_2$ (20 volumes)

General purpose reagent (Hopkin and Williams).

Weight per Ml about 1.02 g.

Chloride 0.0015% max.

Non-volatile matter 0.2% max.

6% W/V $H_2O_2$ minimum.

(e) Manganese Dioxide $MnO_2$ (Precipitated)

General Purpose reagent (Hopkin and Williams)

Acid Insoluble matter 0.2% max.

Lead (Pb) 0.005% max.

80% $MnO_2$ minimum.

2.5.3. Acids.

Listed below are the specifications of the hydrochloric and sulphuric acids used in the leaching solutions together with that of the nitric acid used in dissolving the unleached and leached solids, prior to atomic absorption analysis.

(a) Sulphuric acid - General Purpose Reagent, (Hopkin and Williams).

1.84 grams weight per c.c.

Non-volatile matter 0.015% max.,

Chloride 0.004% max.

Nitrate ($NO_3$) 0.0005% max.,

Heavy metals (Fe) 0.0025% max.,

About 98% W/W $H_2SO_4$

(b) Hydrochloric acid - General Purpose Reagent, (Hopkin and Williams),

Weight per Ml 1.16 grams.

Non-volatile matter 0.005% max.,

Sulphate ($SO_4$) 0.01% max.,

Heavy metals and Iron (Fe) 0.001% max.,

About 32% W/W HCl

(c) Nitric acid - Research Reagent (May and Baker)

Assay 69 - 71% W/W

Chloride (Cl) not more than 0.005%

Sulphate ($SO_4$) not more than 0.01%

Iron (Fe) Not more than 0.002%

Arsenic (As) not more than 0.0001%

Lead (Pb) not more than 0.0002%

Non-volatile residue not more than 0.01%

2.5.4 Reagents for Atomic Absorption Spectrophotometry

Solutions for the calibration of the atomic absorption spectrophotometer were prepared from copper, silver and iron standard solutions (Hopkin and Williams) containing 1000ppm W/V of the respective metals in 0.1 N $HClO_4$. Metal contents are within 0.5% of the nominal value

## SECTION 3

## SILVER-DOPED BORNITE, RESULTS AND DISCUSSION

### 3.1. Leaching Results

Samples of the silver doped bornite containing, 1.20 wt per cent silver, were leached in acidified ferric sulphate solutions using the apparatus and experimental procedure described in section 2.2. The kinetic rate curves for the dissolution can be compared with those previously obtained by Ugarte[11], using an identical leaching technique, for pure synthetic bornite.

The curves shown in Figure 23 were characteristic of the dissolution behaviour of the copper and silver from the silver-doped bornite. The outstanding feature is the almost complete absence of silver in the leach solutions.

The copper dissolved in two distinct stages, a very fast first stage followed by a much slower second stage. This is very similar to the dissolution of copper from pure bornite.

The influence of some leach variables on the dissolution rates was studied. These included temperature, ferric ion concentration,

time and sample size.

### 3.1.1 Temperature

Figure 23 shows the dissolution behaviour of copper and silver from the silver-doped bornite at 60°C and 90°C. The results are tabulated in Tables A-1.1 and A-1.2. The experiments were carried out with a one gram sample of particle size -180 + 125 microns and a solution of ferric sulphate in sulphuric acid. In both experiments the ferric ion concentration was 0.065 M in acid solutions of pH = 1. The acid was required to maintain the ferric ions in solution, preventing their hydrolysis and precipitation.

Prior to these experiments an investigation was carried out to determine the stirring speed required for a turbulent regime to be established in the solution and hence maintaining all the particles in suspension. It was found that for all particle sizes considered, a speed of greater than 1000 r.p.m. was sufficient. However a speed of 1300 r.p.m. was used in these and subsequent experiments to ensure the establishment of this turbulent regime, thus preventing the dissolution rates being controlled by the access of reactants or

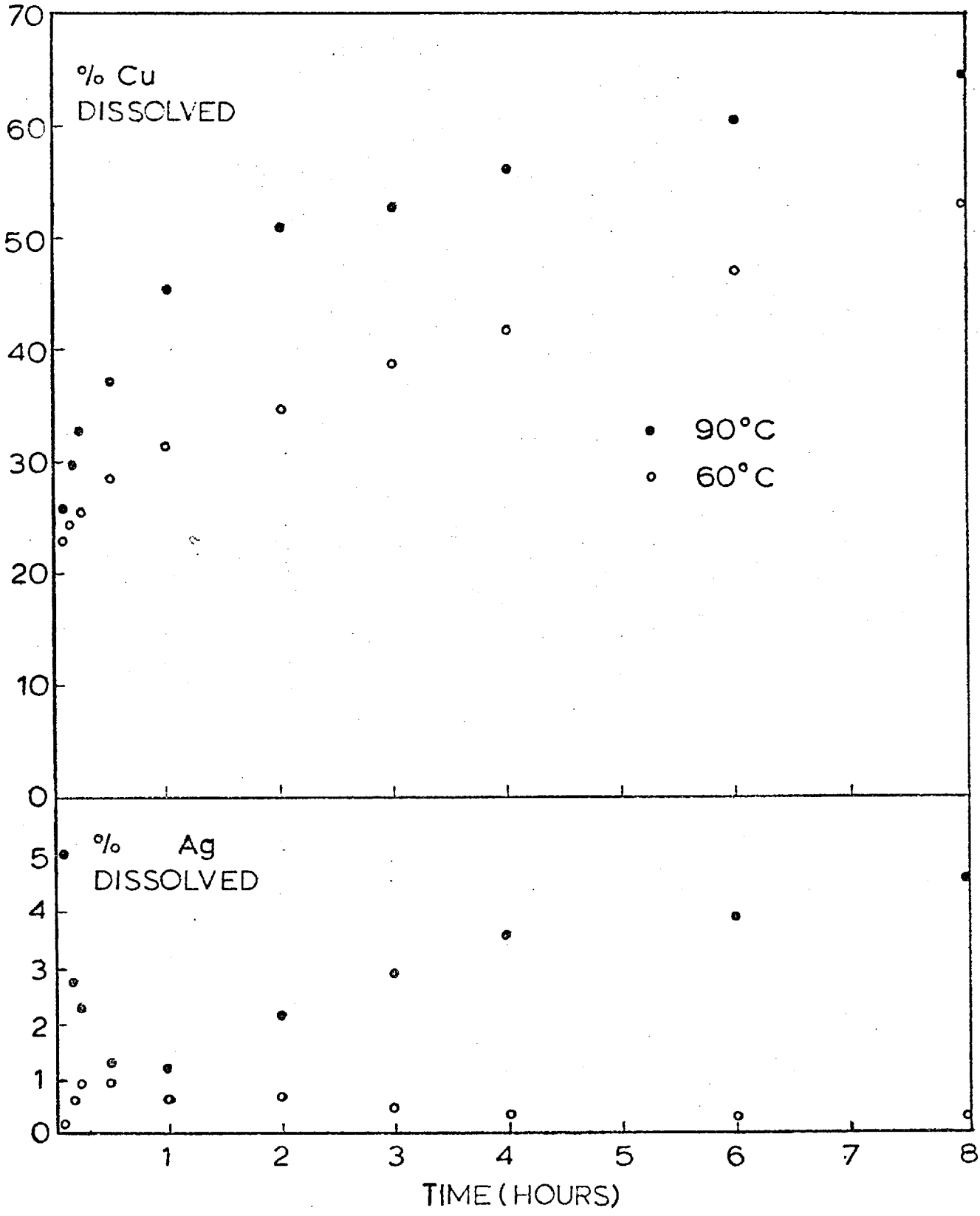


FIGURE 23 : Effect of temperature on the rate of leaching copper and silver from the silver - doped bornite.

products to the surface of the solid.

Figure 2 3 shows that even at the highest temperature (90°C), the amount of silver that dissolved was exceedingly small. After eight hours at 90°C, approximately 4% of the silver had dissolved. In other words, the 200 mls. of leach solution contained approximately 0.5 milligrams of silver from an initial sample content of approximately 12 milligrams of silver. This was about ten times the amount dissolved at 60°C.

The dissolution of the silver was characterised by an initial peak in the dissolution curve, followed by a decrease in the silver content of the solution and then a slow increase. Both the initial and final dissolution rates were faster at the highest temperature. The initial maximum in the silver content of the solution was much greater for the higher temperature and occurred in a much shorter time. It should also be noted that at the higher temperature more silver was removed from the solution after the initial dissolution peak but that the minimum reached was not as low and the subsequent leaching rate faster than at the

lower temperature. However X-ray diffraction analysis and microscopic observations of the residues failed to show the presence of any precipitated phase to explain the decrease in the silver content of the solutions.

The curves obtained for the copper dissolution show the fast first stage and slower second stage characteristic of copper dissolution from pure bornite. At 90°C the fast first stage lasted until about 40% of the copper was dissolved. The leaching curve for the experiment at 60°C showed that this first stage can be divided into two sections. The first section extended until about 25% of the copper was dissolved, showing a leaching rate similar to that occurring in the first stage of the reaction at the higher temperature. The second section, up to 40% of the copper dissolved occurred with a much slower leaching rate.

In general it can be said that the presence of 1.20 weight per cent of silver in bornite had no significant effect on the dissolution of the copper, the kinetic rate curves suggesting that the dissolution mechanism of the bornite remained unaltered. As reported in section 1.2.1,

Ugarte[11] demonstrated that in the first stage of dissolution of the bornite, copper is removed by diffusion through the lattice to form the phase $Cu_3FeS_4$. This fast dissolution stage stops after 40% of the copper has been removed. Subsequently the dissolution rate is much slower with the $Cu_3FeS_4$ being transformed to elemental sulphur through a rate - controlling chemical process.

The X-ray diffraction analyses and the microscopic examinations of the leach residues (sections 3.5 and 3.4) confirm this mechanism. Elemental sulphur and $Cu_3FeS_4$ were the only phases detected, indicating that the silver remained in the original solid material as it transformed from $Cu_5FeS_4$ to $Cu_3FeS_4$ by the diffusion of copper ions into solution. The X-ray pattern for the $Cu_3FeS_4$ phase seemed less well defined than that formed from pure bornite (see Fig. C-1.2) which suggests some degree of distortion within the lattice due to the presence of silver.

The apparent activation energy for the dissolution process can be calculated by writing the Arrhenius equation as:

$$\frac{\text{Log } (K_2) - \text{Log } (K_1)}{1/T_2 - 1/T_1} = - \frac{Ea}{2.303R}$$

Where $K_1$ and $K_2$ are the rates of dissolution at temperatures $T_1$ and $T_2$ respectively, $E_A$ is the apparent activation energy and R is the gas constant. Using the weight per cent dissolved in 5 minutes as a measure of the rate, the activation energy for the copper dissolution in the first stage of the reaction (up to 40% of the copper dissolved) was calculated to be about 0.97 kcals. per mole , while the activation energy for the silver dissolution was found to be about 25.5 kcals. per mole.

Combining the two dissolution processes, and using the total number of moles of copper and silver dissolved in 5 minutes as a measure of the rate, gave an activation energy of about 1.2 kcals per mole.

The low value for the copper dissolution confirms that diffusion controls the first stage of the dissolution of copper from the silver-doped bornite, while the higher value for the silver dissolution indicates some degree of rate control by a chemical process.

The subsequent leaching experiments were all carried out at 60°C since it was found that at higher temperatures, hydrolysis and precipitation of the ferric ions took place if the leaching runs lasted for many hours.

3.1.2 Ferric ion concentration

Figures 24 and 25 show the effects of ferric ion concentration on the dissolution of copper and silver from the silver-doped bornite. The results are presented in Tables A-1.3, A-1.4 and A-1.5. The experiments were carried out at 60°C with 1 gram samples of particle size -180 + 125 microns. The solutions of ferric sulphate in sulphuric acid (pH =1) were stirred at a speed of 1300 rpm

Ferric ion concentrations of 0.01, 0.065 and 0.25 molar were considered. Figure 24 shows that even at the highest concentration, the amount of silver dissolved was very small. At all the ferric ion concentrations, the dissolution curves were characterised by a maximum after about 15 minutes, followed by a decrease and then a slow rise with increase in time. The amount of silver dissolved increased with ferric ion concentration, as did the

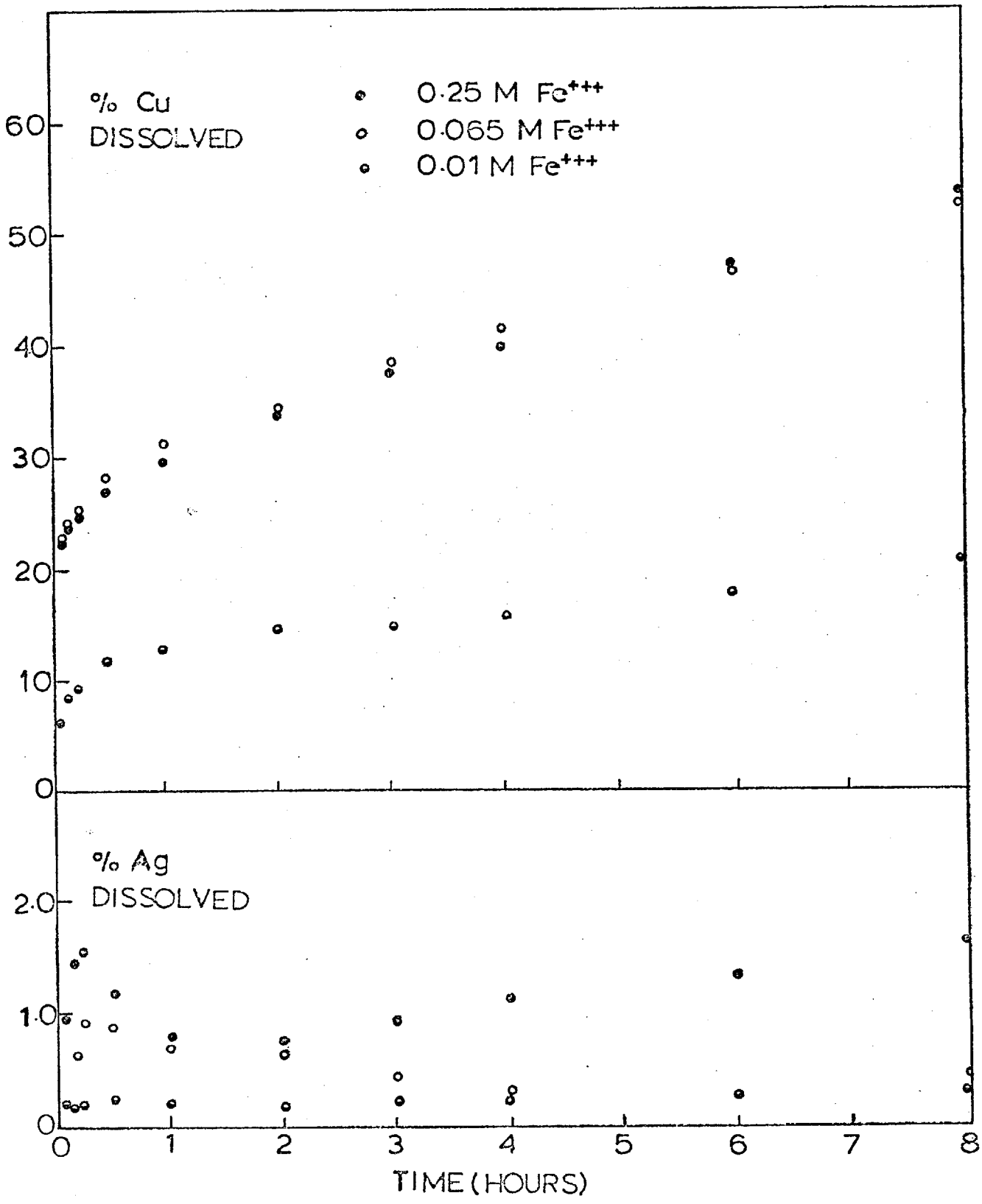


FIGURE 24 : Effect of ferric ion concentration on the rate of leaching copper and silver from the silver - doped bornite.

dissolution rate.

At 0.01 molar ferric ion the dissolution of copper had a very slow rate after about 12% of the copper had dissolved. This was obviously due to the fact that all the ferric ion had been consumed in dissolving this amount of copper. The subsequent very slow increase in the amount of copper dissolved was probably caused by the reoxidation of $Fe^{2+}$ to $Fe^{3+}$ by the air and by the introduction of fresh ferric ion by the sampling technique. This consisted of replacing each 5 mls sample taken from the leaching solution with 5 mls of fresh ferric ion of the appropriate concentration.

The curves for the copper dissolution at the 0.25 molar and 0.065 molar concentrations confirm Ugarte's findings that at concentrations above 0.065M, the rate of dissolution of copper from bornite is independent of ferric ion concentration. In the first two hours of leaching, however, the rate in 0.25M$Fe^{3+}$ was slightly lower than that at 0.065M$Fe^{3+}$. This could be an effect due to the silver dissolution. Slightly more silver was dissolved and subsequently removed from the solution at the

higher $Fe^{3+}$ concentration. If this silver was precipitated in some form on the surface of the particles this would obviously affect the dissolution of the copper.

However it should be pointed out that no evidence for the formation of a precipitated silver-containing phase was found by either X-ray diffraction analysis, or microscopic examination (see sections 3.5, 3.4). Electron-microprobe analysis did show that there was an increase in the silver concentration at the edges of the particles but it appeared that this increase occurred within the original particle and was not due to a surface coating of another phase. (see section 3.3).

Again it can be said that the silver does not affect significantly the dissolution rate of the copper from bornite, even at relatively high $Fe^{3+}$ concentrations. As mentioned in section 2.3 attempts were made to monitor the dissolution of the silver-doped bornite using a calomel electrode and a platinum foil electrode to measure the E.M.F.of the solution as the $Fe^{2+}/Fe^{3+}$ ratio changed due to the dissolution reaction which produces ferrous ions. However

the presence of potassium as KCl in the calomel electrode, caused the precipitation of Jarosite, $KFe_3(SO_4)_2(OH)_6$, and affected the dissolution rate.

The jarosite was identified by its yellow-brown colour and by X-ray diffraction analysis. The d-spacings for a typical precipitate are listed in table B-1.5. The lines other than those of jarosite were identified as due to sulphur. The powder photograph for this precipitate is shown in figure C-1.1.

In a study on the rate of dissolution of chalcopyrite in acidic solutions under oxygen overpressures and at temperatures in the range 135° to 175°C, Yu et al[205] found that the addition of 0.1M$KHSO_4$ or 0.1M$K_2SO_4$ to a 0.5N $H_2SO_4$ solution decreased the leaching rate. As with the present work they found that a yellow precipitate was formed, which was identified as jarosite by X-ray diffraction.

3.1.3 Time.

In order to find out whether the silver enters into solution at some later stage in the dissolution process, the leaching experiments

of the previous section were continued until more than 90% of the copper had dissolved. This took about 30 hours for the 0.065 and 0.25 molar $Fe^{3+}$ solutions. The results are shown in figure 25.

As expected the copper continued to dissolve very slowly in the 0.01 molar solution due to the $Fe^{3+}$ introduced on taking samples and the $Fe^{3+}$ formed by the reoxidation of the $Fe^{2+}$ by air, as mentioned previously. After 46 hours of leaching, 42.33% of the copper had dissolved. The amount of silver dissolved remained very low, being approximately 0.2 per cent of the total silver in the initial sample.

The curves for the copper dissolution in 0.25 molar and 0.065 molar $Fe^{3+}$ solutions clearly show the fast first stage reaction and the slower second stage characteristic of pure bornite. However, at copper dissolutions greater than 80% there was a sharp decline in leaching rate. The microscopic and X-ray studies showed that, as with pure bornite, the elemental sulphur formed in the second stage reaction forms a coating on the particles. This slows down the leaching rate due to the

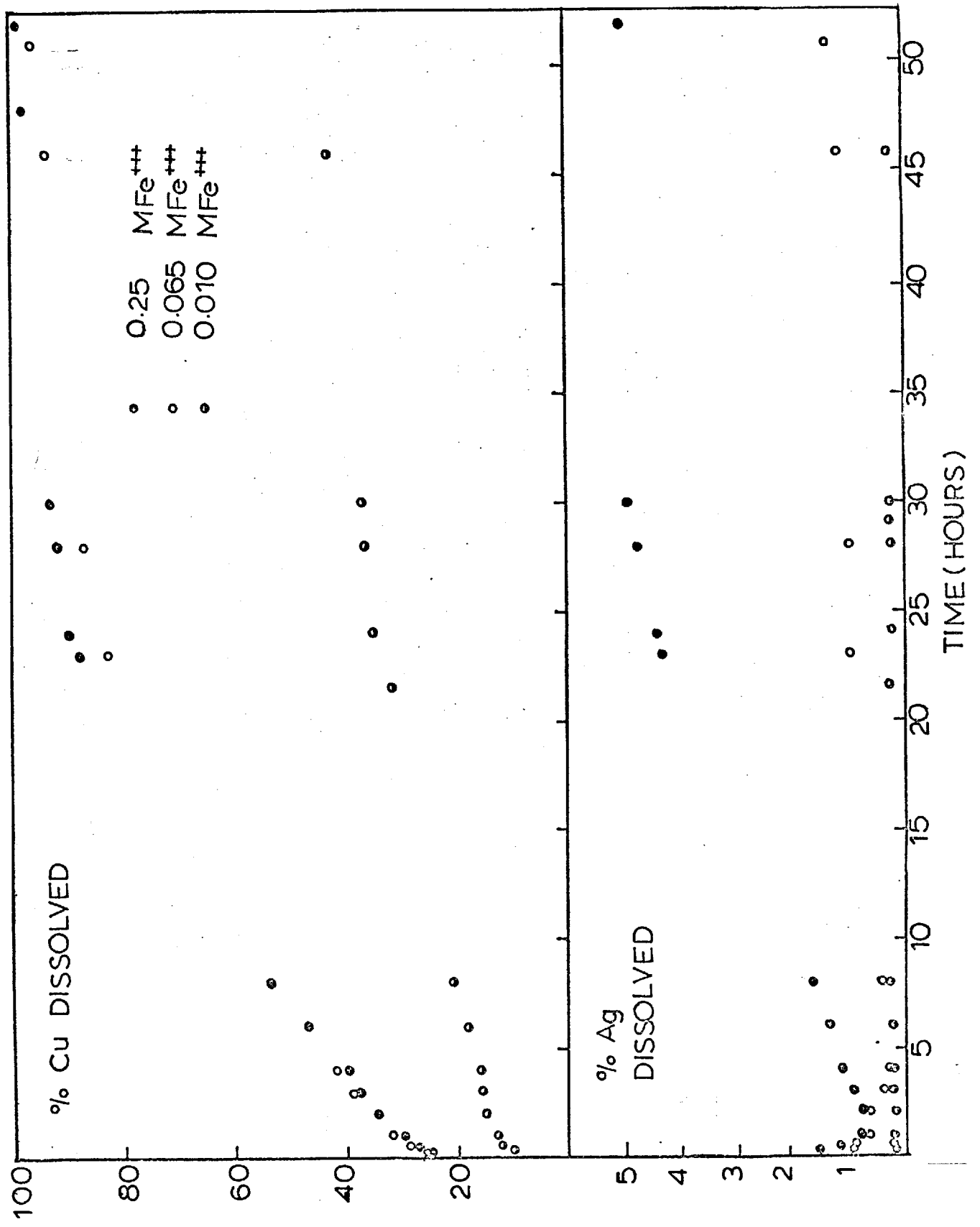


FIGURE 25 : Effect of increased leaching time on the rate of leaching of copper and silver from the silver - doped bornite at different ferric ion concentrations.

reactants and products having to diffuse through this layer. From the curves it can be seen that the effect was greater for the lower concentration (0.065 M$Fe^{3+}$) which is in agreement with the above explanation since the rate of diffusion of the $Fe^{3+}$ ions through the sulphur layer will depend on the bulk concentration of the Ferric ion.

The amount of silver obtained in solution at these two concentrations remains very small, even when more than 90% of the copper had been removed. On increasing the $Fe^{3+}$ concentration from 0.065M to 0.25M the amount of the silver in solution, when almost all the copper had dissolved, was increased from 1.34 to 4.97 weight per cent. In other words, after 52 hours in a 0.25 molar solution of $Fe^{3+}$, only about 0.6 milligrams of silver had dissolved from the initial 1 gram sample containing about 12 milligrams. Hence these leach residues should be silver rich. This was found to be the case by dissolving the residues in nitric acid and analysing the solutions by atomic absorption spectrophotometry, (section 3.2)

It should be noted that the rate of silver

dissolution, after the initial maxima and minima, was much faster for the higher $Fe^{3+}$ concentration, but that the dissolution slowed down as the copper dissolution approached 100%. This suggests that the silver has remained in the original particles which have become coated with sulphur causing a slowing down in the dissolution rates of both copper and silver, and that the undissolved silver has not formed a separate phase by dissolution followed by precipitation.

This is supported by the X-ray and microscopic studies which show no phases other than elemental sulphur and one with the structure of idaite ($Cu_3FeS_4$).

3.1.4 Sample Weight

Figure 26 shows the effect of changing the weight of sample used in the leaching experiments. The experiments were carried out under the same conditions, that is, at 60°C, with a ferric ion concentration of 0.065 M in sulphuric acid (pH = 1), a stirring speed of 1300 rpm and a particle size of -180 + 125 microns. The results are listed in Tables A-1.5 and A-1.6.

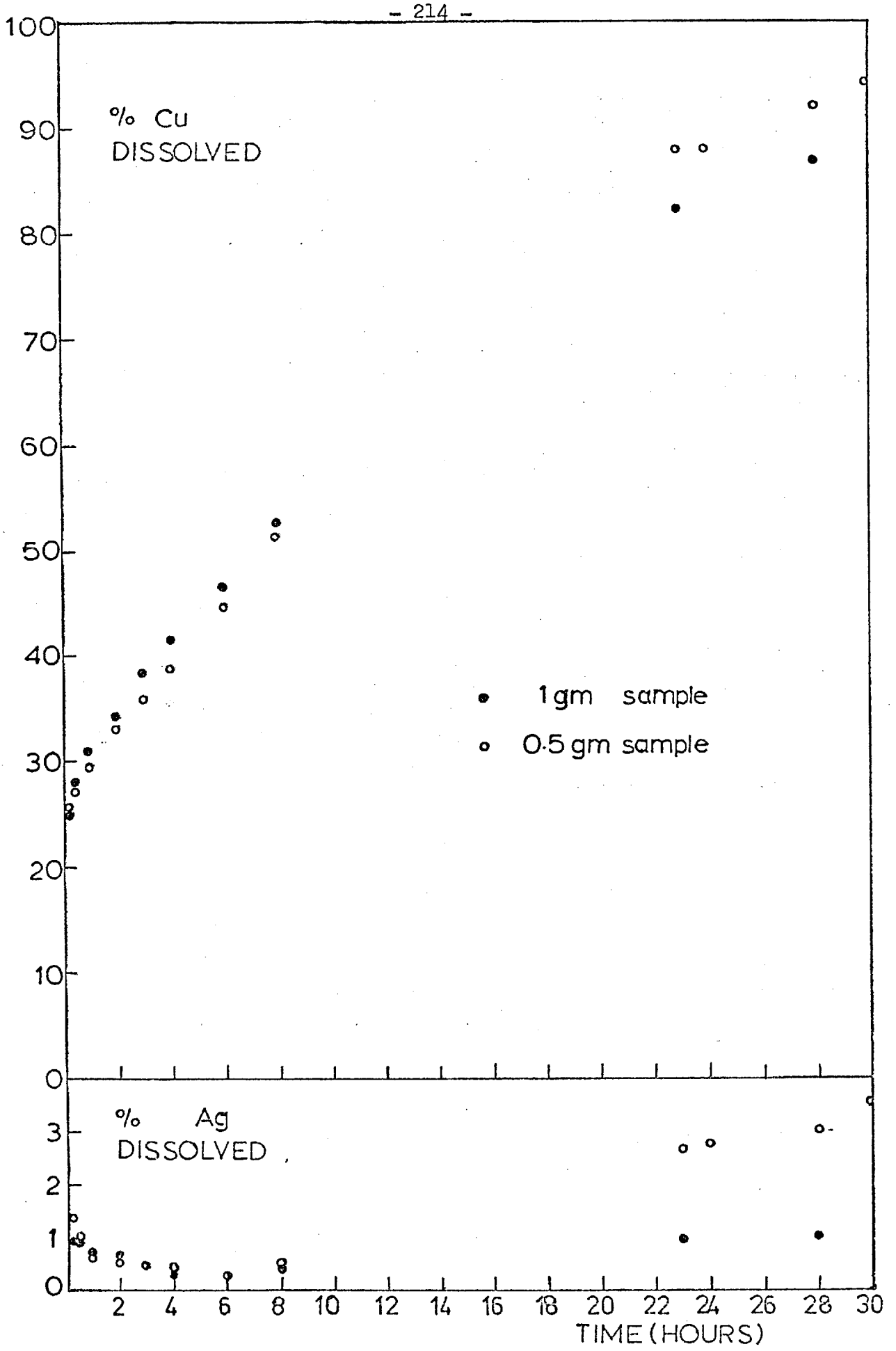


FIGURE 26 : Effect of initial sample weight on the rate of leaching copper and silver from the silver - doped bornite.

When 0.5 grams of solid was used instead of 1 gram, there was no significant effect on the copper dissolution. However there were slight differences. Up to about 40% copper dissolved the 1 gram sample had the slightly faster leaching rate while at higher copper dissolutions the 0.5 gram sample had the slightly faster rate. The latter effect could be explained by the fact that because the same ferric ion concentration was used in both experiments, the amount of ferric ion left in the solution would be greater for the 0.5 gram sample, due to less copper being dissolved in the solution.

The slower rate of the 0.5 gram sample below 40% of the copper dissolved could be due to the fact that more silver per unit mass was dissolved, and then removed from solution, in the initial stages of the dissolution. This again suggests that in the initial stages of the dissolution a small amount of silver is dissolved and then precipitated on the surfaces of the particles, thus slightly affecting the copper dissolution rate. Subsequently the silver dissolves very slowly, the bulk becoming concentrated in the transformed particles with

the structure of idaite.

After the minimum in the silver dissolution curve (which occurred at the same weight of silver dissolved per unit mass) the 0.5 gram sample had a significantly faster leaching rate. This could be due to the same reason as for the faster leaching rate for the copper in the later stages of dissolution i.e., a greater excess of $Fe^{3+}$ in the solution

3.2 Atomic absorption analysis.

The atomic absorption spectro photometer was used to analyse the solid leach residues after removing any elemental sulphur with $CS_2$ (section 2.2) and dissolving the residues in nitric acid (section 2.3). The results for a number of residues are shown in Table 1, together with the weight per cents of copper and silver dissolved from the original samples in the leaching experiments, and the stoichiometric compositions of $Cu_5FeS_4$ (bornite), $CuFeS_2$ (chalcopyrite), and $Cu_3FeS_4$ (idaite). The results are expressed as atomic per cents in Table 2.

As expected, the residues became enriched in silver as the copper is dissolved. It can be seen that the analyses for the residues 1,2, 3 and 4 agree very well with a composition of $(Cu, Ag)_3FeS_4$. X-ray analysis also showed that these residues gave diffraction patterns similar to the idaite phase, $Cu_3FeS_4$ (section 3.5).

The analyses for residues 5 and 6 confirm that the silver remains undissolved even when nearly all the copper has dissolved. In these two cases, at a high silver concentration, the

results do not agree so well with the idaite composition but the total metal : total sulphur ratio was still approximately 1 : 1.

Errors may occur in both the iron and sulphur analyses. If any ferric ions have become hydrolysed during the leaching this would give a higher iron content due to the presence of the iron-containing precipitate while the sulphur content would be higher if the removal of elemental sulphur by $CS_2$ was not complete.

TABLE 1 - Atomic Absorption Analysis of residues.

| Residue | wt % removed | | wt % in residue | | | |
|---|---|---|---|---|---|---|
| | Cu | Ag | Cu | Ag | Fe | S. |
| 1 | 44.68 | 0.20 | 50.91 | 1.65 | 14.57 | 33.17 |
| 2 | 64.29 | 0.86 | 51.78 | 2.81 | 14.66 | 30.75 |
| 3 | 84.04 | 1.76 | 45.50 | 5.00 | 16.03 | 33.47 |
| 4 | 89.67 | 4.97 | 43.32 | 8.09 | 17.36 | 31.23 |
| 5 | 97.79 | 1.20 | 25.14 | 21.02 | 16.94 | 36.90 |
| 6 | 98.76 | 2.16 | 21.15 | 20.98 | 22.24 | 35.63 |
| Initial | - | - | 62.29 | 1.20 | 11.07 | 25.43 |
| $Cu_5FeS_4$ | - | - | 63.33 | - | 11.12 | 25.55 |
| $CuFeS_2$ | - | - | 34.64 | - | 30.42 | 34.94 |
| $Cu_3FeS_4$ | - | - | 50.87 | - | 14.90 | 34.23 |

TABLE 2 - Analyses expressed as Atomic %.

| Residue | At % in residue | | | |
|---|---|---|---|---|
| | Cu | Ag | Fe | S |
| 1 | 37.93 | 0.72 | 12.35 | 48.98 |
| 2 | 39.51 | 1.26 | 12.72 | 46.49 |
| 3 | 34.17 | 2.19 | 13.69 | 49.88 |
| 4 | 33.34 | 3.66 | 15.25 | 47.73 |
| 5 | 19.00 | 9.40 | 16.00 | 55.50 |
| 6 | 16.28 | 9.56 | 19.56 | 54.58 |
| Initial | 49.44 | 0.56 | 10.00 | 40.00 |
| $Cu_5FeS_4$ | 50.00 | - | 10.00 | 40.00 |
| $CuFeS_2$ | 25.00 | - | 25.00 | 50.00 |
| $Cu_3FeS_4$ | 37.50 | - | 12.50 | 50.00 |

## 3.3. Electron Microprobe Analysis.

Although the atomic absorption analyses in the previous section gave the overall compositions of the residues, the electron microprobe was used to investigate the homogeneity and distribution of the elements in the residues. The experimental procedure and the use of the electron microprobe to check the homogeneity of the original synthetic silver-doped bornite have been discussed previously (sections 2.4.3 and 2.1.1, respectively). A typical electron probe trace for the original material is shown in Figure 27.

The results from measurements made at fixed points on the residue particle surface are shown in Table 3 . These spot counts were made at the centres of the particles since accurate measurements were not possible at the edges of the particles because of the cracks and pores that were formed (see section 3.4). The results show that even at high copper dissolutions the composition of the particles remains virtually the same, agreeing well with the formula $(Cu,Ag)_3\ FeS_4$.

It can be seen that the silver content of the particles does not seem to have increased

greatly from the initial content of 1.20 weight per cent. The scatter in the results is probably due to the low beam current (15nA at 25KV) that had to be used (section 2.1.1), and, in the case of silver, the very low values that had to be measured.

The atomic absorption analyses showed much higher silver contents for the same residues and this suggested that the silver was not distributed homogeneously throughout the particles but was concentrated in certain areas. Several traces for Cu, Fe and Ag were made across the leached particles. For the copper and iron traces no consistent differences were found in the bulk of the particles that could not be attributed to topographical features, while at the edges both the copper and iron contents decreased rapidly. The silver traces did not give very consistent results. This was probably due to the low silver content and the low beam current that had to be used to avoid damage to the particles. However, a number of the traces showed that there seemed to be more silver at the edges than in the centres of the particles. One of these traces is shown in Figure 28, together with typical traces for the copper and iron.

This concentration of silver appeared to be within the original particle and was not due to a precipitate on the surface. The X-ray analysis confirmed this and seemed to suggest that these areas of greater silver content still had the $Cu_3FeS_4$ structure since no other phases were detected.

TABLE 3 Electron Probe Analysis of Residues.

| Residue | wt.% in residue (Atomic % in brackets). | | | |
|---|---|---|---|---|
| | Cu | Ag | Fe | S |
| 1 | 54.20 | 1.40 | 15.10 | 29.30 |
| | (41.60) | (0.60) | (13.20) | (44.60) |
| 2 | 50.61 | 1.23 | 16.23 | 31.93 |
| | (38.03) | (0.54) | (13.87) | (47.55) |
| 3 | 48.12 | 1.03 | 16.42 | 34.42 |
| | (35.48) | (0.45) | (13.77) | (50.29) |
| 4 | 48.41 | 1.39 | 16.36 | 33.84 |
| | (35.88) | (0.61) | (13.80) | (49.71) |
| 5 | 49.20 | 1.11 | 15.98 | 33.71 |
| | (36.49) | (0.48) | (13.48) | (49.55) |
| 6 | 51.56 | 1.26 | 17.13 | 30.05 |
| | (39.25) | (0.57) | (14.84) | (45.34) |

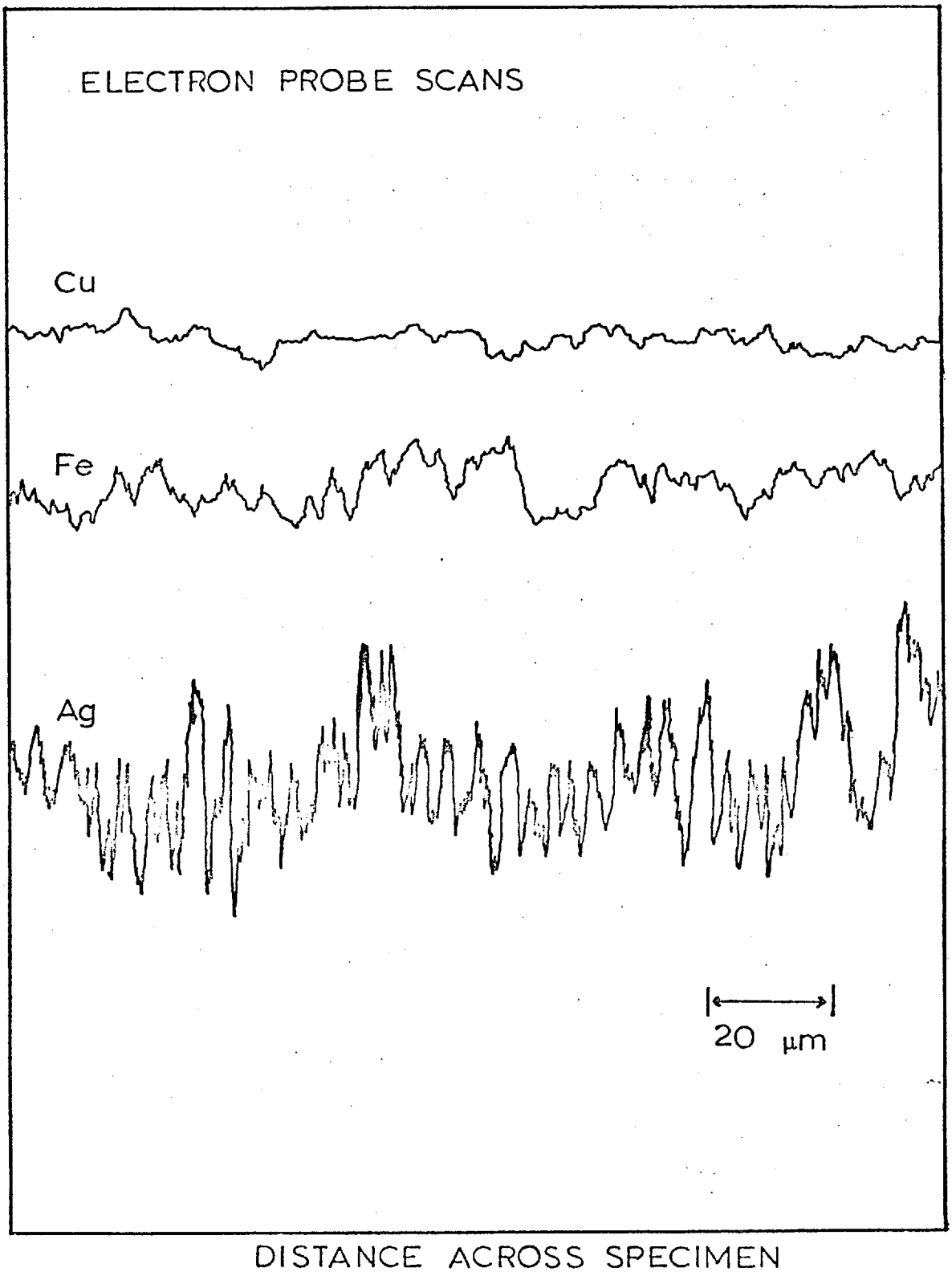


FIGURE 27 : Electron probe scan across an unleached specimen of the silver - doped bornite.

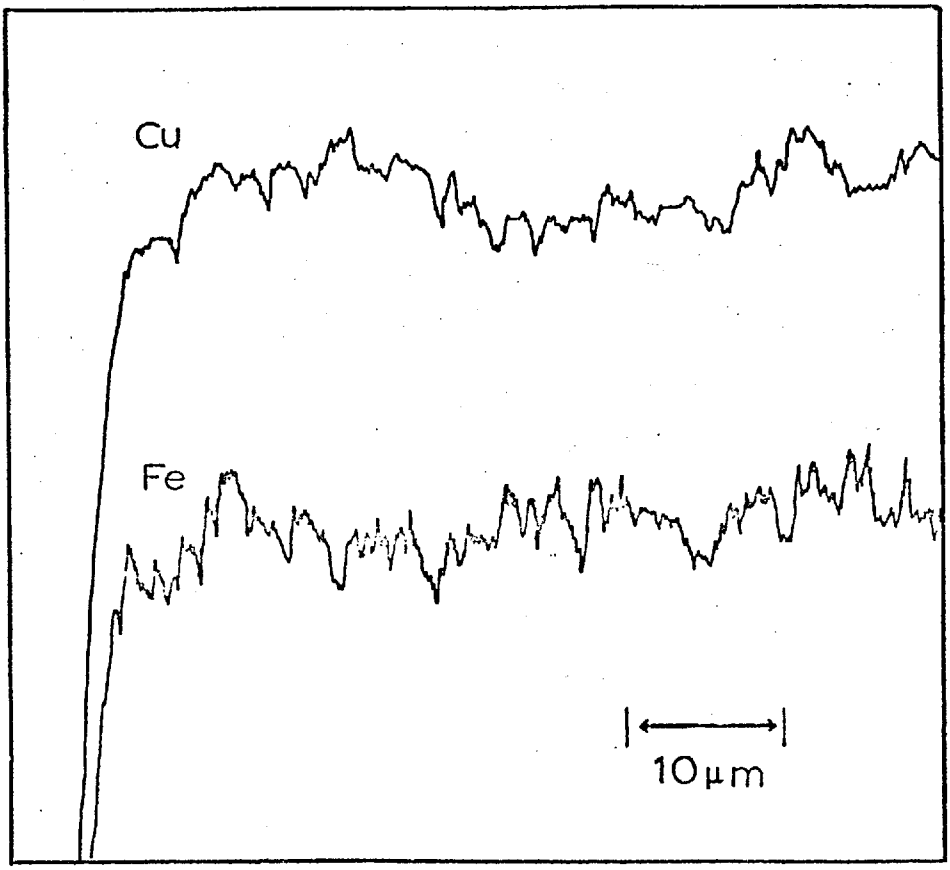


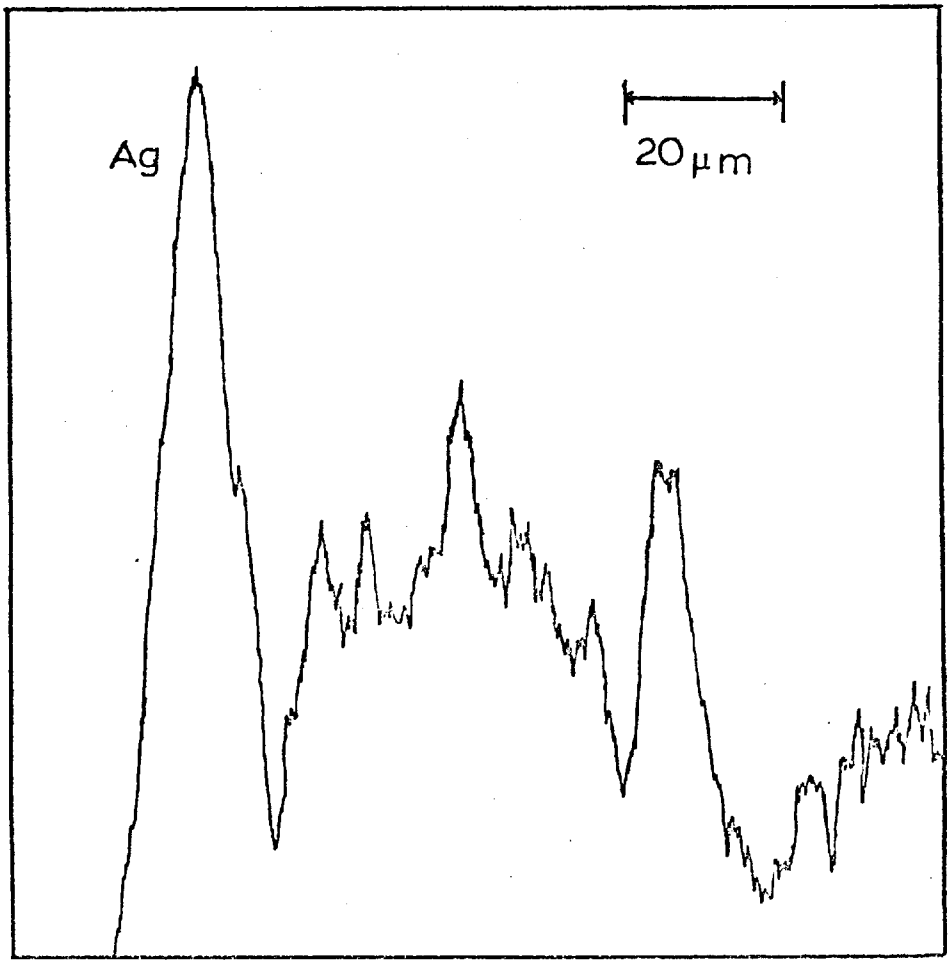


FIGURE 28 : Electron probe scans across leached particles of the silver - doped bornite.

## 3.4 Microscopic Analysis.

The leach residue particles were mounted and polished (section 2.4.1) to study by microscopic means the effect of leaching on the grains of the silver-doped bornite. After leaching, and removal of the elemental sulphur, the particles had a golden colour in a polished mount under reflected light.

Figure C-2.1 shows a particle of the silver-doped bornite after 20.1% of the copper had been dissolved from the sample. The particle still retains the well-defined edges but a number of cracks have formed. This suggests that the removal of copper is carried out by diffusion in the solid state producing a contraction in the unit cell resulting in the development of pores and cracks in the particles.

Figure C-2.2 shows a particle from a sample from which 44.68% of the copper had been dissolved. There are more cracks and pores and attack seems to have started on the edges of the particles. This attack is clearly shown in Figure C-2.3 in a particle from which 64.29% of the copper had been dissolved. This particle also shows the start of a black 'layer'

around the particles which grows in size as more copper is dissolved, as shown in Figures C-2.4 and C-2.5 representing 84.04% and 97.69% of the copper dissolved.

This 'layer' is in fact the hole in the mounting material left due to the elemental sulphur being removed during the polishing of the leach residues. The presence of sulphur was confirmed by X-ray diffraction analysis. In the central parts of the grains it is possible to see the remaining sulphide phase. Electron probe microanalysis performed in this area still gave a composition similar to that given by residues with only about 40% of the copper dissolved (section 3.3).

These observations are in complete agreement with those of Ugarte [11] on the leaching of pure bornite. The retention of the original shape of the particles up to about 40% of the copper dissolved, and the subsequent strong attack on the surface of the particles demonstrates the two stages of the leaching reaction. These are firstly a removal of copper by diffusion in the solid state, and then a chemical attack with the formation of elemental sulphur.

It should be noted that all the residues microscopically examined were homogeneous and no intergrowths of other secondary phases,

## 3.5 X-Ray Diffraction Analysis.

The original material and most of the leach residues were studied by X-ray diffraction. Table B-1.1 compares the measured d-spacings of the silver-doped bornite with pure synthetic bornite and the A.S.T.M. file values. It can be seen that the three patterns are in good agreement. The extra lines in the silver-doped bornite and pure synthetic bornite patterns could not be identified with any phase and were thought to be due to surface oxidation of the samples.

The outstanding feature of the leach residue diffraction patterns was the broadness of some of the lines. This often made it difficult to measure the positions of some of the lines and in these cases the measurements are tabulated as a range of d-spacings. The powder photographs for the residues at different amounts of copper dissolved are shown in Figure C-1.1 and the measured d-spacings are tabulated in Tables B-1.2 and B-1.3.

Table B-1.2 and photographs (b), (c) and (d) in figure C-1.1 show that in the first stage of the dissolution of the silver-doped

bornite there are three noticeable changes in the diffraction pattern of the remaining solid. Firstly, there is a considerable decrease in the number of lines, secondly the lines that remain are displaced, indicating a contraction of the lattice, and thirdly these remaining lines are very broad.

These observations are similar to those of Ugarte[11] on the leaching of pure bornite. According to Ugarte, bornite loses copper in the first stage of the dissolution by diffusion of copper ions in the lattice with a marked contraction of the unit cell until the structure that remains is a chalcopyrite-like structure with a formula unit $Cu_3FeS_4$, known as Idaite.

The contraction in the lattice of the silver-doped bornite as the first 40% of the copper was dissolved can be seen by the displacement of the X-ray line corresponding to d = 1.937 Å in the original silver-doped bornite. Table B-1.2 shows that the line is displaced from 1.937Å to 1.883 - 1.860 Å after 44.68% of the copper has been dissolved.

The d-spacings and intensities of the lines for the sulphide phase formed when about 40% of the copper has dissolved out of the silver-doped bornite are very similar to those obtained by Ugarte for the idaite formed by the leaching of pure bornite. This can be seen by comparing the pattern for a pure bornite with 43.7% Cu removed with the pattern for the silver doped bornite after 44.68% of the copper has been dissolved (Table B-1.2). This suggests that the sulphide phase formed in the first stage of dissolving the silver-doped bornite is also of the structure of idaite, $Cu_3FeS_4$.

The other powder photographs in Figure C-1.1, photographs (e), (f), (g), (h) and (i), and their corresponding d-spacings, listed in Table B-1.3 show that the lines do not move after about 40% of the copper has been removed and that above this amount of copper dissolved the lines of orthorhombic sulphur appear and become stronger in intensity than the lines of the sulphide phase. This indicates that the second stage of dissolution is also similar to that of pure bornite, that is the complete breakdown of the idaite structure to give

elemental sulphur as the copper goes into solution.

This was confirmed by treating the leach residues with $CS_2$ to remove the elemental sulphur and repeating the X-ray analyses. The resulting X-ray diffraction patterns are shown in Figure C-1.2, photographs (b), (c), (d),(e) and (f), and the measured d-spacings are presented in Table B-1.4. These values are very similar to those of idaite, $Cu_3FeS_4$, for all the residues and clearly show that the sulphide phase formed after 40% of the copper has been removed remains unchanged for the rest of the leaching reaction.

However, the leaching results and atomic absorption analysis of the residues (sections 3.1. and 3.2) showed that during this dissolution of copper, only a small amount of silver dissolved, the bulk of the silver remaining in the solid residues. Both microscopic examination and electron probe micro-analysis failed to detect any secondary phase of silver formed by solid state transformation or precipitation.

In figure C-1.2 photographs (h), (i), and (j) are the X-ray diffraction patterns for silver, silver sulphate and silver sulphide respectively. Comparing these patterns with those for the leach residues shows that none of these silver compounds seemed to be present in the residues.

At this point, however, it should be noted that there are limits to the detection ability of the X-ray diffraction technique. Klug and Alexander[179] state that many crystalline substances give such sharp powder patterns that they are detectable when present to the extent of one to two per cent, or less, in a mixture. Other materials give such poor patterns that, although they can readily be identified when alone, they may not be detected when present in a mixture even to the extent of 50%. Little work has been done to determine the amounts of crystalline substances determinable by X-rays in the presence of other materials. However, in work on the phase relations in the Au-Ag-Te system, Cabri[180] stated that with a Guinier-De Wolff camera he was able to show the presence of very small amounts of some phases, less than $\frac{1}{2}$ wt.% in some cases.

To investigate whether small amounts of silver compounds could be detected, two powdered mixtures of pure bornite and pure silver sulphide were analysed by X-ray diffraction. One mixture contained about 1% of silver sulphide and the other contained about 6%. The lines of silver sulphide were visible in both X-ray photographs. In the case of the 1% silver sulphide mixture only a few of the strongest lines were visible, but for the 6% mixture a number of lines were detected.

The conclusion was that it was thought that if silver was present as some secondary phase, it would easily be identified by the X-ray diffraction technique, especially as some of the residues contained up to 20% silver (section 3.2, Table 1).

Since no such phase was detected, this suggests that the silver remains as an isomorphous constituent in the copper-iron sulphide during the transformation from bornite to idaite as copper is dissolved, and that this idaite becomes silver-rich during the second stage of copper dissolution. The electron probe analysis results (Table 3 and Figure 28)

showed that silver was present in the transformed particles at about the same concentration as in the original bornite, and that there was some build up of silver at the edges of the particles as the dissolution of copper continued.

Although Ugarte noted that the idaite formed during the leaching of pure bornite gave X-ray patterns with very broad lines and a noticeable increase in the background radiation, the effect seemed to be much greater for the silver-doped bornite.

In figure C-1.2 photograph (g) is for a sample of pure bornite from which 38.8% of the copper had been leached. Comparison with photograph (a) in the same figure, which is for a sample of silver-doped bornite from which 44.68% of the copper had been dissolved shows that much broader lines were obtained for the transformation product, idaite, in the present work. This could well be an effect due to the presence of silver in the structure.

Several factors contribute to scattering and diffraction at angles other than those of

the discrete Bragg reflections produced by the characteristic radiation employed. These are, (a) lattice imperfections, (b) general radiation, (c) absorption discontinuities, (d) air scatter, (e) secondary fluorescence radiation, and (f) crystallite size. Of these, (b), (c), (d) and (e) would be the same for all samples, and since the increase in background radiation and broad lines only occurred with the leach residues, the cause must be either (a) lattice imperfections, or (f) crystallite size.

According to Klug and Alexander, in the absence of lattice strains, well crystallised material should give reasonably sharp lines at all angles if the crystallite dimension is larger than 0.1 μm. Only at sizes much less than 0.01 μm do the low angle lines become very broad and diffuse.

In the present work, all of the samples for X-ray diffraction analysis were prepared in the same way, being ground and sieved to produce a powder with a particle size of -45μm. The photographs in Figure C-1.1 show that following this preparation the original samples

and the elemental sulphur produced in the leaching reaction gave sharp lines, and that only the lines corresponding to those of idaite were broad and diffuse. It might be expected that the strongly leached residues, with more than 90% of the copper removed, would give broad lines due to a small residual particle size. However, comparison of photographs (e) and (f) with photograph (a) in Figure C-1.2 show that even after only 44.68% of the copper has been removed the lines were already significantly much broader.

Hence it seems unlikely that crystallite size is the source of the line broadening and more likely that lattice imperfections play the major role.

It is doubtful whether the imperfections are structural faults in the lattice since this usually causes broadening of some lines but not others. In the present case, all of the lines of idaite were broad indicating that the imperfections are more likely due to the presence of strain in the lattice, causing a displacement of the atoms from their ideal sites, or a randomness in the population of the atomic sites in the structure. Both of these effects would be expected if silver ions were present in the lattice of the idaite phase.

## 3.6 Discussion and Comparison with other work.

The structure of bornite is a sphalerite-type skeleton that contains layers of ionically-bound interstitial atoms, Cu(I). Ugarte[11] has demonstrated that the removal of the ionically-bound copper atoms results in the formation of a chalcopyrite-like unit cell with a formula unit $Cu_3FeS_4$.

As has been mentioned in section 1.2.1, it is the removal of the ionically-bound copper that occurs in the first stage of the dissolution of pure bornite. This stage is fast because the copper ions can easily diffuse through the lattice. However this results in a contraction of the unit cell as the structure transforms to that with a formula unit of $Cu_3FeS_4$ (Figure 8) and the more difficult dissolution during the second part of the reaction is explained because the atoms are now covalently bound in a more ordered and compact structure. Thus, the dissolution, through a complete breakdown of this structure, results in the formation of elemental sulphur, with the copper and iron going into solution.

This two-stage mechanism of dissolution also applies to the silver-doped bornite. The silver in the original bornite remains in the solid state during the transformation and seems to become incorporated in the more compact $Cu_3FeS_4$ lattice.

Foreign atoms may be incorporated by crystals in a number of ways. Most important are isomorphous substitution for lattice atoms, assumption of interstitial positions, association with defects and dislocations, and adsorption on surfaces during crystal growth.

For ionic compounds the principal factor that determines the possibility of isomorphous substitution is one of volume, and a good first approximation to prediction of isomorphous substitution is given by Goldschmidt's rule that such substitution is possible if the ionic radii of the two elements being considered are within 15 per cent of one another (181). An appreciable correction is necessary for the coordination number of the ion in the particular structure being considered and such factors as electronegativity, polarizability and ionic potential need to be taken into account.

Fleischer[16] emphasized that the use of ionic or atomic radii in predicting solid solutions in sulphides is of rather little value because of the prevalence of mixed bonding. The covalent bond appears to prevail in many, but an unknown degree of transition to the ionic bond or, in some cases, the metallic bond[154] is indicated by certain physical properties.

The metal atoms, Cu(I) and Fe(III), which make up the sphalerite type-skeleton of the bornite structure are tetrahedrally co-ordinated to the sulphur atoms, while the interstitial ionic copper atoms were assumed to be Cu(I) because the preferred coordination of Cu(I) is tetrahedral[149]. Hence the tetrahedral covalent radius of silver should apply in a rough qualitative way to its probable substitution for copper. The difference in the covalent radii of the two elements, Ag(1.52Å), Cu (1.35Å), is, however, significant and approaches the limit permitted for extensive substitution, according to the Goldschmidt rule. The semiconductor properties of bornite also suggests some metallic bonding in the mineral and the atomic radius of silver might

be applied. The difference between the atomic radii of the two elements, Ag (1.40Å), Cu (1.24Å), is, however, again significant.

Despite this the present work suggests that the bornite lattice can hold up to 1.20 weight per cent of silver. The silver could replace the tetrahedally coordinated Cu(I) in the sphalerite-like skeleton, $Cu_3FeS_4$, or the Cu(I) ions in the tetrahedral interstices.

It is well known that silver participates in tetrahedral structures[182] and that silver is contained in many sulphides and probably substitutes for copper in copper sulphide lattices (15). Among the known tetrahedral compounds of silver are $AgFeS_2$, $AgAlS_2$, $AgGaS_2$ and $AgInS_2$, which have similar structures to that of chalcopyrite i.e., a complicated tetrahedral structure based on the sphalerite lattice. Tetrahedral arrangements of sulphur around silver have also been found in the minerals tetrahedrite-tennantite, $(CuAgFe)_{12}(SbAs)_4S_{13}$, proustite, $Ag_3AsS_3$, and pyragyrite, $Ag_3SbS_3$.[181]

In comparing the crystal chemistry of

copper and silver minerals, Povarrenkyh[183] stated that the difference in interatomic distances is relatively large at coordination numbers 2 and 3 but it decreases 10% at coordination number 4. Hence at low coordination numbers of atoms, replacements are practically absent, but in minerals with tetrahedral coordination the Ag ⟶ Cu isomorphic replacement is performed within a wide range. Thus silver may substitute for copper in the tetrahedrite-tennantite lattice up to 25% or more, resulting in a regular increase in the size of the unit cell with silver content[184].

Other sulphosalts which contain varying amounts of copper and silver include Polybasite, $(Ag,Cu)_{16}Sb_2S_{11}$, Pearceite $(Ag,Cu)_{16}AsS_{11}$ and Freibergite $(Cu,Ag,Zn,Fe)_{12}(Sb,As,)_4S_{13}$[15,155]. Skinner[143] also found evidence that stromeyerite had a measureable composition range extending from CuAgS towards $Cu_2S$ but not significantly towards $Ag_2S$. Skinner's suggested formula of $Cu_{1+X}Ag_{1-X}S$ where x ranges from 0 to 0.1 has been verified in field studies.[155]

Hence there is a considerable evidence for

the isomorphic replacement of copper by silver, and vice versa, in many copper-silver minerals. There is also a vast amount of literature on the silver content of other sulphides and sulphosalts, much of which is summarized by Fleischer[16] and Boyle[15]. Among the copper sulphides that contain some silver, Boyle lists the following:

| Sulphide | | Silver content in ppm |
|---|---|---|
| Digenite | $Cu_{2-x}S$ | 10 - 1000 |
| Chalcocite | $Cu_2S$ | 1 - 1000(up to 1%) |
| Bornite | $Cu_5FeS_4$ | 1 - 1000 |
| Chalcopyrite | $CuFeS_2$ | 5 - 3, 300 |
| Stannite | $Cu_2FeSnS_4$ | up to 1% |
| Covellite | CuS | Traces to 500 ppm. |

However, much higher silver contents have been recorded. Ottemann and Frenzel[185] found five mineral occurences of covellite in which from 2.4 to 16.7 wt.% of the copper was replaced by silver. Schwartz[139] suggested that up to 15% of $Ag_2S$ may substitute for $Cu_2S$ in chalcocite, but this was not supported by other work. Skinner[143] found that chalcocite could dissolve up to $1.83 \pm 0.37$ mole.% $Ag_2S$ at 63°C, the chalcocite acting as a host forming a solid solution in which silver

replaced copper.

Prouvost [186] produced a chalcopyrite containing about 5 to 8% silver by heat treating a sample of the mineral after depositing a small amount of silver on its surface. It was noted that the presence of silver in solid solution gave a greenish appearance to the chalcopyrite. Hawley and Nichol [17] found that, although it had an ionic radius too large to easily substitute for $Fe^{2+}$, $Cu^{2+}$ or $Cu^{+}$, silver was clearly concentrated in chalcopyrite areas rather than pyrite or pyrrhotite areas. This preferential concentration was taken as a reflection that the element was more acceptable in certain lattices than in others.

Goldschmidt[181] classified chalcopyrite as a more effective host mineral for silver than sphalerite but not as effective as Galena. It was suggested that the ions of silver are captured in the tetrahedral interstices between four sulphur ions. Goldschmidt calculated that the sum of the normal (6 coordinated) ionic radii of silver and sulphur is 2.87Å, which after correction for tetrahedral coordination, and for polorization of ions, gives

an interionic distance of 2.43Å.

This silver-sulphur distance is very close to the Ag - S distance in Stromeyerite (2.40 Å) which is identical to that found in the tetrahedrally coordinated structures of proustite and pyrargyrite.(141) It can be compared with following Cu - S distances for copper minerals with tetrahedral coordination.(187)

| | | | |
|---|---|---|---|
| Covellite | 2.31Å | Stannite(136) | 2.31 Å |
| Cubanite | 2.31Å | Tennantite | 2.28Å |
| Chalcopyrite | 2.28Å | Tetrahedrite | 2.34Å |

Although there does not seem to be very close agreement between the Cu - S distances and the Ag - S distance, as has already been pointed out, these minerals can retain much silver in their lattices. Since many of these minerals have structures similar to the sphalerite-like skeleton of bornite, it seems the replacement of the tetrahedrally coordinated copper by silver in the bornite lattice would also be quite feasible, as was found.

The silver could also replace the interstitial ionically bound copper atoms. Manning(188,189),

in experiments on the doping of sphalerite with copper and iron, showed that the interstitial sites are stable with respect to metal occupation. He calculated that if the copper atoms lie at the centres of undistorted sphalerite interstitial sites, then Cu - S bond lengths are 2.74Å. This is considerably larger than Goldschmidt's value of 2.43Å for the Ag - S distance and seems to suggest that silver incorporation could be quite possible in the interstitial sites of the sphalerite-like structure.

The structure that remains after the 1st stage of leaching is the sphalerite type skeleton of formula unit $Cu_3FeS_4$, known as idaite. All the above structural considerations apply to the silver that is obviously present in this structure. The silver may be in interstitial positions or may replace copper from its lattice positions. However some of the Cu(I) atoms in the original structure must become Cu (II) to retain electrical neutrality, hen ce not all the copper atoms will be replaceable by the Ag (I) atoms. The presence of the silver ions in the more compact $Cu_3FeS_4$ latticeproduces the line broadening in

the X-ray diffraction patterns described in sections 3.5.

Idaite was first named and described by Frenzel [190] as a supergene sulphide with a formula $Cu_5FeS_6$ which is formed, characteristically by the alteration of bornite. However Sillitoe and Clark [159] showed that the phase formed from Bornite in the oxidation zones of copper deposits had a composition of $Cu_3FeS_4$, which agrees with the findings of Levy[160], Ugarte[11], and the present work. Levy pointed out that since the X-ray data given by Frenzel bears close resemblance to the tetragonal patterns of stannite and mawsonite, idaite of formula $Cu_3FeS_4$ represents the tin-free end member of the $Cu_{2+x}\ Sn_{1-x}\ FeS_4$ solid solution series.

The other end member is stannite, $Cu_2FeSnS_4$, a tetrahedral quaternary compound of the type $Cu_2$ - II - IV - $S_4$ with a tetragonal superstructure based on the sphalerite structure with dimensions analagous to those of the chalcopyrite cell. [191]

Stannite is of interest in the present

discussion because it has been found that its copper is partially replaceable by silver. Moh [192] synthesised the compound Ag Cu Fe Sn $S_4$ but was not able to form the compound $Ag_2$ Fe Sn $S_4$, although it has been suggested as a possible tetrahedral compound.[191] Also the Sn - S distance in stannite is 2.43Å, which agrees exactly with the Ag - S distance calculated by Goldschmidt. However the replacement of Sn (IV) by Ag (1) would require oxidation of the Cu(I) and Fe(II) in the stannite structure to the higher oxidation states of Cu(II) and Fe(III).

It might be expected that the presence of silver would in some way influence the dissolution rate of the bornite and the reaction product idaite. It is an impurity in solid solution and may cause non-stoichiometry in the mineral composition and influence the electronic properties of the host crystal or affect the atomic spacing in the structure due to lattice distortion, all of which have been identified as factors affecting the chemical reactions of minerals. Prosser [8] pointed out that these factors would only be of importance in processes where the rate of chemical reaction or mass transfer through a solid phase was rate-

determining. Since the first stage of dissolution of bornite is by the diffusion of copper ions through the lattice, and the second stage is rate controlled by the chemical reaction by which $Cu_5FeS_4$ breaks down to elemental sulphur, the silver impurity could influence both stages of dissolution

The dissolution curves for the silver-doped bornite at 60°C and 90°C are shown in Figures 29 and 30 and compared with those obtained by Ugarte for pure bornite at the same temperatures, ferric ion concentrations and with the same leaching system. At both temperatures the rate of dissolution of copper has not changed significantly. However the rate of dissolution of copper from the silver-doped bornite is slightly lower than from the pure bornite in the first-stage of the dissolution reaction. This could be due to the slightly different leaching conditions used by Ugarte. He used a stirring speed to 950 rpm and a particle size of -150 + 105 microns compared to 1300 rpm and -180 + 125 microns used in the present work. The difference in stirring speed would not be expected to affect the leaching rate since both speeds were

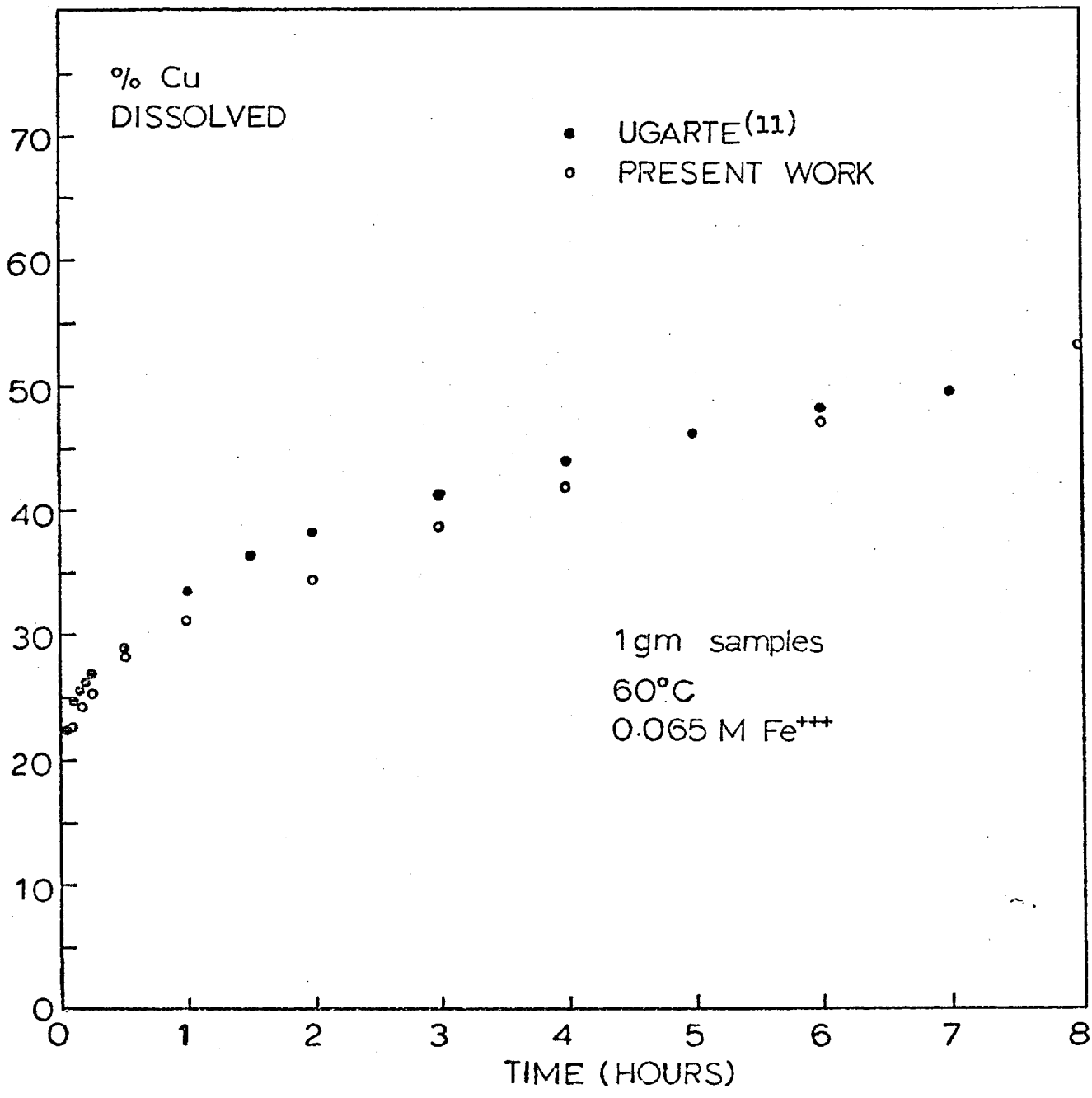


FIGURE 29 : Comparison of dissolution curve of silver - doped bornite at 60°C with that obtained by Ugarte[11] for pure bornite at 60°C.

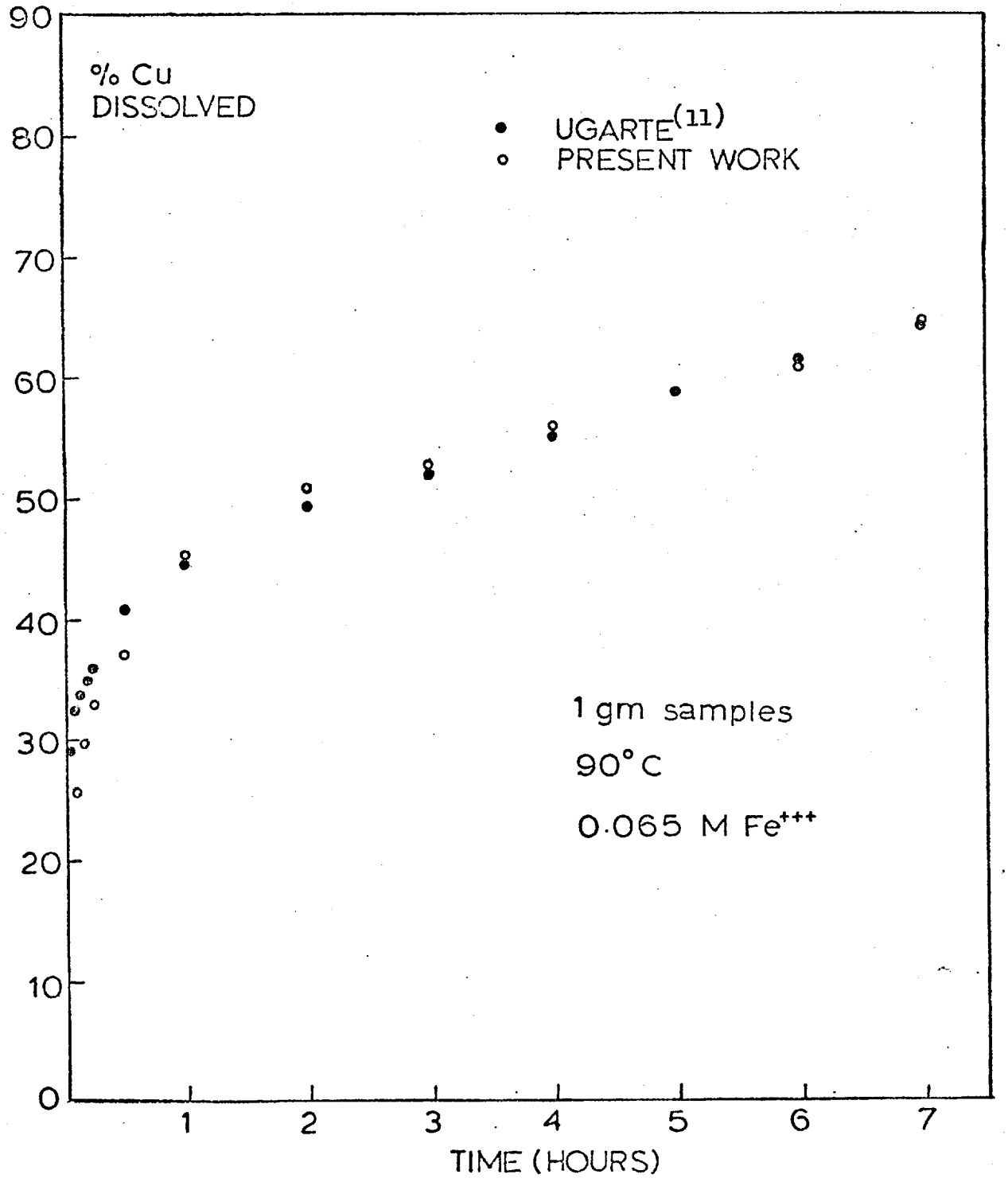


FIGURE 30 : Comparison of dissolution curves of silver - doped bornite and pure bornite at 90°C.

chosen to ensure that all the particles were maintained in suspension. However, the difference in particle size would have an effect.

Ugarte found that a reduction in particle size increased the rate of the first stage of the bornite dissolution reaction due to the rate-controlling step being the diffusion of copper ions in the lattice. A reduction in particle size reduces the distances of the diffusion and thus increases the rate of dissolution. Since the experimental results suggest the same dissolution mechanism for the silver-doped bornite, the slightly larger particle size of the silver-doped bornite would be expected to slightly reduce the dissolution rate of the copper, as was found.

An alternative explanation could involve the decrease in the silver content of the solutions in the initial stages of dissolution (see Figures 23 - 26). If one postulates that the small amount of silver initially dissolved was reprecipitated on the particle surfaces, this would also lead to a

reduction in the dissolution rate of the copper due to the reaction having to occur through this layer. Similar curves were obtained by Gerlach et al [116] for the dissolution of antimony from NiSbS and $Cu_3SbS_4$ due to the formation of basic antimony sulphate of low solubility which slowed down the dissolution rates for Ni and Cu. However the amount of silver 'precipitated' in the present work is so small that the effect, if any, would probably be negligible.

Apart from this slight reduction in the initial stage dissolution rate, the silver doped bornite seems to behave exactly like pure bornite with temperature and ferric ion concentration having effects which are in good agreement with other studies on bornite.

The activation energy value of 0.97 kcals per mole for the Cu dissolution in the first stage is somewhat lower than the values obtained by other authors for the dissolution of bornite. Ugarte[11] obtained a value of 2.1 ± 0.1 kcals per mole for the first stage of the reaction, while average values for the overall dissolution of 5.5 ± 1.4 and 5.7 ± 1.3 kcals per mole were reported by Kopylov and Orlov[93], and Dutrizac et al[94], respectively.

The low value obtained in the present work could be explained by two reasons. Firstly, the present calculations were based on the amount of Cu dissolved after 5 minutes by which time

the first stage of the dissolution could well have been nearing completion. Hence a more accurate activation energy value would probably have resulted with data obtained at a shorter leaching time.

Secondly, with a diffusion mechanism as postulated for the first stage of dissolution of bornite, it is apparent that the rate of copper dissolution will be dependent on the amount of copper dissolved, i.e., the rate will be dependent on the diffusion gradient in the lattice, or the coating thickness of the transformed phase, whichever mechanism applies. Thus when determining the apparent activation energy of the reaction, the rate of copper dissolution at each temperature must be measured when the same amount of copper has been removed, i.e., when the particles are in the same state. Hence measuring the rate in terms of the time required to dissolve a given copper percentage, instead of the amount of copper leached from the sulphide after a certain time, would eliminate some errors due to the variation of rate with per cent Cu dissolved. However since the first half of the reaction is extremely fast, the shape of curve is difficult to determine, and the rate had to be determined from the amount of copper dissolved after five minutes. (However this method was possible with tromeyerite, see section 5.1.1).

Other authors have found that the presence of silver as a 'doping' addition

often has a much more significant effect on the dissolution behaviour of other solids. Simkovich and Wagner [111] studied the kinetics of dissolution of lead sulphide as a function of stoichiometry and as a function of doping additions, silver sulphide, $Ag_2S$, and bismuth sulphide. In 6M nitric acid, the roles of dissolution of PbS were : PbS + $\frac{1}{2}$ mole % $Ag_2S$ > PbS (stoichiometric) > PbS + $\frac{1}{2}$ mole % $Bi_2S_3$ ≥ PbS (S excess) > PbS (Pb excess). With hydrochloric acid there was a much less pronounced difference between the dissolution rates of the doped and undoped crystals.

Carlson and Mikkola [112] studied the effect of cold work and Alloying additions on the kinetics of dissolution of copper in aqueous Cupric ammonium carbonate solution. Generally, solute additions (Zr, Cr) decreased the dissolution rate; however, the rate was found to pass through a minimum as a function of Ag content with additions of more than 0.15 wt. % Ag causing the dissolution rate to increase. The alloy with the highest silver content (0.5 wt. % Ag) gave a dissolution rate of 250 $mg/cm^2$ - hr compared to that of pure Cu of 184 $mg/cm^2$ hr. Measurements using an

electron microscope showed a considerable silver build up at the surface during dissolution.

Based on these observations the authors interpreted the effect of the Ag additions in terms of two distinct processes. At low levels ( < 0.15 weight per cent) the Ag decreases the dissolution rate simply through a mechanical blocking of the dissolution process, which is in general agreement with a model based on mixed reaction-diffusion control. The authors explained the build up of silver that occurs at the surface during the dissolution process as due to the low solubility of silver in cupric ammonium carbonate solution. At high concentrations ( > 0.15%), a sufficient amount is present to form a continuous layer of relatively pure silver which becomes fractured or fragmented by the combined chemical and mechanical forces of the dissolution processes.

Hence the increase in dissolution rate for the high Ag content alloy over that of pure Cu was thought to be the result of two factors: (a) the nonuniform attack promoted by the fragmented surface layer which leads to removal

of sizeable pieces of material through both chemical attack and mechanical forces, and (b) the electochemical effect of the Ag-rich layer in promoting chemical attack of the base material.

In contrast to the above findings, it has been shown that the presence of silver does not affect the dissolution of chalcopyrite or zinc sulphide. Baur el al [108] found that the addition of silver metal powder to an equal weight of chalcopyrite produced practically no increase in the amount of copper dissolved, while copper and iron powders increased the dissolution rate markedly (section 1.3). This was explained by the fact that the couple $Ag^{o}/CuFeS_2$ does not increase the anodic voltage of the chalcopyrite to the point of discharge of oxygen, by the oxidation of water, which would result in an increase in oxygen concentration on the mineral surface and an increase in the dissolution rate.

These authors also noted that although the presence of argentous ions in solution produces striking effects because of the exchange mechanism existing between lattice copper ions

and solution silver ions resulting in the probable formation ofargentite with copper going into solution, this had little effect on the dissolution of chalcopyrite. This was probably because silver is only slightly soluble in the weak sulphuric acid used as the leaching agent.

Similarly it has been shown that although silver can replace zinc in the lattice of zinc sulphide, one $Zn^{2+}$ ion being replaced by two $Ag^{+}$ ions producing a silver sulphide layer at the surface [193], the presence of silver does not catalyse the oxidation of zinc sulphide under acid pressure leaching conditions [114]. It was assumed that the oxidation potential of the silver was outside the required limits for effective mediation and catalysis of the electrochemical reactions occurring as the zinc sulphide dissolved.

It seems likely that the lack of enhancement of copper from silver-doped bornite that was found in the present work could be explained by similar electrochemical considerations. An explanation based on the fact that the silver was only present in a small amount seems unlikely, since Simkovich and Wagner, and Carlson and Mikkola, obtained increased dissolution rates with only small additions of silver.

SECTION 4

## EXPERIMENTS ON SILVER COMPOUNDS

Since there was no appreciable dissolution of silver in the leaching solutions used in section 3, a number of experiments were carried out on the solubility of silver sulphate and silver sulphide in similar solutions, in the absence of copper.

### 4.1. Solubility of Silver Sulphate.

The solubility of the silver sulphate was measured to make sure that the silver from the silver-doped bornite was not being dissolved and then precipitated as the sulphate. X-ray and microscopic analysis already indicated that this was not the case but because the silver is present in such small quantities it was decided to recheck by solubility measurements using a simple technique first used by Ward (194).

The silver sulphate was prepared by dissolving pure silver in hot sulphuric acid, evaporating off some of the liquid and crystallising the sulphate by cooling. The x-ray diffraction pattern of the solid was in complete agreement with that listed in the A.S.T.M. X-ray index file.

The solubility was measured in a solution containing 0.065M $Fe^{3+}$ in $H_2SO_4$, with a pH of 1 at temperatures from 35°C to 90°C. The results, expressed as grams of silver sulphate per litre, are shown in Figure 31. The solubilities compare with values of 5.7 gms/litre at 0°C, 14.1 gms/litre at 100°C [195] and 7.8 gms/litre at 25°C [15] for silver sulphate in water.

4.2. Solubility of Silver Sulphide.

The dissolution of silver sulphide was investigated using the same procedure and apparatus as in the leaching experiments (section 2.2). A 0.065M ferric ion solution in $H_2SO_4$ (pH1) was used at 60 and 90°C. The weight of silver dissolved in 200 mls of solution is plotted as a function of time for each temperature in Figure 32.

The silver sulphide was prepared as a precipitate by mixing solutions of sodium sulphide and silver sulphate. After washing in distilled water and acetone, the powder gave an X-ray pattern in good agreement with that listed in the A.S.T.M X-ray Index file (Table B-1.6). The residues from the dissolution experiments

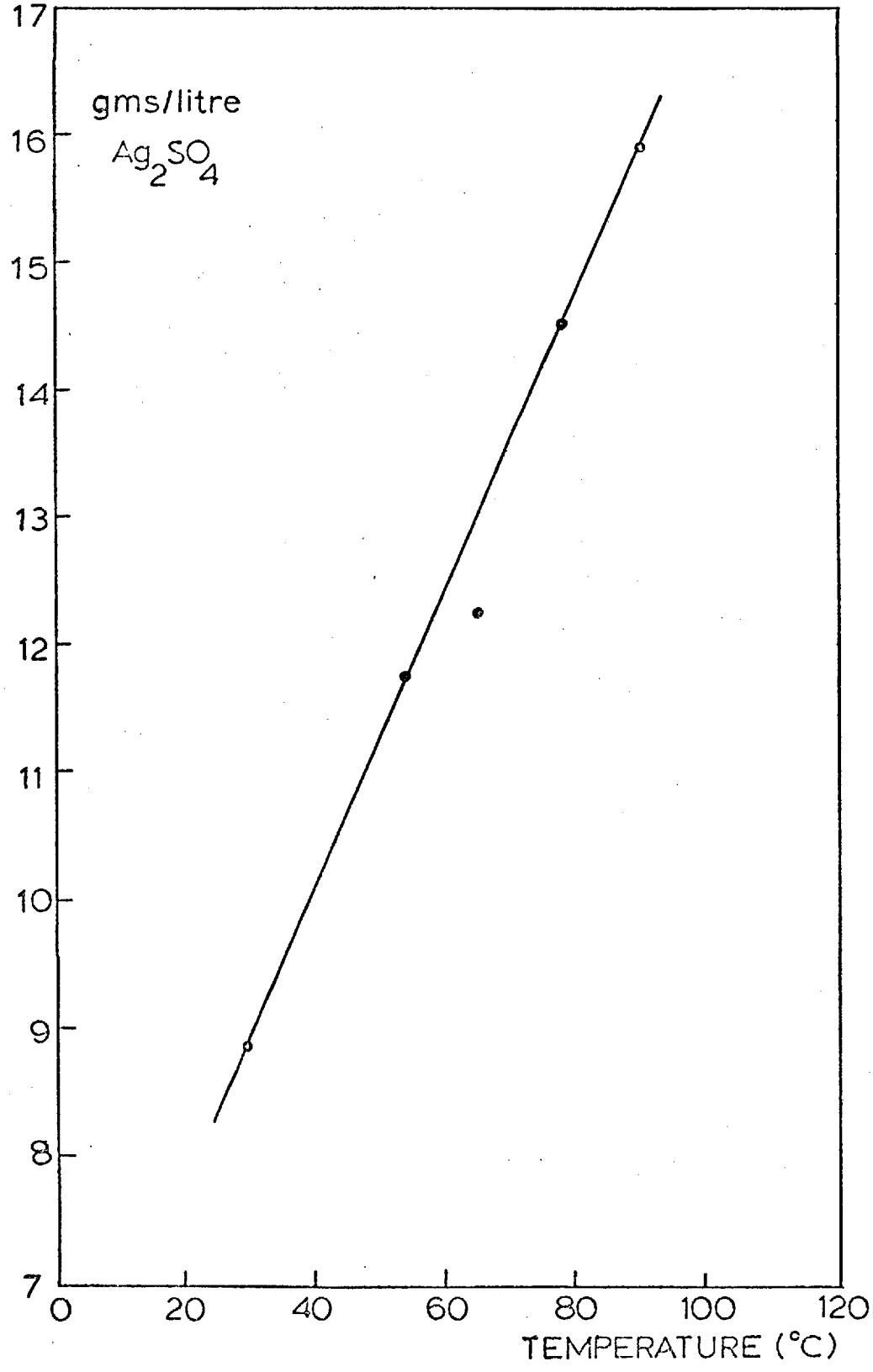


FIGURE 31 : Solubility of silver sulphate in a 0.065M $Fe^{3+}$ solution, in $H_2SO_4$ (pH 1), as a function of temperature.

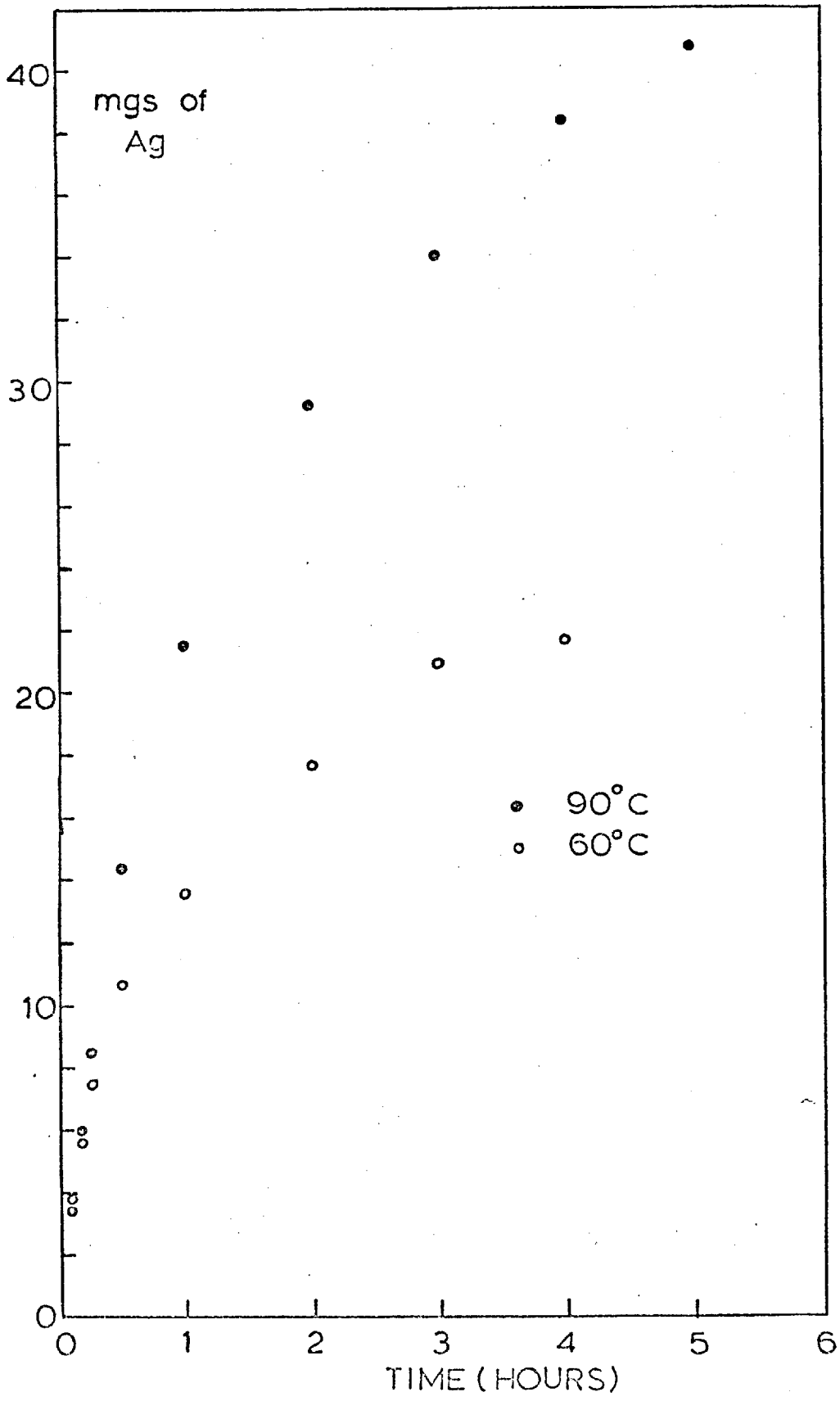


FIGURE 32 : Solubility of silver sulphide in a 0.065M $Fe^{3+}$ solution , in $H_2SO_4$(pH 1), as a function of time at 60°C and 90°C.

were also analysed by X-ray diffraction.

The pattern for the residue after dissolution at 60°C could be indexed as a mixture of silver sulphide and orthorbombic sulphur (Table B-1.7) while the pattern for the residue from the 90°C dissolution (Table B-1.8) seemed to be a mixture of silver sulphide and a phase with a diffraction pattern very close to that of jarosite, $KFe_3(SO_4)_2(OH)_6$, and argentojarosite, $Ag_2Fe_6(OH)_{12}(SO_4)_4$ (see Tables B-1.5 and B-1.8).

## 4.3. Discussion

Both the silver sulphate and silver sulphide solubilities show that the ferric sulphate solution could dissolve more silver than is present in the silver doped bornite samples used in the previous leaching experiments. A one gram sample contained 12 milligrams of silver which according to both figure 31 and 32 should dissolve easily in the leach solutions and precipitation of sulphate or sulphide should not occur.

This can also be shown by calculations involving the solubility products of silver sulphate and sulphide. In section 3.1.3 it was

mentioned that after 52 hours in 200 mls of 0.25M ferric sulphate solution 0.6 milligrams of silver had dissolved. Calculation of the function $(Ag^+)^2 \times (SO_4^{2-})$, where $(Ag^+)$ and $(SO_4^{2-})$ are the concentrations of the species expressed in moles per litre, gives a value of about $2.90 \times 10^{-10}$. This is considerably lower than the solubility product of silver sulphate[15] $1.24 \times 10^{-5}$.

Using the solubility results in Figure 31, the solubility product of $Ag_2SO_4$ was calculated to be $3.24 \times 10^{-5}$ at 35°C and $2.42 \times 10^{-4}$ at 65°C. Using the latter value it was calculated that 0.4 grams of silver could be dissolved in 200 mls of 0.25M ferric sulphate solution. This compares with the 0.6 milligrams actually found in the leaching experiment. Thus the precipitation as sulphate does not seem to explain why only small amounts of silver entered the solution.

For the precipitation of silver sulphide, sulphide ion, $S^{2-}$, must be present. From the solubility product of silver sulphide[195] $1.6 \times 10^{-49}$, and the above amount of silver known to be in solution (0.6 mg), the concentration of

sulphide ion required for precipitation of $Ag_2S$ was calculated to be about $2.07 \times 10^{-36}$ moles/litre. However, by using the solubility products[195] of cupric sulphide ($8.5 \times 10^{-45}$) and cuprous sulphide ($2 \times 10^{-47}$) it can be shown that the presence of this amount of sulphide ion in the solution would limit the amount of copper in 200 mls of solution to $5.22 \times 10^{-8}$ grams due to cupric sulphide precipitation or $3.95 \times 10^{-5}$ grams due to cuprous sulphide precipitation. The rate curves (Figures 23 to 26) show that this precipitation did not occur.

Considering 100% copper dissolution from a 1 gram sample gives a possible sulphide ion concentration of $1.7 \times 10^{-43}$ from the cupric sulphide solubility product, and $8 \times 10^{-45}$ from the cuprous sulphide solubility product. Using the solubility product of $Ag_2S$ shows that solutions containing up to these amounts of sulphide ion could hold up to about 21 and 96 milligrams of silver, respectively, compared to the actual value of 0.6 milligrams. Hence precipitation of silver as silver sulphide seems unlikely to occur.

The dissolution of silver sulphide in 200

mls of 0.065M $Fe^{3+}$ solution seems to reach a maximum of 22 mgs at 60°C (Figure 32). Calculation of the ratio $(Ag^{+})\ (Fe^{2+})/\ (Fe^{3+})$ gives a value of 0.0001562, which is considerably lower than the equilibrium ratios observed by other authors (see section 1.1.2). This suggests that the reaction stops for a reason other than its nearing equilibrium; perhaps the sulphur produced in the reaction forms a layer around the particles. A microscopic examination was attempted but the silver sulphide was too fine for successful mounting and polishing of the residues. The presence of sulphur suggests that the dissolution reaction is :

$$Ag_2S + Fe_2(SO_4)_3 = Ag_2SO_4 + 2FeSO_4 + S^{o} \quad (4.3.1)$$

The low equilibrium constants found by other authors (section 1.1.2) suggest that when the silver-doped bornite is leached, the copper is selectively dissolved and the ferrous ion produced inhibits subsequent silver dissolution. After the above solubility considerations, this seems more likely than that the silver is precipitated as sulphide or sulphate. However, later work on the dissolution of copper and silver from stromeyerite (sections 5.1.7 and 5.1.8)

showed that the major factor in inhibiting silver dissolution seems to be the presence of copper ions in solution.

It was noted that a jarosite-type phase was produced on dissolving silver sulphide in the ferric solution at 90°C. Its yellow-brown colour and the similarities between its X-ray pattern and those of other jarosites suggests that the phase is argentojarosite. May et al[196] have recently synthesised argentojarosite and their d-spacings are listed in Table B-1.8 for comparison.

The formation of an argentojarosite precipitate in the present experiments seems to be consistent with previous observations. May et al precipitated their argentojarosite in $HNO_3$ and $H_2SO_4$ solutions by dissolving silver sulphate in the boiling solutions, adding ferric sulphate, and refluxing at 97°C for a number of hours. Fairchild[197] formed it by heating a saturated solution of silver sulphate in ferric sulphate to between 110 and 200°C in evacuated sealed tubes.

SECTION 5

## STROMEYERITE, RESULTS AND DISCUSSION

### 5.1. Leaching Results.

The general characteristics of the dissolution of stromeyerite, $Cu_{1.07}Ag_{0.93}S$, in acidic ferric sulphate solutions are shown in Figure 33. 50% of the copper dissolved in a very short time, but the second stage of the dissolution was extremely slow. For the conditions of Figure 33, 50% of the copper dissolved in 30 minutes, but in the following $8\frac{1}{2}$ hours only a further 10% dissolved. (see Table A-2.1).

The amount of silver that dissolved was extremely small. This was so under all the conditions tried with acidic ferric sulphate solutions (pH1). Because of this most of the silver dissolution results are not presented graphically but are given in Tables A-2.1 to A-2.19 as either weight per cents or actual weights dissolved.

The effects of temperature, ferric ion concentration, stirring speed, sample weight and particle size on the dissolution of copper were investigated. The stromeyerite was also leached in chloride solutions, hydrogen peroxide,

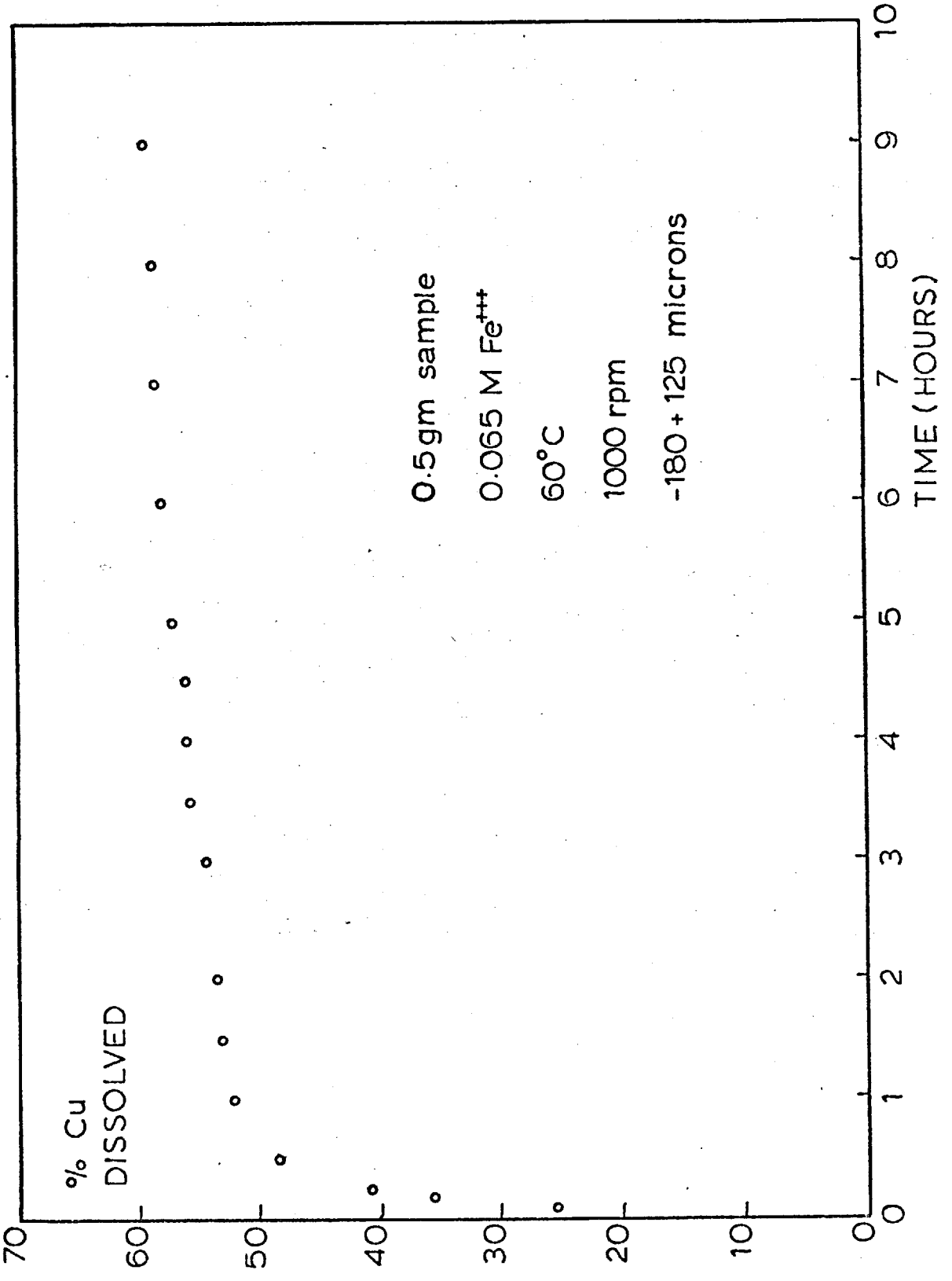


FIGURE 33 : General charecteristics of the dissolution of copper from stromeyerite, $Cu_{1.07}Ag_{0.93}S$.

and a solution containing a suspension of managanese dioxide, to compare the effects of different oxidants.

5.1.1. Temperature.

Increasing the temperature from 30°C to 90°C increased the rate of dissolution of copper in the first stage of the dissolution process (up to 50% of the copper dissolved) but seemed to have little effect on the slower second stage (Figure 34). The dissolution of silver increased slightly with increasing temperature, but the amounts were very small (Tables A-2.2 to A-2.7).

The experiments were carried out from 30 to 90°C with 0.5 gram samples of particle size -180 + 125 microns in a 0.1M ferric sulphate solution with a pH of 1 stirred at 1300 rpm.

The activation energy of the first part of the reaction was determined by plotting the reciprocal of the absolute temperature against the logarithm of the weight % of Cu dissolved in 5 minutes, using data from the above Tables, to give the Arrhenius plot as in Figure 35. This seems to show two distinct lines, one

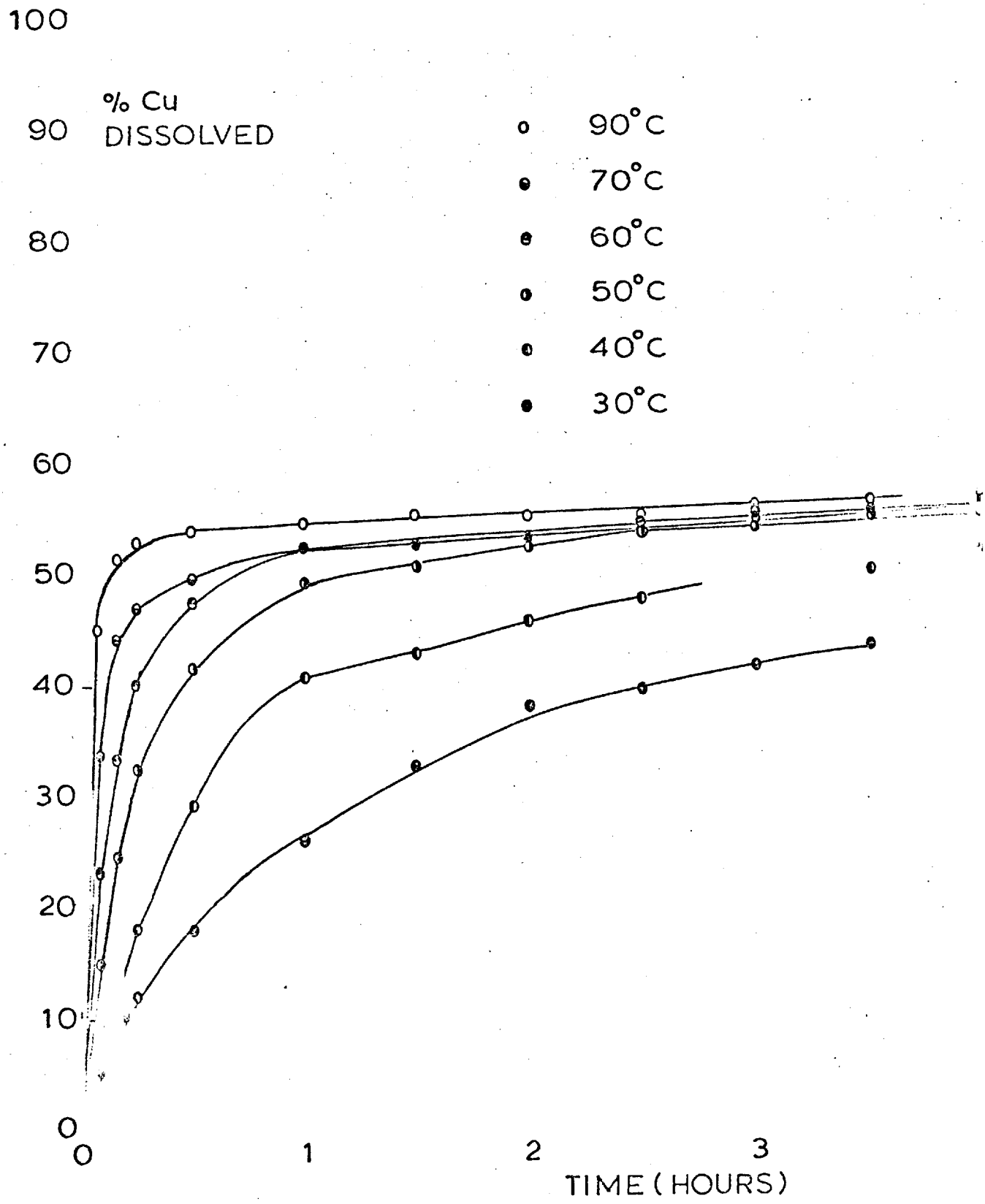


FIGURE 34 : Effect of temperature on the dissolution of copper from stromeyerite.

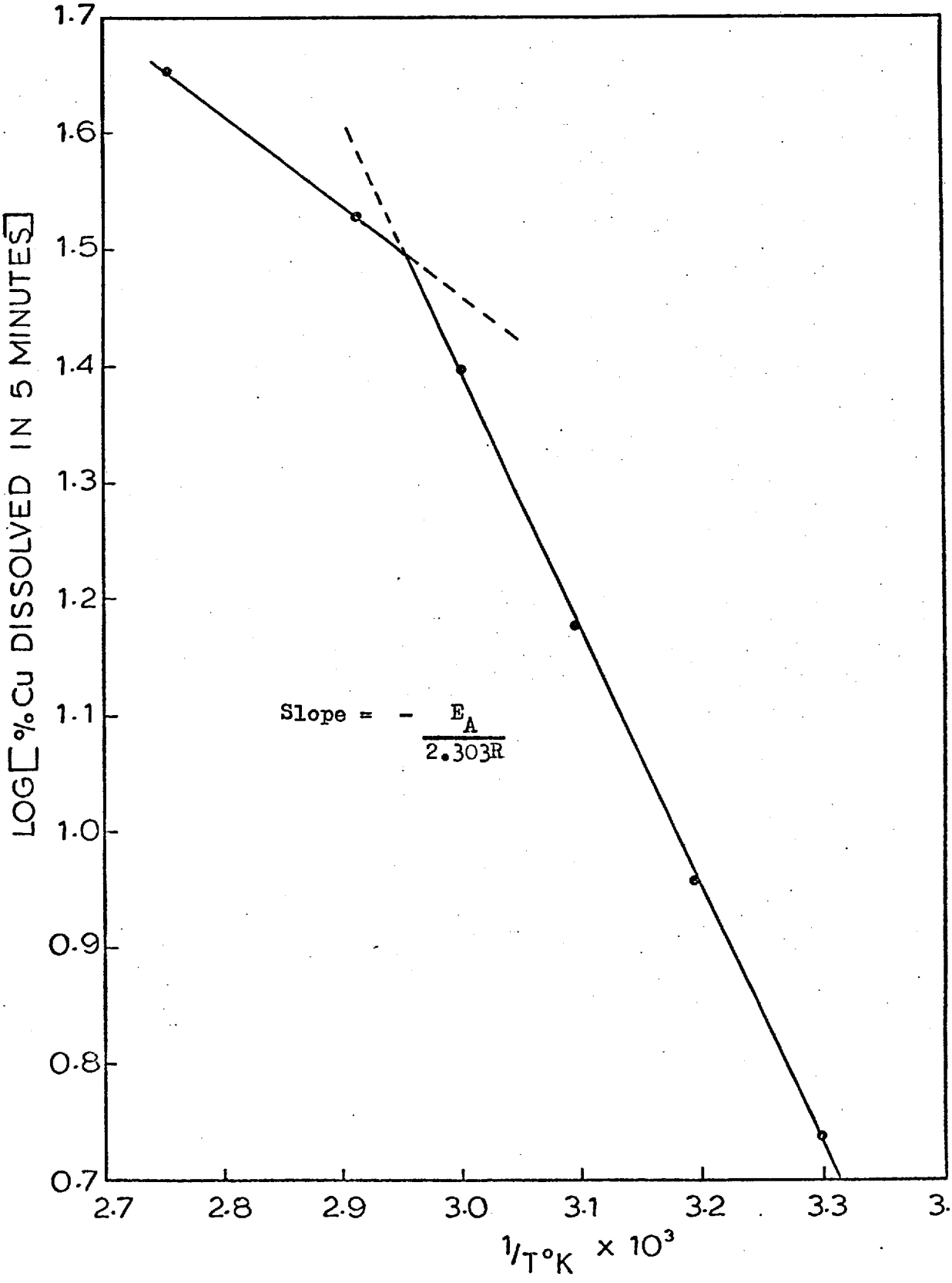


FIGURE 35 : Determination of the activation energy of the first stage of the dissolution of copper from stromeyerite using the wt.% of copper dissolved in 5 minutes as a measure of the rate. ($E_A$= activation energy, R= gas constant).

occurring below 70°C and one between 70°C and 90°C, suggesting that there are two competing reactions. The respective values of the apparent activation energies were calculated to be 10.09 Kcals per mole at the lower temperatures, and 3.66 Kcals per mole at the higher temperatures.

From the considerations discussed in section 3.6 on the determination of the activation energy of the silver-doped bornite, it is known that a more accurate method of determining the activation energy would be to use the times required to dissolve a given copper percentage as the basis of the measured rates at the different temperatures. In the case of the silver-doped bornite the initial dissolution rate was too fast for accurate determinations of those times, but in the case of stromeyerite, the shape of the curves can clearly be drawn, (Fig. 34) and the time taken to dissolve a certain copper percentage can be estimated at the different temperatures.

The data in Table A-2.20 was used to plot Figure 36. The curves still have the features of Figure 35, but it is noticeable that for the

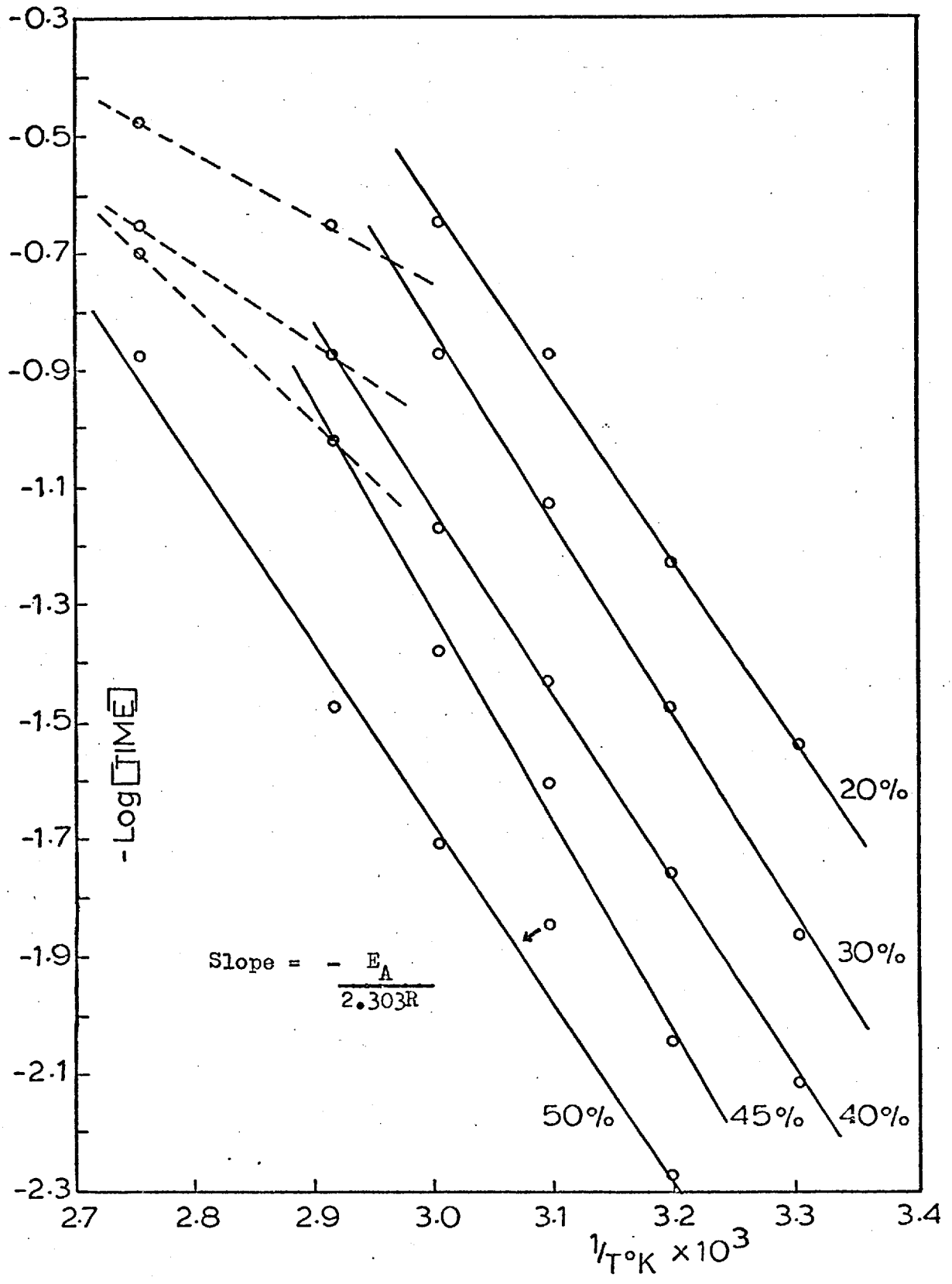


FIGURE 36 : Determination of the activation energy of the first stage of the dissolution of copper from stromeyerite using the reciprocal of the time to dissolve a certain wt. % of copper as a measure of the rate.

plot for 50% copper dissolved, all the points lie approximately on the same straight line, although the points are more scattered. Straight lines were drawn through the points for temperatures of 70°C and below, and also through the 70°C and 90°C points. The latter lines were drawn merely to calculate a value for the activation energy above 70°C and do not imply that the reaction has the same activation energy at 70°C and 90°C.

The calculated activation energies were as follows: (in Kcals per mole)

| % Cu dissolved. | < 70°C | > 70°C |
|---|---|---|
| 20% | 14.20 | - |
| 30% | 15.21 | 5.23 |
| 40% | 14.64 | 6.53 |
| 45% | 16.50 | 9.15 |
| 50% | 14.15 | 14.15 |

These results can be interpreted in one of two ways depending on whether one considers the date used in the above Figures for the 90°C run to be accurate or not. If one considers that the rate of copper dissolution at 90°C is so fast that accurate estimates of times to dissolve certain copper percentages cannot be made, the

data, and thus the different activation energies calculated above 70°C, can be ignored. In this case one supposes that the activation energy of the dissolution reaction in the first stage of the leaching process is given by the average value from the above values obtained at less than 70°C, i.e., approximately 15 kcals per mole. This is lower than normally expected of a chemically controlled reaction and too high for a transport controlled reaction. It seems to indicate an intermediate process where the rate is controlled by both chemical and diffusion factors.

This seems to be in agreement with the mechanism proposed from the X-ray diffraction analyses (section 5.2) and supported by microscopic and electron probe work (sections 5.4. and 5.5.). Equations 5.2.1., 5.2.2 and 5.2.3 show that the reaction proceeds by the diffusion of copper out of the stromeyerite which transforms via the phases $Ag_{1.2}\ Cu_{0.8}\ S$ and $Ag_{1.55}\ Cu_{0.45}\ S$ to silver sulphide, $Ag_2S$, at the same time as covellite, CuS, is being 'precipitated' along certain crystallographic planes. This latter part of the reaction could well be the chemical reaction that increases the

activation energy above that normally associated with diffusion processes.

However if one considers that the data for the 90°C leach run is accurate, the lower activation energies at temperatures greater than 70°C indicate that the chemical reaction becomes less rate determining at these higher temperatures, i.e., the 'precipitation' of CuS becomes easier. This again seems quite feasible from the proposed reaction mechanism.

The increase in activation energy with percentage of copper dissolved could also be simply due to inaccuracies in the data used, or due to the 'precipitation' of CuS becoming more difficult and hence more rate determining as the reaction nears completion. At the end of the first stage of the dissolution, after 50% of the copper has dissolved, the reaction seems to have the same rate determining factors over the whole temperature range, as witnessed by the points all falling on or about the same line (Figure 36).

The apparent independence of the rate of the second stage of dissolution of any change

in temperature suggests that the second stage reaction, the dissolution of covellite, was inhibited by the silver sulphide remaining in the residues. King [9] showed that the rate of dissolution of covellite is controlled by a chemical process, which is dependent on temperature, whereby elemental sulphur is formed via the phase $Cu_{0.8}S$.

5.1.2. Ferric ion concentration.

The results are presented in Figure 37 and Tables A-2.6, and A-2.9 to A-2.11. These show that above 0.065M$Fe^{3+}$, the ferric ion concentration has little effect on the rate of dissolution of copper from stromeyerite. The experiments were carried out at 0.01M, 0.065M, 0.10M and 0.25M $Fe^{3+}$ concentrations with 0.5 gram samples of particle size -180 + 125 microns at a temperature of 60°C and a stirring speed of 1300 rpm; the solutions having a pH of 1.

At the concentration of 0.01M $Fe^{3+}$ the rate of the first stage of the dissolution reaction was reduced considerably, but the rate of the second stage, after 50% of the copper had been removed, was the same as at the higher ferric ion concentrations. Thus it seems that the

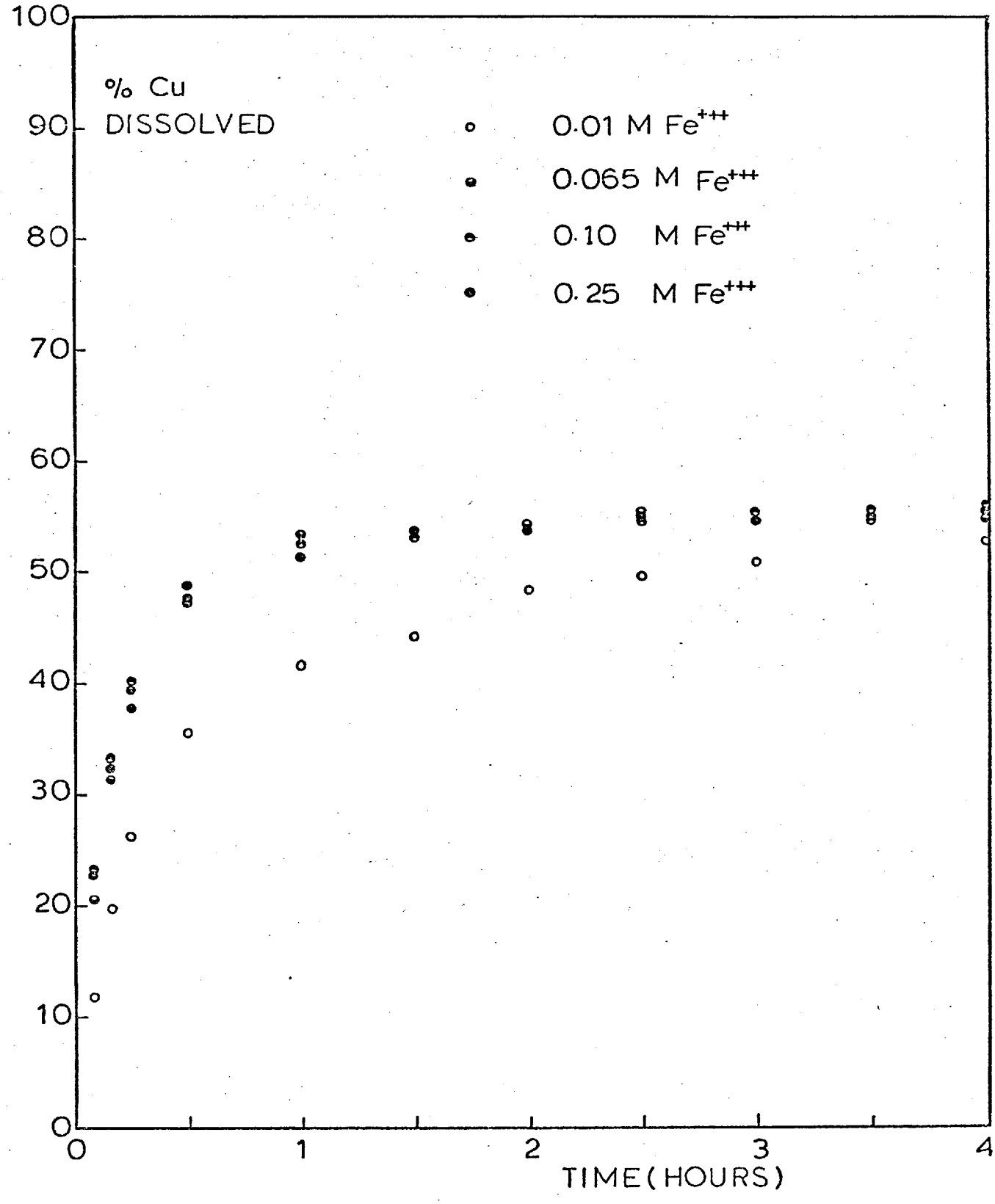


FIGURE 37 : Effect of ferric ion concentration on the dissolution of copper from stromeyerite.

second stage of the dissolution of copper is independent of ferric ion concentrations down to 0.01 M$Fe^{3+}$.

Very little silver was dissolved at all ferric ion concentrations, but the amount does increase with increase in $Fe^{3+}$ concentration (see above Tables). At the higher concentrations (0.10M and 0.25 M) a definite maximum occurs in the silver content of the solutions after about 15 minutes. This is very similar to the behaviour of the silver dissolved from the silver-doped bornite (Section 3.1).

Leaching a sample of stromeyerite in $H_2SO_4$ acid solution (pH1) with no ferric ion present showed that only 0.1% of the copper was dissolved in $3\frac{1}{2}$ hours, while the amount of silver in solution was too small to measure accurately (Table A-2.8).

The reaction mechanism postulated in section 5.2 and equations 5.2.1 to 5.2.4 shows that for completion of the first stage of the reaction, with 50% of the copper dissolved, 1.07 moles of ferric ion are required per one mole of stromeyerite. From this it can be calculated

that 200 mls of 0.01M $Fe^{3+}$ solution is more than sufficient to dissolve this amount of copper from the 0.5 gram sample used. Hence the slower rate at the 0.01M $Fe^{3+}$ concentration is due to some rate determining step, either a chemical reaction or a diffusion process, which becomes less important at higher ferric ion concentrations.

Above 50% of copper dissolved, the dissolution of copper is by the chemical reaction whereby covellite, CuS is transformed to elemental sulphur via the non-stoichometric phase $Cu_{0.8}S$ (section 5.2, equations 5.2.5 , 5.2.6). It would be expected that this rate-determining chemical process would be dependent on the ferric ion concentration. Hence the apparent independence of the second stage of the dissolution observed over the whole range of ferric ion concentrations suggests that another process is rate determining. This could well be a diffusion process connected with the $Ag_2S$ which remains as a layer around the leached samples (see microscopic section 5.4), and thus inhibits the dissolution of copper.

5.1.3 Stirring Speed

In Figure 38 are shown the results of two identical leaching experiments but with the solutions stirred at different speeds. The results are also presented in Tables A-2.1 and A-2.10.

0.5gm samples of particle size -180 + 125 microns in 0.065M $Fe^{3+}$ solutions at 60°C were stirred at 1000 and 1300 rpm, respectively. The difference in stirring speed has little effect on the leaching rate and dissolution characteristics of the copper from stromeyerite.

The initial rate for the experiment at 1000 rpm seems to be slightly faster but this could be experimental error due to the very fast reaction rate in the first stage of dissolution up to 50% of the copper dissolved.

Again very small amounts of silver dissolved but more seems to be dissolved at the higher stirring speed (see above Tables). However it is difficult to perceive any trends due to the very small amounts of silver involved, e.g. at 1000 rpm, 0.048% of the silver had dissolved after 9 hours.

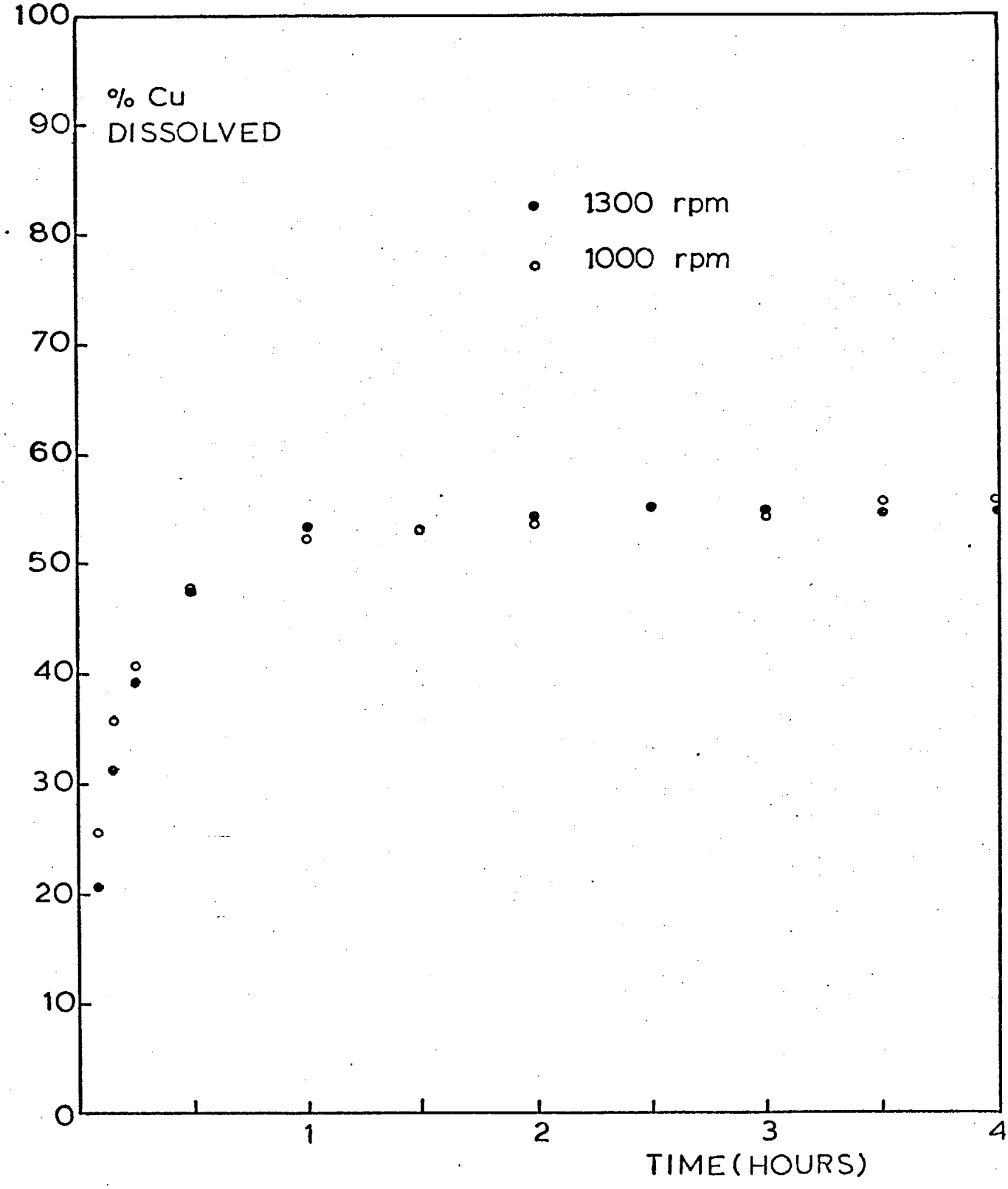


FIGURE 38 : Effect of stirring speed on the dissolution of copper from stromeyerite.

These observations indicate that the diffusion of ferric ions from the solution to the surface of the particles is not the rate-controlling step in either the first or second stage of the dissolution reaction.

5.1.4 Particle size.

Increasing the particle size from -85 + 120 mesh to -40 + 50 mesh reduced the dissolution rate of copper from stromeyerite during the first stage of the dissolution process. This suggests that a solid-state diffusion process is important in the first stage of the dissolution process (up to 50% of the copper dissolved) since increasing the particle size would increase the distances over which diffusion has to occur, slowing down the dissolution rate of the diffusing species.

The mechanism postulated in section 5.2 shows that copper diffuses from the stromeyerite which transforms via the phases $Ag_{1.2}\ Cu_{0.8}\ S$ and $Ag_{1.55}\ Cu_{0.45}\ S$ to $Ag_2S$, as covellite seperates out. Thus the above observations are in agreement with this mechanism.

The results in Figure 39 were obtained with

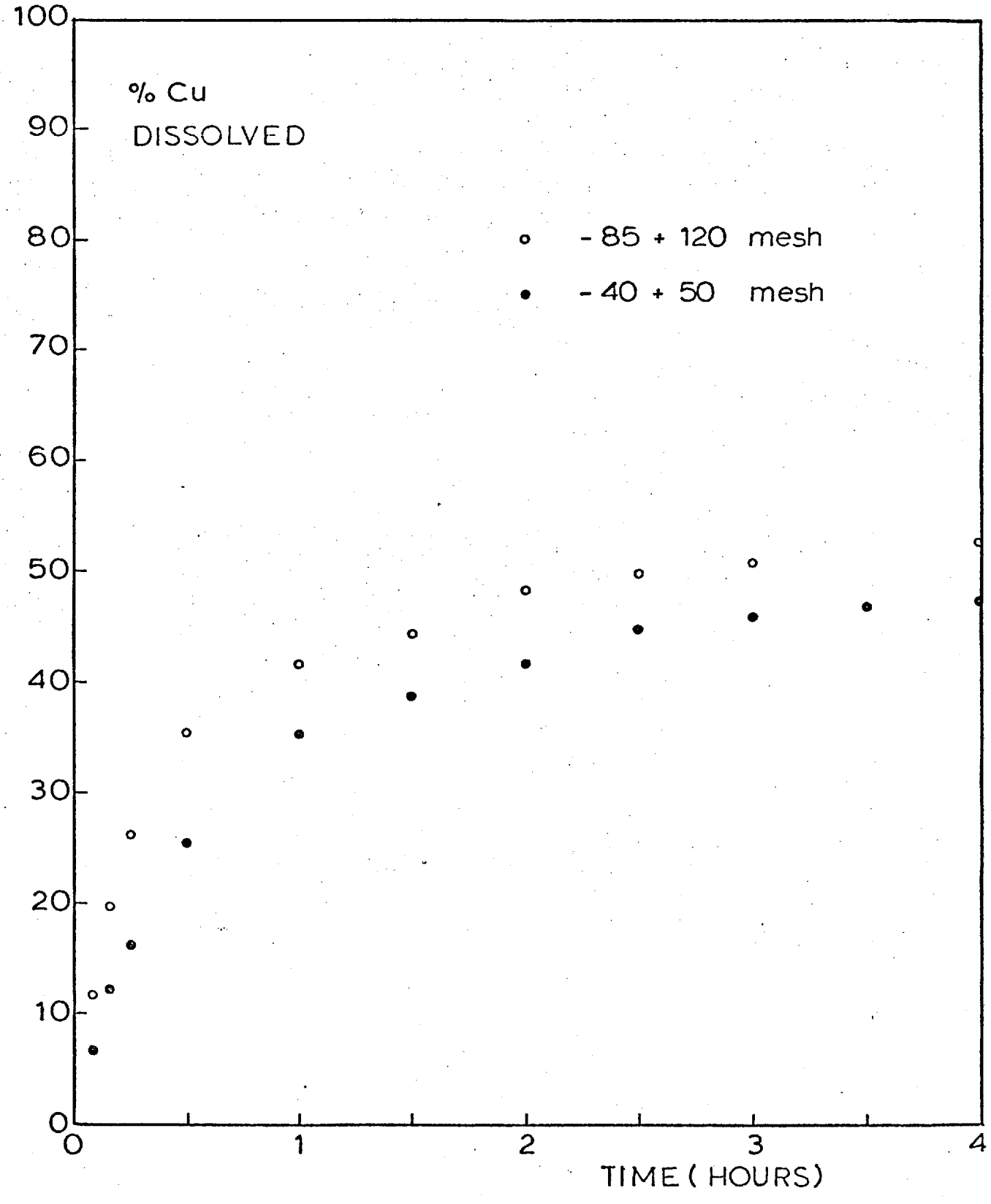


FIGURE 39 : Effect of particle size on the dissolution of copper from stromeyerite.

0.5 gram samples, a stirring speed of 1300 rpm and a temperature of 60°C using 0.01M $Fe^{3+}$ solutions (pH1). The rate of the second stage of the dissolution process appeared to be unaffected by the change in particle size. Increasing the particle size reduces the surface area and hence it would be expected to decrease the rate of any chemical process at the surface, i.e. the dissolution of covellite. That this second stage of the reaction is also unaffected by temperature, ferric ion concentration or stirring speed suggests that the reaction is inhibited in some way. Microscopic examination (section 5.4) suggests that this is due to the residual silver sulphide.

Particle size seemed to have no effect on the silver dissolution. The results in Tables A-2.9 and A-2.12 show that the amounts of silver dissolved remained very small.

5.1.5 Weight of sample.

The effect of decreasing the weight of the sample, used in the experiments from 0.5 grams to 0.1 grams is shown in Figure 40. Both experiments were carried out at 60°C in a 0.1M $Fe^{3+}$ solution stirred at 1300 rpm and both

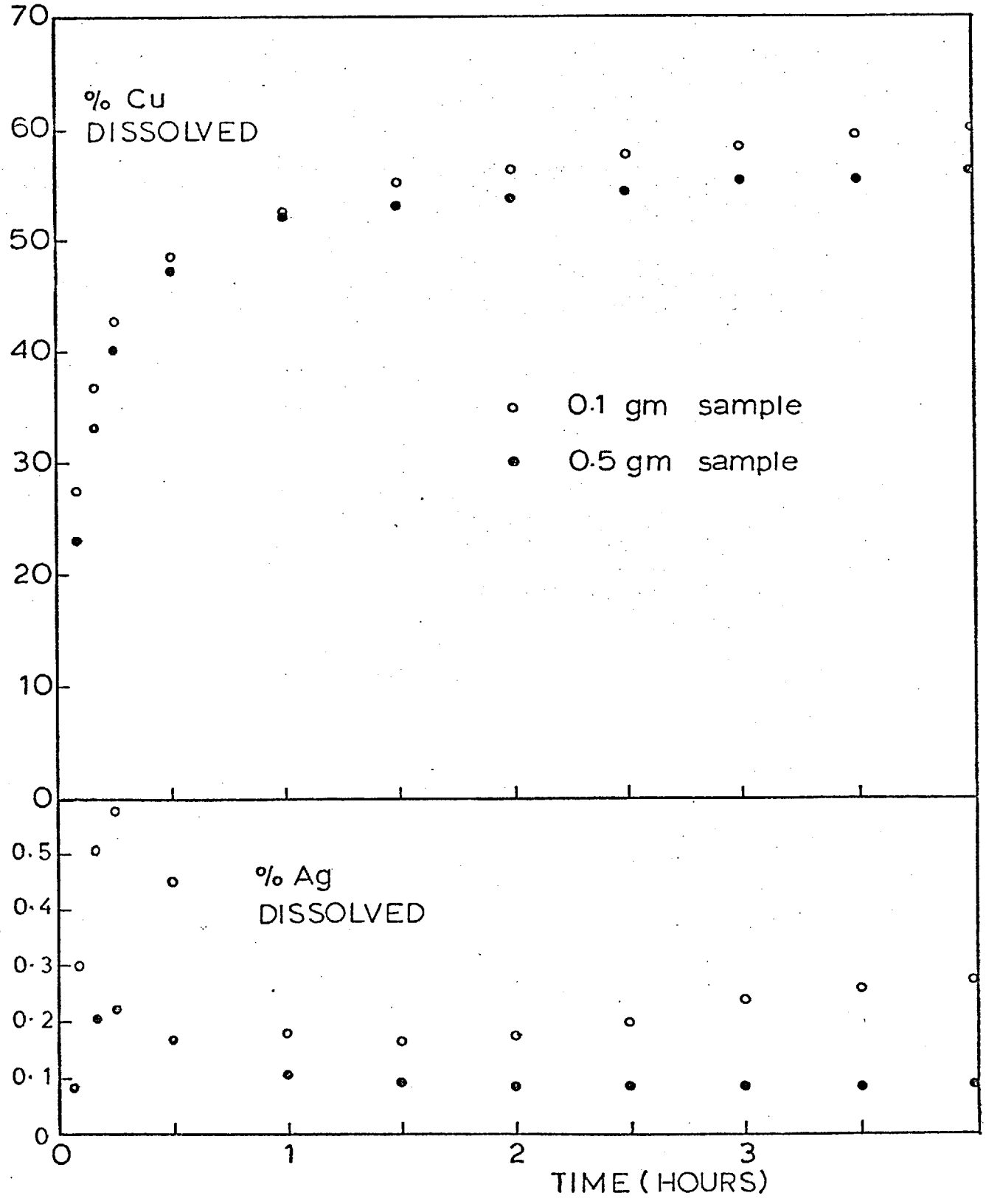


FIGURE 40 : Effect of sample weight on the dissolution of silver and copper from stromeyerite.

samples had a particle size of -180 + 125 microns. The results are also presented in Tables A-2.6 and A-2.13.

The 0.1 gram sample appears to have the faster initial rate but,as with the slight difference observed with change in stirring speed, this could be because of experimental errors due to the rapidity of the initial reaction stage. It should be noted that after one hour, the same weight per cent of copper had been dissolved from both samples. However, in the second stage of the dissolution (above 50% of the copper dissolved) the 0.1 gram sample clearly had a faster copper dissolution rate, indicating that the inhibiting factor on the chemical dissolution of the covellite was less effective, probably due to the greater excess of ferric ion remaining after the first stage of dissolution. This would be expected if the inhibiting factor was a layer of $Ag_2S$ at the surface.

The silver dissolutions are also plotted as weight per cents in Figure 40. As can be seen,the amounts of silver dissolved are very small and the dissolution curves have the same

characteristics as was found with the silver doped bornite, having initial maxima followed by a decrease in the silver content of the solutions and then an increase with a very slow rate.

The weight of the sample seems to have a marked effect on the silver dissolution, the percentage of silver dissolved being greater for the smaller sample. This could simply be due to less ferric ion being converted to ferrous ion because less total weight of copper has been dissolved from the smaller sample.

Hence although the actual weights of copper and silver dissolved from the smaller sample are considerably less, on a weight per cent basis the rates of copper and silver dissolution are increased by reducing the sample weight or, in other words, by increasing the ratio of volume of solution to weight of sample.

5.1.6. Effect of Chloride ion.

Stromeyerite was also leached in solutions containing chloride ion. Figure 41 shows the dissolution curves for stromeyerite in a 0.1M Ferric Chloride solution in 0.1M HCl, containing

4M NaCl, and in a 0.1M HCl solution containing 3.3M NaCl. The results are also presented in Tables A-2.14 and A-2.15. The dissolution curve for stromeyerite in 0.1M ferric sulphate (Table A-2.6) is included in Figure 41 for comparison.

The presence of chloride ion enhanced the dissolution of silver but considerably reduced the copper dissolution. In the chloride solution containing ferric ion, after a fast initial dissolution rate, the silver and copper dissolutions proceeded very slowly suggesting some sort of inhibiting effect on the reaction. The actual weights of the metals in the 200 mls of leaching solution remained fairly constant after about half an hour. The increase in the total weight per cent of the metals dissolved after this time seemed to be due to the sampling technique whereby the sample volume (5 mls) was replaced by fresh solution. Thus more copper and silver dissolved to attain the original concentrations in the leaching solution, which had been reduced by the introduction of this fresh solution.

In the case of the chloride solution

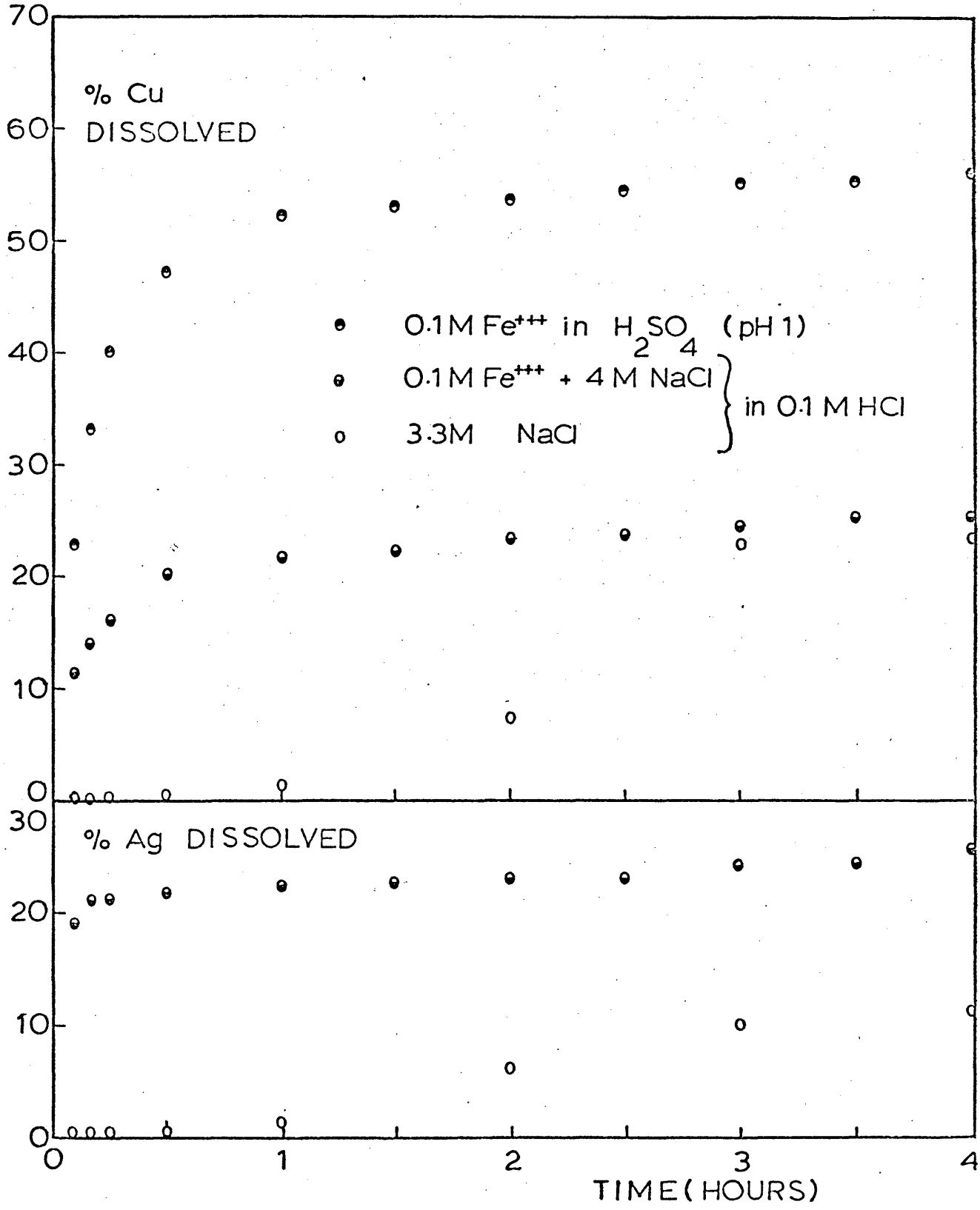


FIGURE 41 : Effect of chloride ion on the dissolution of silver and copper from stromeyerite.

containing no ferric ion, the copper and silver contents of the leaching solution also reached constant values, after an initial period when little dissolution of either copper or silver occurred and a definite smell of $H_2S$ was noted.

X-ray diffraction analysis (section 5.2) showed that with chloride ion present, silver chloride and elemental sulphur are formed. It thus seems likely that these phases form a layer on the particles and effectively halt the dissolution reaction. Because of the inhibiting effect on the copper dissolution it is difficult to determine whether the reaction mechanism is the same as in sulphate solutions. However no sulphate ion was found by analysis of the solutions by nephelometric means (section 2.3) ).

Later chloride leaching experiments on a mixed sulphide material containing stromeyerite, showed that silver dissolves as the complex $AgCl_3^{2-}$ in these solutions (section 6.1.5).

5.1.7 Leaching with Hydrogen Peroxide.

Using a solution of 20-volume hydrogen peroxide in sulphuric acid (pH1) instead of a

ferric ion solution gave exactly the same type of copper leaching curve, as can be seen in Figure 42. After an initial fast dissolution, which was slightly slower than with ferric sulphate leaching, the rate became extremely slow after 50% of the copper dissolved. A solution containing 1 part of 20-volume hydrogen peroxide to four parts of sulphuric acid (pH1) was used with a 0.5 gm sample of particle size -180 + 125 microns with the solution stirred at 1300 rpm at 60°C.

Figure 42 also shows that a solution of hydrogen peroxide and distilled water (in the ratio 1 to 4) had little effect on the stromeyerite. The results of both experiments are given in Tables A-2.16 and A-2.17.

X-ray diffraction analysis of the residue after 55.76% of the copper had dissolved showed it to be a mixture of silver sulphide and covellite, CuS, in agreement with the dissolution mechanism postulated in section 5.2. Thus the mechanism does not seem to be affected by the change in oxidant.

The amount of silver dissolved is again

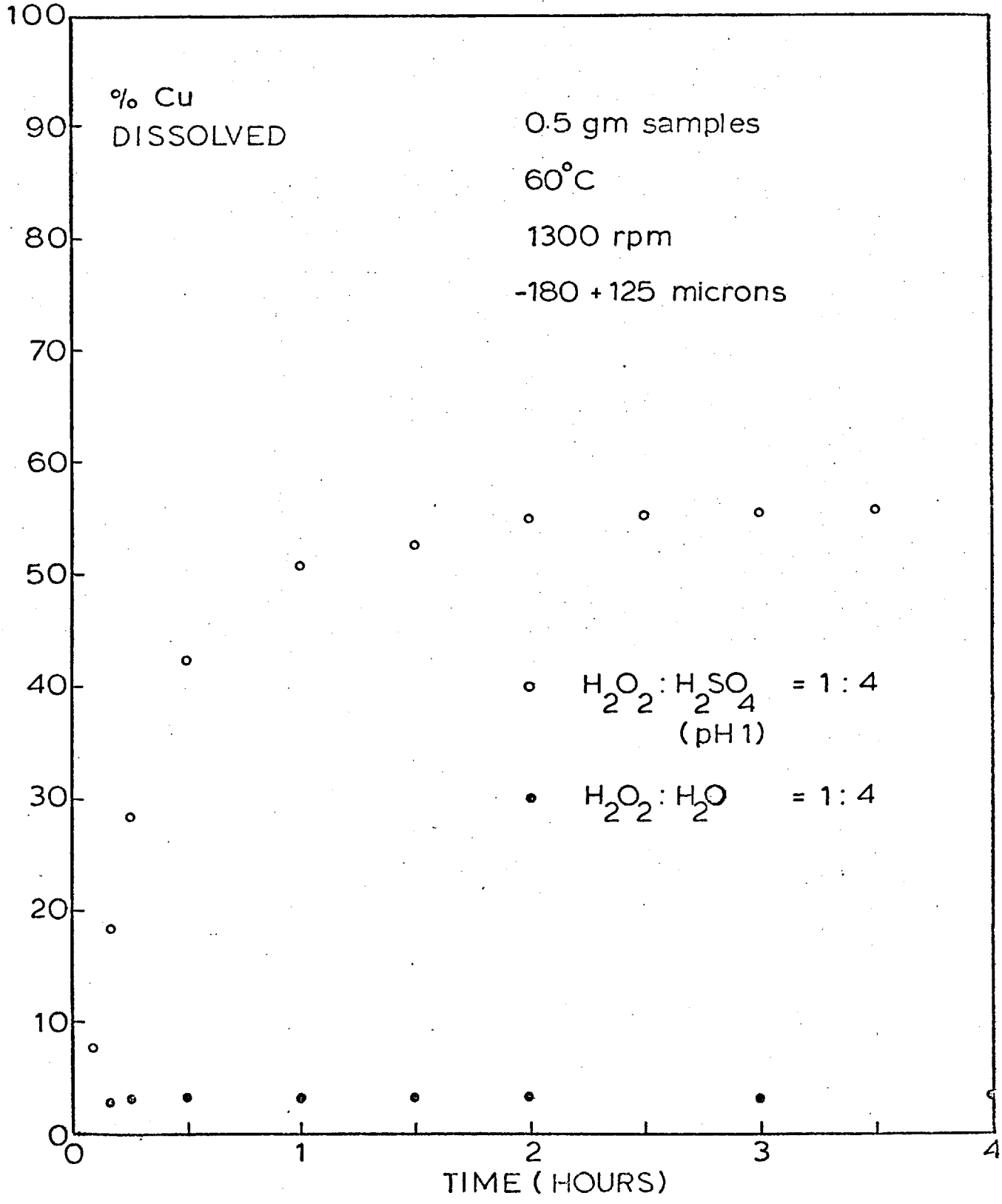


FIGURE 42 : Dissolution of copper from stromeyerite in Hydrogen Peroxide solutions.

very small even in the second stage of the reaction when the silver-copper sulphides have transformed to silver sulphide. Thus although changing the sample weight and thus increasing the Ferric to Ferrous ratio (due to less weight of copper being dissolved) seemed to have an effect on the silver dissolution, from the present results it seems that this is not the primary reason why silver does not dissolve in ferric sulphate solutions. It now seems likely that it is the presence of cupric ions in the solution that is the dominant factor.

5.1.8 Leaching with Manganese Dioxide.

In Figure 43(a) and Tables A - 2.18 and A-2.19 are shown the effect of adding a suspension of manganese dioxide to the leaching system. Both experiments were carried out at 60°C with a 0.5 gram sample of particle size -180 + 125 microns stirred at 1300 rpm. 0.3205 grams of powdered manganese dioxide were added to the 200 mls of leaching solution. The weight was calculated as the theoretical requirement for the dissolution of the stromeyerite, and its intermediate products silver sulphide and covellite, by the reactions:

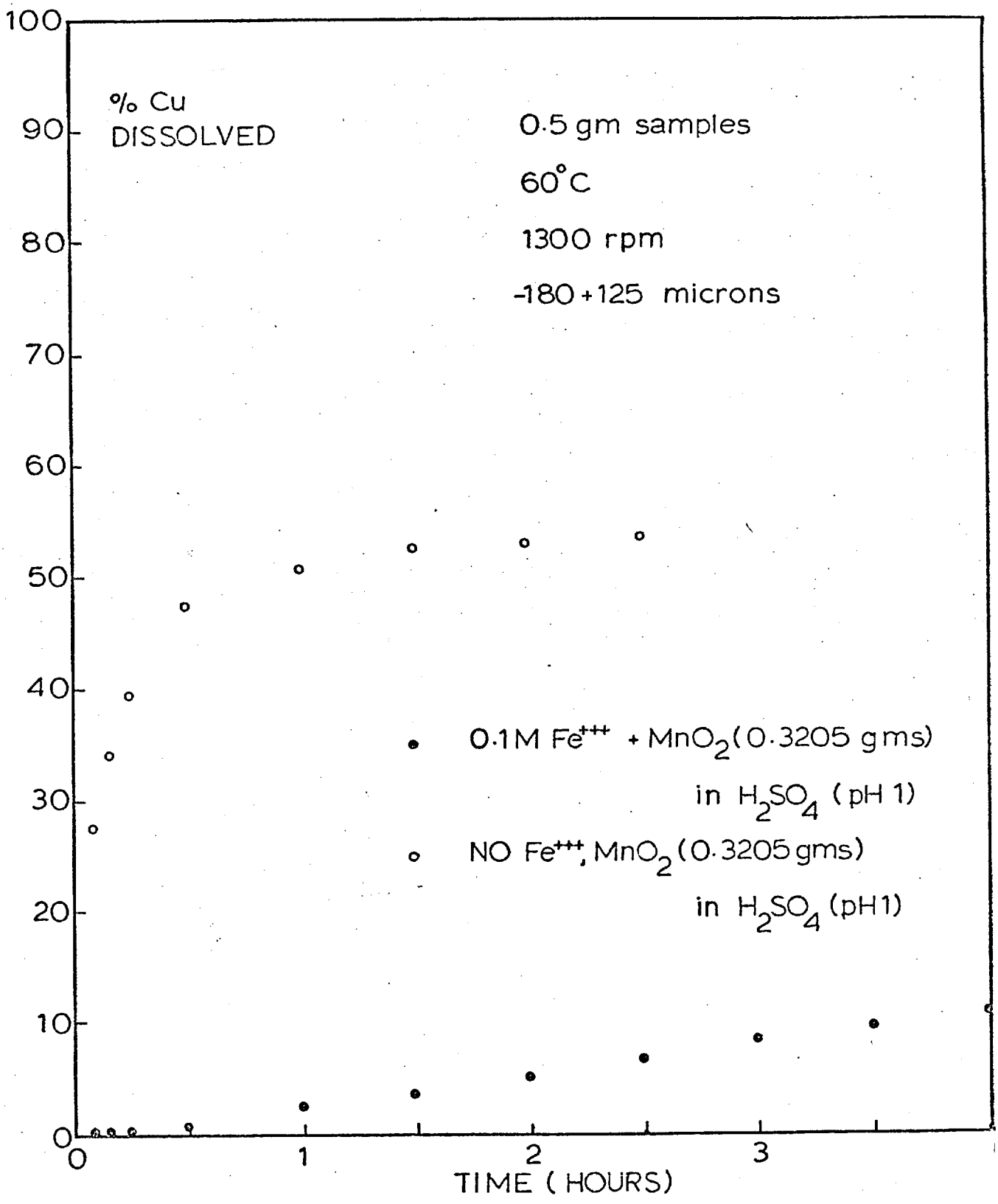


FIGURE 43(a) : Dissolution of copper from stromeyerite in leach solutions containing Manganese Dioxide.

$$2CuAgS + MnO_2 + 2H_2SO_4 = CuS + Ag_2S + CuSO_4 + MnSO_4 + 2H_2O \quad (5.1.1)$$

$$CuS + MnO_2 + 2H_2SO_4 = CuSO_4 + MnSO_4 + 2H_2O + S \quad (5.1.2)$$

$$Ag_2S + MnO_2 + 2H_2SO_4 = Ag_2SO_4 + MnSO_4 + 2H_2O + S \quad (5.1.3)$$

These equations are based on the reaction proposed by Subramanian and Kanduth[198] for the manganese dioxide - sulphuric acid leaching of the CuS formed during the activation of chalcopyrite. The formula CuAgS was used in equation (5.1.1) because only an estimate of the theoretical $MnO_2$ requirement was needed. Using the correct formula of $Cu_{1.07}Ag_{0.93}S$ gave a theoretical $MnO_2$ requirement of 0.3445 grams, not significantly different from 0.3205 grams.

Adding manganese dioxide to a solution of 0.1M ferric sulphate (pH1) had little effect on the copper dissolution, the leaching curves having the same characteristic fast first stage and slower second stage. The silver dissolution was also unaffected, suggesting that the dissolution mechanism remained

unaltered. With a suspension of manganese dioxide in $H_2SO_4$ (pH1), with no ferric ion present, the dissolution of copper was very slow and had a linear rate, after a short period (30 minutes) when little copper was dissolved. This indicates that in the previous experiment the oxidation was still primarily by ferric ion being reduced to ferrous ion.

Analysis of the leach solution samples for manganese showed that in both experiments there was a linear relationship between the number of moles of copper dissolved and the number of moles of manganese in solution (Figure 43(b)). In the absence of ferric ion the molar ratio of Cu to Mn was 0.625 : 1 with 12.33% of the manganese dioxide consumed in 4 hours, while the Cu to Mn ratio in the ferric ion solution was 0.87 : 1 with 44.14% of the manganese dioxide consumed in $2\frac{1}{2}$ hours.

With Mn(IV) acting as the oxidant, itself being reduced to the soluble ion Mn(II), the theoretical molar ratio of Cu to Mn should be 1 : 1. The fact that more manganese occurs in solution is obviously due to some of the

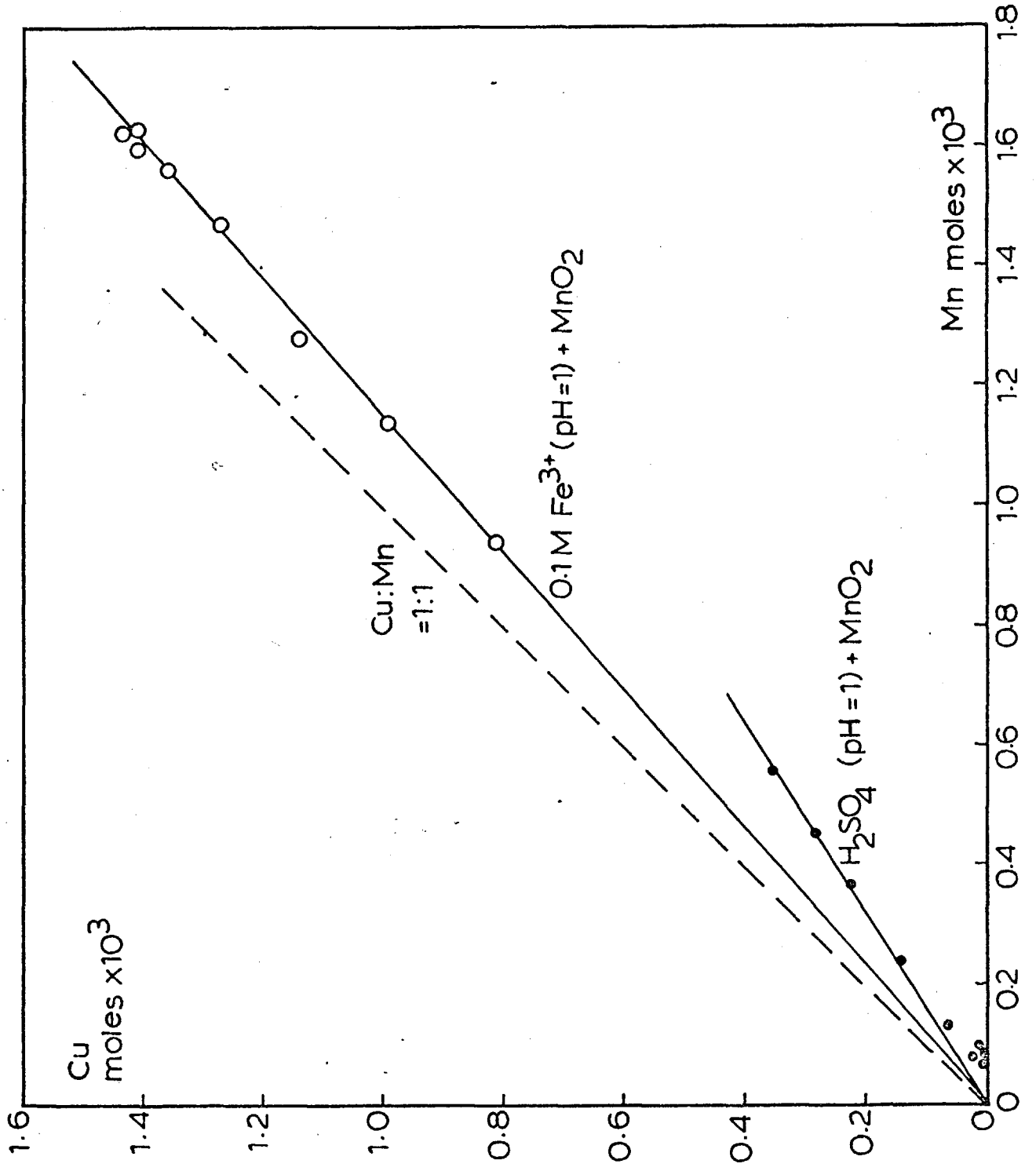


FIGURE 43(b) : Plot of the number of moles of copper dissolved and the number of moles of manganese in solution, when leach solutions containing Manganese Dioxide are used.

manganese dioxide simply dissolving in the solution. This was more noticeable in the absence of ferric ion because the consumption of manganese dioxide by the oxidation of the sulphide and subsequent dissolution of copper was very small due to the slow leaching kinetics.

The much greater consumption in the presence of ferric ion was probably due to the reoxidation of the ferrous ion, produced in the dissolution reaction, to ferric ion (which would also give a theoretical Cu : Mn molar ratio of 1 : 1). Thus in this particular experiment the lack of substantial dissolution of silver in either the first or second stages of the reaction cannot be explained by the presence of ferrous ion producing an adverse ferric to ferrous ratio. This supports the findings on leaching with hydrogen peroxide (section 5.1.7).

## 5.2. X-ray Diffraction Analysis.

The synthetic stromeyerite and the solid residues from the leaching experiments were studied by X-ray powder diffraction analysis using the equipment and method described in section 2.4.4.

The X-ray powder photographs of the leach residues obtained by dissolution of the stromeyerite in the various leaching agents are shown in Figures C-1.3 and C-1.4. Photographs (b) to (j) in Figure C-1.3 are for residues obtained by repeating the leaching run at 30°C and 0.1M $Fe^{3+}$ concentration (Table A-2.2) and extracting samples of solid at regular intervals. Data obtained from measurements on these photographs of both d-spacings and relative intensities are tabulated in Tables B-2.2 to B-2.10.

Photographs (k) in Figure C-1.3 and (a) to (f) in Figure C-1.4 are for residues obtained from ferric sulphate leaching under different conditions of temperature, ferric ion concentration, etc. The d-spacings and relative intensities measured from these photographs are tabulated in Tables B-2.11 to B-2.16.

The differing conditions did not seem to affect the dissolution mechanism. This was confirmed by repeating the leach run at 60°C and 0.01M $Fe^{3+}$ (Table A-2.9) concentration and taking samples of solid. The X-ray patterns and d-spacings of these residues were in good agreement with those of photographs (b) to (j) in Figure C-1.3.

Photograph (g) in Figure C-1.4 is for the residue from leaching stromeyerite in hydrogen peroxide, and photographs (j) to (m) in the same figure are for residues from leaching stromeyerite in a 0.1M $Fe^{3+}$ solution containing 4M NaCl. The d-spacings and relative intensities are listed in Table B-2.17, and Tables B-2.18 to B-2.21 respectively.

As mentioned previously, the pattern obtained for the synthetic stromeyerite was in excellent agreement with that of the synthetic phase $Cu_{1.07}Ag_{0.93}S$ of Djurle[133], and the pattern obtained from a natural crystal of stromeyerite by Suhr[140] (who gave the formula as CuAgS). The three patterns are compared in Table B-2.1, and the X-ray pattern for the synthetic stromeyerite of the present work is shown in photograph (a), Figure C-1.3, for Cu

radiation, and photograph (i), Figure C-1.4, for Co radiation.

Examination of the X-ray patterns in Figure C-1.3 and the data in Tables B-2.2 to B-2.16 show that as the stromeyerite was leached in the ferric sulphate solution, the lines of stromeyerite became steadily weaker while there was a large increase in the numbers of lines in the patterns. However after about 50% of the copper has dissolved, a number of these lines disappear. These X-ray patterns were compared with those of McKinstryite[145], $Cu_{0.8}Ag_{1.2}S$, Jalpaite[144], $Ag_3CuS_2$, silver sulphide $Ag_2S$, and covellite, CuS, as well as those of the synthetic phases $Ag_{1.2}Cu_{0.8}S$ and $Ag_{1.55}Cu_{0.45}S$, prepared by Djurle[133] (Tables B-5.1 to B-5.7).

This comparison shows that the residues with less than 50% of copper removed seem to consist of McKinstryite, jalpaite, silver sulphide and mixtures thereof. The stromeyerite residues with up to 18.06% of the copper removed have X-ray patterns which can be attributed to a mixture of unleached stromeyerite and McKinstryite. The residue patterns seem to agree more closely with Skinner's d-values for

the naturally occurring McKinstryite (Table B-5.1), than with Djurle's d-values for the synthetic $Cu_{0.8}Ag_{1.2}S$ phase (Table B-5.2). Above 18.06% of copper removed the lines of jalpaite begin to appear and the residues seem to be a mixture of McKinstryite and jalpaite. The lines of jalpaite agree well with the d-spacings of both the naturally occurring jalpaite of Grybeck and Finney, $Ag_3CuS_2$, (Table B-5.4), and with the synthetic $Ag_{1.55}Cu_{0.45}S$ phase of Djurle (Table B-5.3).

As more copper is removed from the residues the lines of jalpaite become stronger in intensity until 41.72% of the copper has been removed when the lines of $Ag_2S$ begin to appear. After 47.37% of the copper has been removed it is obvious that silver sulphide is the main phase present with a number of lines also suggesting the presence of covellite, CuS.

Thus it seems that during the fast first stage of the dissolution of stromeyerite in acidic ferric sulphate solutions when 50% of the copper, and very little of the silver, was dissolved, there is a solid-state transformation series of the form :

$Cu_{1.07}Ag_{0.93}S$ - $Cu_{0.8}Ag_{1.2}S$ - $Cu_{0.45}Ag_{1.55}S$-$Ag_2S$, with the remaining undissolved copper present as covellite, CuS. No sulphur was detected in this first stage of dissolution by X-ray or microscopic examination, and no sulphate ion was detected in the leaching experiments with chloride solutions (section 5.1.6). Hence a number of theoretical equations can be written for the dissolution:

$$Ag_{0.93}Cu_{1.07}S + 0.45Fe^{3+} = 0.775Ag_{1.2}Cu_{0.8}S + 0.225CuS + 0.225Cu^{2+} + 0.45Fe^{2+} \quad (5.2.1.)$$

$$0.775Ag_{1.2}Cu_{0.8}S + 0.35Fe^{3+} = 0.6Ag_{1.55}Cu_{0.45}S + 0.175CuS + 0.175Cu^{2+} + 0.35Fe^{2+} \quad (5.2.2)$$

$$0.6Ag_{1.55}Cu_{0.45}S + 0.27Fe^{3+} = 0.465Ag_2S + 0.135CuS + 0.135Cu^{2+} + 0.27Fe^{2+} \quad (5.2.3)$$

This gives an overall reaction for the first stage of dissolution of :

$$Ag_{0.93}Cu_{1.07}S + 1.07Fe^{3+} = 0.465Ag_2S + 0.535CuS + 0.535Cu^{2+} + 1.07Fe^{2+} \quad (5.2.4)$$

21.03% of the copper is dissolved by equation (5.2.1), 16.35% by equation (5.2.2) and 12.62% by equation (5.2.3). Hence, theoretically, the residues should be wholly McKinstryite due to reaction (5.2.1) when 21.03% of the

copper has been removed, above which jalpaite should appear by reaction (5.2.2) and be the predominant phase after 37.38% of the copper has been dissolved, when silver sulphide should begin to appear by reaction (5.2.3). The overall reaction should be complete after 50% of the copper has dissolved with the residue consisting of a mixture of silver sulphide and covellite, CuS. These predictions are in good agreement with the findings by X-ray diffraction analysis and the observed appearance and disappearance of the various phases that have been reported above.

The above equations show that at each step in the dissolution of the copper, as the copper silver sulphide phase is transformed, covellite, CuS, is formed. Examination of the d-spacings for the residues showed that the presence of CuS does not become evident until about 47% of the copper has been removed and even then only a few of its lines are visible. This could be due to one or more of the following factors:

(i) the X-ray diffraction lines of CuS could be 'masked' by the lines of the copper-silver sulphides. The residues containing mixtures of these sulphides have a

large number of diffraction lines in their X-ray patterns, some of which coincide with those of CuS. Thus the lines of CuS may not become evident until only $Ag_2S$ is present since this phase has comparatively fewer lines than the other phases;

(2) The CuS could be formed as very small crystallites which would produce very weak and diffuse lines[179] (section 3.5), and hence make identification difficult;

or

(3) the CuS could form solid-solutions with the copper-silver sulphides, having the structure of the copper-silver sulphides, the composition transforming from the original $Cu_{1.07}Ag_{0.93}S$ via $Cu_{0.84}Ag_{0.93}S$ and $Cu_{0.67}Ag_{0.93}S$ to $Cu_{0.535}Ag_{0.93}S$, at which point CuS begins to separate out, probably due to the $Ag_2S$ being less accommodating to the impurity CuS. New mineral occurrences have shown that silver can replace copper in the covellite structure to a large degree (up 16.7 weight per cent Ag)[185].

This third factor would mean that in the electron probe traces across the samples that had been leached on one face (section 5.5), in going from unleached to leached material there would be a gradual change in the silver and copper traces as the sample composition went from $Cu_{1.07}Ag_{0.93}S$ to $Cu_{0.67}Ag_{0.93}S$ followed by large variations in the silver and copper traces due to the mixture of $Ag_2S$ and CuS. In fact Figure 46 shows that there was no gradual change and large variations occur in the copper and silver traces almost immediately, indicating separate areas of high copper with low silver (CuS) and low copper with high silver (copper-silver sulphide phases). Thus it seems that the difficulty in identifying covellite, CuS, in the residues with less than about 40% of the copper removed was due to the first two of the above factors, i.e., 'masking' of the lines which are probably weak and diffuse.

The X-ray patterns of the residues with more than 50% of the copper removed show no significant changes, the residues remaining as a mixture of covellite and silver sulphide, with the X-ray diffraction lines of elemental

sulphur (orthorhom bic) appearing in the residue with 77.58% of the copper removed.

This is to be expected since any increase in the copper dissolution above 50% will be due to the dissolution of the covellite which, according to King [9], dissolves to form elemental sulphur via the non-stoichiometric phase $Cu_{0.8}S$, which has the covellite structure. Hence the equations can be written:

$$0.535CuS + 0.214Fe^{3+} = 0.535Cu_{0.8}S + 0.214Fe^{2+} + 0.107Cu^{2+} \qquad (5.2.5)$$

and

$$0.535Cu_{0.8}S + 0.856Fe^{3+} = 0.428Cu^{2+} + 0.856Fe^{2+} + 0.535S \qquad (5.2.6)$$

This shows that a further 10% of the copper (i.e., more than 60% of the total copper) has to be dissolved before the appearance of sulphur in the residues. This is in agreement with the findings of the X-ray diffraction analysis, the microscopic examination and the A.A. analysis.

Hence the overall reaction for the dissolution of copper from stromeyerite can be written as:

$$Ag_{0.93}Cu_{1.07}S + 2.14Fe^{3+} = 0.465Ag_2S + 1.07Cu^{2+} + 0.535S + 2.14Fe^{2+} \qquad (5.2.7)$$

The leaching results (section 5.1.7) showed that using hydrogen peroxide as the oxidant instead of ferric ion did not seem to change the mechanism of the dissolution of copper. This was confirmed by the X-ray diffraction pattern (photograph (g) in Figure C-1.4) and the measured d-spacings (Table B-2.17), which showed that the residue (with 55.76% of the copper dissolved) consisted of a mixture of silver sulphide and CuS.

The mechanism of the dissolution of stromeyerite in the chloride solutions was difficult to determine since the reaction was almost brought to a halt after about 20% of the silver and 20% of the copper had been dissolved (section 5.1.6). The X-ray diffraction patterns (photographs (j) to (m) in Figure C-1.4) and the measured d-spacings (Tables B-2.18 to B-2.21) show that a precipitate of silver chloride is formed and it is this that probably inhibits the dissolution. The measured d-spacings also show the presence of the copper-silver sulphide phases, CuS and silver sulphide, indicating that the same

mechanism as for ferric sulphate leaching occurs for the copper dissolution. Elemental sulphur was also produced in the residues, suggesting that there is a chemical reaction occurring by which silver was dissolved and elemental sulphur produced.

Thus the residue after 25.17% Cu and 25.58% Ag had been removed consisted of a mixture of silver sulphide, copper sulphide (CuS), elemental sulphur and silver chloride.

## 5.3 Atomic Absorption Analysis of residues.

A number of the leach residues were dissolved in hot nitric acid and the solutions analysed for copper and silver. The results are shown in Table 4 and are compared with the compositions of the various copper-silver sulphides.

X-ray analysis showed that in the first stage of the dissolution reaction (complete after 50% of the copper has dissolved) the stromeyerite is transformed to a mixture of silver sulphide and copper sulphide, CuS, via the copper-silver sulphide phases $Ag_{1.2}Cu_{0.8}S$ and $Ag_{1.55}Cu_{0.45}S$. Equation 5.2.4 shows that one mole of stromeyerite produces 0.465 moles of silver sulphide and 0.535 moles of CuS. The calculated weight and mole per cents of the constituents of this mixture are presented in Table 4 and show good agreement with the A.A. analysis of the residues with about 50% of the copper dissolved.

Above 50% of copper dissolved, subsequent dissolution of copper is from the copper sulphide, CuS, with the silver remaining as silver sulphide. King[9] found that the copper

was removed from covellite until the formula was $Cu_{0.8}S$ before elemental sulphur was formed. This means that over 60% of the copper has to be dissolved from stromeyerite before sulphur is formed. This seems to be supported by the residue analyses, the residue with 61.76% of the Cu dissolved showing no significant increase in sulphur content, while the residue with 77.58% of the copper dissolved shows a marked increase, together with the expected rise in the silver to copper ratio.

TABLE 4 Analysis of Residues by A.A. Spectrophotometry.

| | Weight per cent | | | Atomic per cent | | | Molar Ratios | |
|---|---|---|---|---|---|---|---|---|
| Wt%Cu removed | Cu | Ag | S | Cu | Ag | S | Ag/Cu | Ag+Cu/S |
| 47.37 | 23.09 | 56.72 | 20.19 | 23.91 | 34.61 | 41.46 | 1.447 | 1.412 |
| 50.60 | 22.68 | 59.29 | 18.03 | 24 29 | 37.42 | 38.28 | 1.539 | 1.612 |
| 55.34 | 20.06 | 59.08 | 20.86 | 20.85 | 36.17 | 42.97 | 1.734 | 1.326 |
| 57.50 | 20.24 | 60.19 | 19.56 | 21.42 | 37.53 | 41.04 | 1.751 | 1.436 |
| 61.76 | 20.12 | 58.69 | 21.19 | 20.81 | 35.75 | 43.43 | 1.718 | 1.302 |
| 77.58 | 12.18 | 55.90 | 31.92 | 11.24 | 30.37 | 58.38 | 2.703 | 0.713 |
| $Ag_{1.55}Cu_{0.45}S$ | 12.55 | 73.38 | 14.07 | 15.00 | 51.66 | 33.33 | 3.444 | 2.000 |
| $Ag_3CuS_2$ | 14.08 | 71.70 | 14.21 | 16.67 | 50.00 | 33.33 | 3.000 | 2.000 |
| $Ag_{1.2}Cu_{0.8}S$ | 23.94 | 60.96 | 15.10 | 26.66 | 40.00 | 33.33 | 1.500 | 2.000 |
| CuAgS | 31.23 | 53.01 | 15.76 | 33.33 | 33.33 | 33.33 | 1.000 | 2.000 |
| $Cu_{1.07}Ag_{0.93}S$ | 33.93 | 50.06 | 16.00 | 35.66 | 31.00 | 33.33 | 0.869 | 2.000 |
| 0.465 moles $Ag_2S$ + 0.535 moles CuS | 20.43 | 60.29 | 19.27 | 21.70 | 37.72 | 40.56 | 1.738 | 1.465 |

5.4 Microscopic examination.

Microscopic examination of the polished residues from the ferric sulphate leaching, mounted in Araldite resin, clearly showed the solid-state changes occurring during the dissolution of stromeyerite. A number of photographs of particles from samples, from which different amounts of copper have been dissolved, are presented in appendix C, Figures C-2.6 to C-2.14.

As soon as copper dissolution began a blue phase appeared at the edges of the particles. Figure C-2.6 shows that by the time 10.44% of the copper had dissolved this blue phase occurred throughout the particles in certain preferred directions. Figures C-2.7 and C-2.8 show the increase in the amount of blue phase as more copper was dissolved (26.15 and 39.64%, respectively) and also show that a light-coloured phase remained as an intergrowth.

This is in complete agreement with the reaction mechanism given by equations (5.2.1) to (5.2.4) which postulates that as copper is dissolved, the stromeyerite is transformed to the phases $Ag_{1.2}Cu_{0.8}S$ and then $Ag_{1.55}Cu_{0.45}S$

with the formation of covellite, CuS, which is known to have an indigo blue colour. Structural considerations (section 5.6) make it reasonable to expect this covellite to form along certain crystallographic planes, thus giving the particles the appearance in Figures C-2.6, C-2.7 and C-2.8.

Figure C-2.9 shows a particle with 50.06% of copper dissolved, which according to equation 5.2.4 marks the end of the first stage of dissolution, the residue now consisting of a mixture of $Ag_2S$ and CuS. The particle has a light blue appearance which on higher magnification can be seen more clearly as a fine intergrowth of the blue phase (CuS) and a light-coloured phase (presumably $Ag_2S$).

This latter conclusion is supported by the fact that this light-coloured phase turns black after only a few minutes of exposure to the microscope light. This is a well known characteristic of silver minerals[199], especially silver sulphide and was also observed in examining the original stromeyerite (see below).

Furthermore it can be seen that in the

first stage of the dissolution, with up to 50% of the copper dissolved, the particles retain their original shape, no attack occurring at the surfaces of the particles. This is in agreement with a reaction mechanism in which dissolution occurs by diffusion of copper ions out of the structures, rather than by a chemical process.

The anisotropism and polarisation colours of stromeyerite and its residues were examined by polarised light. The 'oleander leaf' structure described by Ramdohr[166] and mentioned earlier (section 2.1.3) was much more pronounced under polarised light. Both the unleached stromeyerite and the covellite in the residues showed the strong anisotropism and characteristic polarisation colours described for these minerals[202].

When 50% of the copper had dissolved, the dissolution in the second stage occurred much more slowly with elemental sulphur being formed (section 5.2). Figure C-2.10 shows a particle from a residue with 77.58% of the copper dissolved. The less well-defined edges suggest that a chemical attack is occurring. The dark

areas around the particle are probably holes left by the elemental sulphur removed during polishing. The light-coloured phase, which is now the major constituent of the particles, turned black in a very few minutes similar to the phase in the particle with 50.06%Cu removed (see above). This supports the previous conclusions that the silver remained as $Ag_2S$.

To show more clearly the formation of the various phases, a number of solid samples of stromeyerite were mounted in araldite and placed in a stirred 0.1M$Fe^{3+}$ solution at 60°C so that only one face of the sample was in contact with the solution (section 2.2). The samples were leached for various lengths of time and then sectioned, mounted and polished to show the extent of leaching into the solid samples.

Figure C-2.11 shows a solid sample that was in contact with the solution for 4 hours. The blue phase (CuS) has begun to form at the edge and along certain crystallographic planes into the centre of the solid. A noticeable feature is that the light-coloured phase in which the CuS was formed is of a much lighter

colour than the original stromeyerite. This indicates that stromeyerite is transforming not only to covellite but to another phase as well.

Figure C-2.11 also shows the 'oleander leaf' structure of the unleached stromeyerite and the dark spots due to the effect of the intense microscope light. Figures C-2.12, C-2.13, and C-2.14 show the gradual spread of the intergrowth of the blue phase and light-coloured phase into the solid specimens for leaching times of 24 hours, 48 hours and 7 days, respectively. As the leaching progresses it can be seen that a light-coloured layer remains at the solid edge and increases in thickness. X-ray diffraction analysis of powders scratched from the surfaces of these solid samples gave X-ray patterns typical of the leached particulate residues after 50% of the copper had dissolved, i.e., a mixture of $Ag_2S$, CuS and a trace amount of $Ag_{1.55}Cu_{0.45}S$.

Hence the slowness of the second stage of the copper dissolution is not only due to the slow leaching kinetics of CuS but also the fact that further dissolution of copper has to occur through a progressively thickening layer of residual $Ag_2S$. These conclusions and findings are supported by the electron probe traces (section 5.5.).

## 5.5. Electron Probe Microanalysis.

Electron probe microanalysis was performed on polished samples of both unleached stromeyerite and the leach residues. As already reported this method confirmed the homogeneity of the synthetic material and showed no variation of composition across the lamellae ('oleander leaf') structure visible under the microscope. (Figure 44).

As with the original synthesised samples (section 2.1.3), the residues were damaged by a high beam current (100nA) so all the samples were examinedat lower current of 50nA. Measurements, or even spot counts, were not really practical on such a material under these conditions, and instead the residues were examined by taking electron probe traces across the particles and solid sample residues for the various constituent elements.

Figure 45 shows a trace for copper and silver across a particle with just over 50% of the copper dissolved. The larger variations in the copper trace clearly indicate the formation of two distinct phases, one of high Cu and the other of low Cu. The variations

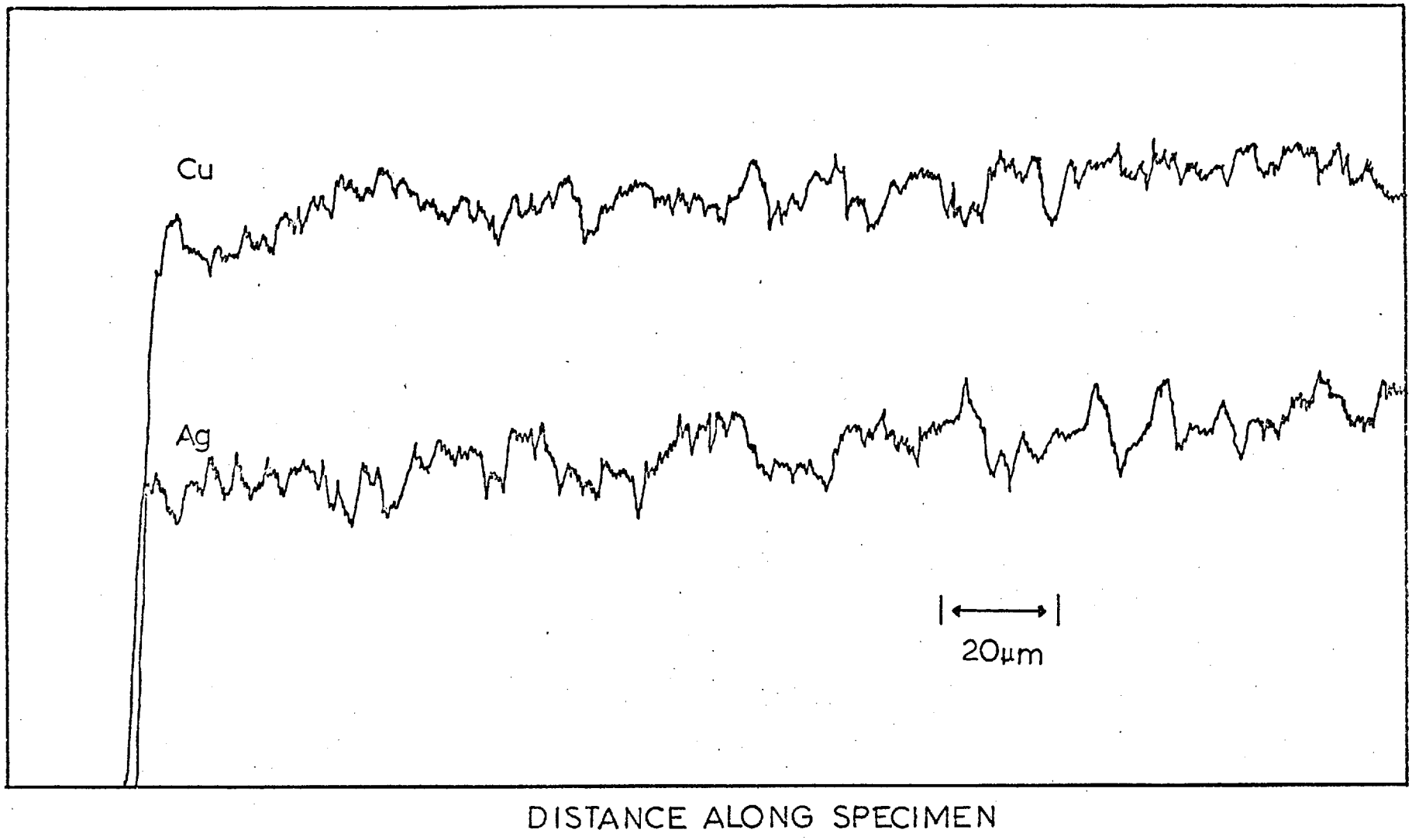


FIGURE 44 : Electron probe trace across an unleached specimen of stromeyerite.

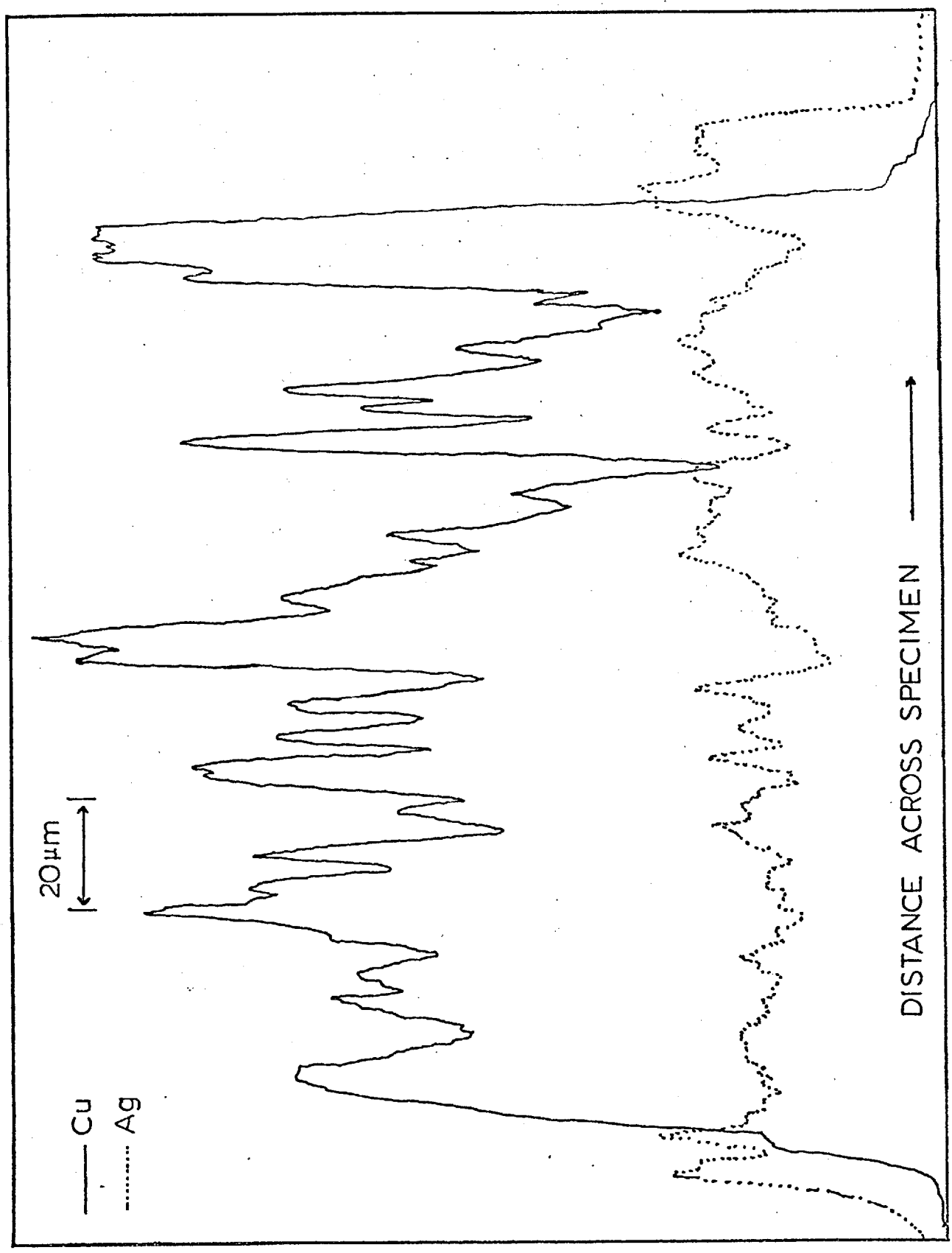


FIGURE 45 : Electron probe trace across a leached particle of stromeyerite.

in the silver trace are not as pronounced because a smaller scale was used, but it is noticeable that the copper and silver traces seem to have an inverse relationship, areas of high Cu having low Ag content, and vice versa. Also noticeable are the regions of high silver content occurring at the edges of the particle.

These observations are seen more clearly in Figure 46, which is a trace across the solid sample shown in Figure C-2.14. Both the copper and silver show substantial variations in composition nearer the leached edge, with the copper and silver traces opposed to each other. At the edge itself the trace shows a decrease in the copper content but an increase in silver content.

The region of very large compositional variation corresponds to the area of the intergrowth of the blue and light-coloured phases (CuS and sulphide containing silver, respectively), while the high silver region at the edge corresponds to the light-coloured band ($Ag_2S$) at the surface of the sample and described in section 5.4.

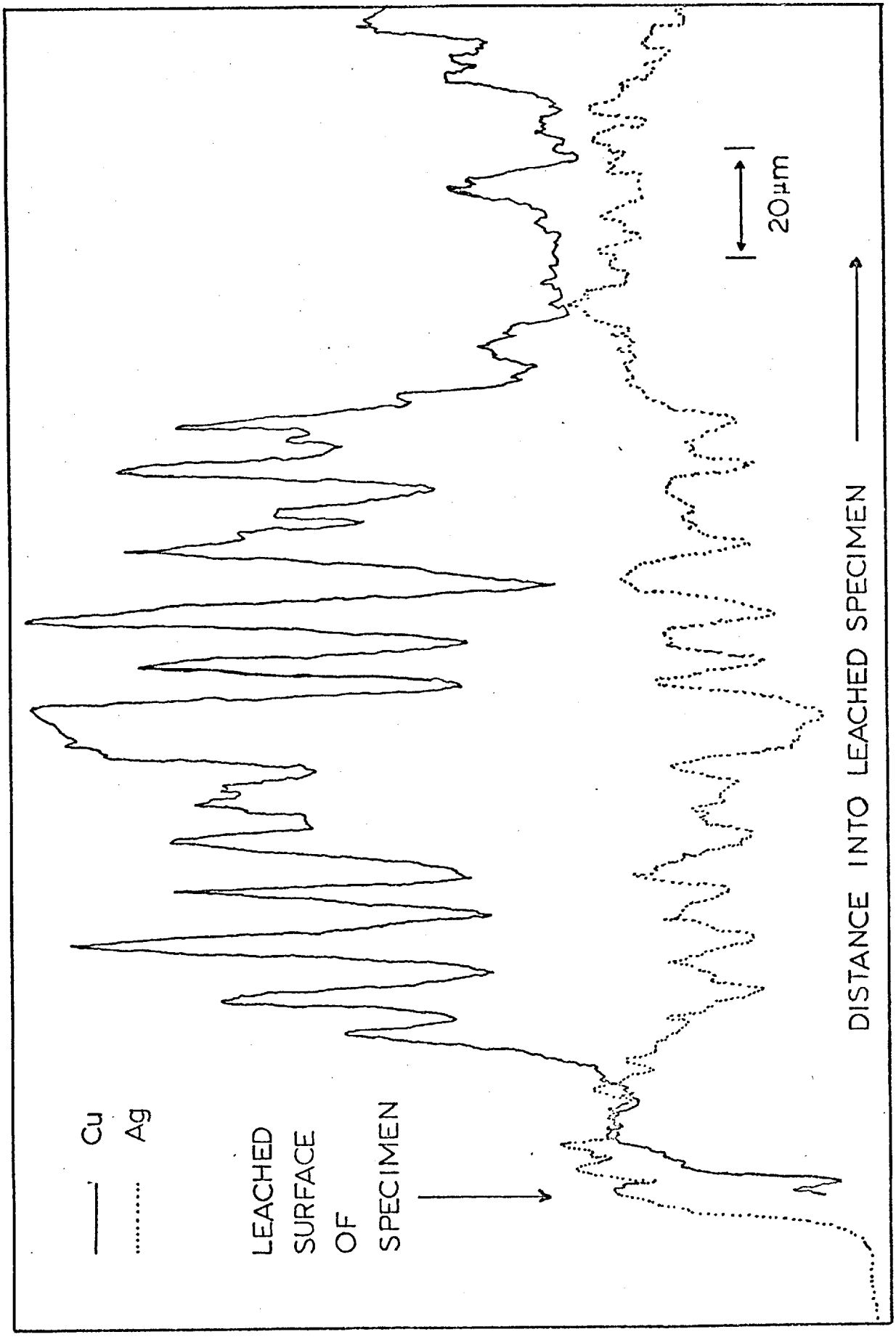


FIGURE 46 : Electron probe trace from the centre to the leached surface of a stromeyerite specimen.

Figure 46 also shows that there is no gradual variation in the copper and silver contents as the trace goes from unleached to leached material but that two distinct phases form immediately. Thus, this defeats any idea that the dissolution is occurring by a mechanism involving the formation of a series of solid solutions of copper and silver as considered in section 5.2.

## 5.6 Discussion and Comparison with other work.

The results of leaching the silver-doped bornite seemed to indicate that the reason for the very small dissolution of silver was the formation of ferrous ion (and thus an adverse ferric:ferrous ratio) by the dissolution of copper from the bornite. This was supported by the literature on the equilibrium reaction, $Ag + Fe^{3+} = Fe^{2+} + Ag^{+}$, (section 1.1.2) which show that this reaction has a very small equilibrium constant. It also seemed to be supported by the increase in silver dissolution from stromeyerite on increasing the ferric ion concentration or reducing the sample weight (thereby decreasing the amount of ferrous ion produced due to less copper being dissolved).

However the use of hydrogen peroxide as an oxidant did not significantly affect the dissolution of silver and neither did the presence of manganese dioxide which reoxidised the ferrous ion to ferric ion. These results suggest that although the ferric to ferrous ratio may affect the dissolution of silver, it is not the primary reason for the silver remaining in the solid state as either an isomorphous impurity in the case of the silver-doped bornite, or as a sulphide in the case of

stromeyerite.

The lack of any significant silver dissolution in the first stage of the dissolution of stromeyerite seems to be due to the favoured reaction being as in equations (5.2.1) to (5.2.4). The copper diffuses out of the stromeyerite which transforms, via the intermediate phases known as McKinstryite and jalpaite, to silver sulphide, the remaining 50% of the copper being 'precipitated' as covellite.

In the second stage of the reaction the covellite (CuS) dissolves by a chemically controlled reaction, via the non-stoichometric phase $Cu_{0.8}S$, to form elemental sulphur. This reaction, however, is stifled by the silver not dissolving and remaining as silver sulphide in the particle residues.

It was shown in section 4 that silver, as the sulphate, is fairly soluble in ferric ion solutions, and that silver sulphide dissolves to form elemental sulphur with a jarosite forming at high temperatures. Calculations also showed that if the limiting factor for silver solubility was the solubility product

of silver sulphide , then only a small amount of the copper could be held in solution.

As mentioned previously (section 1.1.1), many investigations and processes have shown that silver and its sulphide can be dissolved by ferric sulphate, other ferric salts and ferric-ferrous leach liquors. Lee and Muir[36] found that the use of an oxidising agent such as manganese dioxide or potassium permanganate increased the silver extraction from ores due to a more favourable balance being maintained between ferric and ferrous ions, while Azerbaeva and Tseft[42] dissolved synthetic silver sulphide in ferric sulphate and ferric chloride - ferrous chloride solutions.

Hence the above evidence suggests that the ferric-ferrous ratio is not the dominant factor preventing the dissolution of silver sulphide in the second stage of the dissolution of stromeyerite. It seems more likely that it is an electrochemical process, somewhat akin to a cementation reaction, whereby cathodic deposition (or non-dissolution) of the more positive component and anodic dissolution of the less positive component takes place. This

suggestion is supported by other work. Baur et al[108] noted that the presence of argentous ion in their leaching solutions for chalcopyrite produced striking effects because of the exchange mechanism existing between lattice copper ions and solution silver ions, resulting in the probable formation of argentite with copper going into solution. Also the precipitation of silver in the native form and as sulphides, by the reaction of silver-bearing solutions with various sulphides, including covellite, chalcocite, bornite and chalcopyrite, is one of the many mechanisms for the secondary enrichment of silver deposits[15], and copper metal has been used in a cementation reaction for the deposition of silver[200].

A literature survey found only one paper on the dissolution of stromeyerite in which Potashnikov et al[47] dissolved stromeyerite in nitric acid solutions and obtained an activation energy of 5 kcals. per mole which compares with the 15 kcals. per mole at temperatures below 70°C, and 5-15 kcals. per mole above 70°C, of the present work. These authors did not discuss the dissolution mechanism.

The mechanism proposed in the present work is similar in many ways to the dissolution mechanism proposed by King[9] for chalcocite in acidic ferric chloride solutions. The chalcocite, $Cu_2S$, dissolves in two stages. In the first it transforms via a series of non-stoichiometric phases between $Cu_2S$ and CuS to form an intermediate product of covellite, CuS. The copper is removed by diffusion in the lattices of the non-stoichiometric phases, the process having an activation energy of 0.82 kcals. per mole. The covellite then dissolves by a chemically controlled reaction with an activation energy of about 25 kcals. per mole to form elemental sulphur (orthorhom bic) via the non-stoichiometric phase $Cu_{0.8}S$.

Stromeyerite undergoes similar transformations (equations 5.2.1 to 5.2.6). Copper diffusion is important in the first stage of the dissolution as the stromeyerite transforms via the phases $Ag_{1.2}Cu_{0.8}S$ and $Ag_{1.55}Cu_{0.45}S$ to form a mixture of silver sulphide and covellite. The activation energy of this process is somewhat higher than for chalcocite suggesting some degree of chemical control.

The dissolution of copper in the second stage of the stromeyerite reaction, i.e., the dissolution of covellite, should be comparable to the second stage of the chalcocite reaction. However, as has been mentioned previously, the residual silver sulphide inhibits the chemical reaction. A similar, but less marked, effect was noted as the covellite produced from chalcocite dissolved. This was due to the presence of sulphur in the pores which resulted in a reduction in the area of $Cu_{0.8}S$ available for attack by the ferric solution.

These observations on stromeyerite are very similar to those made by Cooke[29] on the dissolution of the silver-antimony sulphide, pyrargite. He found that the mineral turned black in the ferric sulphate-sulphuric acid solutions and suggested that this was due to an accumulation of silver sulphide on the surface as antimony dissolved.

It has already been pointed out that structurally there are many similarities between stromeyerite and silver sulphide, and stromeyerite and McKinstryite (sections 1.4.1 and 1.4.4, respectively). Bragg and Claringbull

showed that the projected structure of acanthite, $Ag_2S$, on the (010) plane is very similar to the structure of stromeyerite projected on the (001) plane, as shown in Figure 17. Frueh also noted that the planar copper-sulphur layers in stromeyerite parallel to the (001) plane are very similar to those in covellite, which has a hexagonal unit cell. Thus it seems reasonable to suggest that the covellite 'precipitates' from the copper-silver sulphide phases, because of its different structure, along planes parallel to the (001) planes of stromeyerite, i.e., along the c axis. Microscopic examination (section 5.4) clearly showed that covellite was being formed along certain crystallographic directions.

This mechanism of covellite formation seems to be supported by the apparent structural relationships between stromeyerite and mckinstryite discussed by Skinner et al[145]. They noted, amongst other things (see section 1.4.4), that the 'b' lattice parameter of mckinstryite (15.7Å) is approximately equal to twice the 'c' parameter of stromeyerite (15.9Å). Thus the separation of mckinstryite and covellite, caused by the removal of some of the copper from

stromeyerite, would seem to be quite feasible in the planes parallel to the (001) plane.

Although, no data is available at the moment on the distribution of copper and silver atoms in the jalpaite and mckinstryite structures to confirm these suggestions, the existence of the various phases formed in the dissolution mechanism is in complete agreement with the phase relations of the Cu-Ag-S system as determined by Skinner[143]. He found that covellite existed stably with stromeyerite, β-phase (mckinstryite), jalpaite and acanthite, $Ag_2S$, while native sulphur could coexist stably only with covellite or acanthite (section 1.5.1, Figure 19).

Recent mineralogical studies have confirmed that mckinstryite is an alteration product of stromeyerite and that the presence of covellite is a feature of this alteration. In a study on the occurrences of mckinstryite, Clark and Rojkovic[203] found that the association mckinstryite - covellite was a consistent feature and they calculated that the proportions of the two minerals approximated those which would result from the breakdown of stromeyerite

with minor loss of copper. Similarly Bergstol and Vokes[204] found that the association mckinstryite - covellite was a feature of a polymetallic sulphide deposit. No covellite was observed other than in association with mckinstryite and the authors concluded that mckinstryite was an alteration product of stromeyerite, in agreement with Clark and Rojovic. Both of these studies support the findings of the present work.

SECTION 6

## MIXED SULPHIDE MATERIAL. RESULTS AND DISCUSSION.

### 6.1. Leaching.

The mixed sulphide material consisted of a mixture of bornite, α-chalcopyrite and stromeyerite, with an overall composition of 54.50% Cu, 10.37% Ag, 10.65%Fe and 24.47% sulphur. The approximate quantities of the minerals were estimated to be 70% Bornite, 20% stromeyerite and 10% chalcopyrite (section 2.1.2).

When the material was crushed to prepare samples for the leaching runs, no preferential fracturing of the material occurred, so the relative amounts and distribution of the three sulphides varied from particle to particle within a particular sample (see Fig. C-2.15). Hence different particles in the same sample could have different leaching rates due to these differences. It follows from this that some slight reservation should be expressed in comparing the leaching data from one sample with another sample due to these same differences, i.e., a different distribution of constituents in the particles of the samples.

To ensure that there were no wide variations in the compositions of the samples, before each leaching run a small amount of the leach sample was dissolved in nitric acid and the solution analysed by atomic absorption spectrophotometry. The copper, iron and silver analyses were always in good agreement with the overall composition, within experimental error. This was probably due to the fact that the minerals were present as very fine intergrowths and therefore with a large enough sample the overall compositions of the samples did not vary.

The general characteristics of the dissolution of copper and silver from the mixed sulphide material in acidic ferric sulphate solutions (pH1) are shown in Figure 47 and Table A-3.1. As with the silver-doped bornite and pure stromeyerite, very little silver went into solution. Figure 61 compares the leaching characteristics of this mixed sulphide material with the theoretical behaviour calculated from the leaching rates of the pure minerals, bornite, chalcopyrite and stromeyerite. It can be seen that the mixed sulphide material leached much faster than was expected. The effects of

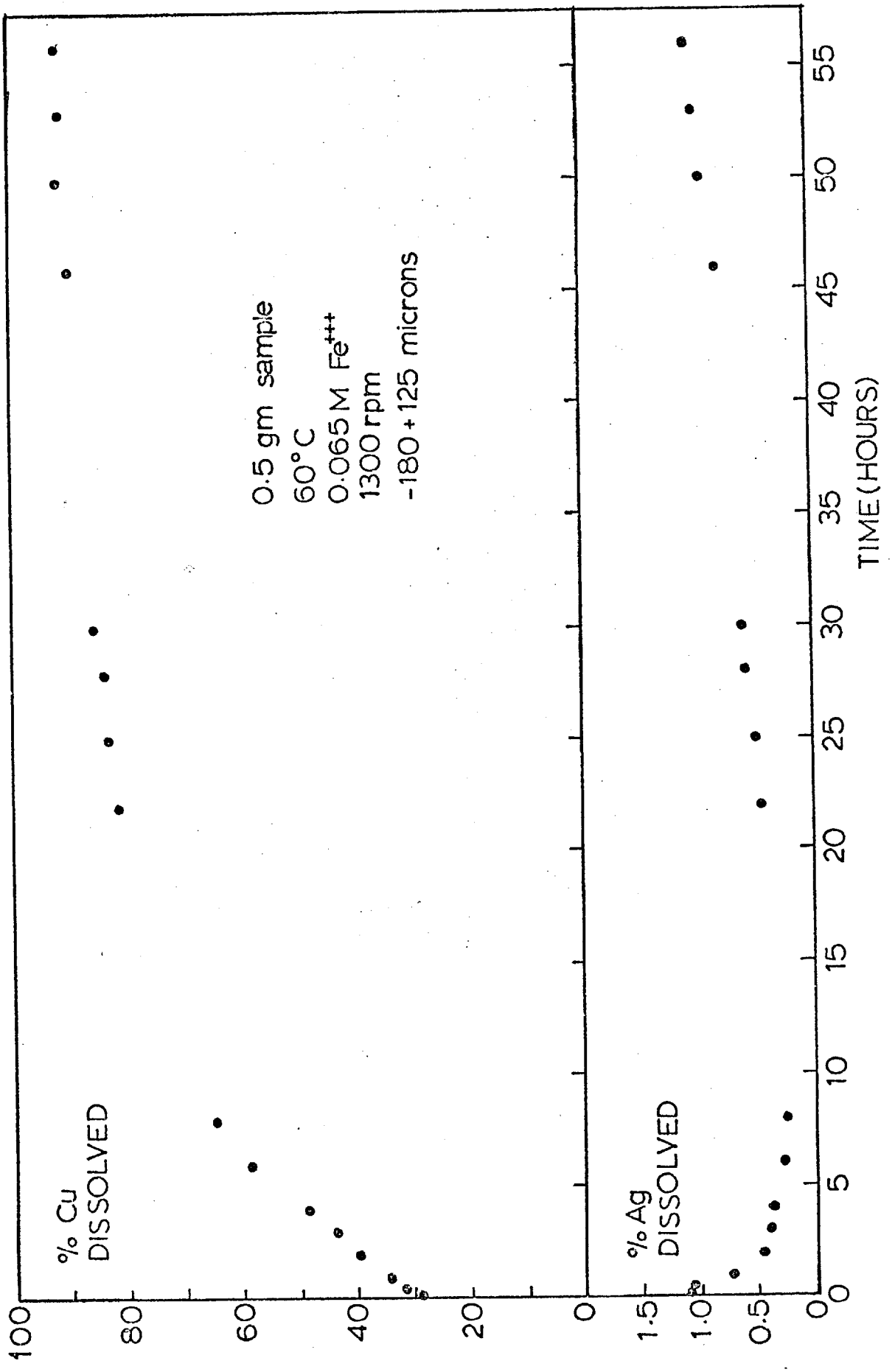


FIGURE 47 : General charecteristics of the dissolution of copper and silver from the mixed sulphide material.

temperature, ferric ion concentration, sample weight, and particle size and chloride ion on the dissolution rate of Cu and Ag from the mixed sulphide material were investigated.

6.1.1. Temperature.

Experiments were carried out at 30°C, 60°C and 90°C with 0.5 gram samples in solutions with a ferric ion concentration of 0.065M in sulphuric acid (pH1). As in previous experiments the solution was stirred at a speed of 1300 rpm. The results are presented in Figure 48 and Tables A-3.1 to A-3.3.

The effect of increasing the temperature is to increase the rate of copper dissolution quite markedly from 30°C to 60°C but less so from 60°C to 90°C. At 90°C the dissolution of copper occurs in two stages, a very fast first stage lasting until about 60% of the copper has dissolved, and a slower second stage. The results at 60°C and 30°C show that the first stage can be further subdivided into a fast section up to 30% of the copper dissolved and a slower second section which has a much faster rate at 60°C than at 30°C.

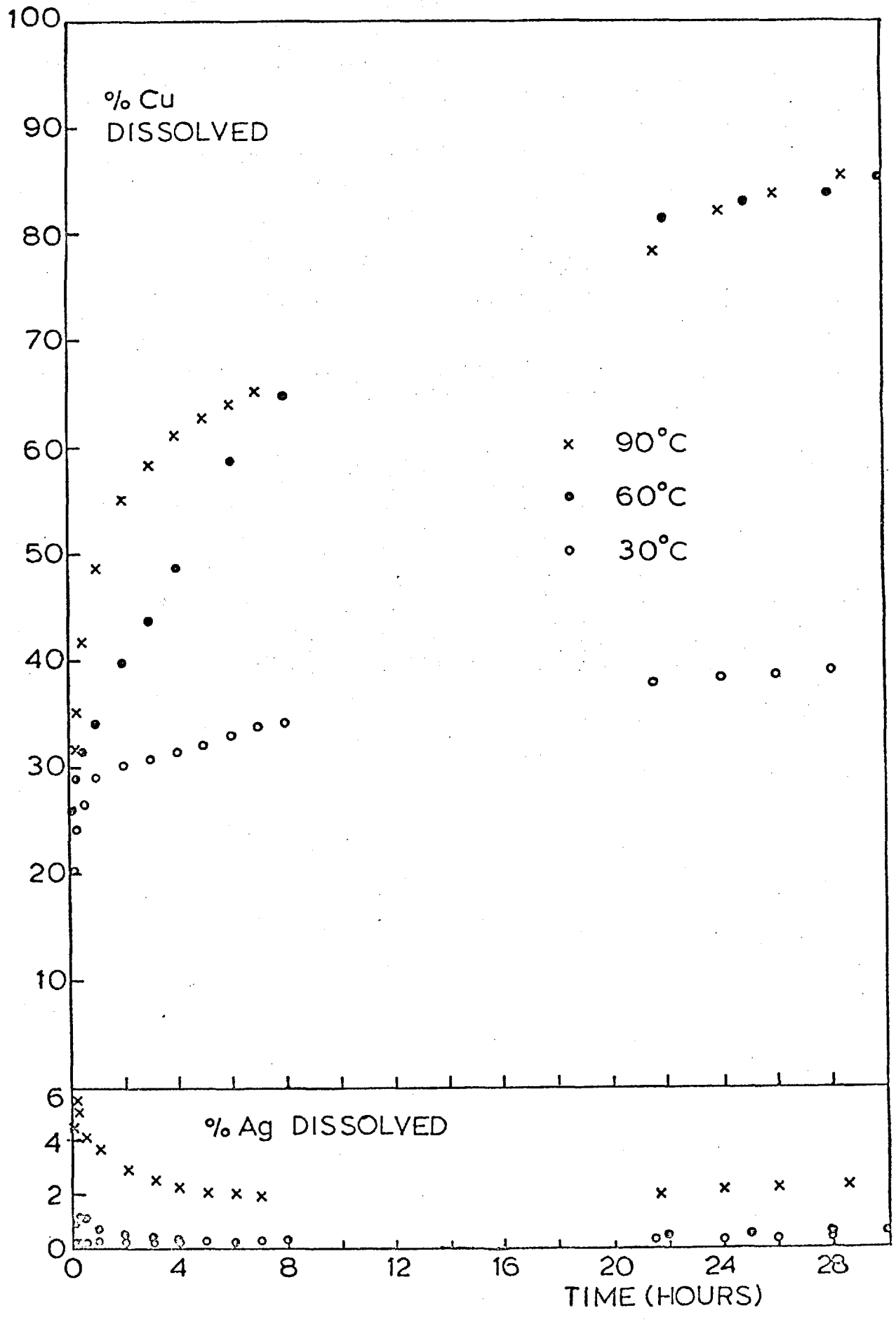


FIGURE 48 : Effect of temperature on the dissolution of copper and silver from the mixed sulphide material.

It is interesting to note that although the leaching rate of the first stage is much faster at 90°C than at 60°C, after 24 hours of leaching there is little difference in the total per cent of the copper that has been dissolved.

The characteristics of the silver dissolution were very similar to those of the silver dissolution for the silver-doped bornite and from pure stromeyerite. The silver content of the solutions reaches an initial peak then decreases and subsequently increases at a very slow rate. The height of the initial peak and the amount of silver 'removed' from solution varied with temperature. More silver was dissolved and subsequently 'removed' from solution at the higher temperature. This suggests that if this silver which is initially dissolved is precipitated in some form that affects the dissolution process, the effect would be greater at 90°C. It can be seen that there is a sharp reduction in the leaching rate of the copper at 90°C when about 55% of the copper has been removed and that this corresponds to a minimum in the silver content of the solution. Less silver is removed from the solution at 60°C and there is not such a marked reduction in the

copper leaching rate. However it should be noted that no precipitated compound of silver was detected by microscopic or X-ray analysis and that the 4% reduction in silver content of the solution at 90°C only represents a total weight of 2 mg of silver.

These observations suggest that either the silver removed from solution is re-incorporated in the lattices of the copper sulphides or that any precipitate of silver is not present in sufficient amounts for detection by X-ray analysis. It is also doubtful whether such small quantities would have a significant effect on the dissolution rate of copper.

From the estimated composition of the mixed sulphide material it can be calculated that 81.22% of the total copper is present as bornite, 12.43% is present as stromeyerite and 6.3% is present as chalcopyrite. It is known that 40% of the copper from bornite and 50% of the copper from stromeyerite, that is 32.48% and 6.22%, respectively, of the copper in the mixed sulphide material, dissolves out very quickly in the initial stages of dissolution. In fact it has been found that at 30°C only 27%

of the copper from bornite (21.93% of the copper in the mixed sulphide material) dissolves out quickly followed by a slower section to a maximum of about 40%[11]. In section 5.1 it has been shown that the dissolution of stromeyerite when 50% of the copper has been removed is also very slow. Hence at 30°C, if one considers the dissolution of copper from chalcopyrite to be negligible in comparison, it would be expected that the total copper dissolution from the mixed sulphide material would be due to the fast first stages of bornite and stromeyerite dissolution giving an overall dissolution of 28.15%, followed by a slower section to give a maximum dissolution of about 38.7%. This is in good agreement with the experimental results at 30°C (Figure 48, Table A-3.3).

The faster dissolution rates at the higher temperatures, which would be expected from the known leaching behaviours of stromeyerite and bornite, are obviously due to the conditions being more favourable for the second stages of the dissolution processes of stromeyerite and bornite since X-ray analysis and microscopic examination showed that the residues after

about 90% of the copper had dissolved consisted mainly of undissolved chalcopyrite, silver sulphide (from the stromeyerite) and elemental sulphur. Thus the fact that the rate of copper dissolution is almost the same at 60°C and 90°C when between 80 and 90% of the copper has dissolved is probably due to the dissolution of α-chalcopyrite not being greatly affected by temperature[12] and the inhibiting effect of a sulphur and silver sulphide layer (see microscopic and electron probe sections).

6.1.2. Ferric Ion concentration.

The rate of dissolution of copper from the mixed sulphide material increased with increase in the ferric ion concentration of the leaching solution. Experiments were carried out at 60°C using $Fe^{3+}$ concentrations of 0.01, 0.065, 0.10, 0.25 and 0.50M., the other conditions remaining the same, i.e., 0.5. gm sample of particle size -180 + 125 microns, the solution (at pH1) being stirred at 1300 rpm. The results are presented in Tables A-3 .1 and A-3.4 to A-3.7.

Figure 49 shows that for $Fe^{3+}$ concentrations above 0.065M, the rate of the first stage of the dissolution seems very little affected by

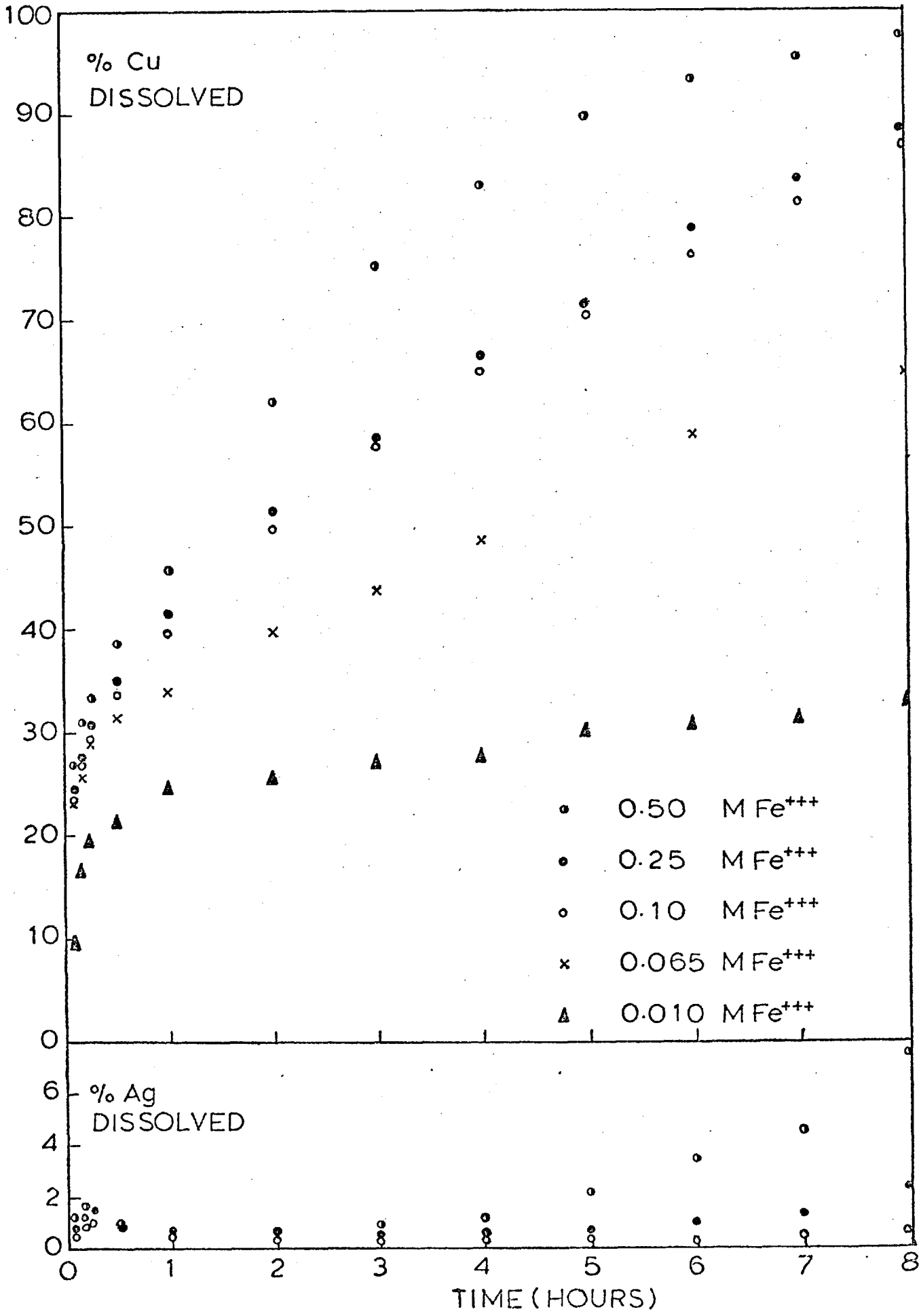


FIGURE 49 : Effect of ferric ion concentration on the dissolution of silver and copper from the mixed sulphide material.

any variation, while the second, slower stage is quite markedly affected up to concentrations of 0.5M. The silver dissolution characteristics are not greatly affected by an increase in the $Fe^{3+}$ concentration, although the final dissolution rate, after the initial rise and fall in the silver content of the solution, is much faster for the highest $Fe^{3+}$ concentration, 0.5M.

From previous work it is known that copper dissolution from bornite[11] and stromeyerite (section 5.1.2) is independent of $Fe^{3+}$ concentration above 0.065M while chalcopyrite is not affected significantly by increasing the $Fe^{3+}$ concentration from 0.01M to 0.1M[12]. The increase in copper dissolution rate from the mixed sulphide material up to $Fe^{3+}$ concentrations of 0.5M could be explained by electrochemical or mineralogical factors.

Since the minerals in the mixed sulphide material are in good electrical contact it could be that an electrochemical process becomes important whereby one or more of the sulphides is preferentially dissolved by a galvanic corrosion mechanism which depends on the $Fe^{3+}$ concentration. (see section 1.3). Alternatively the effect could be due to the presence of the

very fine intergrowth of stromeyerite in the bornite phase. Microscopic examination showed that, as the sulphide material was leached, cracks and pits seemed to be preferentially formed along this intergrowth. This would effectively increase the surface area and thus increase the number of sites that chemical attack on the bornite could take place.

However the chemical attack on pure bornite, whereby the intermediate leach product $Cu_3FeS_4$ is transformed to elemental sulphur, is independent of $Fe^{3+}$ concentrations above 0.065M. Hence the Cu dissolution dependence on the $Fe^{3+}$ concentration up to 0.5M could be due to the rate controlling step now being the diffusion of ferric ions in the pits and cracks to the unreacted surfaces of the bornite phase.

Figure 50 shows the dissolution of silver from the mixed sulphide material at a number of $Fe^{3+}$ concentrations for leaching times up to 30 hours. It can be seen that whereas temperature has a marked effect on the initial peak in the silver dissolution (Fig. 48), increasing the $Fe^{3+}$ concentration has little effect but greatly increases the final rate of dissolution

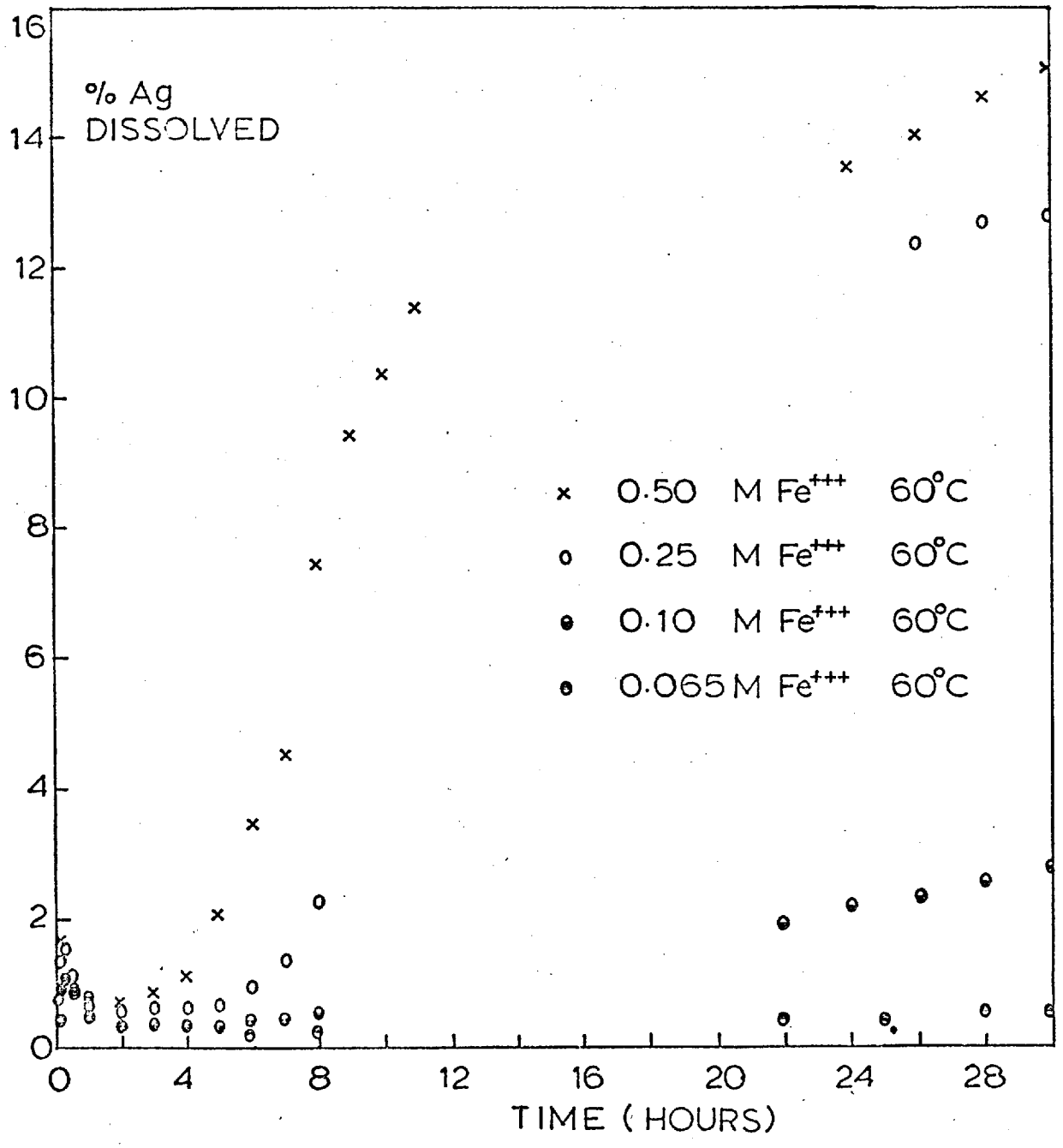


FIGURE 50 : Effect of ferric ion concentration on the dissolution of silver from the mixed sulphide material.

of silver. This indicates that there is a chemical reaction occurring which is probably the dissolution of the silver sulphide formed from the stromeyerite. Again this may be affected by electrochemical and mineralogical factors.

6.1.3. Particle size.

Experiments were carried out at 60°C with a 0.5 gm sample in a 0.1M $Fe^{3+}$ solution, the particle size being -85 + 120 mesh and -40 + 50 mesh. The results are presented in Figure 51 and Tables A-3.5 and A-3.8.

Increasing the particle size caused a marked reduction in the dissolution of copper from the mixed sulphide material. This would be expected in the first stages of dissolution, since, initially, copper dissolves from both bornite and stromeyerite by the diffusion of copper ions in the solid state. Increasing the particle size increases the diffusion distances and hence decreases the dissolution rate.

However, the large difference in leaching rate after about 2 hours cannot be explained by this mechanism since both stromeyerite and bornite

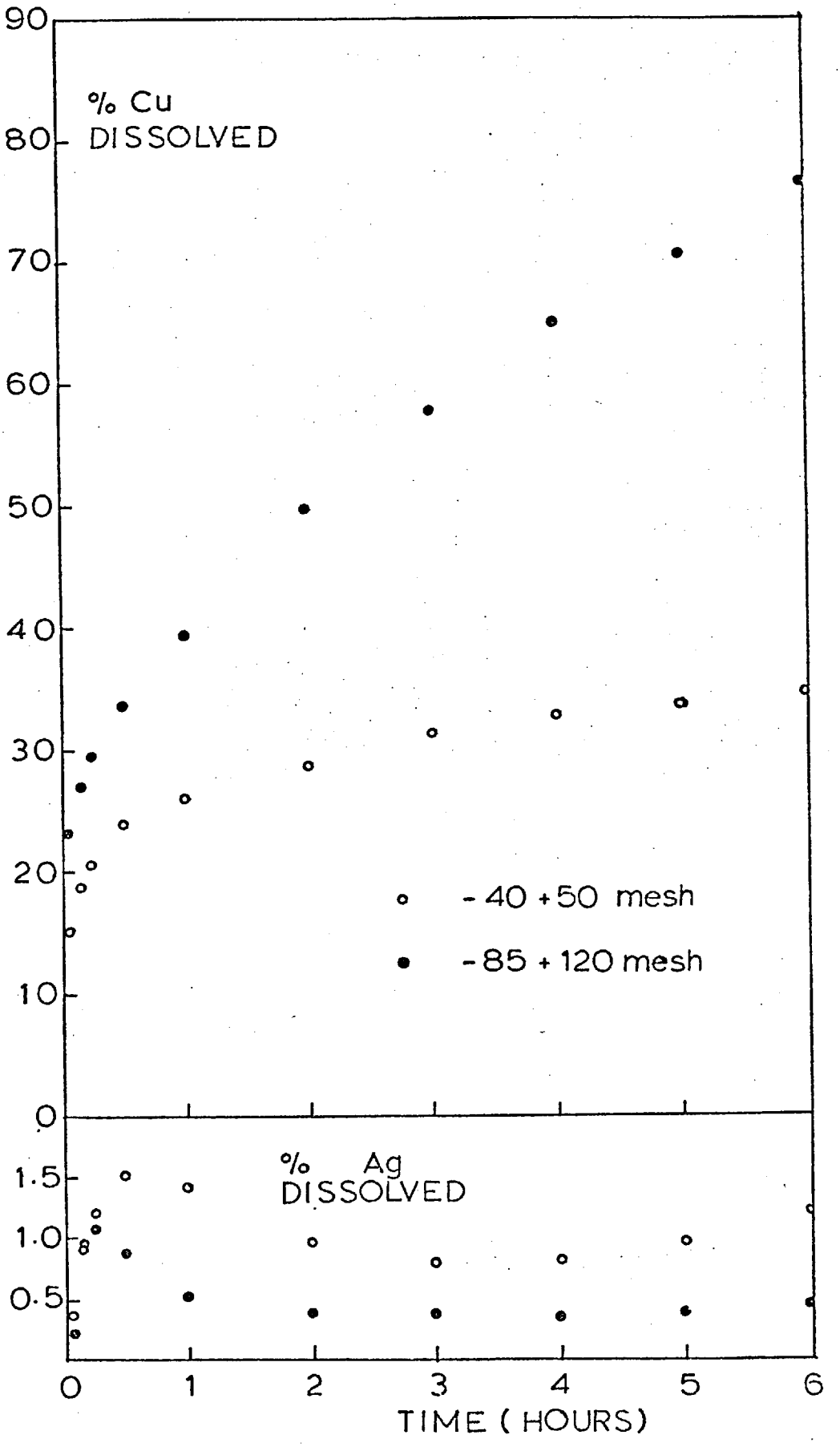


FIGURE 51 : Effect of increasing the particle size on the dissolution of copper and silver from the mixed sulphide material.

undergo chemical transformations in their second stages of leaching, (the dissolution of chalcopyrite can be ignored since it is so slow, and chalcopyrite is present in such small quantities). It could be explained by the same electrochemical and mineralogical factors mentioned in section 6.1.2.

Increasing the particle size reduces the surface area, and thus decreases the sites available for electrochemical activity and also increases the distances that the ferric ion has to diffuse along the pores and cracks in the material. The overall effect is a reduction in the copper dissolution rate.

The silver dissolution was greater with the larger particle size, as would be expected from the previous work (section 5.1.4), since the cupric ion and ferrous ion concentrations in the solution are less than those obtained with the smaller particle size.

6.1.4 Sample Weight.

Figure 52 shows that increasing the sample weight used in the experiments from 0.5 gms to 1 gm did not seem to affect the dissolution of

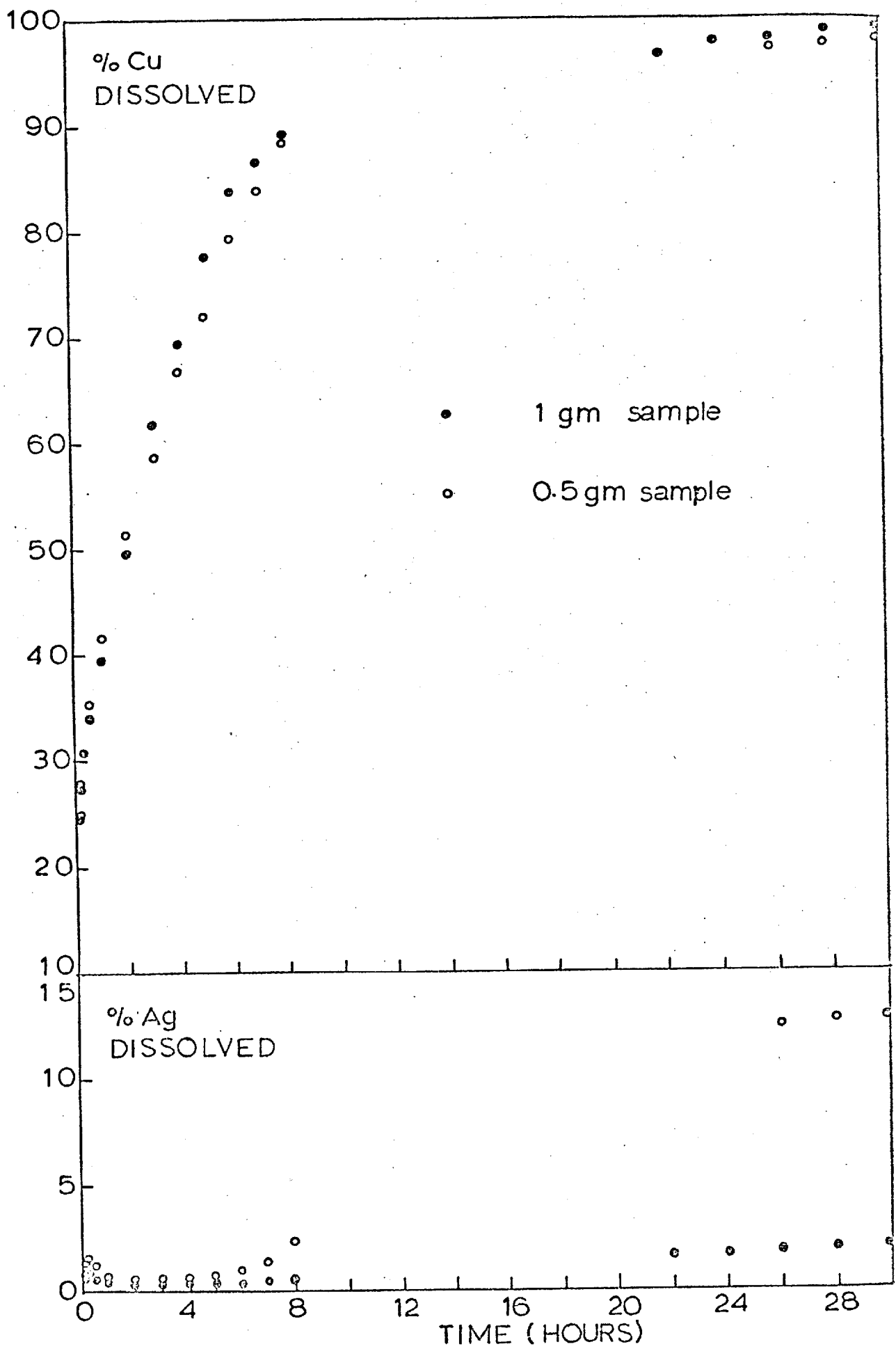


FIGURE 52 : Effect of sample weight on the dissolution of copper and silver from the mixed sulphide material.

copper to any great extent. Both experiments were carried out at 60°C in a 0.25M $Fe^{3+}$ solution. The results are presented in Tables A-3.6 and A-3.9.

The silver dissolution, however, increases when the sample weight is decreased. Decreasing the sample weight of both stromeyerite and the silver-doped bornite had a similar effect (sections 5.1.5 and 3.1.4). It is thought that this is due to less actual weight of copper being dissolved so that the cupric ion and ferrous ion concentrations, which adversely affect the silver dissolution, are considerably lower.

6.1.5. Effect of Chloride ion.

Figure 53 compares the use of a ferric chloride solution with a ferric sulphate solution of the same $Fe^{3+}$ concentration (0.1M), all other conditions being the same. There was a decrease in the dissolution rate of the copper with the chloride solution, while there was a slight increase in the silver dissolution, which did not show the characteristic peak in the initial stages of dissolution observed in sulphate solutions. X-ray analysis showed

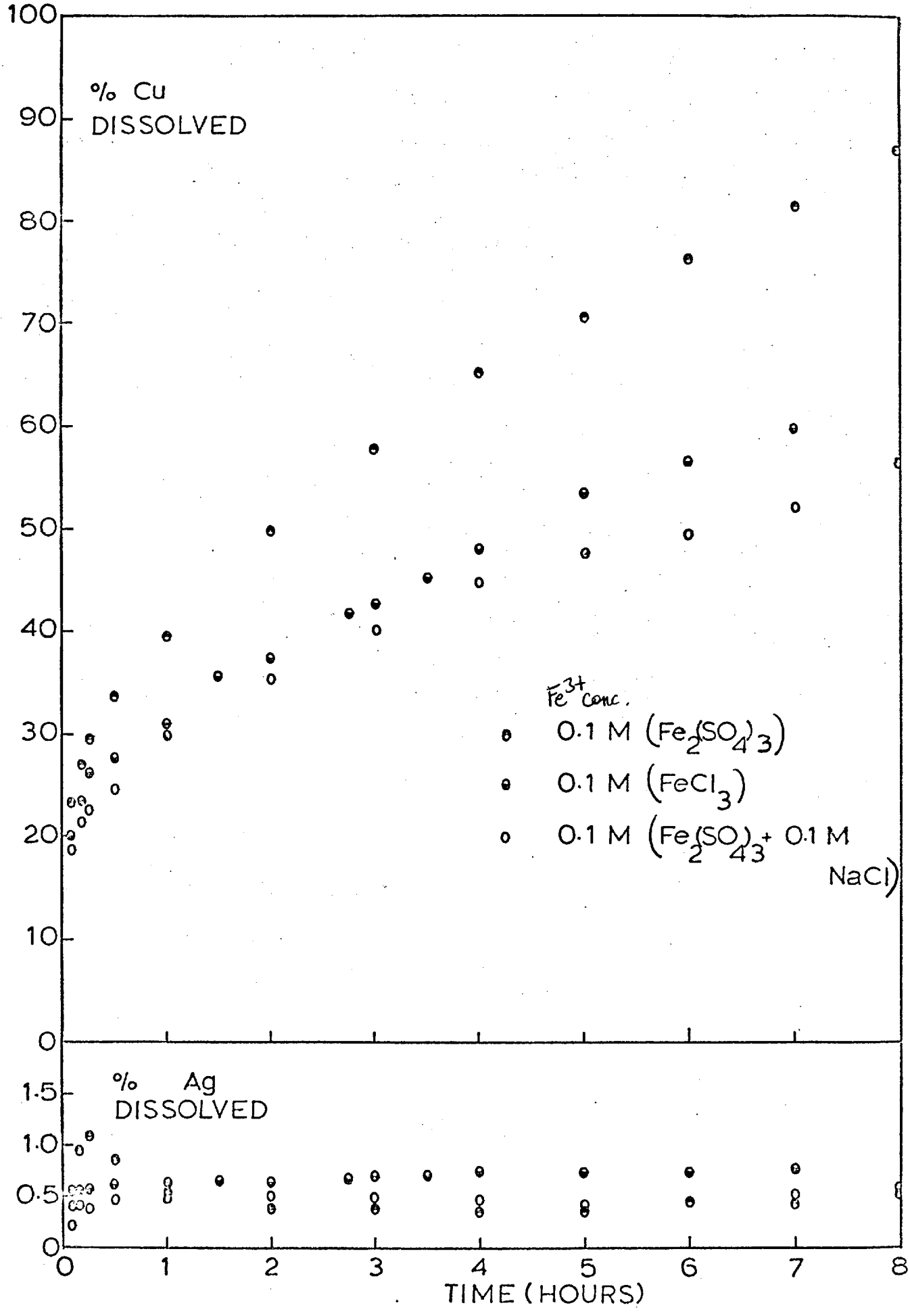


FIGURE 53 : Effect of chloride ion on the dissolution of copper and silver from the mixed sulphide material.

that silver chloride had been precipitated and this may have had an inhibiting effect on the reaction (section 6.2).

The addition of 0.1M NaCl to a ferric sulphate solution had a similar effect, both the copper and silver dissolutions being slightly lower than with the ferric chloride solution, (Figure 53).

A number of experiments were carried out using ferric chloride solutions in 0.1M HCl containing different amounts of NaCl. The results are presented in Figures 54 and 55, and listed in Tables A-3.10 to A-3.15. For NaCl concentrations of 1,1.5 and 3M,the dissolution of copper does not seem to be greatly affected by increasing the chloride concentration. The curves are not consistent with any particular trend, but at all these NaCl concentrations, the copper dissolution rate is still slightly slower than that obtained by using a 0.1M ferric sulphate solution.

Increasing the chloride concentration to 4.4M NaCl caused a significant increase in the copper dissolution, the copper dissolving at a rate that was slightly faster than with

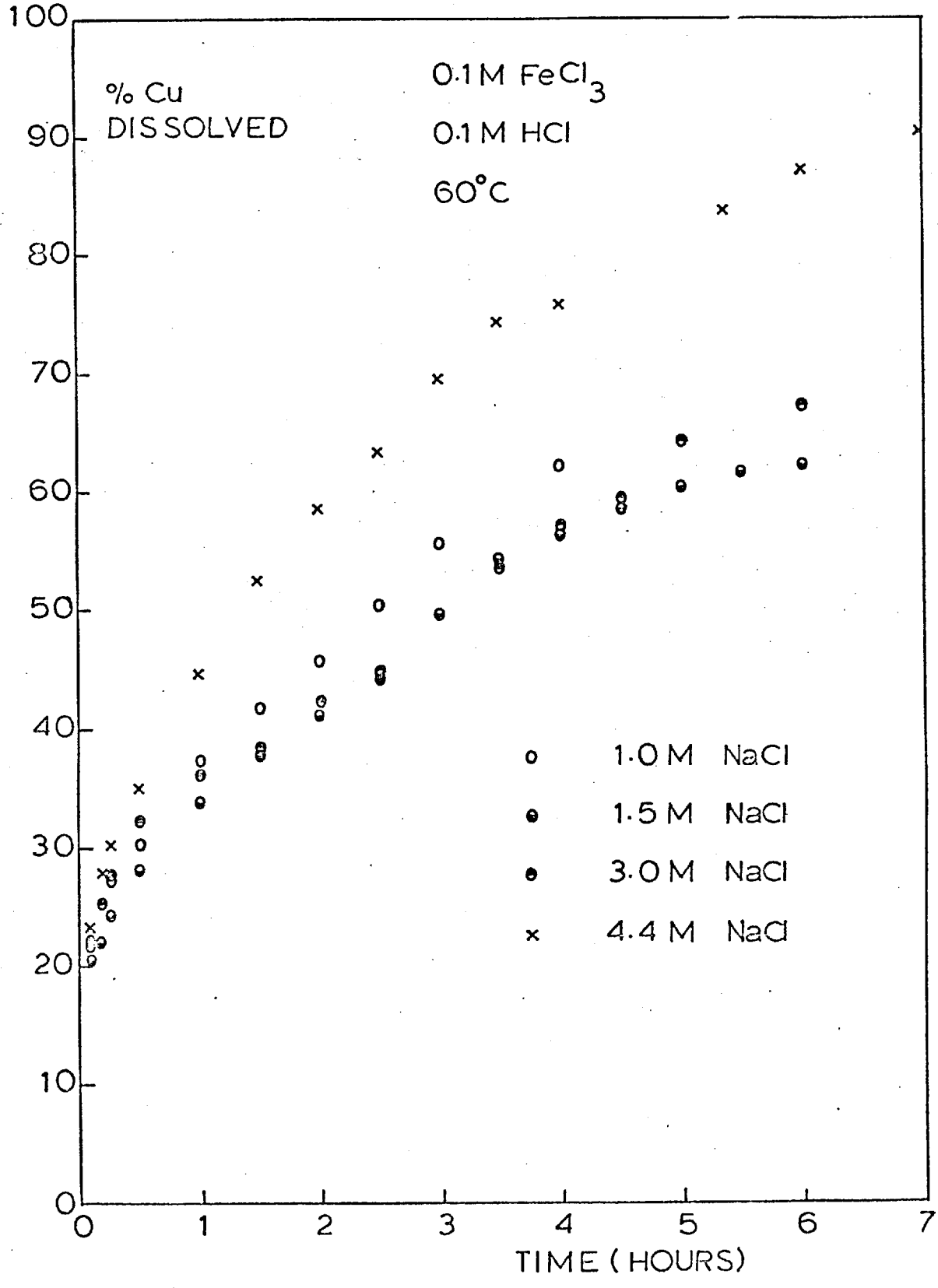


FIGURE 54 : Effect of different concentrations of NaCl on the dissolution of copper from the mixed sulphide material.

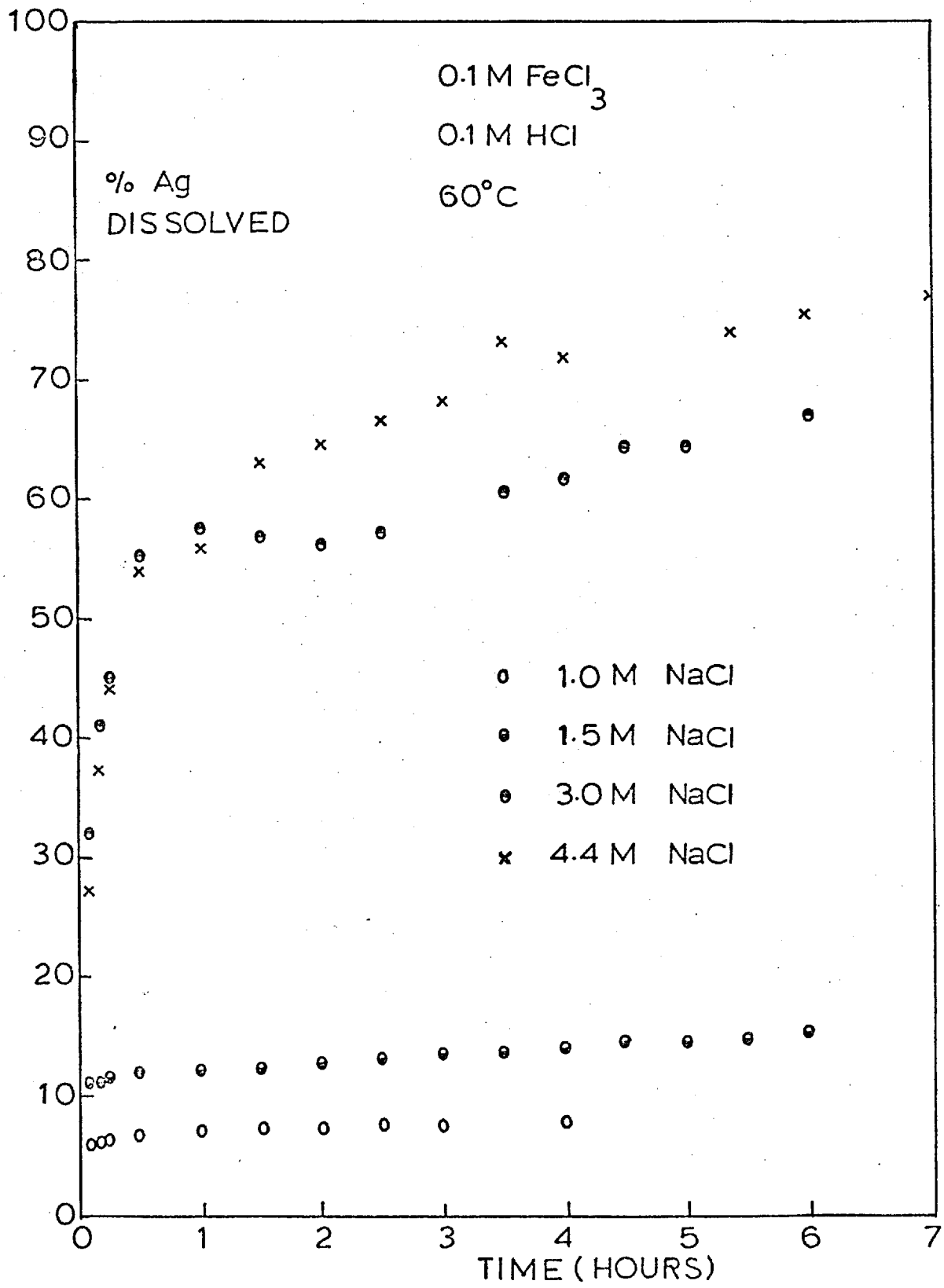


FIGURE 55 : Effect of different concentrations of NaCl on the dissolution of silver from the mixed sulphide material.

the 0.1M ferric sulphate solution.

Figure 55 shows that increasing the NaCl concentration in the leaching solutions from 1M to 4.4M markedly increased the amount of silver dissolved from the mixed sulphide material. At all the chloride concentrations the amount of silver in the leach solutions reached an almost constant value after a short time. Hence although the curves in Figure 55 show that after an initial fast dissolution rate there is a very slow increase in the amount of silver dissolved, this is due to the sampling technique whereby replacing the solution sample with fresh solution results in a slight decrease in the silver concentration of the leach solutions.

The results were somewhat erratic at the higher chloride concentrations. This could be explained by the silver chloride that was formed in all the experiments (section 6.2). Microscopic examination suggested that this silver chloride formed a layer around the particles with the elemental sulphur that was also formed during the reaction. It was apparent that this layer was not very adhesive because the leach solutions became cloudy due

to a fine, white suspension, identified as silver chloride. The samples of the leach solutions were centrifuged before analysis by atomic absorption, but the readings were still very 'noisy' and this caused some error in the analyses.

The enhanced dissolution of silver in the chloride solutions is obviously due to the formation of some soluble silver-chloride complex ion. In section 1.1.3 work on the known complexes has been discussed, with the presence of $AgCl_2^-$, $AgCl_3^{2-}$ and $AgCl_4^{3-}$ being noted under different conditions.

Since the silver concentrations in the leach solutions reach almost constant values after a certain length of time, these values were used in the graphical method of Garret et al[71] to find the complex formed in the present experiments. Garret et al wrote the general equation that represents the increased solubility of silver chloride as:

$AgCl(S) + nCl^- = AgCl_{n+1}^{-n}$ (complexion) (6.1.1).

with the equilibrium constant, $K = \frac{(a)_{AgCl^{-n}_{n+1}}}{(a)^n_{Cl^-}}$ (6.1.2).

where (a) = activity = $M\gamma$ (M = molarity, $\gamma$ = activity coefficient).

Thus $\log K = \log(a)_{AgCl_{n+1}^{-n}} - n \log(a)_{Cl^-}$ (6.1.3).

and $\log(a)_{AgCl_{n+1}^{-n}} = n \log(a)_{Cl^-} + \log K$ (6.1.4).

Therefore plotting $\log(a)_{AgCl_{n+1}^{-n}}$ versus $\log(a)_{Cl^-}$ gives a line of slope n and an intercept of log K. This was done using the data in Table A-3.16 to obtain the straight line plot in Figure 56. The line had a slope of 2.02 (ignoring the point for 3.4M $Cl^-$) and gave a value for K of -4.1. Therefore the chief reaction resulting in the increased dissolution of silver in the chloride concentration range 1 to 4.4M must be:

$AgCl(S) + 2Cl^- = AgCl_3^{2-}$ (6.1.5.)

with K, the equilibrium constant, = $7.943 \times 10^{-5}$.

In Garret's determination and in the present calculations, $\log M_{Cl^-}$ is actually plotted against $\log M_{Ag}$ complex. This is justified if n = 1 for in that case $\gamma AgCl_2^- / \gamma Cl^- = 1$; it can also be justified if n = 2 for, according to the Debye-Huckel relationship $-\log \gamma = CZ_1 Z_2 \sqrt{I}$, it can be shown that at a given concentration (value of I) :

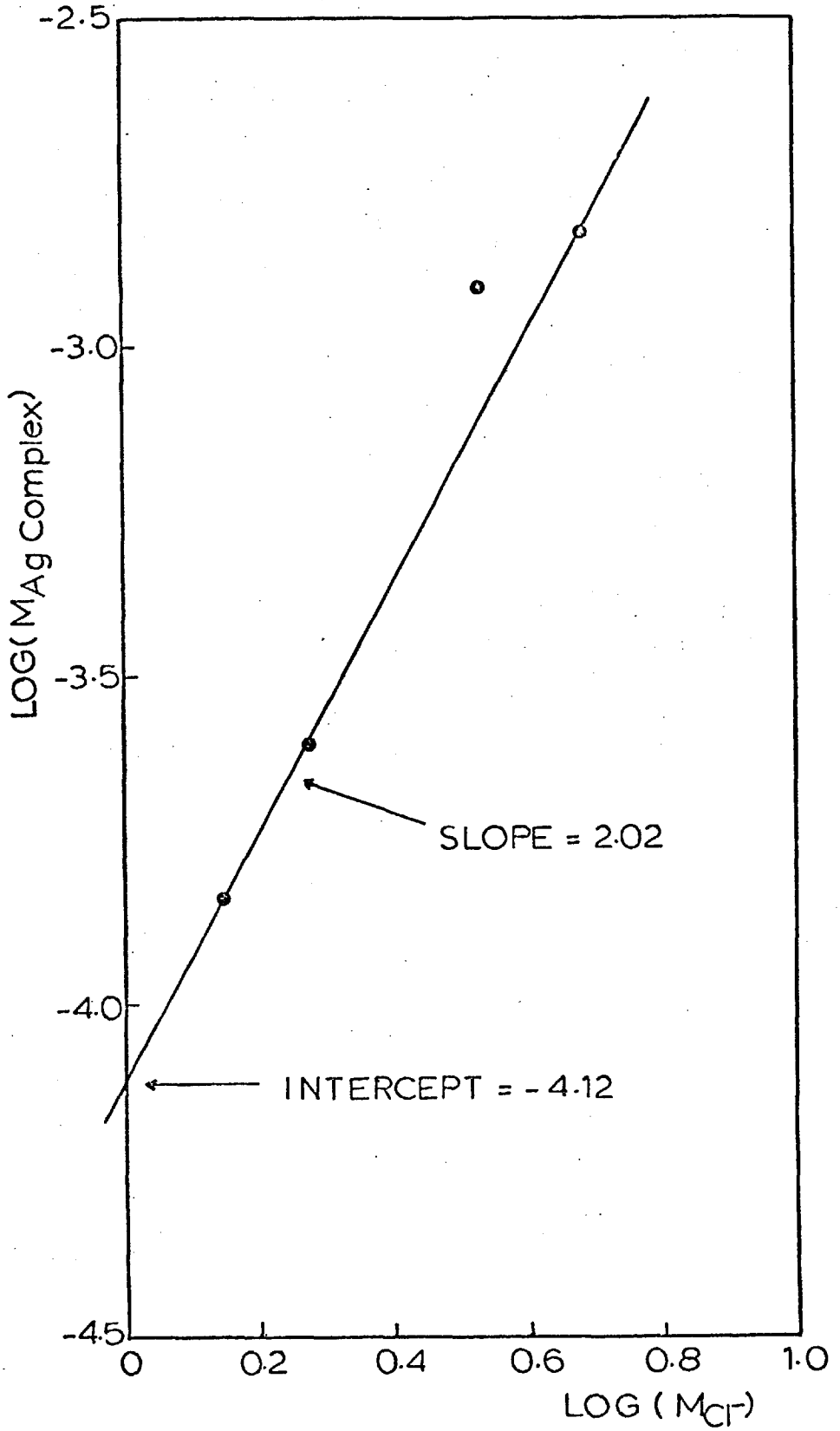


FIGURE 56 : Determination of the complex formed between silver and chloride ion.

$\log\gamma$ (bivalent ion ) = 2 $\log\gamma$(univalent ion)

or $\gamma(11) = \gamma(1)^2$

Hence the expression (6.1.4) can be written

$$\log K = \log MAgCl_3^{2-} + \log \gamma AgCl_3^{2-} - 2 \log MCl^- - 2 \log \gamma Cl^-$$

which reduces to

$$\log K = \log MAgCl_3^{2-} - 2 \log MCl^- \qquad (6.1.5)$$

## 6.2 X-ray Diffraction Analysis.

The X-ray data for the mixed sulphide material is presented in Table B-3.1 and compared with the d-spacings of bornite, chalcopyrite and stromeyerite to show that the synthetic material is a mixture of these three sulphides. This is also apparent on comparing the X-ray diffraction photographs (a), (b), (c) and (d), in Figure C-1.5.

That samples of this mixed sulphide material could contain varying amounts of the three constituent sulphides is illustrated by Figures 57 and 58. These are microdensitometer traces from the X-ray patterns of two different samples. The strongest lines of bornite, chalcopyrite and stromeyerite are indicated and clearly show that different amounts of the sulphides are present in the two samples, giving a difference in the relative intensities of the lines.

The X-ray patterns of the residues from leaching the mixed sulphide material with acidic ferric sulphate solutions are shown in Figure C-1.5 and the measured d-spacings are presented in Tables B-3.2 and B-3.3. These

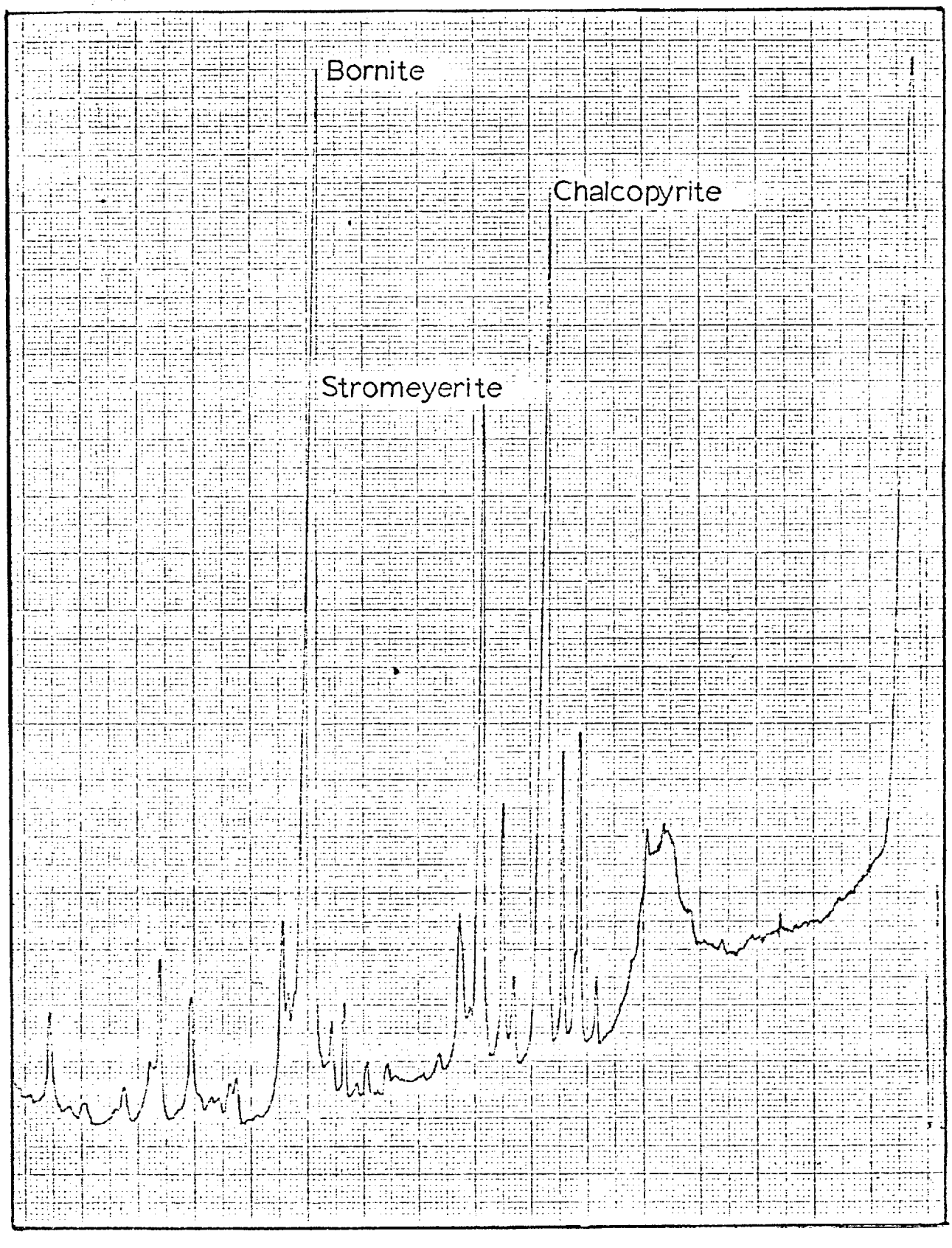


FIGURE 57 : Microdensitometer trace from the X-ray diffraction pattern of sample (A) of the mixed sulphide material.

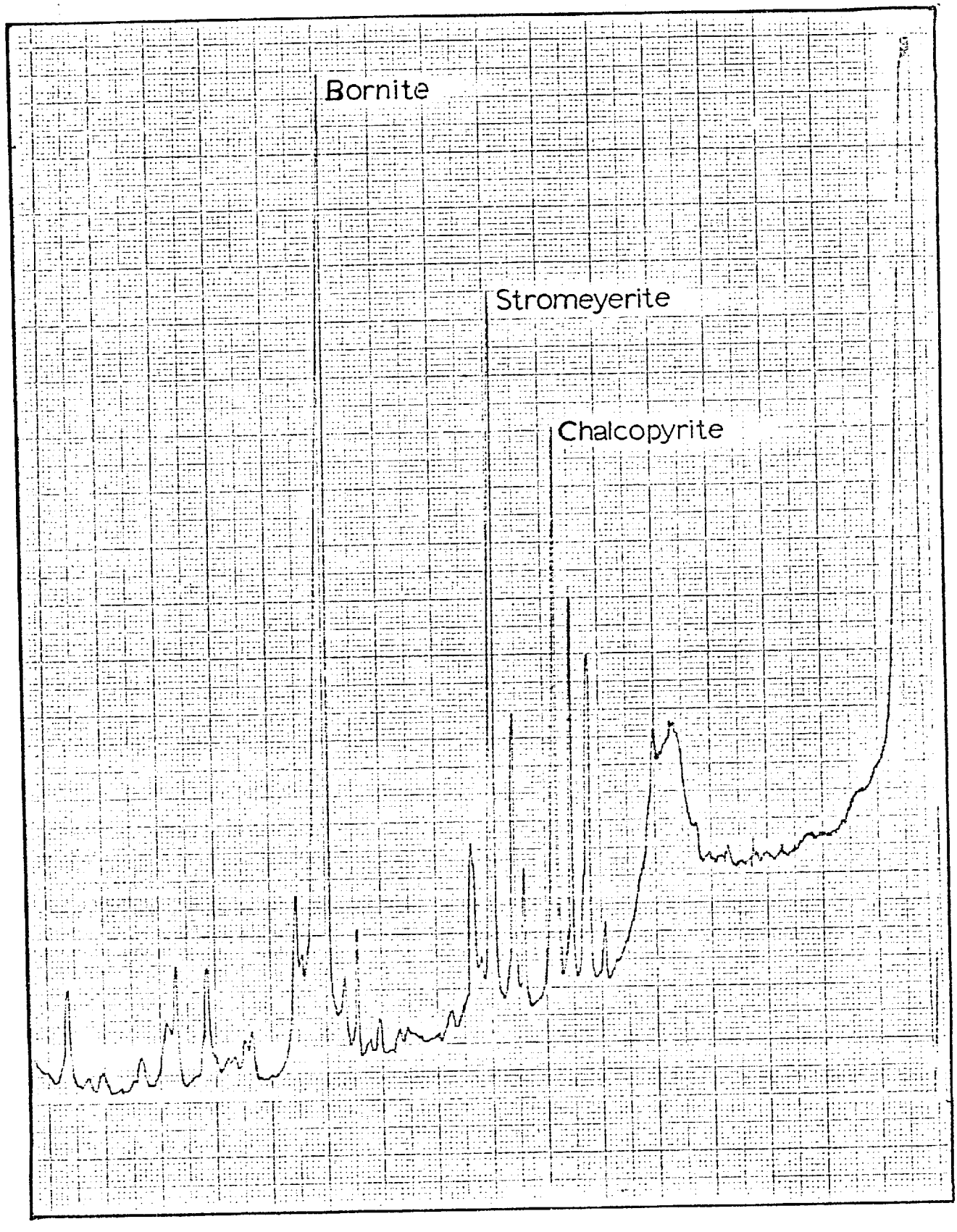


FIGURE 58 : Microdensitometer trace from the X-ray diffraction pattern of sample (B) of the mixed sulphide material.

results suggest that the mechanisms of dissolution of the three constituent sulphides in the mixed sulphide material are the same as for the pure minerals.

The d-spacings that can be attributed to the leached bornite show the gradual decrease that is characteristic of the first stage of leaching pure bornite when copper diffuses out of the lattice causing a contraction of the unit cell (Figure 8) and forming the phase $Cu_3FeS_4$ [11]. This is clearly illustrated in Figure C-1.5 and in Table B-3.2 by the reflections at d = 3.164 and d = 1.936 Å. The former decreases to 3.082 and the latter to 1.888Å, after 39.45% of the copper from the mixed sulphide material has dissolved. Above this amount of copper dissolved, the transformation product of bornite, idaite, dissolves by a chemical reaction to produce elemental sulphur[11], as evidenced by the diffraction lines of the idaite remaining stationary and the emergence of elemental sulphur (orthorhombic ) diffraction lines, which were clearly visible after 69.00 and 93.00% of the copper had been dissolved (see Table B-3.3 and photographs (l) and (m) in Figure C-1.5.).

The residue with 93% of the copper dissolved was treated with carbon disulphide to remove the elemental sulphur. The X-ray pattern and d-spacings of the remaining residue (Figure C-1.5, photograph (n), and Table B-3.4) show that, after this amount of copper had dissolved, all of the bornite had dissolved leaving a residue of undissolved chalcopyrite and silver sulphide.

The presence of chalcopyrite in the residue indicates that it leaches much slower than bornite, as has already been mentioned (section 1.2.2). Its dissolution mechanism also seems to be unchanged in the presence of the other sulphides. The diffraction lines showing no movement and indicating that dissolution is by a chemical process[12].

The presence of silver sulphide indicates that the stromeyerite dissolves by the same mechanism as described in section 5.2 for the pure mineral which produces a mixture of silver sulphide and covellite after the first stage of copper dissolution and leaves a residue of silver sulphide after dissolution of the covellite in the second stage.

The presence of jalpaite, Mckinstryite and covellite were difficult to detect from the X-ray patterns probably due to the large number of diffraction lines and the fact that these species would only be present in small quantities. The presence of silver sulphide seemed to be indicated by the patterns for the residues with 23.30% copper removed and above.

Films (b), (c), (d), (e), and (f) in Figure C-1.6 are the X-ray diffraction patterns for the residues of the mixed sulphide material after leaching in the chloride solutions described in section (6.1.5). The d-spacings are presented in Table B-3.5 and comparison with the d-spacings of sulphur, silver chloride and chalcopyrite shows that these three species are present in all the residues. No other silver phases were detected but some of the lines indicate that trace amounts of bornite are still present in some of these residues. The more copper that is removed the stronger the lines of sulphur appear, and the more silver dissolved the weaker the lines of silver chloride. The lines for chalcopyrite remain the same as in the unleached material.

## 6.3 Atomic Absorption Analysis of residues.

Analyses of the leach residues after leaching in acidic ferric sulphate solutions and removal of the elemental sulphur are presented in Table 5. Very little can be determined about the dissolution behaviour of the mixture of sulphides from these analyses which just give the overall compositions of the residues. It can be seen that the residues become steadily richer in silver as the copper is dissolved and that the copper to iron molar ratio becomes very close to 1 : 1. This is expected from the X-ray diffraction analysis which showed that after the removal of elemental sulphur, the residues with greater than 90% of the copper dissolved consist of undissolved chalcopyrite and silver sulphide (section 6.2)

TABLE 5 : Analysis of Residues by A.A. Spectrophotometry.

| Wt.% Dissolved | | Compositions of Residues (weight % and Atomic %) | | | | | | | |
|---|---|---|---|---|---|---|---|---|---|
| Cu | Ag | Copper | | Silver | | Iron | | Sulphur | |
| | | Wt.% | At.% | Wt.% | At.% | Wt.% | At.% | Wt.% | At.% |
| 34.66 | 1.218 | 48.87 | 39.16 | 10.03 | 4.73 | 13.55 | 12.35 | 27.55 | 43.74 |
| 38.91 | 0.313 | 47.82 | 39.38 | 12.63 | 6.12 | 14.26 | 13.34 | 25.26 | 41.14 |
| 51.39 | 0.073 | 43.16 | 36.06 | 14.71 | 6.50 | 14.92 | 14.11 | 27.21 | 43.31 |
| 58.86 | 0.233 | 41.47 | 33.14 | 13.43 | 6.32 | 16.14 | 14.67 | 28.96 | 45.86 |
| 93.69 | 1.079 | 19.95 | 17.56 | 36.95 | 19.16 | 16.06 | 16.08 | 27.03 | 47.17 |
| 97.30 | 5.200 | 15.73 | 14.45 | 42.62 | 23.06 | 17.19 | 17.96 | 24.46 | 44.52 |
| 97.52 | 2.000 | 15.72 | 15.98 | 53.78 | 32.20 | 11.22 | 12.98 | 19.28 | 38.83 |
| 97.61 | 15.385 | 11.89 | 11.54 | 52.97 | 30.29 | 11.54 | 12.74 | 23.60 | 45.40 |

## 6.4. Microscopic Examination.

Figure C-2.15 shows the condition of the unleached sample. A full description of the mixed sulphide material has been given in section 2.1.2. The stromeyerite appears to be a bluish grey in contrast to the light coloured polished sections of the pure mineral described in section 5.4. Although most authors have described stromeyerite as having a steel-grey colour, it has been noted that it often appears blue on exposed surfaces[201].

The particles of the mixed sulphide material showed no preferential fracturing but it should be noted that the relative amounts of the different phases varied from particle to particle. Hence the dissolution rate of each individual particle may be different, but the leaching rate of a particular phase would be expected to be the same unless there is some electrochemical effect on the leaching process.

For these reasons it is difficult to show the progress of leaching in a series of photomicrographs. However certain observations can be made. Figure C-2.16 shows a particle from which 7-8% of the copper has been removed.

Cracks have begun to appear in the particle and pits have appeared in the chalcopyrite. Figure C-2.17 shows a particle from a residue with 23.30% of the copper removed. Pits and cracks have formed in the bornite phase while the stromeyerite and chalcopyrite appear almost unattacked except at the edges of the particle. Figure C-2.18 shows a particle from the same residue with just bornite and the stromeyerite intergrowth present. The pits that have formed seem to follow along the direction of the intergrowth suggesting that this intergrowth plays an important part in the dissolution of the mixed sulphide material.

Figure C-2.19 shows the growth of these pits, as more copper was dissolved, with the chalcopyrite still relatively unattacked but some removal of stromeyerite has taken place. Figure C-2.20 shows a particle where more than 90% of the copper had been dissolved. The large dark areas are probably due to the removal, during polishing, of a coating of sulphur (identified by X-ray diffraction, section 6.21). The preferential attack along the intergrowth can clearly be seen. It is this preferential leaching and the cracks that

are formed that may explain the very fast dissolution rate of the mixed sulphide material.

Figures C-2.21 and C-2.22 show the effect of leaching the material in chloride solutions. A definite layer was formed around the particles and X-ray diffraction analysis suggested it to be a mixture of sulphur and silver chloride (section 6.2). Attack started immediately at the edges and there seemed to be no preferential leaching behaviour. Hence the chloride solutions seemed to dissolve the phases at about the same rate, while the ferric sulphate solutions dissolved the bornite and stromeyerite with the chalcopyrite much slower. The dissolution of the bornite seemed to be enhanced by the presence of the intergrowth of stromeyerite.

## 6.5. Electron Microprobe Analysis.

It was not possible to make any quantitative measurements on the mixed sulphide material residues because of the pits and cracks (section 6.4.) and the beam damage that occurs (section 2.1.2). However a number of electron microprobe traces were carried out on the leached material and these can be compared with the traces in Figure 59 for the unleached material which were discussed in section 2.1.2.

Figure 60 shows two iron-silver traces across particles from samples with more than 90% of the copper dissolved (similar to Figure C-2.20). Areas of high silver are still areas of low iron content. The iron content is almost uniform with areas of high silver at the edges of the leached particles. This is consistent with the X-ray analysis which showed that above 90% of copper dissolution, when the elemental sulphur had been removed the residues were essentially undissolved chalcopyrite and silver sulphide. The silver sulphide would surround the residual chalcopyrite since it is formed from the stromeyerite which occurred between the chalcopyrite and the, now dissolved,

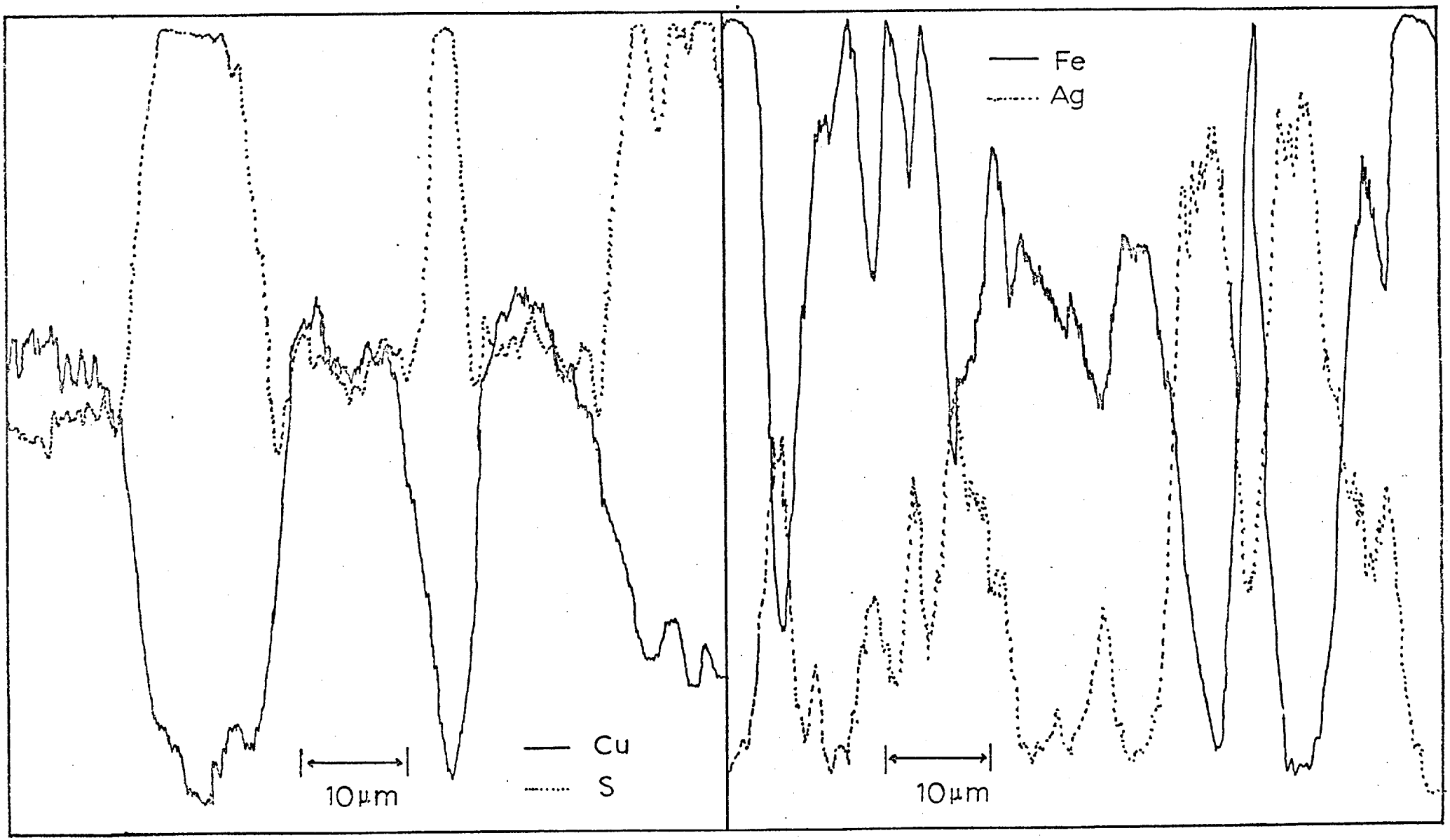


FIGURE 59 : Electron probe trace across a sample of unleached mixed sulphide material.

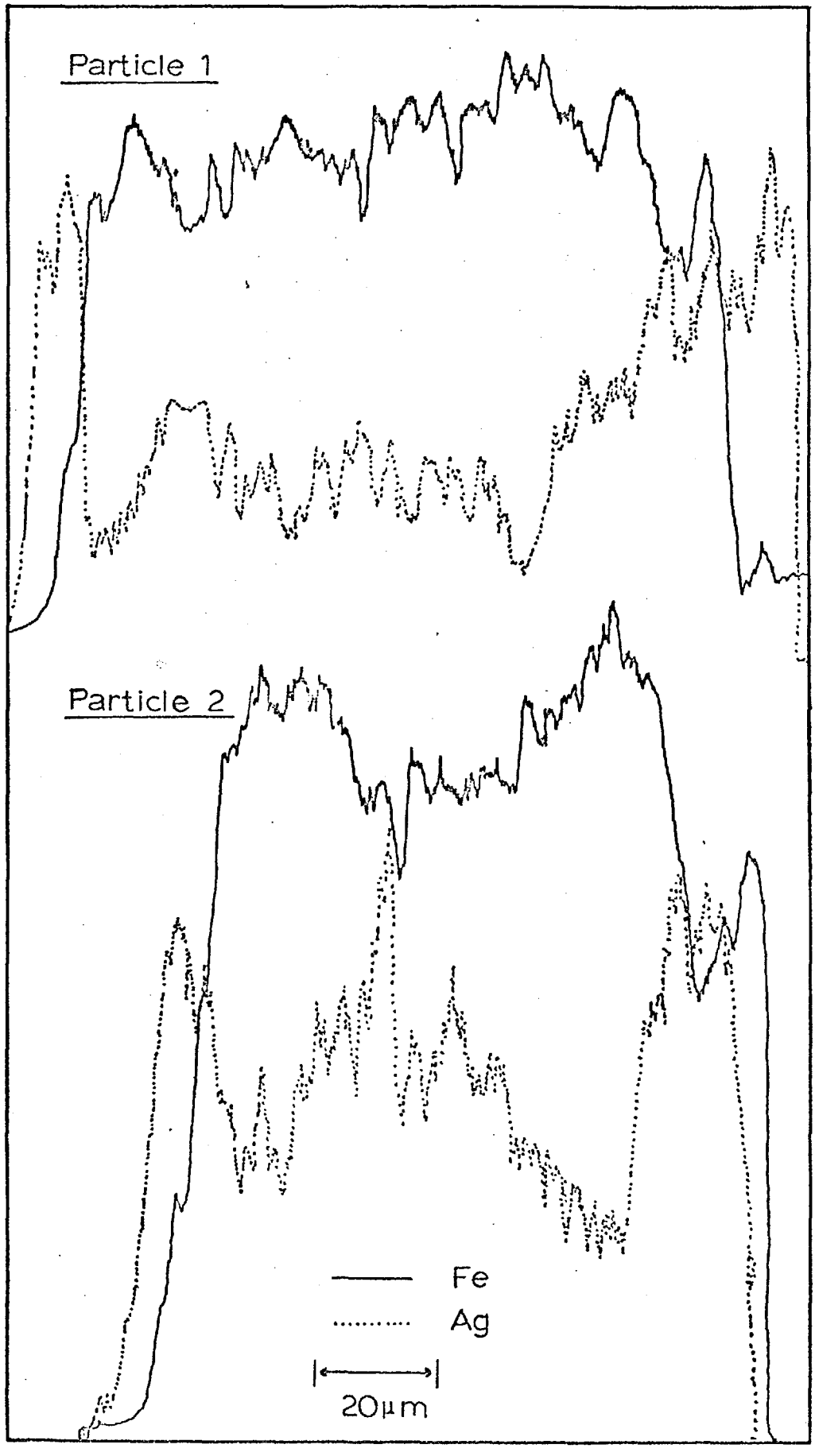


FIGURE 60 : Electron probe trace across leached particles of the mixed sulphide material.

bornite in the original samples.

The presence of this silver phase around the chalcopyrite may inhibit the dissolution of the chalcopyrite as it did with the dissolution of the covellite in the second stage of the dissolution of stromeyerite (section 5.1.).

## 6.6. Leaching of mixtures of the pure minerals.

As has been mentioned earlier, copper dissolved from the mixed sulphide material much faster than from pure bornite. The material was estimated to contain 70% bornite, 10% chalcopyrite and 20% stromeyerite. Since the leaching characteristics of all three minerals are now known, the theoretical amount of copper that should dissolve out can be calculated and compared with the actual experimental results from the mixed sulphide material leach runs.

The data used to calculate this theoretical leaching rate is presented in Table A-4.1, and the calculated copper dissolution is presented in Tables A-4.2 and Figure 61 where it is compared with the experimental leaching behaviour of the mixed sulphide material. The data in Table A-4.1 was obtained from the following sources:

Pure Bornite (Ugarte)[11]: Leach run at 60°C with a 0.065M $Fe^{3+}$ solution

Pure Chalcopyrite: (Ferreira)[12]: Leach run at 80°C with a 0.1M $Fe^{3+}$ solution.

Pure stromeyerite (present work): Leach run at 60°C with a 0.1M $Fe^{3+}$ solution (Table A-2.6).

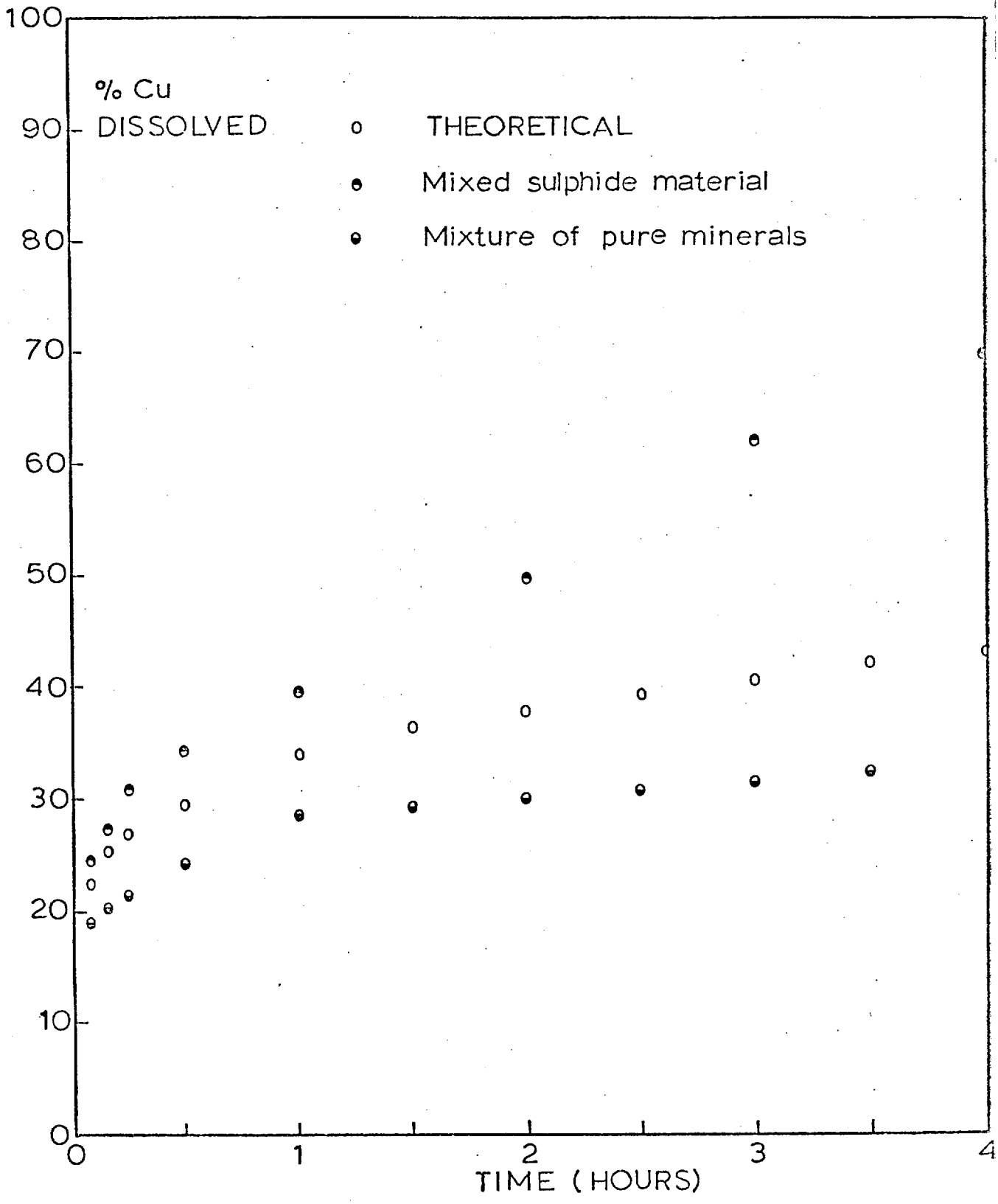


FIGURE 61 : Comparison of the dissolution of copper from a mixture of the pure minerals, bornite, stromeyerite, and chalcopyrite, with that from the mixed sulphide material and the expected dissolution.

The mixed sulphide material data was taken from Table A-3.9 (60°C , 0.25M $Fe^{3+}$ concentration).

As can be seen in Figure 61 there is a considerable difference between the actual weight per cent of copper dissolved and the theoretical amounts predicted from the leaching characteristics of the separate minerals. To investigate this further, a number of leaching experiments were carried out with mixtures of the pure minerals.

A mixture of 0.7 grams of pure bornite, 0.1 grams pure chalcopyrite and 0.20 grams of pure stromeyerite (i.e., with the same proportions as the mixed sulphide material) was leached in a solution of 0.25M $Fe^{3+}$ in $H_2SO_4$ (pH1) at 60°C. The copper in the mixture was calculated as 54.58% of the total weight, in good agreement with the composition of the mkxed sulphide material (54.50 wt.% Cu). The copper dissolution is presented in Table A-4.3 and is plotted in Figure 61 as the total weight % of copper in solution versus time.

It can be seen that the dissolution of

copper from the mixture of pure minerals was slower than that predicted and much slower than the dissolution from the mixed sulphide material, although it has the same leaching characteristics of a fast first stage followed by a slower second stage. From these results it seems that one or more of the sulphides, bornite, chalcopyrite and stromeyerite, has an inhibiting effect on the dissolution of copper from the other sulphides. The faster dissolution rate of the mixed sulphide material now seems to be more likely to be explained by mineralogical factors such as the presence of the fine intergrowth of stromeyerite in the bornite phase along which pits and cracks seem to form, effectively reducing the particle size and increasing the surface area for attack (section 6.4, Figure C-2.18).

To check the inhibiting effect of the sulphides on each other, a mixture of 0.7 grams of bornite and 0.1 grams of chalcopyrite, and a mixture of 0.7 grams of bornite and 0.2 grams of stromeyerite were both separately leached at 60°C in solutions containing 0.1M $Fe^{3+}$ in $H_2SO_4$ (pH1). The results are presented in Tables A-4.4 and A-4.5, and Figures 62 and 63.

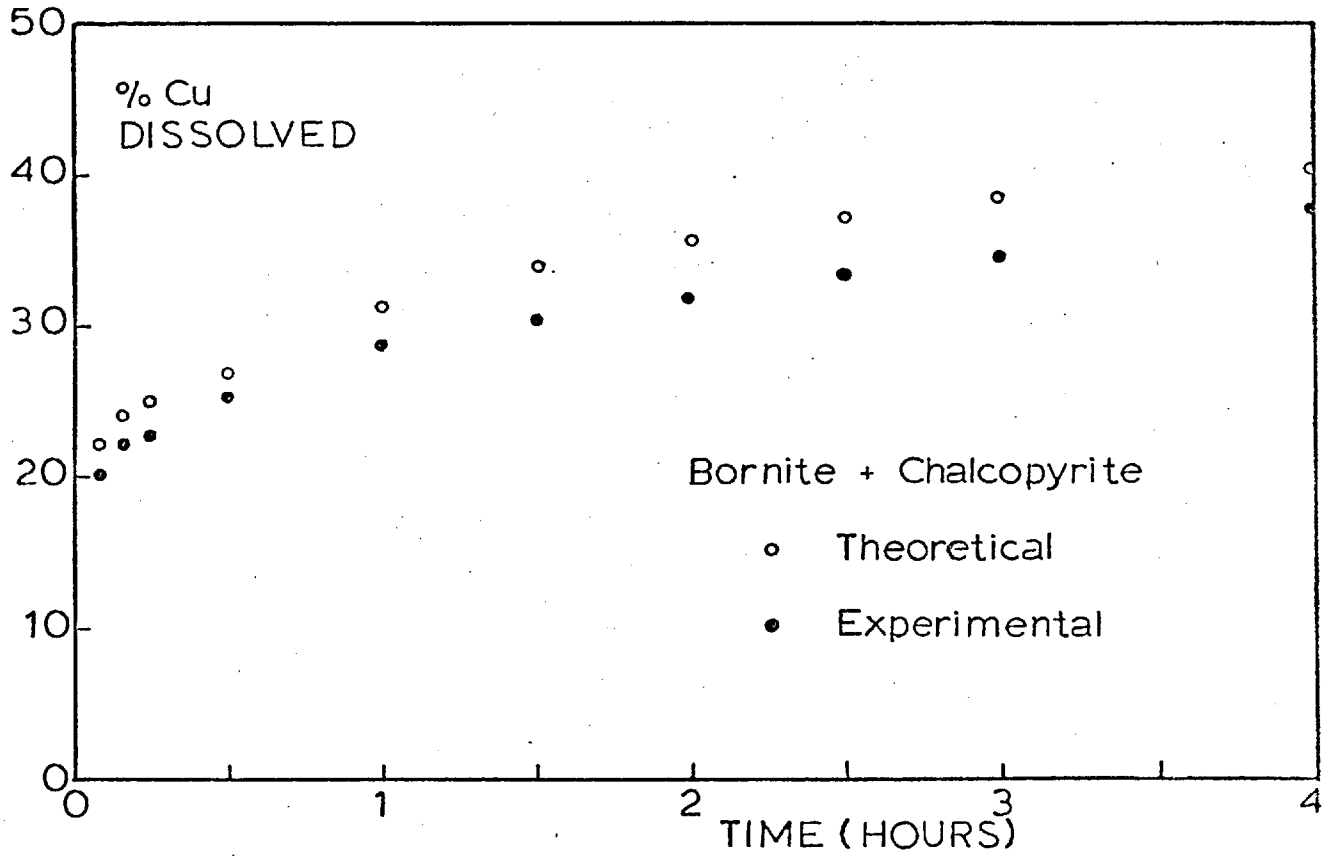


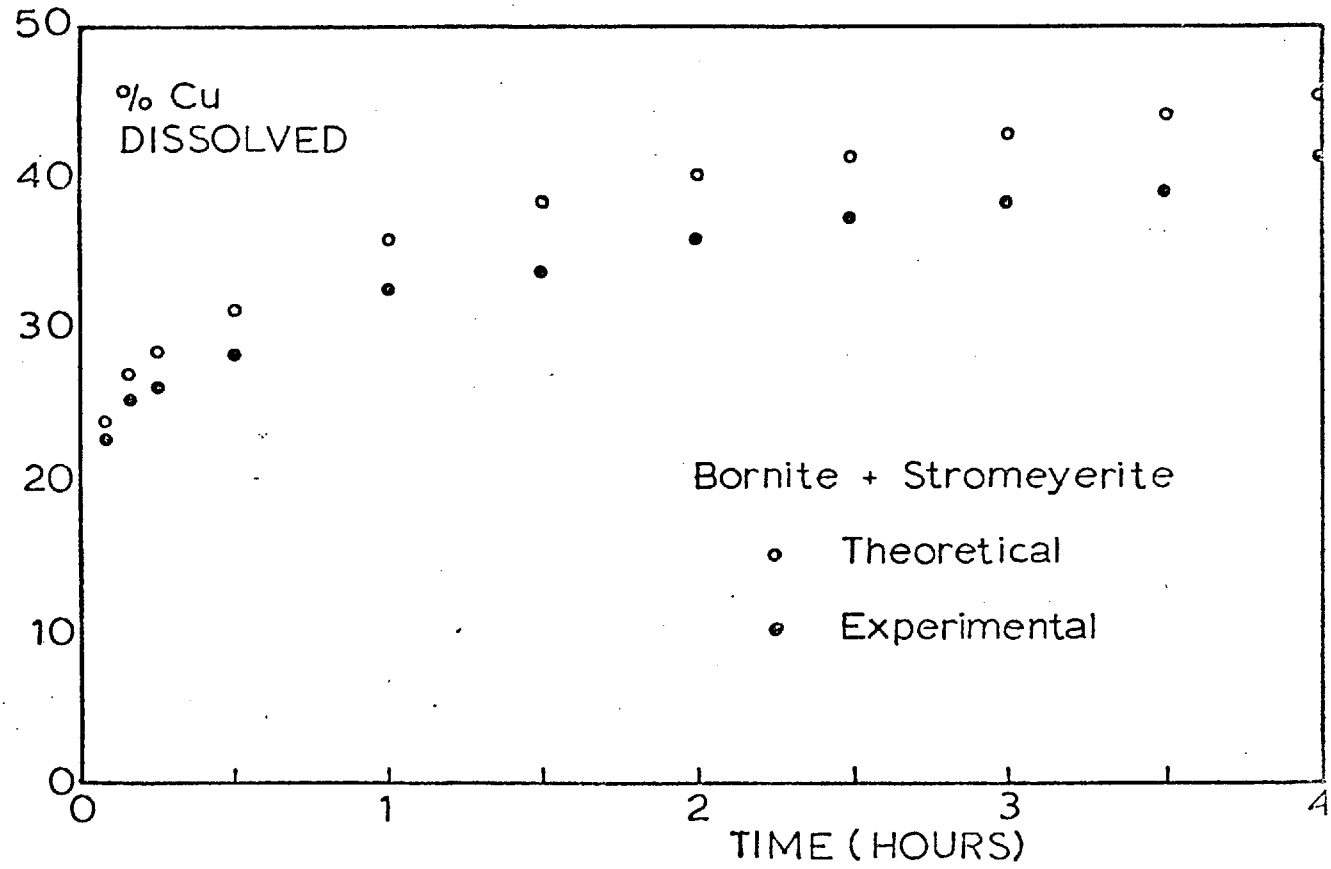


FIGURE 62 : Comparison of the dissolution of copper from (a) a mixture of bornite (0.7gms) and chalcopyrite (0.1gms), and (b) a mixture of bornite (0.7gms) and stromeyerite (0.2gms), with the expected dissolutions.

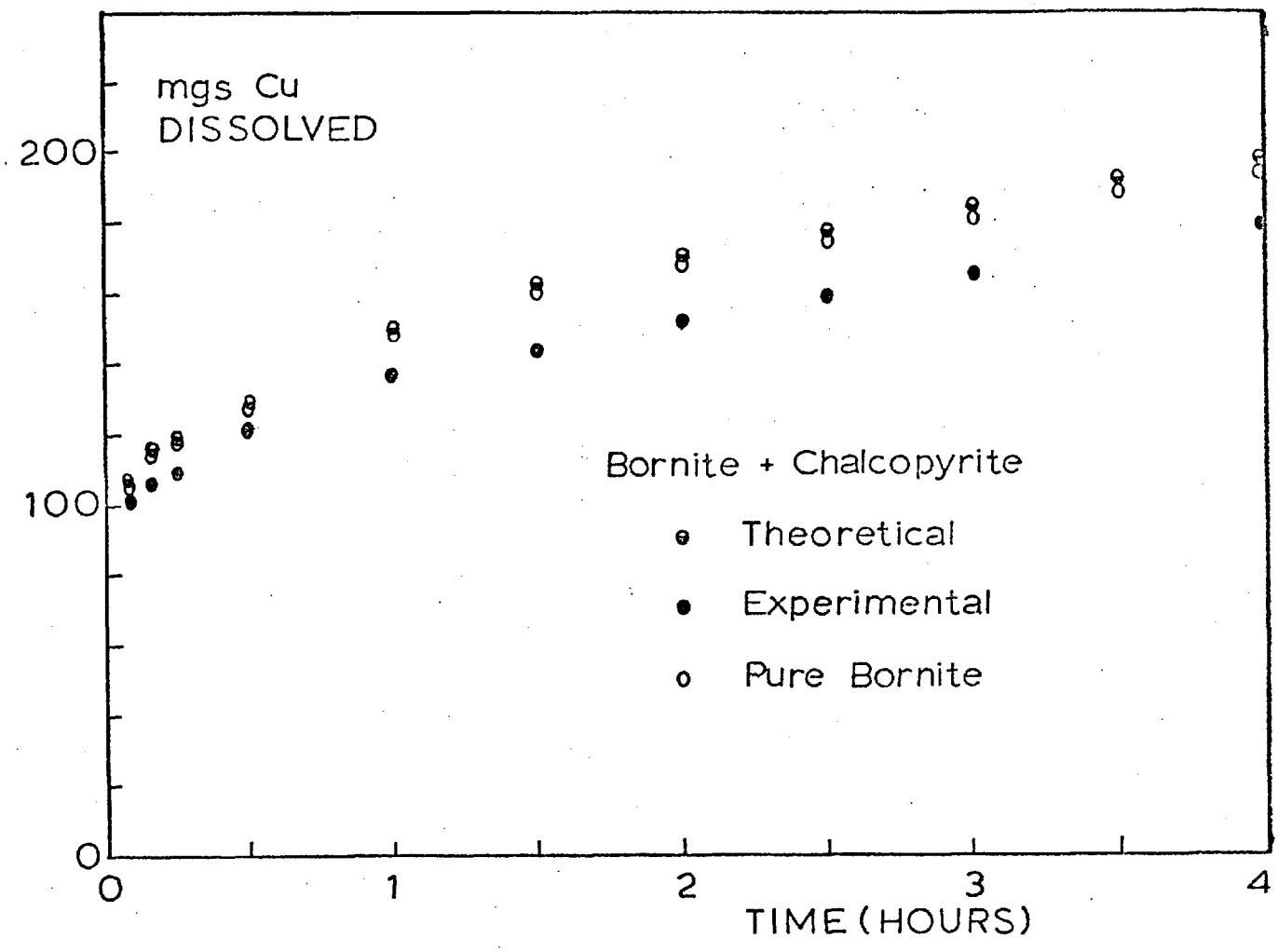


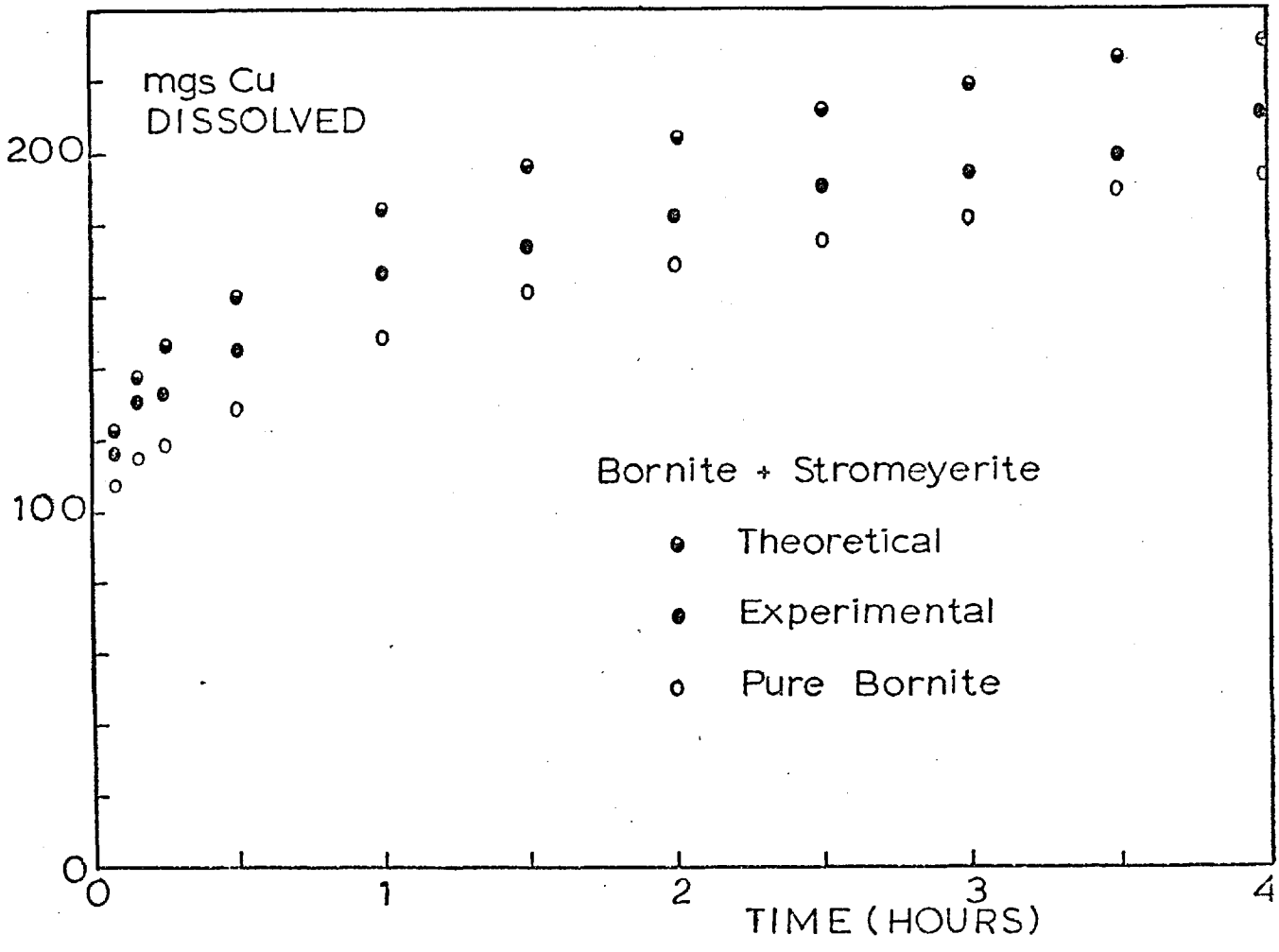


FIGURE 63 : Comparison of the weight of copper dissolved from the mixtures with the expected weights.

Figure 62 shows that the dissolution of copper from both mixtures, expressed as weight % of the total copper, was less than the theoretical weight % predicted from Table A-4.1 and presented in Tables A-4.4 and A-4.5. The dissolution curves of the mixtures of pure minerals, however, still retain the same characteristics.

Figure 63 shows the same results presented as total weight of copper dissolved and they are compared with the dissolution of copper from 0.7 grams of pure bornite (data from Table A-41). There is now an obvious difference between the leaching behaviour of the two mixtures. In the case of the bornite-chalcopyrite mixture it can be seen that the experimental amount of copper dissolved is not only less than the theoretical expected amount but is also less than the amount that would dissolve from the bornite alone. This suggests that the presence of 0.1 gram of chalcopyrite has an inhibiting effect on the dissolution of the 0.7 grams of bornite.

In the case of the bornite-stromeyerite mixture the experimental amount of copper dissolved is greater than the amount that can

be explained by the dissolution of bornite alone but is still less than the amount that should be present in the solution if the two minerals have no effect on eachother. Hence either the stromeyerite affects the dissolution of copper from bornite or bornite has an inhibiting effect on the stromeyerite dissolution.

Although the rate of dissolution of copper was somewhat slower, the characteristics of the leaching curves in the Figures 62 and 63, together with the X-ray diffraction data (presented in Tables B-4.1 to B-4.3, and Figure C-1.6, photographs (h), (i) and (j)) indicate that the mechanisms of dissolution of the pure minerals are unaffected by the presence of the other sulphides. This conclusion is supported by the photomicrograph of the bornite-chalcopyrite-stromeyerite mixture residue in Figure C-2.23, showing one particle of each of the sulphides. The stromeyerite particle has the same appearance as that in Figure C-2.9, and the chalcopyrite and bornite particles have the same appearance as those presented by Ferreira [12] and Ugarte [11].

## 6.7. Discussion and Comparison with Other Work.

The results of the mixed sulphide material leaching and the leaching of the mixtures of pure minerals indicated that the dissolution mechanism of each of the three sulphides was unaltered in the presence of the other sulphides. This conclusion was supported by the characteristics of the dissolution curves, the X-ray diffraction analysis and the microscopic examinations. However Figure 61 clearly shows that the dissolution of copper from the mixed sulphide material was considerably greater than that theoretically predicted from leaching data on the pure minerals.

It was noted that $Fe^{3+}$ concentration had a far greater effect than expected on the dissolution of copper from the mixed sulphide material, and that increasing the particle size considerably decreased the copper dissolution rate. These effects seemed to show the importance of either electrochemical or mineralogical factors, or both, on the dissolution process. It would be these same factors that caused the much faster leaching rate of the mixed sulphide material compared to the predicted rate.

The mineralogicsl factors are associated with the way in which the different sulphides are distributed in the mixed sulphide material. The stromeyerite is not only deposited between the chalcopyrite and bornite phases but is also present as a fine intergrowth in the bornite phase. As the bornite leaches, copper diffuses out and there is a contraction in the unit cell as the bornite transforms to idaite. This contraction causes a number of pits and cracks to form, which, microscopic examination showed, seemed to be preferably formed along the boundary with the intergrowth of stromeyerite. Obviously the formation of cracks would be much easier at these boundaries, especially since the stromeyerite is also leaching and transforming to covellite and silver sulphide. The formation of these cracks effectively reduces the particle size of the particles and increases the surface area and thus, as long as the ferric ion concentration is sufficient to enable easy diffusion into the cracks, the dissolution of the bornite will be enhanced.

As mentioned in section 1.3 an electrochemical or galvanic dissolution mechanism requires good electrical contact between the

different sulphides. The distribution of the sulphides in the mixed sulphide material ensures this condition and leads to the possibility that electrochemical effects may enhance the dissolution of one or more of the sulphides and thus explain the faster than predicted leaching rate for the material.

Dutrizac et al[122, 123] obtained good electrical contact between different sulphides by using sintered discs and investigated the effects of various impurity sulphides on the dissolution of bornite and chalcopyrite. The authors found that the accelerating effect of pyrite on both chalcopyrite and bornite dissolution and the inhibiting effect of galena on chalcopyrite dissolution were consistent with a galvanic mechanism for the dissolutions. According to galvanic corrosion theory, the dissolution of sulphides is an electrochemical process. On the surface of the 'pure' sulphide certain regions such as grain boundaries, impurity atom sites, dislocations, etc., become anodic; the remainder of the surface is cathodic. The actual dissolution (i.e., oxidation) occurs in the anodic regions, while the oxidant is reduced at the cathodic sites. The

electron transfer is completed through the conducting sulphide mineral.

If the sulphide was in contact with a second mineral having a more positive potential, then this second mineral would become cathodic, and the original sulphide would become the anode. Thus the dissolution of the original sulphide would be favoured under these conditions provided that the reduction step can occur easily on the surface of the second sulphide mineral. Conversely when the sulphide is in contact with a mineral having a lower rest potential, the dissolution of the first sulphide is retarded while that of the second mineral is accelerated.

Gottschalk and Buehler[120] arranged a selection of minerals according to their measured electrode potentials in a series analogous to the electrochemical series. This series, in order of decreasing nobility (i.e., increasing reactivity), was: marcasite, argentite, chalcopyrite, molybdenite, covellite, bornite, pyrrhotite, chalcocite and sphalerite.

Wright[13] has reviewed other work on the

measurement of the electrode potentials of minerals and has concluded that, although there are many difficulties in experimentally measuring the electrode potentials of minerals and the order of the above series appears to differ slightly in different solutions, the overall trend is essentially the same. Thus chalcopyrite is more noble than bornite and it would be expected that when in contact, the chalcopyrite would be cathodic and the bornite anodic so that the dissolution of the chalcopyrite is retarded while that of the bornite is accelerated.

No data has been found for the electrode potential of stromeyerite but the above series shows that Argentite, $Ag_2S$, is more noble than chalcopyrite, bornite and covellite. Hence argentite would be expected to act as the cathode in the anodic dissolution of both chalcopyrite and bornite, as well as covellite. The latter observation is important not only in the dissolution of the mixed sulphide material but also in the dissolution of pure stromeyerite. After the first stage of dissolution stromeyerite forms an intimate mixture of covellite and silver sulphide. From the electrochemical

considerations the dissolution of covellite will be favoured. The results in section 5.1 show that this was the case, the reaction, however, being slowed down by the residual silver sulphide.

Hence the accelerated dissolution rate of the mixed sulphide material could also be explained by electrochemical (galvanic) interactions between the separate sulphides. The fact that X-ray diffraction and microscopic examinations showed that chalcopyrite and $Ag_2S$ remain in the residues, when virtually all the bornite has dissolved, is consistent with both the electrochemical and the mineralogical considerations. Since in both cases it is the bornite dissolution that is enhanced.

However the experimental results presented in Figure 61 showed that the copper dissolution from a mixture with the same relative proportions ions of the three minerals was less than that from the mixed sulphide material and also less than that predicted from the dissolution characteristics of the three individual sulphides. The difference between the mixture and the mixed sulphide material could be explained by

the electrochemical or mineralogical factors discussed above. However the difference with the predicted dissolution rate can only be explained by chemical or electrochemical factors.

Figures 62 and 63 showed that copper dissolution from the bornite-chalcopyrite and bornite-stromeyerite mixtures is inhibited in some way. With sintered discs, Dutrizac et al found that with chalcopyrite containing bornite as an impurity, the mixtures appeared to dissolve slightly more rapidly than the weighted sum of the dissolution rates of the pure sulphides,[123] in accordance with the electrochemical considerations discussed above, but that additions of chalcopyrite to bornite slightly decreased the dissolution rates of the bornite-chalcopyrite mixtures,[122] in accordance with the present work. However this latter effect was thought by Dutrizac et al to be due to the rate-controlling step of bornite dissolution still being mass transport across a liquid boundary layer adjacent to the disc. This is not the case in the present work.

X-ray analysis and microscopic examination showed that the separate sulphides still

dissolved by the same mechanisms and no new phases were noted that could affect the dissolution rate. Hence it seems unlikely that purely chemical effects cause the decrease in dissolution rate but that electrochemical effects are the major factor.

The use of mixtures of separate particles of the different minerals means that good electrical contact is not possible since the particles touch at only a few contact points which are frequently broken by agitation of the solution. Despite this, many authors have explained the changes occurring in dissolution rates on the addition of a separate component (sulphide or non-sulphide) as due to electrochemical phenomena (section 1.3).

The work of Baur et al[108] is of special interest in the present discussion since it shows that the presence of the much more noble silver did not affect the copper dissolution from chalcopyrite. This was thought to be due to the $Ag/CuFeS_2$ couple not increasing the anodic voltage sufficiently to alter the rate-controlling process. This work also shows that additions of a less noble nature than chalcopyrite, such as copper and iron powders, can

markedly affect the dissolution rate of the copper by altering the process from an anodic to a cathodic mechanism of dissolution.

Thus it seems that the lower dissolution rates of the mixture of pure minerals could be explained by electrochemical effects. This leads one to conclude that the electrochemical effects on the mixed sulphide material, if any do occur, would inhibit rather than accelerate the dissolution of copper. Therefore it seems that the major factor in accelerating the dissolution of copper from the mixed sulphide material is of a mineralogical nature.

The other important result from the leaching of this mixed sulphide material was the marked effect that chloride ion had on the dissolution of silver (section 6.1.5). Figure 56 clearly demonstrates that in the NaCl concentration range considered (1 to 4.4M), the complex formed between silver and chloride ion, which thus enhances the dissolution of silver, is of the form $AgCl_3^{2-}$ and the dissolution is expressed by equation 6.1.5. The value for the stability constant ($\log k = 4.12$) is in good agreement with other values[63].

The presence of silver as the complex $AgCl_3^{2-}$ in the leach solutions seems to be in good agreement with previous work, fully reviewed in section 1.1.3. Forbes[66] stated that it was the stable species below 1.5N $Cl^-$, while Garret[71] demonstrated by the same graphical method used in section 6.1.5 that it was the dominant species up to concentrations of 0.9 Moles of KCl per 1000 gms of water. Leden[74] stated that in a solution of 5M NaCl about 1/3 or $\frac{1}{2}$ of the silver is present as $AgCl_4^{3-}$, the rest is $AgCl_3^{2-}$, while in 1M NaCl 80 - 90% is $AgCl_3^{2-}$.

Leiser[76] thought that $AgCl_3^{2-}$ was the dominant species above 0.2M NaCl and Marcus[78] determined that it was the predominant species in the range 0.002-12M HCl. However Chateau and Hervier[77] found no evidence for the species in 0.5 to 1.5M KCl solutions and explained their data in terms of coexisting $AgCl_2^-$ and $AgCl_4^{3-}$ complexes. Finally, Ciantelli[81] plotted the concentration of the species against $Cl^-$ concentration, Figure 4(a), which showed that $AgCl_3^{2-}$ is the dominant complex from 0.5 to 4M NaCl. This is in excellent agreement with the present findings.

Despite this increased solubility in chloride solutions, the dissolution of the silver from the mixed sulphide material by the ferric sulphate solutions was still very small. From the results in sections 3.1, 5.1 and 6.1, it seems that although a temperature rise increased the silver dissolved in the initial stages and an increase in the $Fe^{3+}$ concentration increased the rate of the later stages of dissolution, the major factors affecting the silver dissolution were sample weight and particle size. Decreasing the sample weight or increasing the particle size increased the amount of silver dissolved. Both of these changes result in a smaller copper dissolution, and a smaller $Fe^{2+}$ production. Since the silver dissolution was still very small in the absence of $Fe^{2+}$ ion (section 5.1.7 and 5.1.8) it is suggested that it is the presence of cupric ion in the solution that inhibits the silver dissolution. This would be consistent with electrochemical considerations with the more noble constituent, silver, acting as the cathode for the less noble constituent, copper, which anodically dissolves.

The increase in the silver dissolution

with chloride solutions is in agreement with the findings of many other workers on the dissolution of silver from ores and concentrates [8,9,14,15,24] (section 1.1.1). Christensen[26], Oldright[32] and Traill et al[33] were among the early workers who used NaCl in $Fe^{3+}$ ion solutions to dissolve silver. Azerbaeva and Tseft[42] showed that almost complete dissolution of $Ag_2S$ in $Fe^{3+}$ -$Fe^{2+}$ solutions only occurred in the presence of sodium or ammonium chloride due to the increased solubility of the AgCl formed on the surface. The presence of AgCl in the leach residues of the mixed sulphide material seems to indicate a similar reason for the increased silver dissolution.

SECTION 7

## SUMMARY OF RESULTS

### 7.1. Silver-doped Bornite.

The presence of 1.20 wt. % silver as an isomorphous constituent had little effect on the dissolution characteristics of bornite in acidified ferric sulphate solutions. The leaching of the bornite proceeded in two stages. In the first part of the reaction, bornite ($Cu_5FeS_4$) is rapidly transformed to idaite ($Cu_3FeS_4$), by the diffusion of copper ions in the solid state. Very little of the silver dissolved, the bulk remaining as an isomorphous constituent of the idaite. During the second part of the reaction the surface of the idaite formed is increasingly attacked, producing a direct transformation to elemental sulphur by a chemical reaction. Again very little of the silver dissolved, the idaite becoming silver-rich. The presence of the silver caused some lattice distortion as evidenced by the broad X-ray diffraction lines. No phases other than idaite or elemental sulphur were detected.

### 7.2 Stromeyerite

Stromeyerite ($Cu_{1.07}Ag_{0.93}S$) dissolved in acidified ferric sulphate solutions in two distinct stages. In the first stage copper dissolved from the stromeyerite which underwent a solid-state transformation via the phases $Ag_{1.2}Cu_{0.8}S$ and $Ag_{1.55}Cu_{0.45}S$ to form silver sulphide, $Ag_2S$. During this transformation, covellite, CuS, was precipitated along certain crystallographic planes and at

the completion of the first stage of the copper dissolution the solid consisted of an intimate mixture of $Ag_2S$ and CuS, with 50% of the copper dissolved. The second stage of the copper dissolution, the transformation of CuS via the non-stoichiometric phase $Cu_{0.8}S$ to form elemental sulphur by a chemical reaction, was extremely slow and seemed to be inhibited by the silver sulphide which did not dissolve.

The dissolution mechanism of the stromeyerite was unaltered when solutions containing hydrogen peroxide and a suspension of manganese dioxide were used. These studies indicated that the lack of silver dissolution was due not only to the adverse ferric/ferrous ratio in the solutions but also the presence of cupric ion. The presence of chloride ion enhanced the silver dissolution, but the formation of a silver chloride precipitate stopped the reaction.

7.3. Mixed Sulphide Material

Copper dissolved from the mixed sulphide material, containing approximately 70% bornite, 10% α-chalcopyrite and 20% stromeyerite, much faster than was theoretically predicted and much faster than from a mixture of separate particles of the three minerals. The dissolution mechanisms of each of the three sulphides were unaltered by the presence of the other sulphides, and the increased dissolution rate of the copper could be explained by both electrochemical and mineralogical factors. Very little silver dissolved in the acidified ferric sulphate solutions but considerable amounts dissolved at high chloride ion concentrations. Experiments showed that this was due to the formation of a complex ion, $AgCl_3^{2-}$.

ACKNOWLEDGEMENTS.

The author wishes to express his gratitude to Dr. A.R. Burkin for his advice, encouragement and supervision during the course of the research work and in the production of this thesis. The author also wishes to thank Dr. A.J. Monhemius for his initial encouragement and supervision during the first year of the research work.

The author is indebted to numerous staff and postgraduate students within the Metallurgy department, especially those of the Hydrometallurgy group, for their advice and assistance. In particular the author would like to thank Mr. J. Burgess for his practical advice, Mr. C. Monk for the electron probe microanalyses, and the Photographic section for the reproduction of the photographs. Special thanks are due to Mrs. V. Northover Smith for her fast and efficient typing.

Acknowledgement is due to the Science Research Council for their financial assistance over the last three yaars.

Thanks are also due to many friends and acquaintances of the author for their interest and companionship during the period of this work. Above all, the author wishes to express thanks to members of his family, especially his mother and father, for their interest and consideration throughout the three years of this work.

MICHAEL JAMES SHERIDAN.
ROYAL SCHOOL OF MINES
LONDON, S.W.7.

# APPENDIX A

## EXPERIMENTAL RESULTS FROM THE LEACHING RUNS

## A-1 : Silver-doped Bornite Leaching Results

### TABLE A-1.1

Sample weight : 1 gram
Sample size : -180 +125 microns
Stirring speed : 1300 rpm
Temperature : 60°C
Solution : 0.065M $Fe^{3+}$ in $H_2SO_4$ ( pH 1 )

| Time | wt.% Cu | wt.% Ag |
|---|---|---|
| 5mins. | 22.72 | 0.21 |
| 10 " | 24.02 | 0.67 |
| 15 " | 25.32 | 0.94 |
| 30 " | 28.23 | 0.92 |
| 1 hour | 31.29 | 0.69 |
| 2 " | 34.41 | 0.66 |
| 3 " | 38.55 | 0.43 |
| 4 " | 41.66 | 0.31 |
| 6 " | 46.74 | 0.27 |
| 8 " | 52.88 | 0.42 |

### TABLE A-1.2

1 gram
-180 +125 microns
1300 rpm
90°C
0.065M $Fe^{3+}$ in $H_2SO_4$ ( pH 1 )

| wt.% Cu | wt.% Ag |
|---|---|
| 25.64 | 5.03 |
| 29.73 | 2.76 |
| 32.70 | 2.32 |
| 37.00 | 1.30 |
| 45.22 | 1.20 |
| 50.75 | 2.14 |
| 52.56 | 2.86 |
| 55.98 | 3.54 |
| 60.42 | 3.81 |
| 64.29 | 4.51 |

### TABLE A-1.3

Sample weight : 1 gram
Sample size : -180 +125 microns
Stirring speed : 1300 rpm
Temperature : 60°C
Solution : 0.01M $Fe^{3+}$ in $H_2SO_4$ ( pH 1 )

| Time | wt.% Cu | wt.% Ag |
|---|---|---|
| 5 mins. | 6.40 | 0.23 |
| 10 " | 8.48 | 0.16 |
| 15 " | 9.48 | 0.20 |
| 30 " | 11.95 | 0.24 |
| 1 hour | 12.87 | 0.21 |
| 2 " | 14.77 | 0.18 |
| 3 " | 15.11 | 0.22 |
| 4 " | 15.61 | 0.23 |
| 6 " | 18.03 | 0.27 |
| 8 " | 20.99 | 0.28 |
| 21.5 " | 30.88 | 0.20 |
| 23 " | - | - |
| 24 " | 32.38 | 0.20 |
| 28 " | 35.97 | 0.21 |
| 30 " | 36.28 | 0.18 |
| 46 " | 42.33 | 0.22 |
| 48 " | - | - |
| 52 " | - | - |

### TABLE A-1.4

1 gram
-180 +125 microns
1300 rpm
60°C
0.25M $Fe^{3+}$ in $H_2SO_4$ ( pH 1 )

| wt.% Cu | wt.% Ag |
|---|---|
| 22.42 | 0.98 |
| 23.87 | 1.49 |
| 24.46 | 1.57 |
| 26.96 | 1.19 |
| 29.51 | 0.81 |
| 34.03 | 0.78 |
| 37.84 | 0.94 |
| 39.81 | 1.16 |
| 47.08 | 1.36 |
| 53.40 | 1.67 |
| - | - |
| 87.65 | 4.32 |
| 89.35 | 4.42 |
| 91.32 | 4.76 |
| 92.68 | 4.90 |
| - | - |
| 97.20 | - |
| 98.44 | 4.97 |

TABLE A-1.5

| | |
|---|---|
| Sample weight | 1 gram |
| Sample size | -180 +125 microns |
| Stirring speed | 1300 rpm |
| Temperature | 60°C |
| Solution | 0.065M $Fe^{3+}$ in $H_2SO_4$ (pH 1) |

| Time | wt.% Cu | wt.%Ag |
|---|---|---|
| 5 mins. | 22.72 | 0.21 |
| 10 " | 24.02 | 0.67 |
| 15 " | 25.32 | 0.94 |
| 30 " | 28.23 | 0.92 |
| 1 hour | 31.29 | 0.69 |
| 2 " | 34.41 | 0.66 |
| 3 " | 38.55 | 0.43 |
| 4 " | 41.66 | 0.31 |
| 6 " | 46.74 | 0.27 |
| 8 " | 52.88 | 0.42 |
| 23 " | 82.21 | 0.94 |
| 24 " | - | - |
| 28 " | 86.83 | 0.96 |
| 30 " | - | - |
| 46 " | 93.71 | 1.14 |
| 51 " | 96.26 | 1.34 |

TABLE A-1.6

| | |
|---|---|
| | 0.5 grams |
| | -180 +125 microns |
| | 1300 rpm |
| | 60°C |
| | 0.065M $Fe^{3+}$ in $H_2SO_4$ ( pH 1 ) |

| wt.% Cu | wt.% Ag |
|---|---|
| 20.66 | 0.40 |
| 24.80 | 1.21 |
| 25.68 | 1.34 |
| 27.12 | 1.01 |
| 29.60 | 0.63 |
| 33.11 | 0.51 |
| 35.89 | 0.49 |
| 38.73 | 0.26 |
| 44.57 | 0.27 |
| 51.31 | 0.50 |
| 87.75 | 2.62 |
| 87.76 | 2.75 |
| 91.89 | 2.98 |
| 93.91 | 3.48 |
| - | - |
| - | - |

## A-2 : Stromeyerite Leaching Results

TABLE A-2.1

| | |
|---|---|
| Sample weight | 0.5 grams |
| Sample size | -180 +125 microns |
| Temperature | 60°C |
| Stirring speed | 1000 rpm |
| Solution | 0.065M $Fe^{3+}$ in $H_2SO_4$ ( pH 1 ) |

| Time | wt.% Cu | wt.% Ag | wt. Ag (gms. x$10^6$) |
|---|---|---|---|
| 5 mins. | 25.55 | 0.065 | 164 |
| 10 " | 35.79 | 0.134 | 336.1 |
| 15 " | 40.95 | 0.158 | 394.1 |
| 30 " | 47.75 | 0.137 | 341.9 |
| 1 hour | 52.23 | 0.065 | 161.9 |
| 1.5 " | 53.30 | 0.063 | 155.2 |
| 2 " | 53.62 | 0.048 | 120.3 |
| 3 " | 54.47 | 0.043 | 108.0 |
| 3.5 " | 55.70 | 0.041 | 102.4 |
| 4 " | 55.92 | 0.044 | 110.0 |
| 4.5 " | 56.03 | 0.041 | 101.7 |
| 5 " | 57.19 | 0.045 | 113.2 |
| 6 " | 58.06 | 0.046 | 115.0 |
| 7 " | 58.32 | 0.044 | 110.7 |
| 8 " | 58.56 | 0.047 | 118.3 |
| 9 " | 59.38 | 0.048 | 120.1 |

TABLE A-2.2

Sample weight : 0.5 grams
Sample size : -180 +125 microns
Stirring speed : 1300 rpm
Temperature : 30°C
Solution : 0.1M $Fe^{3+}$ in $H_2SO_4$ (pH 1)

| Time | wt.% Cu | wt. Ag ($g.x10^6$) |
|---|---|---|
| 5 mins. | 5.44 | 32 |
| 10 " | 10.44 | 26.8 |
| 15 " | 12.17 | 37.4 |
| 30 " | 18.06 | 38.3 |
| 1 hour | 26.15 | 45.2 |
| 1.5 " | 32.96 | 46.3 |
| 2 " | 38.16 | 47.3 |
| 2.5 " | 39.64 | 54.4 |
| 3 " | 41.72 | 55.6 |
| 3.5 " | 43.54 | 62.8 |
| 4 " | - | - |
| 4.5 " | - | - |
| 5 " | - | - |

TABLE A-2.3

0.5 grams
-180 +125 microns
1300 rpm
40°C
0.1M $Fe^{3+}$ in $H_2SO_4$ (pH 1)

| wt.% Cu | wt.Ag ($gx10^6$) |
|---|---|
| 9.04 | - |
| 13.03 | - |
| 18.33 | - |
| 29.32 | - |
| 40.89 | - |
| 42.92 | - |
| 45.89 | - |
| 47.85 | - |
| 49.83 | - |
| 50.33 | - |
| 52.02 | - |
| 53.72 | - |
| 54.25 | - |

Final solution contained 0.000064 gms Ag (0.026 wt.%)

TABLE A-2.4

Sample weight : 0.5 grams
Sample size : -180 +125 microns
Stirring speed : 1300 rpm
Temperature : 50°C
Solution : 0.1M $Fe^{3+}$ in $H_2SO_4$ (pH 1)

| Time | wt.% Cu | wt.Ag ($g.x10^6$) |
|---|---|---|
| 5 mins. | 14.96 | - |
| 10 " | 24.81 | - |
| 15 " | 32.52 | - |
| 30 " | 41.63 | - |
| 1 hour | 49.26 | - |
| 1.5 " | 50.89 | - |
| 2 " | 52.68 | - |
| 2.5 " | 54.02 | - |
| 3 " | 54.59 | - |
| 3.5 " | 55.31 | - |

Final solution contained 0.000093 gms Ag (0.038 wt.%)

TABLE A-2.5

0.5 grams
-180 + 125 microns
1300 rpm
70°C
0.1M $Fe^{3+}$ in $H_2SO_4$ (pH 1)

| wt.% Cu | wt.Ag ($g.x10^6$) |
|---|---|
| 33.88 | 562 |
| 44.01 | 568 |
| 47.01 | 537 |
| 49.61 | 530 |
| 52.24 | 550 |
| 52.68 | 445 |
| 53.54 | 386 |
| 53.21 | 358 |
| 54.62 | 339 |
| 54.27 | 319 |

TABLE A-2.6

Sample weight : 0.5 grams
Sample size : -180 +125 microns
Stirring speed : 1300 rpm
Temperature : 60°C
Solution : 0.1M $Fe^{3+}$ in $H_2SO_4$ (pH 1)

| Time | wt.% Cu | wt.Ag ($g.x10^6$) |
|---|---|---|
| 5 mins. | 23.04 | 196 |
| 10 " | 33.37 | 478 |
| 15 " | 40.12 | 518 |
| 30 " | 47.48 | 391 |
| 1 hour | 52.45 | 252 |
| 1.5 " | 53.03 | 217 |
| 2 " | 53.60 | 200 |
| 2.5 " | 54.47 | 191 |
| 3 " | 55.61 | 195 |
| 3.5 " | 55.24 | 194 |
| 4 " | 56.06 | 198 |

TABLE A-2.7

0.5 grams
-180 +125 microns
1300 rpm
90°C
0.1M $Fe^{3+}$ in $H_2SO_4$ (pH 1)

| wt.% Cu | wt.Ag ($g.x10^6$) |
|---|---|
| 45.09 | 218 |
| 51.53 | 247 |
| 53.08 | 281 |
| 54.05 | 304 |
| 54.66 | 323 |
| 55.23 | 298 |
| 55.13 | 335 |
| 55.44 | 342 |
| 56.32 | 340 |
| 56.59 | 347 |
| 57.15 | 354 |

TABLE A-2.8

Sample weight : 0.5 grams
Sample size : -180 +125 microns
Temperature : 60°C
Stirring speed : 1300 rpm
Solution : $H_2SO_4$ (pH 1)

| Time | wt.% Cu | wt.Ag ($g.x10^6$) |
|---|---|---|
| 5 mins | 0.004 | - |
| 10 " | 0.004 | - |
| 15 " | 0.009 | - |
| 30 " | 0.019 | - |
| 1 hour | 0.029 | - |
| 1.5 " | 0.051 | - |
| 2 " | 0.082 | - |
| 2.5 " | - | - |
| 3 " | - | - |
| 3.5 " | 0.103 | - |
| 4 " | - | - |

TABLE A-2.9

0.5 grams
-180 +125 microns
60°C
1300 rpm
0.01M $Fe^{3+}$ in $H_2SO_4$ (pH 1)

| wt.% Cu | wt.Ag ($g.x10^6$) |
|---|---|
| 11.77 | 22 |
| 19.87 | 22.5 |
| 26.39 | 23 |
| 35.57 | 17.5 |
| 41.72 | 15.9 |
| 44.47 | 18.3 |
| 48.45 | 18.7 |
| 49.70 | 19.1 |
| 50.98 | 19.5 |
| - | - |
| 52.65 | 35.9 |

TABLE A-2.10

Sample weight : 0.5 grams
Sample size : -180 +125 microns
Stirring speed : 1300 rpm
Temperature : 60°C
Solution : 0.065M $Fe^{3+}$ in $H_2SO_4$ (pH 1)

| Time | wt.% Cu | wt.Ag ($g.x10^6$) |
|---|---|---|
| 5 mins. | 20.52 | 132 |
| 10 " | 31.22 | 227 |
| 15 " | 39.22 | 272 |
| 30 " | 47.55 | 269 |
| 1 hour | 53.41 | 245 |
| 1.5 " | - | - |
| 2 " | 54.21 | 211 |
| 2.5 " | 55.31 | 184 |
| 3 " | 54.47 | 177 |
| 3.5 " | 54.33 | 161 |
| 4 " | 54.55 | 160 |

TABLE A-2.11

0.5 grams
-180 +125 microns
1300 rpm
60°C
0.25M $Fe^{3+}$ in $H_2SO_4$ (pH 1)

| wt.% Cu | wt.Ag ($g.x10^6$) |
|---|---|
| 22.98 | 320 |
| 32.40 | 398 |
| 37.32 | 497 |
| 48.83 | 419 |
| 51.22 | 189 |
| 53.59 | 133 |
| 53.63 | 135 |
| 54.83 | 147 |
| 54.84 | 155 |
| 54.83 | 167 |
| 55.37 | 170 |

TABLE A-2.12

Sample weight : 0.5 grams
Sample size : -40 +50 mesh
Stirring speed : 1300 rpm
Temperature : 60°C
Solution : 0.01M $Fe^{3+}$ in $H_2SO_4$ (pH 1)

| Time | wt.% Cu | wt.Ag ($g.x10^6$) |
|---|---|---|
| 5 mins. | 6.80 | 18 |
| 10 " | 12.12 | 16 |
| 15 " | 16.35 | 19 |
| 30 " | 25.53 | 19 |
| 1 hour | 35.23 | 14 |
| 1.5 " | 38.80 | 18 |
| 2 " | 41.68 | 14 |
| 2.5 " | 44.92 | 18 |
| 3 " | 45.93 | 19 |
| 3.5 " | 46.95 | 19 |
| 4 " | 47.37 | 20 |

TABLE A-2.13

0.1 grams
-180 +125 microns
1300 rpm
60°C
0.1M $Fe^{3+}$ in $H_2SO_4$ (pH 1)

| wt.% Cu | wt.Ag ($g.x10^6$) |
|---|---|
| 27.53 | 152 |
| 36.89 | 256 |
| 42.95 | 292 |
| 48.69 | 229 |
| 52.48 | 92 |
| 55.07 | 84 |
| 56.29 | 89 |
| 57.68 | 99 |
| 58.35 | 121 |
| 59.30 | 131 |
| 59.94 | 137 |

TABLE A-2.14

Sample weight : 0.5 grams
Sample size : -180 +125 microns
Stirring speed : 1300 rpm
Temperature : 60°C
Solution : 0.1M $Fe^{3+}$ in HCl (0.1M) containing 4M NaCl

| Time | wt.% Cu | wt.% Ag |
|---|---|---|
| 5 mins. | 11.44 | 18.92 |
| 10 " | 14.09 | 21.27 |
| 15 " | 16.21 | 21.30 |
| 30 " | 20.25 | 21.81 |
| 1 hour | 21.97 | 22.56 |
| 1.5 " | 22.48 | 22.67 |
| 2 " | 23.64 | 23.18 |
| 2.5 " | 23.70 | 23.20 |
| 3 " | 24.50 | 24.73 |
| 3.5 " | 25.35 | 24.21 |
| 4 " | 25.17 | 25.58 |

TABLE A-2.15

0.5 grams
-180 +125 microns
1300 rpm
60°C
0.1M HCl containing 3.3M NaCl

| wt.% Cu | wt.% Ag |
|---|---|
| 0.194 | 0.130 |
| 0.228 | 0.147 |
| 0.340 | 0.184 |
| 0.507 | 0.268 |
| 1.680 | 1.370 |
| - | - |
| 7.84 | 6.36 |
| - | - |
| 23.00 | 10.27 |
| - | - |
| 23.40 | 11.24 |

TABLE A-2.16

Sample weight : 0.5 grams
Sample size : -180 +125 microns
Stirring speed : 1300 rpm
Temperature : 60°C
Solution : 1 part $H_2O_2$ (20 vol.) to 4 parts $H_2SO_4$ (pH 1)

| Time | wt.% Cu | wt.Ag ($g.x10^6$) |
|---|---|---|
| 5 mins. | 7.92 | 10 |
| 10 " | 18.43 | 14 |
| 15 " | 28.47 | 18 |
| 30 " | 42.42 | 15 |
| 1 hour | 50.81 | 15 |
| 1.5 " | 52.90 | 16 |
| 2 " | 55.02 | 9 |
| 2.5 " | 55.39 | 16 |
| 3 " | 55.58 | 16 |
| 3.5 " | 55.76 | 13 |

TABLE A-2.17

0.5 grams
-180 +125 microns
1300 rpm
60°C
1 part $H_2O_2$ (20 vol.) to 4 parts $H_2O$

| wt.% Cu | wt.Ag ($g.x10^6$) |
|---|---|
| - | - |
| 2.83 | 10 |
| 3.12 | 7 |
| 3.42 | 10 |
| 3.37 | 10 |
| 3.36 | 15 |
| 3.40 | 13 |
| - | - |
| 3.20 | 16 |
| - | - |

| | TABLE A-2.18 | TABLE A-2.19 |
|---|---|---|
| Sample weight : | 0.5 grams | 0.5 grams |
| Sample size : | -180 +125 microns | -180 +125 microns |
| Stirring speed : | 1300 rpm | 1300 rpm |
| Temperature : | 60°C | 60°C |
| Solution : | $H_2SO_4$ (pH 1) containing 0.3205 grams $MnO_2$ | 0.1M $Fe^{3+}$ in $H_2SO_4$ (pH 1) containing 0.3205 gms $MnO_2$ |

| Time | wt. % Cu | wt.Ag | wt.% Cu | wt. Ag($g.x10^6$) |
|---|---|---|---|---|
| 5 mins. | 0.30 | - | 27.65 | 226 |
| 10 " | 0.41 | - | 34.02 | 313 |
| 15 " | 0.49 | - | 39.64 | 179 |
| 30 " | 0.88 | - | 47.50 | 149 |
| 1 hour | 2.56 | - | 50.98 | 120 |
| 1.5 " | 3.65 | - | 52.75 | 103 |
| 2 " | 5.38 | - | 53.06 | 91 |
| 2.5 " | 6.72 | - | 53.64 | 110 |
| 3 " | 8.50 | - | - | - |
| 3.5 " | 9.76 | - | - | - |
| 4 " | 10.70 | - | - | - |

Data for Figure 43(b) :

| | Moles x $10^3$ | | Moles x $10^3$ | |
|---|---|---|---|---|
| Time | Cu | Mn | Cu | Mn |
| 5 mins. | 0.008 | 0.069 | 0.818 | 0.942 |
| 10 mins. | 0.011 | 0.092 | 0.988 | 1.143 |
| 15 " | 0.013 | 0.101 | 1.138 | 1.289 |
| 30 " | 0.023 | 0.086 | 1.268 | 1.470 |
| 1 hour | 0.068 | 0.136 | 1.361 | 1.564 |
| 1.5 " | - | - | 1.408 | 1.600 |
| 2 " | 0.144 | 0.245 | 1.416 | 1.632 |
| 2.5 " | - | - | 1.432 | 1.623 |
| 3 " | 0.227 | 0.371 | - | - |
| 4 " | - | - | - | - |
| 5 " | 0.349 | 0.560 | - | - |

Data for Figure 36: TABLE A-2.20

| | | % Copper Dissolved | | | | | | | | | |
|---|---|---|---|---|---|---|---|---|---|---|---|
| | | 20% | | 30% | | 40% | | 45% | | 50% | |
| °C | $1/T^{\circ}K \times 10^{3}$ | Time | Log(1/t) | Time | Log(1/t) | Time | Log(1/t) | Time | Log(1/t) | Time | Log(1/t) |
| 30 | 3.300 | 34.5 | -1.5378 | 73.5 | -1.8663 | 147 | -2.1673 | - | - | - | - |
| 40 | 3.195 | 17.0 | -1.2304 | 30.0 | -1.4771 | 58.5 | -1.7672 | 112.5 | -2.0511 | 187.5 | -2.2730 |
| 50 | 3.096 | 7.5 | -1.8751 | 13.5 | -1.1303 | 27.0 | -1.4314 | 40.5 | -1.6075 | 70.5 | -1.8482 |
| 60 | 3.003 | 4.5 | -0.6532 | 7.5 | -0.8751 | 15.0 | -1.1761 | 24.0 | -1.3802 | 51.0 | -1.7076 |
| 70 | 2.915 | - | - | 4.5 | -0.6532 | 7.5 | -0.8751 | 10.5 | -1.0212 | 30.0 | -1.4771 |
| 90 | 2.755 | - | - | 3.0 | -0.4771 | 4.5 | -0.6532 | 5.0 | -0.6990 | 7.5 | -0.8751 |

## A-3 : Mixed sulphide material Leaching Results

### TABLE A-3.1

Sample weight : 0.5 grams
Sample size : -180 +125 microns
Temperature : 60°C
Stirring speed : 1300 rpm
Solution : 0.065M $Fe^{3+}$ in $H_2SO_4$ (pH 1)

| Time | wt.% Cu | wt.% Ag |
|---|---|---|
| 5 mins | 23.04 | 0.39 |
| 10 " | 25.73 | 0.91 |
| 15 " | 28.93 | 1.09 |
| 30 " | 31.54 | 1.07 |
| 1 hour | 34.03 | 0.73 |
| 2 " | 39.86 | 0.45 |
| 3 " | 43.80 | 0.39 |
| 4 " | 48.56 | 0.38 |
| 6 " | 58.72 | 0.26 |
| 8 " | 64.81 | 0.24 |
| 22 " | 81.18 | 0.43 |
| 25 " | 82.98 | 0.47 |
| 28 " | 83.61 | 0.56 |
| 30 " | 85.01 | 0.57 |
| 46 " | 89.04 | 0.79 |
| 50 " | 91.01 | 0.90 |
| 53 " | 90.19 | 0.98 |
| 56 " | 90.93 | 1.00 |

### TABLE A-3.2

Sample weight : 0.5 grams
Sample size : -180 +125 microns
Temperature : 90°C
Stirring speed : 1300 rpm
Solution : 0.065M $Fe^{3+}$ in $H_2SO_4$ (pH 1)

| Time | wt.% Cu | wt.% Ag |
|---|---|---|
| 5 mins. | 27.15 | 4.45 |
| 10 " | 31.68 | 5.45 |
| 15 " | 35.21 | 5.06 |
| 30 " | 41.93 | 4.12 |
| 1 hour | 48.61 | 3.64 |
| 2 " | 55.06 | 2.93 |
| 3 " | 58.35 | 2.47 |
| 4 " | 61.32 | 2.26 |
| 5 " | 62.85 | 2.11 |
| 6 " | 64.04 | 2.07 |
| 7 " | 65.21 | 1.97 |
| 8 " | - | - |
| 21 " | 78.19 | 1.94 |
| 21.5" | - | - |
| 24 " | 82.03 | 2.08 |
| 26 " | 83.73 | 2.22 |
| 28 " | 85.44 | 2.36 |

### TABLE A-3.3

0.5 grams
-180 +125microns
30°C
1300 rpm
0.065M $Fe^{3+}$ in $H_2SO_4$ (pH 1)

| wt.% Cu | wt.% Ag |
|---|---|
| 14.63 | 0.038 |
| 20.32 | 0.087 |
| 24.12 | 0.109 |
| 26.53 | 0.121 |
| 29.00 | 0.187 |
| 30.04 | 0.188 |
| 30.72 | 0.196 |
| 31.40 | 0.166 |
| 32.08 | 0.218 |
| 33.13 | 0.223 |
| 33.82 | 0.228 |
| 34.11 | 0.262 |
| - | - |
| 37.77 | 0.286 |
| 38.16 | 0.273 |
| 38.54 | 0.278 |
| 38.91 | 0.313 |

TABLE A-3.4

Sample weight : 0.5 grams
Sample size : -180 + 125microns
Temperature : 60°C
Stirring speed : 1300 rpm
Solution : 0.01M $Fe^{3+}$ in $H_2SO_4$ (pH 1)

| Time | wt.% Cu | wt.% Ag |
|---|---|---|
| 5 mins. | 9.64 | 0.021 |
| 10 " | 16.67 | 0.035 |
| 15 " | 19.65 | 0.036 |
| 30 " | 21.41 | 0.058 |
| 1 hour | 24.67 | 0.046 |
| 2 " | 25.69 | 0.055 |
| 3 " | 27.09 | 0.065 |
| 4 " | 27.88 | 0.083 |
| 5 " | 30.44 | 0.085 |
| 6 " | 30.72 | 0.095 |
| 7 " | 31.28 | 0.089 |
| 8 " | 32.77 | 0.090 |
| 21.5 " | 45.81 | 0.066 |
| 22.0 " | - | - |
| 24.0 " | 48.25 | 0.063 |
| 26.0 " | 49.45 | 0.072 |
| 28.0 " | 51.39 | 0.073 |
| 30.0 " | - | - |

TABLE A-3.5

0.5 grams
-180 +125 microns
60°C
1300 rpm
0.10M $Fe^{3+}$ in $H_2SO_4$ (pH 1)

| wt.% Cu | wt.% Ag |
|---|---|
| 23.30 | 0.41 |
| 27.01 | 0.96 |
| 29.50 | 1.09 |
| 33.88 | 0.89 |
| 39.45 | 0.53 |
| 49.73 | 0.39 |
| 57.70 | 0.39 |
| 65.00 | 0.36 |
| 70.57 | 0.38 |
| 76.35 | 0.46 |
| 81.21 | 0.45 |
| 86.83 | 0.51 |
| - | - |
| 97.85 | 1.93 |
| 98.09 | 2.18 |
| 97.11 | 2.30 |
| 98.03 | 2.55 |
| 98.86 | 2.74 |

TABLE A-3.6

Sample weight : 0.5 grams
Sample size : -180 +125 microns
Temperature : 60°C
Stirring speed : 1300 rpm
Solution : 0.25M $Fe^{3+}$ in $H_2SO_4$ (pH 1)

| Time | wt.% Cu | wt.% Ag |
|---|---|---|
| 5 mins. | 24.85 | 0.81 |
| 10 " | 27.85 | 1.36 |
| 15 " | 30.92 | 1.51 |
| 30 " | 35.33 | 1.19 |
| 1 hour | 41.78 | 0.66 |
| 2 " | 51.52 | 0.56 |
| 3 " | 58.60 | 0.63 |
| 4 " | 66.61 | 0.61 |
| 5 " | 71.79 | 0.68 |
| 6 " | 79.28 | 0.98 |
| 7 " | 83.93 | 1.37 |
| 8 " | 88.32 | 2.24 |
| 24 " | - | - |
| 26 " | 97.04 | 12.34 |
| 28 " | 97.21 | 12.68 |
| 30 " | 97.52 | 12.72 |

TABLE A-3.7

0.5 grams
-180 +125 microns
60°C
1300 rpm
0.5M $Fe^{3+}$ in $H_2SO_4$ (pH 1)

| wt.% Cu | wt.% Ag |
|---|---|
| 26.99 | 1.31 |
| 31.16 | 1.69 |
| 33.57 | 1.46 |
| 38.59 | 1.03 |
| 45.73 | 0.78 |
| 62.02 | 0.72 |
| 75.20 | 0.88 |
| 83.18 | 1.14 |
| 89.84 | 2.07 |
| 93.32 | 3.47 |
| 95.47 | 4.53 |
| 97.58 | 7.45 |
| - | 13.53 |
| - | 14.05 |
| - | 14.62 |
| - | 15.06 |

TABLE A-3.8

| | |
|---|---|
| Sample weight | 0.5 grams |
| Sample size | -40 +50 mesh |
| Temperature | 60°C |
| Stirring speed | 1300 rpm |
| Solution | 0.1M $Fe^{3+}$ in $H_2SO_4$ (pH 1) |

| Time | wt.% Cu | wt.% Ag |
|---|---|---|
| 5 mins. | 15.19 | 0.36 |
| 10 " | 18.80 | 0.61 |
| 15 " | 20.51 | 1.20 |
| 30 " | 24.01 | 1.51 |
| 1 hour | 26.04 | 1.44 |
| 2 " | 28.70 | 0.98 |
| 3 " | 31.34 | 0.79 |
| 4 " | 32.71 | 0.82 |
| 5 " | 33.72 | 0.96 |
| 6 " | 34.66 | 1.22 |
| 7 " | - | - |
| 8 " | - | - |
| 22 " | - | - |
| 24 " | - | - |
| 26 " | - | - |
| 28 " | - | - |
| 30 " | - | - |

TABLE A-3.9

| | |
|---|---|
| | 1.0 grams |
| | -180 +125 microns |
| | 60°C |
| | 1300 rpm |
| | 0.25M $Fe^{3+}$ in $H_2SO_4$ (pH 1) |

| wt.% Cu | wt.% Ag |
|---|---|
| 24.54 | 0.33 |
| 27.36 | 0.61 |
| 30.78 | 0.70 |
| 34.27 | 0.58 |
| 39.48 | 0.33 |
| 49.75 | 0.26 |
| 61.91 | 0.23 |
| 69.58 | 0.19 |
| 77.76 | 0.24 |
| 83.91 | 0.26 |
| 86.50 | 0.33 |
| 89.11 | 0.38 |
| 96.51 | 1.52 |
| 97.80 | 1.61 |
| 97.98 | 1.72 |
| 98.80 | 1.79 |
| 99.30 | 1.85 |

TABLE A-3.10

| | |
|---|---|
| Sample weight | 0.5 grams |
| Sample size | -180 +125 microns |
| Temperature | 60°C |
| Stirring speed | 1300 rpm |
| Solution | 0.1M $Fe^{3+}$ in $H_2SO_4$ (pH 1) containing 0.1M NaCl |

| Time | wt.% Cu | wt.% Ag |
|---|---|---|
| 5 mins. | 18.64 | 0.268 |
| 10 " | 21.31 | 0.406 |
| 15 " | 22.57 | 0.378 |
| 30 " | 24.58 | 0.483 |
| 1 hour | 29.92 | 0.492 |
| 1.5 " | - | - |
| 2 " | 35.39 | 0.504 |
| 2.5 " | - | - |
| 3 " | 40.24 | 0.490 |
| 3.5 " | - | - |
| 4 " | 44.83 | 0.227 |
| 5 " | 47.67 | 0.434 |
| 6 " | 49.46 | 0.472 |
| 7 " | 52.00 | 0.521 |
| 8 " | 56.41 | 0.579 |

TABLE A-3.11

| | |
|---|---|
| | 0.5 grams |
| | -180 +125 microns |
| | 60°C |
| | 1300 rpm |
| | 0.1M $Fe^{3+}$ (as $FeCl_3$) in HCl (0.1M) |

| wt.% Cu | wt.% Ag |
|---|---|
| 19.99 | 0.571 |
| 23.43 | 0.562 |
| 26.21 | 0.599 |
| 27.76 | 0.621 |
| 30.98 | 0.628 |
| 35.56 | 0.650 |
| 37.47 | 0.649 |
| 41.80 | 0.671 |
| 42.73 | 0.700 |
| 45.31 | 0.700 |
| 48.12 | 0.722 |
| 53.54 | 0.728 |
| 56.69 | 0.742 |
| 59.70 | 0.772 |
| - | - |

TABLE A-3.12

Sample weight : 0.5 grams
Sample size : -180 +125 microns
Stirring speed : 1300 rpm
Temperature : 60°C
Solution : 0.1M $Fe^{3+}$ (as $FeCl_3$) in 0.1M HCl containing 1M NaCl

| Time | wt.% Cu | wt.% Ag |
|---|---|---|
| 5 mins. | 21.78 | 5.87 |
| 10 " | 25.28 | 6.14 |
| 15 " | 27.48 | 6.46 |
| 30 " | 30.49 | 6.82 |
| 1 hour | 37.51 | 7.15 |
| 1.5 " | 41.74 | 7.48 |
| 2 " | 45.85 | 7.44 |
| 2.5 " | 50.62 | 7.64 |
| 3 " | 55.69 | 7.56 |
| 3.5 " | - | - |
| 4 " | 62.24 | 7.96 |
| 4.5 " | - | - |
| 5 " | - | - |
| 5.5 " | - | - |
| 6 " | - | - |

TABLE A-3.13

0.5 grams
-180 +125 microns
1300 rpm
60°C
0.1M $Fe^{3+}$ (as $FeCl_3$) in 0.1M HCl containing 1.5M NaCl

| wt.% Cu | wt.% Ag |
|---|---|
| 20.55 | 11.27 |
| 22.06 | 11.22 |
| 24.38 | 11.83 |
| 28.13 | 12.19 |
| 33.94 | 12.39 |
| 37.91 | 12.42 |
| 41.15 | 12.95 |
| 44.46 | 13.23 |
| 49.61 | 13.52 |
| 54.47 | 13.79 |
| 56.45 | 14.08 |
| 58.45 | 14.86 |
| 60.46 | 14.65 |
| 61.71 | 14.94 |
| 62.15 | 15.55 |

TABLE A-3.14

Sample weight : 0.5 grams
Sample size : -180 +125 microns
Stirring speed : 1300 rpm
Temperature : 60°C
Solution : 0.1M $Fe^{3+}$ (as $FeCl_3$) in 0.1M HCl containing 3M NaCl

| Time | wt.% Cu | wt.% Ag |
|---|---|---|
| 5 mins. | 22.18 | 32.16 |
| 10 " | 25.32 | 41.05 |
| 15 " | 27.79 | 45.01 |
| 30 " | 32.52 | 55.41 |
| 1 hour | 36.24 | 57.50 |
| 1.5 " | 38.57 | 56.82 |
| 2 " | 42.40 | 56.23 |
| 2.5 " | 44.83 | 57.46 |
| 3 " | - | - |
| 3.5 " | 53.77 | 60.56 |
| 4 " | 56.62 | 61.85 |
| 4.5 " | 59.14 | 64.37 |
| 5 " | 64.29 | 64.44 |
| 6 " | 67.13 | 66.97 |
| 7 " | - | - |

TABLE A-3.15

0.5 grams
-180 +125 microns
1300 rpm
60°C
0.1M $Fe^{3+}$ (as $FeCl_3$) in 0.1M HCl containing 4.4CM NaCl

| wt.% Cu | wt.% Ag |
|---|---|
| 23.30 | 27.37 |
| 27.92 | 37.31 |
| 30.25 | 44.01 |
| 35.01 | 53.94 |
| 44.65 | 55.80 |
| 52.48 | 63.08 |
| 58.65 | 64.52 |
| 63.29 | 66.55 |
| 69.67 | 68.01 |
| 74.34 | 73.13 |
| 75.96 | 71.79 |
| - | - |
| 83.82 | 73.85 |
| 87.07 | 75.34 |
| 90.35 | 76.84 |

TABLE A-3.16 : Data for Figure 56; Determination of Silver Chloride complex ion.

| $(Ag)^{*1}$ mg/ml | $(Ag)$ M x$10^4$ | $Log(M_{Ag})$ | $(Cl^-)^{*2}$ M | $Log(M_{Cl^-})$ |
|---|---|---|---|---|
| 0.0157 | 1.455 | $\bar{4}.1629$ $(-3.8371)$ | 1.40 | 0.1461 |
| 0.0270 | 2.510 | $\bar{4}.3997$ $(-3.6003)$ | 1.90 | 0.2788 |
| 0.1330 | 12.320 | $\bar{3}.0908$ $(-2.9092)$ | 3.40 | 0.5315 |
| 0.1550 | 14.370 | $\bar{3}.1574$ $(-2.8426)$ | 4.80 | 0.6812 |

*1 : The maximum silver concentration reached in each of the leach solutions.

*2 : The sum of NaCl molarity + 0.1M HCl + 0.1M $FeCl_3$

A-4 : Mixtures of Pure Minerals, Leaching Results

TABLE A-4.1 : Dissolution rates of the minerals

| Time | Bornite (0.7gms) | | Stromeyerite (0.2gms) | | Chalcopyrite (0.1gms |
|---|---|---|---|---|---|
| | wt.% Cu | wt. Cu mgms | wt.% Cu | wt. Cu mgms | wt.% Cu | wt. Cu mgms |
| 5 mins | (24) | (106.3) | 23.04 | 15.63 | (1.5) | (0.52) |
| 10 " | (26) | (115.2) | 33.37 | 22.64 | (2.6) | (0.90) |
| 15 " | 26.82 | 118.83 | 40.12 | 27.23 | (3.0) | (1.04) |
| 30 " | 28.91 | 128.10 | 47.48 | 32.22 | (4.0) | (1.38) |
| 1 hour | 33.47 | 148.30 | 52.45 | 35.59 | 4.7 | 1.63 |
| 1.5 " | 36.19 | 160.35 | 53.03 | 35.98 | (6.0) | (2.08) |
| 2 " | 37.98 | 168.29 | 53.60 | 36.37 | 6.8 | 2.36 |
| 2.5 " | 39.50 | 175.11 | 54.47 | 36.96 | (7.4) | (2.56) |
| 3 " | 40.98 | 181.67 | 55.16 | 37.43 | 8.0 | 2.77 |
| 3.5 " | 42.65 | 188.98 | 55.24 | 37.49 | (8.6) | (2.98) |
| 4 " | 43.62 | 193.37 | 56.06 | 38.04 | 9.1 | 3.15 |
| 4.5 " | 44.84 | 198.78 | 56.08 | 38.06 | (9.6) | (3.33) |
| 5 " | 45.71 | 202.54 | 57.19 | 38.81 | 9.9 | 3.43 |

( ) = Value estimated from graph.

Bornite values from Ugarte[11], Chalcopyrite values from Ferreira[12], Stromeyerite values from Table A-2.6.

TABLE A-4.2 : Bornite(0.7gms) + Chalcopyrite(0.1gms) + Stromeyerite(0.2gms) mixture

| | TOTAL COPPER DISSOLVED (wt. in milligrams) | | | |
|---|---|---|---|---|
| | Predicted (from Table A-4.1) | | Mixed sulphide material (table A-3.9) | |
| Time | wt. | wt.% | wt. | wt.% |
| 5 mins. | 122.45 | 22.44 | 133.8 | 24.54 |
| 10 " | 138.74 | 25.42 | 149.14 | 27.36 |
| 15 " | 147.10 | 26.95 | 167.79 | 30.78 |
| 30 " | 161.70 | 29.63 | 186.81 | 34.27 |
| 1 hour | 185.52 | 33.99 | 215.20 | 39.48 |
| 1.5 " | 198.41 | 36.35 | - | - |
| 2 " | 207.02 | 37.93 | 270.20 | 49.75 |
| 2.5 " | 214.63 | 39.32 | - | - |
| 3 " | 221.87 | 40.65 | 337.47 | 61.91 |
| 3.5 " | 229.45 | 42.04 | - | - |
| 4 " | 234.56 | 42.97 | 379.24 | 69.58 |
| 4.5 " | 240.17 | 44.00 | - | - |
| 5 " | 244.78 | 44.85 | 423.86 | 77.76 |

TABLE A-4.3

Sample : 0.7gms Bornite + 0.1gms Chalcopyrite + 0.2gms Stromeyerite
Sample size : -180 +125 microns
Stirring speed : 1300 rpm
Temperature : 60°C
Solution : 0.25M $Fe^{3+}$ in $H_2SO_4$ (pH 1)

| | COPPER DISSOLVED | | SILVER DISSOLVED |
|---|---|---|---|
| Time | wt.(mgs) | wt.% | wt. (gms x$10^6$) |
| 5 mins. | 103.40 | 18.94 | 88 |
| 10 " | 110.48 | 20.24 | 98.2 |
| 15 " | 117.18 | 21.46 | 216.6 |
| 30 " | 132.74 | 24.20 | 111.9 |
| 1 hour | 155.41 | 28.47 | 68.5 |
| 1.5 " | 159.52 | 29.22 | 45.8 |
| 2 " | 163.14 | 29.89 | 32.7 |
| 2.5 " | 168.44 | 30.71 | 61.1 |
| 3 " | 172.77 | 31.65 | 77.1 |
| 3.5 " | 177.04 | 32.43 | 90.6 |
| 4.5 " | 179.32 | 32.85 | 106.5 |
| 5 " | 183.07 | 33.54 | 116.7 |

TABLE A-4.4

Sample: ; 0.7gms Bornite + 0.1gms Chalcopyrite
Sample size : -180 +125 microns
Stirring speed : 1300 rpm
Temperature : 60°C
Solution : 0.1M $Fe^{3+}$ in $H_2SO_4$ (pH 1)

COPPER DISSOLVED

| Time | EXPERIMENTAL wt.(mgs) | wt.% | CALCULATED (from Table A-4.1) wt.(mgs) | wt.% |
|---|---|---|---|---|
| 5 mins | 102 | 21.34 | 106.82 | 22.35 |
| 10 " | 106.55 | 22.29 | 116.10 | 24.29 |
| 15 " | 109.65 | 22.94 | 119.87 | 25.08 |
| 30 " | 121.76 | 25.47 | 129.48 | 27.09 |
| 1 hour | 137.58 | 28.78 | 149.93 | 31.37 |
| 1.5 " | 144.68 | 30.27 | 162.43 | 33.98 |
| 2 " | 152.88 | 31.98 | 170.65 | 35.70 |
| 2.5 " | 159.71 | 33.41 | 177.67 | 37.17 |
| 3 " | 165.62 | 34.65 | 184.44 | 38.59 |
| 3.5 " | - | - | 191.96 | 40.16 |
| 4 " | 179.10 | 37.47 | 196.52 | 41.12 |
| 4.5 " | 182.82 | 38.25 | 202.11 | 42.28 |
| 5 " | 187.55 | 39.24 | 205.97 | 43.09 |

TABLE A-4.5

Sample : 0.7gms Bornite + 0.2gms Stromeyerite
Sample size : -180 +125 microns
Stirring speed : 1300 rpm
Temperature : 60°C
Solution : 0.1M $Fe^{3+}$ in $H_2SO_4$ (pH 1)

COPPER DISSOLVED

| Time | EXPERIMENTAL wt.(mgs) | wt.% | CALCULATED (from Table A-4.1) wt.(mgs) | wt.% |
|---|---|---|---|---|
| 5 mins. | 116.5 | 22.76 | 121.97 | 23.86 |
| 10 " | 130.41 | 25.48 | 137.84 | 26.96 |
| 15 " | 133.10 | 26.01 | 146.06 | 28.57 |
| 30 " | 145.27 | 28.39 | 160.32 | 31.36 |
| 1 hour | 166.80 | 32.59 | 183.89 | 35.97 |
| 1.5 " | 173.06 | 33.82 | 196.33 | 38.41 |
| 2 " | 182.88 | 35.74 | 204.66 | 40.04 |
| 2.5 " | 190.86 | 37.29 | 212.07 | 41.49 |
| 3 " | 194.93 | 38.09 | 219.10 | 42.86 |
| 3.5 " | 199.51 | 38.99 | 226.47 | 44.30 |
| 4 " | 211.60 | 41.35 | 231.41 | 45.27 |

# APPENDIX B

## X-RAY POWDER

## DIFFRACTION DATA



Abbreviations used for line intensities :

vst : very strong

st : strong

m : medium

vw : very weak

vvw : very, very weak

sh : shadow (indistinct line)

) : brackets indicate a broad line

I : relative intensity of line

d : 'd' spacings, measured in Ångstroms

B-1 : Silver-doped Bornite, X-ray Data.

TABLE B-1.1 : X-ray patterns for the silver-doped Bornite and pure Bornite, compared with Ugarte's Bornite and the A.S.T.M. X-ray Index File values.

| Synthetic Ag-doped Bornite | | Synthetic Bornite | | Bornite (11) | | Bornite (207) | |
|---|---|---|---|---|---|---|---|
| dÅ | I | dÅ | I | dÅ | I | dÅ | I |
| 6.324 | vw | 6.313 | vw | - | | | |
| 5.471 | vw | 5.475 | vw | | | | |
| 4.786 | vw | 4.788 | vw | | | | |
| 4.072 | w | 4.070 | w | 4.07 | m | 4.08 | 10 |
| 3.870 | vw | 3.862 | vw | - | - | - | - |
| - | - | - | - | - | - | 3.64 | 5 |
| - | - | - | - | - | - | 3.48 | 5 |
| 3.305 | m | 3.300 | m | 3.30 | m | 3.31 | 40 |
| 3.261 | w | 3.261 | w | 3.26 | vw | - | - |
| 3.162 | st | 3.156 | st | 3.16 | vw | 3.18-3.15 | 60 |
| 3.006 | vw | 3.014 | vw | 3.00 | vw | 3.01 | 5 |
| 2.804 | w | 2.804 | m | 2.80 | m | 2.80-2.81 | 20 |
| 2.735 | m | 2.736 | m | 2.73 | m | 2.74-2.73 | 50 |
| 2.628 | vw | 2.633 | vw | 2.63 | vw | 2.63 | 5 |
| 2.511 | m | 2.510 | m | 2.50 | m | 2.50 | 40 |
| 2.496 | m | 2.495 | m | | | | |
| 2.179 | vw | 2.174 | vw | - | - | - | - |
| 2.135 | w | 2.137 | vw | 2.13 | w | 2.13-2.12 | - |
| 2.107 | w | 2.104 | w | 2.10 | vw | 2.11 | 10 |
| 1.959 | vw | 1.957 | vw | - | - | - | - |
| 1.937 | vst | 1.935 | vst | 1.93 | vst | 1.937 | 100 |
| 1.851 | w | 1.847 | vw | 1.85 | w | 1.850 | 10 |
| 1.795 | vw | 1.791 | vw | - | - | - | - |
| 1.669 | vw | 1.670 | vw | - | - | - | - |
| 1.650 | w | 1.648 | w | 1.65 | m | 1.652 | 30 |
| 1.580 | vw | 1.578 | vw | 1.58 | vw | 1.584 | 10 |
| 1.532 | vw | 1.531 | vw | 1.53 | vw | 1.534 | 10 |
| 1.473 | vw | 1.470 | vw | 1.47 | vw | 1.47 | 5 |
| 1.425 | vw | 1.423 | vw | 1.42 | m | 1.42 | 20 |
| 1.368 | vw | 1.367 | vw | 1.37 | m | 1.37 | 20 |
| 1.337 | vw | 1.337 | vw | 1.34 | w | 1.335 | 5 |
| - | - | - | - | - | - | 1.300 | 5 |
| - | - | - | - | - | - | 1.290 | 5 |

TABLE B-1.2 : X-ray diffraction data for silver-doped Bornite leach residues.

% Cu Dissolved : 20.10

% Ag Dissolved : -

| d Å | I |
|---|---|
| 3.316 | w |
| 3.219 | w |
| 3.170 | vw |
| 3.142 | st |
| 3.062, 3.038 | m |
| 2.723 | m |
| 2.612 | vw |
| 2.523 | vw |
| 2.501 | vw |
| 2.386 | w |
| 2.285 | vw |
| 2.097 | vw |
| 1.980 | vw |
| 1.941 | w |
| 1.928, 1.917 | vst |
| 1.867, 1.858 | w |
| 1.642, 1.636 | w |
| 1.602, 1.560 | vw |
| 1.569 | w |
| 1.359 | w |

% Cu Dissolved : 44.68

% Ag Dissolved : 0.20

| d Å | I |
|---|---|
| 3.269, 3.219 | vw |
| 3.086, 3.032 | st |
| 2.494 | vw |
| 2.292, 2.262 | vw |
| 1.883, 1.860 | st |
| 1.604, 1.581 | w |

Pure Bornite after 43.7% Cu had been dissolved.(11)

| d Å | I |
|---|---|
| 3.2203 | w |
| 3.0178 | vst |
| 2.6217 | w |
| 2.4947 | vw |
| 2.2703 | vw |
| 1.9028 | w |
| 1.8589 | st |
| 1.5876 | m |
| 1.3163 | w |
| 1.2094 | w |
| 1.0790 | w |
| 1.0161 | vw |

TABLE B-1.3 : X-ray diffraction data for silver- doped Bornite leach residues.

| WEIGHT % DISSOLVED | | | | | | | | | | SULPHUR (207) | |
|---|---|---|---|---|---|---|---|---|---|---|---|
| Cu 64.29 Ag 0.86 | | Cu 84.04 Ag 1.76 | | Cu 89.67 Ag 4.97 | | Cu 97.79 Ag 1.20 | | Cu 98.76 Ag 2.16 | | | |
| d Å | I | d Å | I | d Å | I | d Å | I | d Å | I | d Å | I |
| 7.726 | vw | 7.732 | vw | 7.718 | vw | 7.729 | vw | 7.709 | vw | 7.69 | 6 |
| 5.770 | w | 5.751 | w | 5.783 | w | 5.786 | w | 5.756 | w | 5.76 | 14 |
| – | – | – | – | 5.704 | vw | 5.704 | vw | – | – | 5.68 | 5 |
| – | – | – | – | – | – | – | – | – | – | 4.80 | 2 |
| – | – | – | – | – | – | 4.206 | vw | 4.208 | vw | 4.19 | 12 |
| 4.072 | m | 4.060 | w | 4.076 | w | 4.072 | w | 4.603 | w | 4.06 | 11 |
| 3.922 | w | 3.917 | w | 3.925 | w | 3.924 | w | 3.917 | w | 3.91 | 12 |
| 3.861 | st | 3.854 | st | 3.871 | st | 3.864 | vst | 3.861 | vst | 3.85 | 100 |
| 3.585 | w | 3.569 | w | 3.581 | w | 3.578 | w | 3.568 | w | 3.57 | 8 |
| 3.454 | m | 3.449 | m | 3.457 | m | 3.454 | st | 3.450 | m | 3.44 | 40 |
| – | – | – | – | 3.394 | vw | 3.394 | vw | 3.379 | vw | 3.38 | 3 |
| 3.341 | w | 3.333 | m | 3.349 | w | 3.343 | m | 3.339 | m | 3.33 | 25 |
| 3.223 | m | 3.216 | m | 3.228 | m | 3.225 | st | 3.218 | st | 3.21 | 60 |
| 3.116 | w | 3.112 | w | 3.125 | w | 3.119 | m | 3.115 | m | 3.11 | 25 |
| 3.087 | w | 3.083 | w | 3.096 | w | 3.091 | m | 3.087 | m | 3.08 | 17 |
| – | – | – | – | – | – | – | – | – | – | 3.06 | ± |
| 3.069 / 3.035 | st | 3.044 / 3.022 | m | 3.054 / 3.035 | st | 3.053 / 3.029 | vw | 3.049 / 3.019 | st | – | – |
| 2.850 | w | 2.848 | w | 2.854 | w | 2.857 | m | 2.848 | m | 2.842 | 18 |
| 2.737 | vw | – | – | – | – | 2.696 | vw | 2.687 | vw | 2.688 | 2 |
| – | – | – | – | – | – | – | – | – | – | 2.614 | 4 |
| 2.573 | vw | 2.568 | w | 2.577 | vw | 2.572 | vw | 2.569 | vw | 2.569 | 8 |
| 2.538 | vw | – | – | 2.509 | vw | 2.507 | m | 2.503 | vw | – | – |
| 2.503 | vw | 2.498 | w | 2.501 | vw | 2.491 | vw | 2.487 | vw | 2.501 | 7 |
| 2.431 | w | 2.424 | m | 2.432 | w | 2.429 | m | 2.427 | m | 2.424 | 13 |
| – | – | 2.402 | w | 2.418 | vw | 2.410 | vw | 2.410 | vw | 2.404 | 2 |
| 2.379 | vw | 2.378 | w | 2.378 | w | 2.380 | vw | 2.379 | vw | 2.375 | 4 |

TABLE B-1.3 continued :

| d Å | I | d Å | I | d Å | I | d Å | I | d Å | I | d Å | I |
|---|---|---|---|---|---|---|---|---|---|---|---|
| – | – | 2.367 | w | – | – | 2.373 | vw | 2.369 | vw | 2.366 | 4 |
| 2.291 | vw | 2.287 | m | 2.293 | w | 2.294 | m | 2.289 | w | 2.288 | 6 |
| – | – | – | – | – | – | – | – | 2.255 | vw | – | – |
| – | – | – | – | – | – | 2.224 | vw | 2.219 | vw | 2.215 | 2 |
| – | – | – | – | – | – | – | – | 2.147 | vw | 2.146 | 4 |
| 2.113 | vw | 2.113 | m | 2.120 | w | 2.118 | vw | 2.115 | vw | 2.112 | 10 |
| – | – | – | – | – | – | – | – | 2.097 | vw | 2.098 | 2 |
| – | – | – | – | – | – | – | – | 2.081 | vw | – | – |
| – | – | – | – | – | – | 2.061 | vw | 2.059 | vw | 2.057 | 1 |
| – | – | – | – | – | – | – | – | – | – | 2.041 | 1 |
| – | – | – | – | 2.010 | vw | 2.010 | vw | – | – | 2.003 | 2 |
| – | – | – | – | 1.995 | vw | 1.994 | vw | 1.989 | vw | 1.988 | 4 |
| – | – | – | – | 1.963 | vw | 1.962 | vw | 1.958 | vw | 1,957 | 2 |
| – | – | – | – | – | – | 1.929 | vw | 1.928 | vw | 1.926 | 1 |
| – | – | – | – | 1.906 | w | 1.907 | vw | 1.902 | vw | 1.900 | 7 |
| 1.907 | w | 1.902 | m | 1.880) | m | 1.880) | vw | 1.878) | st | – | – |
| 1.878) 1.856) | st | 1.876) 1.855) | m | 1.858) | | 1.865) | | 1.852) | | | |
| – | – | – | – | – | – | 1.857 | vw | – | – | 1.856 | 1 |
| – | – | – | – | – | – | – | – | – | – | 1.838 | 1 |
| 1.824 | vw | 1.824 | vw | 1.826 | w | 1.826 | w | 1.823 | w | 1.823 | 4 |
| 1.783 | vw | 1.782 | w | 1.784 | m | 1.785 | m | 1.783 | w | 1.781 | 11 |
| 1.761 | vw | – | – | – | – | – | – | – | – | – | – |
| 1.757 | vw | 1.755 | vw | 1.757 | w | 1.758 | m | 1.756 | vw | 1.754 | 7 |
| 1.724 | vw | 1.726 | vw | 1.725 | w | 1.727 | w | 1.727 | w | 1.725 | 8 |
| 1.698 | vw | 1.698 | vw | 1.699 | vw | 1.692 | w | 1.698 | w | 1.698 | 7 |
| – | – | – | – | 1.665 | vw | 1.668 | vw | 1.666 | vw | 1.665 | 2 |
| – | – | – | – | – | – | – | – | 1.656 | vw | 1.658 | 2 |
| 1.647 | vw | 1.647 | vw | 1.648 | vw | 1.650 | w | 1.648 | w | 1.647 | 5 |
| 1.624 | vw | 1.622 | vw | 1.623 | w | 1.625 | w | 1.624 | w | 1.622 | 6 |

TABLE B-1.3 continued :

| d Å | I | d Å | I | d Å | I | d Å | I | d Å | I | d Å | I |
|---|---|---|---|---|---|---|---|---|---|---|---|
| – | – | – | – | 1.606 | w | 1.609 | vw | 1.606 | w | 1.607 | 6 |
| 1.608) 1.577) | vw | 1.606 | vw | 1.605) 1.581) | w | – | – | 1.606) 1.574) | w | – | – |
| – | – | – | – | – | – | – | – | – | – | 1.601 | 2 |
| – | – | 1.593 | w | – | – | – | – | – | – | 1.595 | 3 |
| – | – | – | – | 1.564 | vw | 1.565 | vw | 1.563 | vw | 1.563 | 2 |
| – | – | – | – | – | – | 1.543 | vw | 1.541 | vw | 1.542 | 1 |
| – | – | – | – | – | – | 1.533 | vw | 1.529 | vw | 1.531 | 1 |
| – | – | – | – | – | – | – | – | – | – | 1.515 | 1 |
| – | – | – | – | – | – | 1.505 | vw | 1.504 | vw | 1.504 | 1 |
| – | – | – | – | – | – | – | – | – | – | 1.490 | 1 |
| – | – | – | – | 1.475 | vw | 1.476 | vw | 1.475 | vw | 1.475 | 2 |
| – | – | – | – | – | – | 1.461 | vw | 1.460 | vw | 1.461 | 1 |
| – | – | – | – | – | – | – | – | 1.453 | vw | – | – |
| – | – | – | – | 1.438 | vw | 1.441 | vw | 1.438 | vw | 1.439 | 3 |
| – | – | – | – | 1.422 | w | 1.422 | vw | 1.422 | vw | 1.424 | 3 |
| – | – | – | – | 1.417 | w | 1.418 | vw | 1.417 | vw | 1.419 | 1 |
| – | – | – | – | – | – | – | – | – | – | 1.391 | 1 |
| – | – | – | – | – | – | – | – | – | – | 1.362 | 1 |
| – | – | – | – | – | – | – | – | – | – | 1.354 | 3 |

TABLE B-1.4 : X-ray diffraction data for the silver-doped Bornite leach residues after removal of elemental Sulphur by treatment with $CS_2$.

| WEIGHT % DISSOLVED | | | | | | | | | |
|---|---|---|---|---|---|---|---|---|---|
| Cu 64.29 Ag 0.86 | | Cu 84.04 Ag 1.76 | | Cu 89.67 Ag 4.97 | | Cu 97.79 Ag 1.20 | | Cu 98.76 Ag 2.16 | |
| d Å | I | d Å | I | d Å | I | d Å | I | d Å | I |
| 3.268, 3.225 | vw | 3.263, 3.212 | vw | 3.250, 3.204 | vw | 3.290, 3.195 | vw | 3.301, 3.219 | w |
| 3.093, 3.036 | st | 3.099, 3.028 | m | 3.087, 3.025 | st | 3.081, 3.027 | vst | 3.071, 3.030 | vst |
| – | – | – | – | – | – | 2.730 | vw | 2.738, 2.730 | m |
| – | – | 2.631, 2.615 | w | 2.634, 2.608 | vw | – | – | – | – |
| – | – | – | – | 2.291 | vw | 2.496 | vw | – | – |
| – | – | – | – | – | – | – | – | 1.900, 1.895 | st |
| 1.885, 1.867 | st | 1.882, 1.858 | st | 1.878, 1.853 | st | 1.880, 1.855 | st | 1.876, 1.856 | st |
| 1.605, 1.588 | vw | 1.599, 1.583 | w | 1.604, 1.579 | w | 1.599, 1.575 | | 1.596, 1.580 | w |

TABLE B-1.5 : X-ray diffraction data for the Jarosite precipitate.

| Precipitate | | Jarosite[207] | |
|---|---|---|---|
| d Å | I | d Å | I |
| 5.943 | m | 5.94 | 30 |
| 5.735 | m | 5.74 | 20 |
| 5.105 | st | 5.09 | 40 |
| 3.844 | w | – | – |
| 3.658 | m | 3.65 | 10 |
| 3.549 | vw | – | – |
| 3.436 | vw | – | – |
| 3.331 | vw | – | – |
| 3.220 | vw | – | – |
| 3.108 | vst | 3.11 | 60 |
| 3.078 | vst | 3.08 | 100 |
| 2.969 | m | 2.97 | 10 |
| 2.863 | m | 2.87 | 20 |
| 2.543 | m | 2.547 | 30 |
| 2.365 | vw | – | – |
| 2.285 | st | 2.292 | 50 |
| 1.975 | st | 1.978 | 50 |
| 1.933 | w | 1.941 | 20 |
| 1.906 | w | 1.913 | 10 |
| 1.822 | st | 1.823 | 50 |
| 1.773 | vw | – | – |
| 1.737 | vw | – | – |
| 1.716 | vw | – | – |
| 1.690 | vw | – | – |
| 1.622 | vw | – | – |
| 1.593 | vw | – | – |
| 1.572 | vw | – | – |
| 1.560 | vw | – | – |
| 1.552 | vw | – | – |
| 1.537 | m | 1.539 | 30 |
| 1.507 | m | 1.512 | 30 |
| 1.482 | w | 1.484 | 10 |
| 1.344 | m | – | – |
| 1.458 | m | 1.459 | 14 |
| 1.445 | vvw | – | – |
| 1.436 | " | – | – |
| 1.415 | " | – | – |
| 1.406 | " | – | – |
| 1.399 | " | – | – |
| 1.379 | " | – | – |

TABLE B-1.6 : X-ray diffraction data for Silver sulphide.

| Synthetic $Ag_2S$ | | $Ag_2S$[207] | |
|---|---|---|---|
| d Å | I | d Å | I |
| 3.965 | w | 3.96 | 10 |
| 3.575 | w | 3.571 | 6 |
| 3.439 | m | 3.437 | 35 |
| 3.387 | m | 3.383 | 20 |
| 3.081 | st | 3.080 | 60 |
| 2.840 | st | 2.836 | 70 |
| 2.666 | m | 2.664 | 45 |
| 2.608 | vst | 2.606 | 100 |
| 2.585 | m | 2.583 | 70 |
| 2.485 | m | 2.456 | 70 |
| 2.442 | st | 2.440 | 80 |
| 2.423 | m | 2.421 | 60 |
| 2.384 | st | 2.383 | 75 |
| 2.318 | vvw | – | – |
| 2.284 | vvw | – | – |
| 2.255 | vvw | – | – |
| 2.213 | m | 2.213 | 45 |
| 2.094 | vw | 2.093 | 16 |
| 2.084 | m | 2.083 | 45 |
| 2.071 | w | 2.072 | 16 |
| 2.049 | w | 2.047 | 16 |
| 1.997 | w | 1.995 | 16 |
| 1.984 | vvw | – | – |
| 1.965 | w | 1.963 | 20 |
| – | – | 1.935 | 4 |
| 1.919 | vvw | 1.918 | 4 |
| 1.904 | w | 1.903 | 14 |
| 1.868 | w | 1.866 | 16 |
| 1.854 | vvw | – | – |
| 1.817 | vw | 1.816 | 4 |
| 1.797 | vw | 1.798 | 4 |
| 1.786 | vw | – | – |
| 1.732 | w | 1.733 | 12 |
| 1.719 | w | 1.718 | 20 |
| 1.690 | vw | 1.691 | 6 |
| 1.668 | vvw | – | – |
| 1.608 | vw | 1.610 | 4 |
| 1.598 | vvw | – | – |
| 1.586 | w | 1.587 | 14 |
| 1.579 | w | 1.579 | 10 |
| 1.554 | w | 1.554 | 8 |
| 1.546 | vw | – | – |
| 1.539 | w | 1.540 | 8 |
| 1.513 | w | 1.513 | 12 |
| 1.502 | vvw | – | – |
| 1.482 | w | 1.483 | 10 |
| 1.469 | vw | 1.470 | 10 |

TABLE B-1.7 : X-ray diffraction data for the silver sulphide residue after leaching at 60°C.

| d Å | I |
|---|---|
| 3.962 | w |
| 3.861 | vw |
| 3.575 | vw |
| 3.440 | m |
| 3.388 | w |
| 3.215 | vw |
| 3.084 | st |
| 2.841 | st |
| 2.669 | m |
| 2.610 | vst |
| 2.586 | st |
| 2.459 | w |
| 2.444 | st |
| 2.425 | w |
| 2.385 | st |
| 2.318 | vw |
| 2.256 | vw |
| 2.216 | st |
| 2.095 | vw |
| 2.086 | m |
| 2.073 | vw |
| 2.050 | w |
| 1.997 | w |
| 1.987 | vw |
| 1.966 | m |
| 1.940 | vvw |
| 1.918 | vw |
| 1.904 | w |
| 1.869 | w |
| 1.855 | vw |
| 1.817 | vw |
| 1.799 | vw |
| 1.787 | vw |
| 1.733 | w |
| 1.719 | m |
| 1.691 | w |
| 1.669 | vw |
| 1.609 | vw |
| 1.587 | w |
| 1.581 | w |
| 1.555 | w |
| 1.547 | vw |
| 1.540 | w |
| 1.513 | vw |
| 1.482 | w |
| 1.469 | w |
| 1.459 | m |
| 1.445 | vw |
| 1.439 | vw |
| 1.416 | vw |
| 1.406 | vw |

TABLE B-1.8 : X-ray diffraction data for the silver sulphide residue after dissolution at 90°C.

| RESIDUE | | Argentojarosite (196) | | | | RESIDUE | |
|---|---|---|---|---|---|---|---|
| d Å | I | d Å | I | d Å | I | d Å | I |
| 5.948 | st | 5.98 | 50 | - | - | 1.477 | m |
| 5.056 | w | 5.08 | 6 | 1.4690 | 8 | 1.470 | vw |
| 3.958 | w | - | - | - | - | 1.460 | w |
| 3.680 | st | 3.681 | 30 | 1.4537 | 5 | 1.455 | vw |
| 3.575 | w | 3.479 | 1 | - | - | 1.439 | vw |
| 3.393 | m | | | 1.4143 | 3 | 1.417 | vw |
| 3.388 | w | - | - | - | - | 1.393 | vw |
| 3.129 | m | 3.127 | 20 | 1.3892 | 4 | 1.388 | vw |
| 3.082 | w | - | - | 1.3464 | 6 | - | - |
| 3.068 | vst | 3.062 | 100 | | | | |
| 2.977 | w | 2.972 | 15 | | | | |
| 2.841 | m | - | - | | | | |
| 2.779 | m | 2.763 | 20 | | | | |
| 2.667 | m | - | - | | | | |
| 2.610 | st | - | - | | | | |
| 2.587 | m | - | - | | | | |
| 2.530 | m | 2.524 | 30 | | | | |
| 2.459 | m | - | - | | | | |
| 2.444 | st | - | - | | | | |
| 2.424 | m | - | - | | | | |
| 2.385 | st | 2.380 | 5 | | | | |
| 2.314 | m | 2.309 | 8 | | | | |
| 2.230 | st | - | - | | | | |
| 2.215 | m | 2.218 | 30 | | | | |
| 2.122 | vvw | - | - | | | | |
| 2.096 | vw | 2.079 | 2 | | | | |
| 2.086 | m | - | - | | | | |
| 2.074 | vw | - | - | | | | |
| 2.051 | w | - | - | | | | |
| 1.998 | w | - | - | | | | |
| 1.983 | st | 1.9794 | 25 | | | | |
| 1.966 | w | - | - | | | | |
| 1.952 | w | 1.9454 | 3 | | | | |
| 1.905 | w | 1.9000 | 1 | | | | |
| 1.870 | w | - | - | | | | |
| 1.854 | vw | - | - | | | | |
| 1.839 | m | 1.8366 | 20 | | | | |
| 1.754 | vw | - | - | | | | |
| 1.744 | w | - | - | | | | |
| 1.735 | vw | 1.7352 | 4 | | | | |
| 1.721 | m | - | - | | | | |
| 1.693 | m | - | - | | | | |
| 1.686 | vw | 1.6860 | 4 | | | | |
| 1.654 | m | - | - | | | | |
| 1.626 | vw | - | - | | | | |
| 1.613 | w | - | - | | | | |
| 1.584 | w | - | - | | | | |
| 1.573 | vw | - | - | | | | |
| 1.563 | m | 1.5594 | 4 | | | | |
| 1.541 | vw | - | - | | | | |
| 1.533 | m | 1.5286 | 8 | | | | |
| 1.515 | vw | - | - | | | | |
| 1.487 | m | 1.4847 | 5 | | | | |

B-2 : Stromeyerite, X-ray diffraction data.

TABLE B-2.1 : X-ray pattern for the synthetic Stromeyerite compared with the values of Suhr[140] and Djurle[133].

| Stromeyerite $Cu_{1.07}Ag_{0.93}S$ Present Work | | Stromeyerite $Cu_{1.07}Ag_{0.93}S$ Djurle | | Stromeyerite CuAgS Suhr | |
|---|---|---|---|---|---|
| d Å | I | d Å | I | d Å | I |
| 5.266 | vw | - | - | - | - |
| 3.998 | vw | 3.98 | 20 | 3.98 | 10 |
| 3.746 | vvw | - | - | - | - |
| 3.608 | vvw | 3.627 | 20 | - | - |
| 3.474 | st | 3.458 | 60 | 3.46 | 70 |
| 3.322 | st | 3.309 | 60 | 3.33 | 80 |
| 3.069 | m | 3.056 | 40 | 3.07 | 60 |
| 2.734 | vw | - | - | - | - |
| 2.622 | vst | 2.615 | 100 | 2.61 | 100 |
| 2.554 | m | 2.546 | 60 | 2.55 | 60 |
| 2.482 | vw | - | - | - | - |
| 2.407 | vw | - | - | - | - |
| 2.334 | vw | - | - | - | - |
| 2.214 | vw | - | - | - | - |
| 2.112 | w | 2.109 | 20 | 2.10 | 20 |
| 2.078 | m | 2.072 | 40 | 2.07 | 80 |
| 2.036 | st | 2.031 | 60 | - | - |
| 1.997 | st | 1.993 | 60 | 1.99 | 70 |
| 1.979 | vw | - | - | - | - |
| 1.945 | w | - | - | - | - |
| 1.890 | m | 1.885 | 60 | 1.89 | 60 |
| 1.749 | m | 1.745 | 60 | 1.75 | - |
| 1.734 | m | 1.733 | 40 | 1.73 | 40 |
| - | - | 1.728 | 40 | - | - |
| 1.711 | m | 1.708 | 40 | 1.70 | 30 |
| 1.697 | m | 1.693 | 40 | 1.69 | 30 |
| 1.661 | w | - | - | - | - |
| 1.626 | vw | - | - | 1.63 | 10 |
| 1.592 | m | 1.588 | 40 | 1.58 | 20 |
| 1.571 | w | 1.567 | 40 | 1.57 | 10 |
| 1.532 | w | - | - | - | - |
| 1.454 | w | 1.451 | 40 | 1.45 | 20 |
| 1.425 | m | 1.422 | 60 | 1.42 | 60 |
| 1.409 | vw | - | - | - | - |
| 1.394 | vw | - | - | - | - |
| 1.330 | vw | - | - | - | - |
| 1.310 | w | 1.306 | 40 | - | - |
| 1.286 | vw | - | - | - | - |
| 1.277 | vw | - | - | - | - |
| 1.262 | m | 1.258 | 40 | - | - |
| 1.242 | w-m | 1.239 | 40 | - | - |
| 1.234 | w-m | 1.232 | 40 | - | - |

X-ray data for residues of Stromeyerite after leaching in acidic ferric sulphate solutions.

TABLE B-2.2
5.44% Cu Dissolved

| d Å° | I |
|---|---|
| 5.251 | vvw |
| 3.995 | vw |
| 3.917 | vw |
| 3.508 | w |
| 3.465 | st |
| 3.314 | st |
| 3.179 | vw |
| 3.135 | vw |
| 3.062 | m |
| 2.868 | vw |
| 2.805 | vw |
| 2.759 | vvw |
| 2.617 | vst |
| 2.551 | m |
| 2.527 | vvw |
| 2.476 | vvw |
| 2.434 | vvw |
| 2.409 | vw |
| 2.307 | vw |
| 2.190 | vw |
| 2.169 | vvw |
| 2.110 | vw |
| 2.091 | vvw |
| 2.075 | m |
| 2.032 | st |
| 1.994 | st |
| 1.947 | sh |
| 1.888 | m |
| 1.746 | m |
| 1.731 | m |
| 1.709 | m-w |
| 1.693 | m-w |
| 1.658 | vw |
| 1.589 | w |
| 1.568 | w |
| 1.530 | vvw |
| 1.451 | w |
| 1.423 | m |
| 1.327 | vvw |
| 1.307 | w |
| 1.283 | vvw |
| 1.274 | vvw |
| 1.259 | m |
| 1.240 | m |
| 1.232 | m-w |

TABLE B-2.3
10.44% Cu Dissolved

| d Å | I |
|---|---|
| 5.236 | vvw |
| 4.335 | vvw |
| 4.004 | vvw |
| 3.909 | vw |
| 3.515 | vw |
| 3.468 | st |
| 3.317 | st |
| 3.184 | vvw |
| 3.140 | vvw |
| 3.064 | m |
| 2.946 | sh |
| 2.868 | w-m |
| 2.807 | w |
| 2.765 | w |
| 2.617 | vst |
| 2.551 | m |
| 2.527 | vw |
| 2.506 | vw |
| 2.480 | vw |
| 2.439 | vw |
| 2.411 | w |
| 2.359 | vvw |
| 2.309 | w |
| 2.248 | vw |
| 2.191 | vw |
| 2.171 | vw |
| 2.124 | vvw |
| 2.110 | vvw |
| 2.093 | vvw |
| 2.075 | m |
| 2.033 | st |
| 1.995 | st |
| 1.961 | vw |
| 1.948 | vw |
| 1.888 | m |
| 1.746 | m |
| 1.733 | m |
| 1.710 | m |
| 1.694 | m |
| 1.658 | vw |
| 1.622 | vvw |
| 1.590 | m |
| 1.568 | w-m |
| 1.530 | vw |
| 1.452 | w-m |
| 1.424 | m |
| 1.394 | vvw |
| 1.359 | vvw |
| 1.308 | m |
| 1.285 | vvw |
| 1.275 | vvw |
| 1.260 | m |
| 1.241 | m |
| 1.233 | m |

TABLE B-2.4
12.17% Cu Dissolved

| d Å | I |
|---|---|
| 7.008 | vw |
| 5.244 | vw |
| 4.335 | vw |
| 4.004 | vw |
| 3.909 | vw |
| 3.690 | vvw |
| 3.584 | vvw |
| 3.512 | w |
| 3.468 | m |
| 3.320 | st |
| 3.187 | vvw |
| 3.138 | vvw |
| 3.064 | m |
| 2.949 | vvw |
| 2.871 | w-m |
| 2.805 | w |
| 2.761 | vw |
| 2.645 | vvw |
| 2.619 | vst |
| 2.574 | vw |
| 2.551 | m |
| 2.527 | vw |
| 2.508 | vvw |
| 2.480 | vw |
| 2.438 | vw |
| 2.411 | m |
| 2.358 | vw |
| 2.312 | w |
| 2.275 | vw |
| 2.250 | vw |
| 2.190 | vw |
| 2.169 | vw |
| 2.124 | vw |
| 2.095 | vw |
| 2.075 | m |
| 2.035 | st |
| 2.012 | vvw |
| 1.997 | m |
| 1.949 | w-m |
| 1.888 | m |
| 1.747 | m |
| 1.733 | m-w |
| 1.710 | w |
| 1.694 | w |
| 1.659 | vw |
| 1.591 | m |
| 1.570 | w |
| 1.532 | vvw |
| 1.453 | w |
| 1.425 | m |
| 1.358 | vvw |
| 1.308 | w |
| 1.285 | vw |
| 1.260 | m |
| 1.241 | w |
| 1.233 | w |

X-ray data for residues of Stromeyerite after leaching in acidic ferric sulphate solutions.

TABLE B-2.5
18.06% Cu
Dissolved

| d Å | I | d Å | I |
|---|---|---|---|
| 6.988 | vvw | 1.734 | w-m |
| 4.345 | w | 1.713 | w |
| 4.021 | w | 1.696 | w |
| 3.917 | w | 1.658 | vw |
| 3.697 | vw | 1.604 | vvw |
| 3.588 | vw | 1.591 | vw |
| 3.522 | w | 1.571 | vw |
| 3.475 | w | 1.560 | vvw |
| 3.398 | vw | 1.532 | w |
| 3.323 | m | 1.523 | vvw |
| 3.187 | vw | 1.488 | vw |
| 3.141 | vw | 1.454 | w |
| 3.068 | m | 1.426 | m |
| 2.954 | vw | 1.359 | vw |
| 2.919 | vw | 1.309 | w |
| 2.871 | w | 1.286 | vvw |
| 2.808 | w | 1.260 | m |
| 2.764 | w | 1.241 | w |
| 2.646 | vw | 1.233 | w |
| 2.620 | vst | | |
| 2.574 | vw | | |
| 2.555 | vw | | |
| 2.531 | vw | | |
| 2.507 | vw | | |
| 2.480 | vw | | |
| 2.438 | w | | |
| 2.412 | w | | |
| 2.357 | w | | |
| 2.312 | vw | | |
| 2.278 | vw | | |
| 2.255 | vw | | |
| 2.192 | vw | | |
| 2.171 | w | | |
| 2.127 | vw | | |
| 2.094 | vw | | |
| 2.076 | m | | |
| 2.037 | m | | |
| 2.012 | vw | | |
| 1.997 | m | | |
| 1.963 | vw | | |
| 1.950 | w | | |
| 1.889 | m | | |
| 1.846 | vw | | |
| 1.749 | m | | |

TABLE B-2.6
26.15% Cu
Dissolved

| d Å | I | d Å | I |
|---|---|---|---|
| 7.002 | w | 1.952 | w |
| 4.329 | w | 1.889 | w-m |
| 4.021 | vw | 1.847 | vw |
| 3.193 | w | 1.748 | w-m |
| 3.690 | w | 1.734 | w |
| 3.581 | vw | 1.712 | vw |
| 3.519 | m | 1.695 | vw |
| 3.472 | m | 1.603 | vw |
| 3.391 | vw | 1.590 | vw |
| 3.323 | m | 1.571 | vw |
| 3.224 | vw | 1.559 | vvw |
| 3.193 | vw | 1.544 | vvw |
| 3.141 | vw | 1.533 | vw |
| 3.068 | m | 1.488 | vw |
| 2.954 | vw | 1.455 | w |
| 2.917 | vw | 1.426 | m |
| 2.869 | m | 1.398 | vvw |
| 2.808 | m | 1.382 | vvw |
| 2.762 | w | 1.367 | vw |
| 2.694 | vw | 1.309 | vw |
| 2.648 | vw | 1.302 | vw |
| 2.618 | vst | 1.260 | w |
| 2.574 | w | 1.243 | w |
| 2.552 | w | 1.233 | w |
| 2.529 | w | | |
| 2.509 | vw | | |
| 2.482 | w | | |
| 2.438 | w | | |
| 2.412 | w | | |
| 2.357 | w | | |
| 2.330 | vw | | |
| 2.311 | vw | | |
| 2.278 | w | | |
| 2.253 | vw | | |
| 2.214 | vw | | |
| 2.193 | vw | | |
| 2.172 | w | | |
| 2.125 | w | | |
| 2.092 | vw | | |
| 2.074 | m | | |
| 2.034 | m | | |
| 2.013 | vw | | |
| 1.997 | w | | |
| 1.964 | vw | | |

X-ray data for residues of Stromeyerite after leaching in acidic ferric sulphate solutions.

TABLE B-2.7

32.96% Cu Dissolved

| d Å | I | d Å | I |
|---|---|---|---|
| 6.974 | w | 1.888 | w-m |
| 4.334 | w-m | 1.846 | vvw |
| 4.017 | w | 1.747 | w-m |
| 3.908 | w | 1.732 | w |
| 3.686 | w | 1.714 | vw |
| 3.581 | vw | 1.695 | vvw |
| 3.515 | m | 1.603 | vvw |
| 3.472 | w-m | 1.591 | vw |
| 3.394 | vw | 1.571 | w |
| 3.320 | w-m | 1.532 | vw |
| 3.185 | vw | 1.488 | vvw |
| 3.141 | w | 1.454 | vw |
| 3.065 | m | 1.442 | vvw |
| 2.867 | w | 1.426 | w |
| 2.806 | m | 1.396 | vvw |
| 2.762 | m | 1.380 | vvw |
| 2.646 | vw | 1.359 | vvw |
| 2.620 | vst | 1.329 | vvw |
| 2.576 | w | 1.309 | vvw |
| 2.552 | w | 1.287 | vvw |
| 2.527 | w | 1.261 | w |
| 2.507 | vvw | 1.242 | w |
| 2.480 | w | 1.233 | w |
| 2.438 | m | | |
| 2.413 | w | | |
| 2.384 | vw | | |
| 2.357 | m | | |
| 2.330 | vw | | |
| 2.311 | vw | | |
| 2.278 | vw | | |
| 2.252 | vvw | | |
| 2.215 | vw | | |
| 2.189 | vw | | |
| 2.168 | w | | |
| 2.124 | w | | |
| 2.094 | vw | | |
| 2.074 | m | | |
| 2.036 | w-m | | |
| 2.014 | w | | |
| 1.997 | w-m | | |
| 1.964 | vvw | | |
| 1.953 | m | | |
| 1.930 | vw | | |

TABLE B-2.8

38.16% Cu Dissolved

| d Å | I | d Å | I |
|---|---|---|---|
| 6.964 | vw | 1.911 | vvw |
| 4.331 | m | 1.889 | vw |
| 4.023 | vw | 1.877 | vvw |
| 3.910 | vw | 1.845 | vvw |
| 3.684 | w | 1.746 | w |
| 3.576 | w | 1.732 | vw |
| 3.514 | w | 1.714 | vw |
| 3.473 | vw | 1.694 | vvw |
| 3.399 | vvw | 1.586 | vvw |
| 3.319 | vw | 1.568 | vvw |
| 3.140 | vw | 1.531 | vvw |
| 3.066 | m | 1.488 | vvw |
| 2.918 | vvw | 1.454 | vvw |
| 2.868 | w | 1.440 | vvw |
| 2.835 | vvw | 1.424 | vw |
| 2.807 | m | 1.416 | vvw |
| 2.761 | m | 1.396 | " |
| 2.647 | vvw | 1.379 | " |
| 2.617 | st | 1.343 | " |
| 2.576 | vw | 1.285 | " |
| 2.551 | vvw | 1.260 | " |
| 2.530 | vw | 1.232 | " |
| 2.510 | vvw | | |
| 2.486 | w | | |
| 2.438 | m | | |
| 2.413 | vw | | |
| 2.384 | vvw | | |
| 2.355 | m | | |
| 2.328 | vw | | |
| 2.312 | vvw | | |
| 2.276 | w | | |
| 2.256 | vvw | | |
| 2.216 | vvw | | |
| 2.193 | vvw | | |
| 2.169 | w | | |
| 2.124 | w | | |
| 2.094 | vw | | |
| 2.075 | w | | |
| 2.034 | vw | | |
| 2.014 | w | | |
| 1.997 | vw | | |
| 1.951 | w | | |
| 1.930 | vw | | |

X-ray data for residues of Stromeyerite after leaching in acidic ferric sulphate solutions.

TABLE B-2.9

39.64% Cu Dissolved

| d Å | I | d Å | I |
|---|---|---|---|
| 6.991 | w | 1.568 | vw |
| 4.336 | w-m | 1.489 | " |
| 3.910 | vvw | 1.441 | " |
| 3.684 | w | 1.424 | " |
| 3.579 | w | 1.417 | " |
| 3.510 | w-m | 1.395 | " |
| 3.434 | vvw | 1.379 | " |
| 3.383 | vvw | 1.359 | " |
| 3.322 | w | 1.328 | " |
| 3.140 | vvw | 1.282 | " |
| 3.069 | w | 1.259 | " |
| 2.868 | w | 1.233 | " |
| 2.837 | vvw | | |
| 2.805 | m | | |
| 2.757 | m | | |
| 2.614 | st | | |
| 2.581 | vvw | | |
| 2.549 | vvw | | |
| 2.527 | vvw | | |
| 2.483 | w | | |
| 2.436 | m | | |
| 2.413 | vw | | |
| 2.382 | vw | | |
| 2.354 | m | | |
| 2.329 | vw | | |
| 2.311 | vvw | | |
| 2.279 | w | | |
| 2.216 | vvw | | |
| 2.190 | vvw | | |
| 2.167 | w | | |
| 2.123 | w | | |
| 2.093 | vw | | |
| 2.073 | vw | | |
| 2.049 | vvw | | |
| 2.032 | vvw | | |
| 2.015 | w | | |
| 1.993 | vw | | |
| 1.951 | vvw | | |
| 1.930 | vvw | | |
| 1.889 | vvw | | |
| 1.871 | vvw | | |
| 1.747 | vw | | |
| 1.717 | " | | |
| 1.586 | " | | |

TABLE B-2.10

41.72 % Cu Dissolved

| d Å | I | d Å | I |
|---|---|---|---|
| 6.964 | w | 1.487 | vvw |
| 4.331 | m | 1.456 | " |
| 3.897 | vvw | 1.440 | " |
| 3.677 | w | 1.415 | " |
| 3.575 | vw | 1.397 | " |
| 3.503 | vvw | 1.379 | " |
| 3.487 | vvw | 1.358 | " |
| 3.428 | vvw | 1.327 | " |
| 3.380 | vvw | 1.306 | " |
| 3.316 | vw | 1.283 | " |
| 3.134 | vvw | 1.230 | " |
| 3.066 | w | | |
| 2.864 | vw | | |
| 2.833 | vw | | |
| 2.803 | m | | |
| 2.755 | m | | |
| 2.662 | vw | | |
| 2.643 | vvw | | |
| 2.610 | st | | |
| 2.581 | vvw | | |
| 2.527 | vw | | |
| 2.482 | w | | |
| 2.435 | m | | |
| 2.378 | vw | | |
| 2.352 | m | | |
| 2.325 | vw | | |
| 2.273 | w | | |
| 2.213 | vvw | | |
| 2.190 | vvw | | |
| 2.164 | w | | |
| 2.122 | w | | |
| 2.095 | vw | | |
| 2.073 | vw | | |
| 2.046 | vvw | | |
| 2.012 | vw | | |
| 1.958 | vvw | | |
| 1.930 | vw | | |
| 1.900 | vvw | | |
| 1.868 | vvw | | |
| 1.744 | w | | |
| 1.716 | vw | | |
| 1.586 | vvw | | |
| 1.568 | vvw | | |

X-ray data for residues of Stromeyerite after leaching in acidic ferric sulphate solutions.

TABLE B-2.11

47.37% Cu Dissolved

| d Å | I | d Å | I |
|---|---|---|---|
| 6.997 | vw | 1.718 | w |
| 4.343 | w | 1.690 | vvw |
| 3.957 | vw | 1.588 | vw |
| 3.686 | vw | 1.577 | vw |
| 3.581 | vw | 1.568 | vw |
| 3.496 | vw | 1.555 | vw |
| 3.439 | w | 1.538 | " |
| 3.388 | w | 1.512 | " |
| 3.291 | vw | 1.488 | " |
| 3.225 | vw | 1.481 | " |
| 3.082 | st | 1.468 | " |
| 3.053 | w | 1.458 | " |
| 2.839 | m | 1.441 | " |
| 2.812 | st | 1.413 | " |
| 2.759 | m | 1.393 | " |
| 2.726 | w | 1.378 | " |
| 2.666 | m | | |
| 2.608 | st | | |
| 2.586 | m | | |
| 2.487 | w | | |
| 2.459 | w | | |
| 2.440 | st | | |
| 2.424 | w | | |
| 2.383 | w | | |
| 2.358 | st | | |
| 2.327 | w | | |
| 2.273 | w | | |
| 2.217 | m | | |
| 2.169 | w | | |
| 2.125 | m | | |
| 2.095 | vw | | |
| 2.084 | m | | |
| 2.072 | vw | | |
| 2.048 | vw | | |
| 2.012 | w | | |
| 1.995 | w | | |
| 1.965 | w | | |
| 1.931 | w | | |
| 1.901 | m | | |
| 1.847 | w | | |
| 1.799 | vvw | | |
| 1.786 | vvw | | |
| 1.744 | w | | |
| 1.735 | w | | |

TABLE B-2.12

50.60% Cu Dissolved

| d Å | I |
|---|---|
| 3.974 | vw |
| 3.574 | vw |
| 3.444 | w |
| 3.392 | w |
| 3.086 | m |
| 2.843 | st |
| 2.731 | w |
| 2.669 | m |
| 2.612 | st |
| 2.589 | m |
| 2.462 | m |
| 2.447 | st |
| 2.427 | m |
| 2.388 | st |
| 2.219 | m |
| 2.097 | vvw |
| 2.088 | m |
| 2.076 | vw |
| 2.053 | w |
| 2.000 | vw |
| 1.968 | w |
| 1.907 | w-m |
| 1.870 | w |
| 1.736 | vw |
| 1.722 | m |
| 1.693 | w |
| 1.612 | vw |
| 1.590 | vw |
| 1.584 | vw |
| 1.559 | vw |
| 1.544 | vw |
| 1.517 | vw |
| 1.486 | vw |
| 1.472 | vw |
| 1.461 | w |
| 1.419 | vw |

TABLE B-2.13

55.10% Cu Dissolved

| d Å | I |
|---|---|
| 3.959 | w |
| 3.579 | vw |
| 3.437 | m |
| 3.383 | w |
| 3.289 | sh |
| 3.220 | sh |
| 3.081 | st |
| 3.040 | w |
| 2.837 | st |
| 2.804 | sh |
| 2.720 | sh |
| 2.664 | m |
| 2.605 | st |
| 2.582 | m |
| 2.457 | m |
| 2.439 | st |
| 2.421 | m |
| 2.382 | m |
| 2.212 | m |
| 2.082 | m |
| 2.070 | w |
| 2.047 | w |
| 1.994 | w |
| 1.963 | w |
| 1.901 | m |
| 1.866 | w |
| 1.815 | vvw |
| 1.798 | vvw |
| 1.731 | w |
| 1.718 | m |
| 1.689 | vw |
| 1.610 | vw |
| 1.586 | w |
| 1.580 | w |
| 1.553 | vw |
| 1.538 | vw |
| 1.512 | vw |
| 1.481 | vw |
| 1.468 | vw |
| 1.457 | w |

X-ray data for residues of Stromeyerite after leaching in acidic ferric sulphate solutions.

TABLE B-2.14

59.94% Cu Dissolved

| d Å | I |
|---|---|
| 3.979 | w |
| 3.870 | vw |
| 3.586 | vw |
| 3.450 | m |
| 3.398 | m-w |
| 3.091 | st |
| 2.845 | st |
| 2.671 | m |
| 2.616 | st |
| 2.591 | m-w |
| 2.464 | w |
| 2.449 | m |
| 2.430 | m |
| 2.390 | st |
| 2.221 | w-m |
| 2.089 | m |
| 2.077 | vw |
| 2.054 | w |
| 2.000 | w |
| 1.971 | m |
| 1.907 | w |
| 1.872 | w |
| 1.722 | w |
| 1.694 | vw |
| 1.585 | w |
| 1.558 | vw |
| 1.543 | " |
| 1.517 | " |
| 1.485 | " |
| 1.471 | " |
| 1.460 | " |

TABLE B-2.15

61.76% Cu Dissolved

| d Å | I |
|---|---|
| 4.079 | vvw |
| 3.950 | vw |
| 3.565 | vvw |
| 3.439 | m |
| 3.384 | w |
| 3.291 | vvw |
| 3.219 | vvw |
| 3.081 | st |
| 3.035 | vw |
| 2.837 | st |
| 2.723 | vw |
| 2.667 | m |
| 2.607 | st |
| 2.584 | m |
| 2.457 | w |
| 2.441 | m |
| 2.425 | w |
| 2.385 | st |
| 2.214 | m |
| 2.085 | m |
| 2.048 | vw |
| 1.997 | vw |
| 1.965 | vw |
| 1.900 | w |
| 1.866 | vw |
| 1.734 | vw |
| 1.719 | w |
| 1.693 | vvw |
| 1.584 | vw |
| 1.555 | vw |
| 1.543 | vw |
| 1.513 | vw |
| 1.483 | vw |
| 1.470 | vw |
| 1.459 | vw |

TABLE B-2.16

77.58% Cu Dissolved

| d Å | I |
|---|---|
| 5.745 | sh |
| 5.165 | sh |
| 4.077 | vvw |
| 3.967 | m |
| 3.866 | w |
| 3.580 | w |
| 3.445 | m |
| 3.390 | w |
| 3.292 | vw |
| 3.223 | vw |
| 3.087 | st |
| 2.844 | st |
| 2.727 | m |
| 2.669 | m |
| 2.612 | vst |
| 2.590 | m |
| 2.460 | m |
| 2.446 | st |
| 2.427 | m |
| 2.387 | st |
| 2.254 | vw |
| 2.217 | m |
| 2.087 | m |
| 2.051 | w |
| 1.999 | vw |
| 1.966 | w |
| 1.904 | w-m |
| 1.870 | vw |
| 1.821 | sh |
| 1.734 | vw |
| 1.720 | m |
| 1.690 | vw |
| 1.609 | sh |
| 1.583 | w |
| 1.556 | vw |
| 1.541 | vw |
| 1.515 | vw |
| 1.483 | vw |
| 1.469 | vw |
| 1.459 | w |
| several lines | vw |
| 1.418 | vw |
| 1.381 | vw |

TABLE B-2.17 : X-ray data for residue of Stromeyerite leached in Hydrogen Peroxid solution.

55.76% Cu Dissolved

| d Å | I |
|---|---|
| 3.965 | w |
| 3.582 | vw |
| 3.443 | m |
| 3.392 | w |
| 3.293 | vw |
| 3.224 | vw |
| 3.085 | st |
| 3.044 | w |
| 2.843 | st |
| 2.726 | w |
| 2.666 | m |
| 2.611 | st |
| 2.586 | m |
| 2.457 | w |
| 2.445 | st |
| 2.426 | m-w |
| 2.386 | st |
| 2.250 | vw |
| 2.214 | m |
| 2.086 | m |
| 2.050 | vw |
| 1.997 | vw |
| 1.965 | vw |
| 1.900 | m |
| 1.868 | vw |
| 1.817 | vw |
| 1.731 | vw |
| 1.718 | w |
| 1.689 | vw |
| 1.608 | sh |
| 1.585 | sh |
| 1.579 | sh |
| 1.556 | vw |
| 1.541 | vw |
| 1.514 | vw |
| 1.481 | vw |
| 1.469 | vw |
| 1.459 | w |
| 1.442 | vw |
| 1.416 | vw |

X-ray data for residues of Stromeyerite leached in 0.1M $Fe^{3+}$ solution containing 4M NaCl .

TABLE B-2.18

11.44% Cu diss.
18.92% Ag "

| d Å | I |
|---|---|
| 4.315 | vvw |
| 4.031 | vw |
| 3.916 | vw |
| 3.619 | vvw |
| 3.574 | vvw |
| 3.509 | w |
| 3.400 | vvw |
| 3.326 | vw |
| 3.209 | m |
| 3.139 | vvw |
| 3.063 | m |
| 2.866 | w |
| 2.805 | w |
| 2.782 | st |
| 2.768 | w |
| 2.646 | vw |
| 2.611 | st |
| 2.573 | vw |
| 2.527 | vw |
| 2.506 | vvw |
| 2.475 | vw |
| 2.437 | vw |
| 2.409 | w |
| 2.354 | w |
| 2.309 | w |
| 2.273 | w |
| 2.250 | vw |
| 2.190 | w |
| 2.166 | w |
| 2.124 | vw |
| 2.091 | w |
| 2.072 | m |
| 2.034 | vw |
| 2.010 | w |
| 1.996 | vw |
| 1.964 | st |
| 1.948 | w |
| 1.920, 1.901 | vw |
| 1.888 | vw |
| 1.747 | vw |
| 1.675 | w |
| 1.602 | w |
| 1.529 | vw |
| 1.485 | " |
| 1.453 | " |
| 1.438 | " |
| 1.421 | " |
| 1.386 | " |

TABLE B-2.19

20.25% Cu diss.
21.81% Ag "

| d Å | I |
|---|---|
| 3.572 | vw |
| 3.505 | vw |
| 3.443 | w |
| 3.279 | vvw |
| 3.208 | m |
| 3.082, 3.034 | w |
| 2.879 | vw |
| 2.839 | vw |
| 2.805 | vw |
| 2.781 | st |
| 2.726 | vvw |
| 2.615 | w |
| 2.581 | vw |
| 2.487 | vw |
| 2.439 | w |
| 2.385 | w |
| 2.356 | w |
| 2.329 | vw |
| 2.275 | vw |
| 2.214 | vw |
| 2.166 | vw |
| 2.125 | w |
| 2.085 | vw |
| 2.034 | w |
| 2.017 | w |
| 1.996 | w |
| 1.966 | st |
| 1.913, 1.898 | vw |
| 1.888 | vvw |
| 1.744 | vvw |
| 1.716 | vvw |
| 1.677 | w |
| 1.604 | w |
| 1.565 | vvw |
| 1.488 | vvw |

TABLE B-2.20

23.64% Cu diss.
23.18% Ag "

| d Å | I |
|---|---|
| 3.440 | vvw |
| 3.289 | vw |
| 3.210 | m |
| 3.084, 3.036 | m |
| 2.834 | w |
| 2.781 | st |
| 2.727 | w |
| 2.664 | vw |
| 2.617, 2.578 | w |
| 2.441 | w |
| 2.385 | w |
| 2.286 | vvw |
| 2.218 | vw |
| 2.089 | vw |
| 2.044 | vw |
| 2.000 | vw |
| 1.965 | m |
| 1.909, 1.895 | st |
| 1.732 | vw |
| 1.676 | w |
| 1.604 | w |
| 1.562 | vw |
| 1.387 | vw |

TABLE B-2.21

25.17% Cu diss.
25.58% Ag "

| d Å | I |
|---|---|
| 8.194 | w |
| 3.845 | w |
| 3.435 | w |
| 3.343 | w |
| 3.277 | w |
| 3.201 | st |
| 3.045 | m |
| 2.819 | w |
| 2.772 | st |
| 2.722 | w |
| 2.662 | vvw |
| 2.622, 2.579 | vvw |
| 2.427 | vvw |
| 2.381 | vvw |
| 2.094 | vvw |
| 2.041 | w |
| 1.961 | st |
| 1.901, 1.891 | m |
| 1.733 | w |
| 1.672 | w-m |
| 1.601 | w-m |
| 1.555 | vw |
| 1.384 | w |

B-3 : Mixed Sulphide Material, X-ray diffraction data.

TABLE B-3.1 : X-ray pattern for the mixed sulphide material compared with the values for bornite, α-chalcopyrite[207], and stromeyerite[133,207].

| Mixed Sulphide Material | | Bornite (Table B-1.1) $Cu_5FeS_4$ | | α-Chalcopyrite $CuFeS_2$ | | Stromeyerite $Cu_{1.07}Ag_{0.93}S$ | |
|---|---|---|---|---|---|---|---|
| d Å | I | d Å | I | d Å | I | d Å | I |
| 6.333 | vw | 6.313 | vw | – | – | – | – |
| 5.478 | vw | 5.475 | vw | – | – | – | – |
| 4.779 | w | 4.788 | vw | – | – | – | – |
| 4.069 | m | 4.070 | w | – | – | – | – |
| – | – | – | – | – | – | 3.98 | 20 |
| 3.868 | vw | 3.862 | vw | – | – | – | – |
| – | – | – | – | – | – | 3.627 | 20 |
| 3.465 | m | – | – | – | – | 3.458 | 60 |
| 3.307 | m | 3.300 | m | – | – | 3.309 | 60 |
| 3.262 | w | 3.261 | w | – | – | – | – |
| 3.164 | m-st | 3.156 | st | – | – | – | – |
| 3.060 | vw | – | – | – | – | 3.056 | 40 |
| 3.041 | st | – | – | 3.03 | 100 | – | – |
| 2.900 | vvw | 3.014 | vw | – | – | – | – |
| 2.807 | m | 2.804 | m | – | – | – | – |
| 2.739 | m | 2.736 | m | – | – | – | – |
| 2.648 | vvw | – | – | 2.63 | 5 | – | – |
| 2.638 | vw | 2.633 | vw | – | – | – | – |
| 2.615 | st | – | – | – | – | 2.615 | 100 |
| 2.548 | w | – | – | – | – | 2.546 | 60 |
| 2.514 | w | 2.510 | m | – | – | – | – |
| 2.496 | w | 2.495 | m | – | – | – | – |
| 2.398 | vw | – | – | – | – | – | – |
| 2.177 | w | 2.174 | vw | – | – | – | – |
| – | – | 2.137 | vw | – | – | – | – |
| 2.108 | m | 2.104 | w | – | – | 2.109 | 20 |
| 2.072 | w | – | – | – | – | 2.072 | 40 |
| 2.031 | m-st | – | – | – | – | 2.031 | 60 |
| 1.993 | m | – | – | – | – | 1.993 | 60 |
| 1.959 | w | 1.957 | vw | – | – | – | – |
| 1.936 | vst | 1.935 | vst | – | – | – | – |
| 1.885 | w | – | – | – | – | 1.885 | 60 |
| 1.870 | m | – | – | 1.865 | 40 | – | – |
| 1.856 | m-st | 1.847 | vw | 1.854 | 80 | – | – |
| – | – | 1.791 | vw | – | – | – | – |
| 1.746 | m | – | – | – | – | 1.745 | 60 |
| 1.733 | w | – | – | – | – | 1.733 | 40 |
| 1.728 | vw | – | – | – | – | 1.728 | 40 |
| 1.708 | w | – | – | – | – | 1.708 | 40 |
| 1.693 | w | – | – | – | – | 1.693 | 40 |
| 1.668 | w | 1.670 | vw | – | – | – | – |

Continued on following page .....

TABLE B-3.1 continued,

| Mixed Sulphide Material | | Bornite | | α-Chalcopyrite | | Stromeyerite | |
|---|---|---|---|---|---|---|---|
| d Å | I | d Å | I | d Å | I | d Å | I |
| 1.650 | m | 1.648 | w | - | - | - | - |
| 1.592 | m | - | - | 1.591 | 60 | 1.588 | 40 |
| 1.581 | vw | 1.578 | vw | - | - | - | - |
| 1.574 | m | - | - | 1.573 | 20 | - | - |
| 1.566 | vw | - | - | - | - | 1.567 | 40 |
| 1.531 | w | 1.531 | vw | - | - | - | - |
| 1.518 | vw | - | - | 1.518 | 5 | - | - |
| 1.471 | vw | 1.470 | vw | - | - | - | - |
| 1.449 | vw | - | - | - | - | 1.451 | 40 |
| 1.420 | m | 1.423 | vw | - | - | 1.422 | 60 |
| 1.369 | w | 1.367 | vw | - | - | - | - |
| - | | 1.337 | vw | - | - | - | - |

TABLE B-3.2 : X-ray diffraction data for the Mixed Sulphide Material leach residues.

| WEIGHT % Cu DISSOLVED | | | | | | | | | | | | |
|---|---|---|---|---|---|---|---|---|---|---|---|---|
| 0.00 | | 7.50 | | 14.15 | | 23.30 | | 29.50 | | 39.45 | | |
| d Å | I | d Å | I | d Å | I | d Å | I | d Å | I | d Å | I | |
| 6.333 | vw | 6.217 | vvw | 6.235 | vvw | 6.198 | vw | 6.179 | vw | 6.139 | w | |
| 5.478 | vw | – | – | – | – | – | – | – | – | – | – | |
| 4.779 | w | – | – | – | – | – | – | – | – | – | – | |
| 4.069 | m | – | – | – | – | – | – | – | – | – | – | |
| 3.868 | vw | – | – | – | – | – | – | – | – | – | – | |
| – | – | – | – | – | – | – | – | – | – | 3.858 | vvw | |
| 3.465 | m | – | – | – | – | – | – | – | – | – | – | |
| – | – | 3.440 | sh | 3.449 | vvw | 3.449 | vvw | 3.439 | vw | 3.443 | vw | |
| – | – | 3.391 | sh | 3.383 | vvw | 3.400 | vvw | 3.382 | vw | 3.383 | vvw | |
| 3.307 | m | – | – | – | – | – | – | – | – | – | – | |
| 3.262 | w | 3.262 | w | 3.255 | w | 3.245 | w | 3.229 | w | 3.223 | w | |
| 3.164 | st | 3.123 | st | 3.114 | st | 3.105 | st | 3.092 | st | 3.082 | st | |
| 3.060 | vw | – | – | – | – | – | – | – | – | – | – | |
| 3.040 | st | 3.039 | st | 3.044 | st | 3.044 | st | 3.038 | st | 3.037 | st | |
| 2.900 | vvw | – | – | – | – | – | – | – | – | – | – | |
| – | – | 2.842 | vw | 2.840 | w | 2.842 | w | 2.841 | w | 2.838 | w | |
| 2.807 | m | 2.811 | vw | – | – | – | – | – | – | – | – | |
| 2.739 | m | 2.758 | vw | – | – | – | – | – | – | – | – | |
| – | – | 2.707 | m | 2.695 | m | 2.687 | st | 2.677 | m | 2.671 | m | |
| 2.648 | vvw | 2.651 | vvw | 2.656 | vvw | 2.648 | w | 2.649 | w | 2.644 | vw | |
| 2.638 | vw | – | – | – | – | – | – | – | – | – | – | |
| 2.615 | st | 2.612 | vw | 2.613 | w | 2.608 | w | 2.612 | w | 2.605 | vw | |
| – | – | – | – | 2.587 | w | 2.590 | vw | 2.581 | vw | 2.583 | vw | |
| 2.548 | w | – | – | – | – | – | – | – | – | – | – | |
| 2.514 | w | – | – | – | – | – | – | – | – | – | – | |
| 2.496 | w | 2.484 | vvw | 2.471 | vvw | – | – | – | – | – | – | |
| – | – | – | – | – | – | – | – | 2.455 | w | 2.451 | vw | |
| – | – | 2.435 | vvw | – | – | 2.447 | vw | – | – | – | – | |
| – | – | – | – | 2.427 | vvw | – | – | 2.426 | vw | 2.421 | vvw | |

TABLE B-3.2 continued :

| d Å | I | d Å | I | d Å | I | d Å | I | d Å | I | d Å | I |
|---|---|---|---|---|---|---|---|---|---|---|---|
| 2.406 | vw | – | – | – | – | – | – | – | – | – | – |
| – | – | 2.384 | vw | 2.386 | w | 2.386 | vw | 2.381 | w | 2.383 | w |
| – | – | 2.355 | vvw | – | – | – | – | – | – | – | – |
| – | – | 2.217 | sh | 2.221 | sh | 2.221 | vvw | 2.217 | vvw | 2.216 | vw |
| 2.210 | vvw | – | – | – | – | – | – | – | – | – | – |
| 2.177 | w | – | – | – | – | – | – | – | – | – | – |
| 2.108 | m | 2.125 | sh | – | – | – | – | – | – | – | – |
| – | – | 2.086 | sh | 2.085 | sh | 2.090 | vvw | 2.084 | vw | 2.084 | vw |
| 2.072 | w | – | – | – | – | – | – | – | – | – | – |
| – | – | – | – | – | – | – | – | – | – | 2.054 | vvw |
| 2.031 | m-st | – | – | – | – | – | – | – | – | – | – |
| – | – | – | – | – | – | – | – | – | – | 1.992 | vvw |
| 1.993 | m | – | – | – | – | – | – | – | – | – | – |
| 1.959 | w | – | – | – | – | – | – | – | – | – | – |
| 1.936 | vst | 1.910 | vst | 1.907 | vst | 1.900 | vst | 1.890 | vst | 1.888 | vst |
| 1.885 | w | – | – | – | – | – | – | – | – | – | – |
| 1.870 | m | 1.872 | w | 1.874 | w | 1.874 | w | 1.870 | w | 1.871 | w |
| 1.856 | m-st | 1.857 | m | 1.858 | m | 1.858 | m | 1.856 | m | 1.857 | m |
| 1.746 | m | – | – | – | – | – | – | – | – | – | – |
| 1.733 | w | – | – | – | – | – | – | – | – | – | – |
| 1.728 | vw | – | – | – | – | – | – | – | – | – | – |
| 1.708 | w | – | – | – | – | – | – | – | – | – | – |
| 1.693 | w | – | – | – | – | – | – | – | – | – | – |
| 1.668 | w | – | – | – | – | – | – | – | – | – | – |
| 1.650 | m | – | – | – | – | – | – | – | – | – | – |
| – | – | 1.629 | w | 1.626 | w | 1.621 | w | 1.613 | m | 1.611 | m |
| 1.592 | m | 1.593 | w | 1.596 | m | 1.595 | m | 1.592 | m | 1.594 | m |
| 1.581 | vw | 1.575 | w | 1.578 | w | 1.578 | w | 1.576 | w | 1.576 | w |
| 1.574 | m | – | – | – | – | – | – | – | – | – | – |
| 1.566 | vw | 1.559 | vw | 1.557 | vvw | 1.550 | w | 1.543 | w | 1.542 | w |
| 1.532 | w | – | – | – | – | – | – | – | – | – | – |
| 1.518 | vw | – | – | – | – | – | – | – | – | – | – |
| 1.471 | vw | – | – | – | – | – | – | – | – | – | – |
| 1.449 | vw | – | – | – | – | – | – | – | – | – | – |
| 1.420 | m | – | – | – | – | – | – | – | – | – | – |
| 1.369 | w | – | – | | – | | | | | | |

TABLE B-3.3 : X-ray diffraction data for the Mixed Sulphide Material leach residues.

| WEIGHT % Cu DISSOLVED | | | | | | | | SULPHUR[207] | |
|---|---|---|---|---|---|---|---|---|---|
| 49.73 | | 61.70 | | 69.00 | | 93.00 | | | |
| d Å | I | d Å | I | d Å | I | d Å | I | d Å | I |
| – | – | – | – | – | – | 7.742 | vw | 7.69 | 6 |
| 6.189 | vw | 6.191 | vvw | 6.182 | vvw | – | – | – | – |
| – | – | – | – | 5.763 | vw | 5.759 | w | 5.76 | 14 |
| – | – | – | – | – | – | 5.678 | vw | 5.68 | 5 |
| – | – | – | – | – | – | 4.804 | vw | 4.80 | 2 |
| – | – | – | – | 4.730 | vw | 4.740 | vw | – | – |
| – | – | – | – | – | – | 4.204 | w | 4.19 | 2 |
| – | – | – | – | 4.072 | vw | 4.067 | m | 4.06 | 11 |
| – | – | – | – | – | – | 3.949 | vw | – | – |
| – | – | – | – | – | – | 3.912 | w | 3.91 | 12 |
| 3.784 | vw | 3.857 | vw | 3.864 | w | 3.857 | st | 3.85 | 100 |
| – | – | – | – | – | – | 3.570 | w | 3.57 | 8 |
| 3.450 | vw | 3.450 | vw | 3.450 | w | 3.449 | m | 3.44 | 40 |
| 3.387 | vw | – | – | 3.392 | vw | 3.389 | w | 3.38 | 3 |
| 3.332 | vvw | – | – | 3.345 | vw | 3.337 | w | 3.33 | 25 |
| 3.222 | w | 3.222 | w | 3.222 | w | 3.222 | m | 3.21 | 60 |
| – | – | – | – | 3.119 | vvw | 3.113 | w | 3.11 | 25 |
| 3.081 | st | 3.084 | st | 3.084 | st | 3.086 | m | 3.08 | 17 |
| – | – | – | – | – | – | – | – | 3.06 | ± |
| 3.044 | st | 3.040 | st | 3.044 | st | 3.037 | st | – | – |
| 2.839 | vw | 2.841 | w | 2.846 | w | 2.842 | m | 2.842 | 18 |
| – | – | – | – | – | – | 2.833 | m | – | – |
| – | – | – | – | – | – | 2.683 | vvw | 2.688 | 2 |
| – | – | – | – | – | – | – | – | 2.673 | 1 |
| 2.669 | m | 2.671 | m | 2.667 | m | 2.659 | w | – | – |
| 2.648 | vw | – | – | 2.649 | vw | 2.647 | vw | – | – |
| – | – | – | – | – | – | 2.619 | w | 2.621 | 13 |
| – | – | – | – | – | – | – | – | 2.614 | 4 |
| 2.609 | w | 2.610 | w | 2.609 | m | 2.605 | m | – | – |

TABLE B-3.3 continued :

| d Å | I | d Å | I | d Å | I | d Å | I | d Å | I |
|---|---|---|---|---|---|---|---|---|---|
| 2.587 | vw | 2.586 | vw | 2.587 | vw | 2.588 | w | – | – |
| – | – | – | – | – | – | 2.566 | vw | 2.569 | 8 |
| – | – | – | – | – | – | 2.501 | vw | 2.501 | 7 |
| – | – | – | – | – | – | 2.489 | vvw | – | – |
| 2.455 | vw | 2.455 | w | 2.458 | w | 2.458 | w | – | – |
| – | – | 2.437 | vvw | 2.445 | w | 2.440 | m | – | – |
| 2.424 | vvw | 2.424 | vw | 2.428 | w | 2.428 | w | 2.424 | 13 |
| – | – | – | – | – | – | 2.402 | vvw | 2.404 | 2 |
| 2.382 | w | 2.385 | w | 2.387 | w | 2.386 | m | – | – |
| – | – | – | – | – | – | 2.373 | vw | 2.375 | 4 |
| – | – | – | – | – | – | 2.365 | vw | 2.366 | 4 |
| – | – | – | – | 2.311 | vw | – | – | – | – |
| – | – | – | – | 2.288 | vw | 2.284 | w | 2.288 | 6 |
| 2.212 | vw | 2.217 | vw | 2.221 | w | 2.217 | m | 2.215 | 2 |
| – | – | – | – | – | – | 2.143 | w | 2.146 | 4 |
| – | – | – | – | – | – | 2.110 | m | 2.112 | 10 |
| – | – | – | – | – | – | 2.098 | vw | 2.098 | 2 |
| 2.088 | vw | 2.087 | vw | 2.090 | w | 2.087 | m | – | – |
| – | – | – | – | – | – | 2.075 | vw | – | – |
| 2.051 | vvw | – | – | 2.053 | w | 2.050 | vw | 2.057 | 1 |
| – | – | – | – | – | – | 2.044 | vw | 2.041 | 1 |
| 1.999 | vvw | – | – | 1.995 | w | 1.995 | vw | 2.003 | 2 |
| – | – | – | – | – | – | 1.986 | vw | 1.988 | 4 |
| 1.966 | vw | – | – | 1.966 | w | 1.959 | w | 1.957 | 2 |
| – | – | – | – | – | – | 1.923 | vw | 1.926 | 1 |
| – | – | – | – | 1.912 | vw | 1.905 | w | 1.900 | 7 |
| 1.887 | vst | 1.885 | vst | 1.887 | vst | – | – | – | – |
| 1.872 | w | 1.871 | vw | 1.873 | w | 1.873 | st | – | – |
| 1.856 | m | 1.856 | m | 1.859 | w | 1.856 | st | 1.856 | 1 |
| – | – | – | – | – | – | 1.838 | w | 1.838 | 1 |
| – | – | – | – | – | – | 1.826 | vw | 1.823 | 4 |
| – | – | – | – | 1.784 | vw | 1.784 | w | 1.781 | 11 |
| – | – | – | – | – | – | 1.758 | w | 1.754 | 7 |

TABLE B-3.3 continued :

| d Å | I | d Å | I | d Å | I | d Å | I | d Å | I |
|---|---|---|---|---|---|---|---|---|---|
| – | – | – | – | 1.723 | vw | 1.723 | m | 1.725 | 8 |
| – | – | – | – | – | – | 1.715 | m | – | – |
| – | – | – | – | – | – | 1.699 | w | 1.698 | 7 |
| – | – | – | – | – | – | 1.685 | vvw | – | – |
| – | – | – | – | – | – | 1.660 | w | 1.665 | 2 |
| – | – | – | – | – | – | 1.652 | vw | 1.658 | 2 |
| – | – | – | – | – | – | 1.643 | vw | 1.647 | 5 |
| – | – | – | – | – | – | 1.619 | vw | 1.622 | 6 |
| 1.610 | m | 1.609 | m | 1.609 | m | 1.608 | w | 1.607 | 6 |
| 1.594 | m | 1.594 | m | 1.595 | m | 1.595 | st | 1.595 | 3 |
| – | – | – | – | – | – | 1.589 | vw | – | – |
| 1.576 | w | 1.576 | m | 1.577 | m | 1.577 | m | – | – |
| – | – | – | – | – | – | 1.558 | vw | 1.563 | 2 |
| – | – | – | – | – | – | 1.551 | vw | – | – |
| 1.541 | w | 1.539 | w | 1.540 | w | 1.537 | vw | 1.542 | 1 |
| – | – | – | – | – | – | 1.526 | vw | 1.531 | 1 |
| 1.519 | vw | – | – | 1.520 | vw | – | – | – | – |
| – | – | – | – | – | – | 1.510 | vw | 1.515 | 1 |
| – | – | – | – | – | – | 1.500 | vw | 1.504 | 1 |
| – | – | – | – | – | – | 1.483 | vw | 1.490 | 1 |
| – | – | – | – | – | – | 1.478 | vw | 1.475 | 2 |
| – | – | – | – | – | – | 1.470 | vw | – | – |
| – | – | – | – | – | – | 1.465 | vw | 1.461 | 1 |
| – | – | – | – | 1.459 | vw | 1.457 | w | – | – |
| – | – | – | – | – | – | 1.449 | vw | – | – |
| – | – | – | – | – | – | 1.436 | w | 1.439 | 3 |
| – | – | – | – | – | – | 1.417 | vw | 1.419 | 1 |
| – | – | – | – | – | – | 1.413 | vw | – | – |

TABLE B-3.4 : X-ray diffraction data for the mixed sulphide material leach residue with 93.00% of the Cu dissolved, after removal of the elemental sulphur by treatment with $CS_2$.

| Residue 93% Cu Dissolved | | Chalcopyrite (207) | | $Ag_2S$ (207) | | Residue | | Chalcopyrite | | $Ag_2S$ | |
|---|---|---|---|---|---|---|---|---|---|---|---|
| d Å | I | d Å | I | d Å | I | d Å | I | d Å | I | d Å | I |
| 3.96 | vw | - | - | 3.96 | 10 | 1.592 | m | 1.591 | 60 | - | - |
| 3.685 | w | - | - | - | - | 1.587 | vw | - | - | 1.587 | 4 |
| 3.573 | w | - | - | 3.571 | 6 | 1.581 | w | - | - | 1.579 | 10 |
| 3.435 | m | - | - | 3.437 | 35 | 1.574 | w | 1.573 | 20 | - | - |
| 3.380 | m | - | - | 3.383 | 20 | 1.554 | w | - | - | 1.554 | 8 |
| 3.075 | m | - | - | 3.080 | 60 | 1.539 | w | - | - | 1.540 | 8 |
| 3.039 | vst | 3.03 | 100 | - | - | 1.517 | w | 1.518 | 5 | - | - |
| 2.836 | st | - | - | 2.836 | 70 | 1.512 | vw | - | - | 1.513 | 12 |
| 2.705 | w | - | - | - | - | 1.484 | w | - | - | 1.483 | 10 |
| 2.665 | m | - | - | 2.664 | 45 | 1.468 | vw | - | - | 1.470 | 10 |
| 2.608 | st | - | - | 2.606 | 100 | 1.453 | vw | - | - | - | - |
| 2.578 | m | - | - | 2.583 | 70 | 1.446 | vw | - | - | - | - |
| 2.519 | vw | - | - | - | - | 1.416 | vw | - | - | - | - |
| 2.452 | m | - | - | 2.456 | 70 | 1.406 | vw | - | - | - | - |
| 2.436 | m | - | - | 2.440 | 80 | 1.380 | vw | - | - | 1.379 | 6 |
| 2.419 | m | - | - | 2.421 | 60 | | | | | | |
| 2.379 | st | - | - | 2.383 | 75 | | | | | | |
| 2.254 | vw | - | - | - | - | | | | | | |
| 2.209 | m | - | - | 2.213 | 45 | | | | | | |
| - | - | - | - | 2.187 | 40 | | | | | | |
| - | - | - | - | 2.164 | 40 | | | | | | |
| 2.090 | vw | - | - | 2.093 | 16 | | | | | | |
| 2.083 | m | - | - | 2.083 | 45 | | | | | | |
| 2.071 | vw | - | - | 2.072 | 16 | | | | | | |
| 2.047 | w | - | - | 2.047 | 16 | | | | | | |
| 1.995 | w | - | - | 1.995 | 16 | | | | | | |
| 1.983 | vw | - | - | - | - | | | | | | |
| 1.963 | m | - | - | 1.962 | 20 | | | | | | |
| - | - | - | - | 1.935 | 4 | | | | | | |
| 1.917 | vw | - | - | 1.918 | 4 | | | | | | |
| 1.901 | w | - | - | 1.903 | 14 | | | | | | |
| 1.869 | st | 1.865 | 40 | 1.866 | 16 | | | | | | |
| 1.855 | st | 1.854 | 80 | - | - | | | | | | |
| 1.842 | w | - | - | - | - | | | | | | |
| - | - | - | - | 1.816 | 4 | | | | | | |
| - | - | - | - | 1.798 | 4 | | | | | | |
| 1.731 | vw | - | - | 1.733 | 12 | | | | | | |
| 1.718 | m | - | - | 1.718 | 20 | | | | | | |
| 1.697 | w | - | - | - | - | | | | | | |
| 1.690 | vw | - | - | 1.691 | 6 | | | | | | |
| - | | - | - | 1.610 | 4 | | | | | | |

TABLE B-3.5 : X-ray diffraction data for the Mixed Sulphide Material leached in solutions containing Chloride ion.

| SULPHUR (207) | | $CuFeS_2$ (207) | | AgCl (207) | | WEIGHT % DISSOLVED | | | | | | | | | |
|---|---|---|---|---|---|---|---|---|---|---|---|---|---|---|---|
| | | | | | | Cu 56.41 Ag 0.58 | | Cu 62.15 Ag 15.55 | | Cu 67.13 Ag 67.97 | | Cu 95.03 Ag 0.79 | | Cu 90.35 Ag 76.84 | |
| d Å | I | d Å | I | d Å | I | d Å | I | d Å | I | d Å | I | d Å | I | d Å | I |
| 7.69 | 6 | – | – | – | – | 7.741 | vvw | 7.739 | vvw | 7.713 | vvw | 7.695 | vw | 7.722 | vw |
| 5.76 | 14 | – | – | – | – | 5.769 | vw | 5.785 | vw | 5.755 | vw | 5.756 | w | 5.757 | w |
| 5.68 | 5 | – | – | – | – | 5.683 | vvw | – | – | – | – | 5.693 | vw | 5.702 | vw |
| 4.80 | 2 | – | – | – | – | – | – | – | – | – | – | 4.804 | vw | 4.811 | vvw |
| – | – | – | – | – | – | 4.712 | vw | 4.739 | vw | – | – | 4.696 | vw | 4.714 | vw |
| 4.19 | 12 | – | – | – | – | – | – | – | – | – | – | 4.183 | vw | 4.193 | w |
| 4.06 | 11 | – | – | – | – | 4.063 | w | 4.076 | vw | 4.061 | vw | 4.054 | w | 4.064 | w |
| – | – | – | – | – | – | – | – | – | – | 3.989 | vw | – | – | – | – |
| 3.91 | 12 | – | – | – | – | 3.924 | w | 3.928 | vw | 3.926 | vw | 3.912 | w | 3.921 | vw |
| 3.85 | 100 | – | – | – | – | 3.856 | m | 3.871 | m | 3.855 | m | 3.844 | m | 3.853 | st |
| 3.57 | 8 | – | – | – | – | 3.574 | vw | 3.581 | vw | 3.570 | vvw | 3.566 | vw | 3.572 | w |
| 3.44 | 40 | – | – | – | – | 3.450 | w | 3.459 | m | 3.446 | w | 3.440 | m | 3.445 | m |
| 3.38 | 3 | – | – | – | – | 3.384 | vvw | – | – | 3.389 | vvw | 3.377 | vw | 3.385 | vw |
| 3.33 | 25 | – | – | – | – | 3.337 | w | 3.351 | w | 3.339 | w | 3.330 | w | 3.337 | w |
| 3.21 | 60 | – | – | 3.203 | 49 | 3.207 | st | 3.217 | m | 3.212 | m | 3.200 | st | 3.215 | m |
| 3.11 | 25 | – | – | – | – | 3.117 | vw | 3.125 | w | 3.116 | vw | 3.108 | w | 3.112 | w |
| 3.08 | 17 | – | – | – | – | 3.088 | sh | 3.089 | vw | 3.085 | vw | 3.081 | w | 3.084 | w |
| 3.06 | ± | | | | | 3.048 | | | | | | | | | |
| – | – | 3.03 | 100 | – | – | 3.040 | vst | 3.047 | vst | 3.042 | vst | 3.033 | st | 3.038 | vst |
| – | – | – | – | – | – | 2.907 | vw | – | – | – | – | – | – | 2.899 | vw |
| 2.842 | 18 | – | – | – | – | 2.850 | vw | 2.860 | w | 2.848 | vw | 2.842 | w | – | – |
| – | – | – | – | 2.774 | 100 | 2.777 | vst | 2.785 | st | 2.777 | m | 2.770 | vst | 2.775 | vvw |
| – | – | – | – | – | – | – | – | 2.728 | sh | – | – | – | – | 2.725 | vvw |
| 2.688 | 2 | – | – | – | – | – | – | 2.652 | vw | – | – | 2.688 | vvw | 2.692 | vvw |
| – | – | – | – | – | – | 2.646 | vw | – | – | 2.643 | w | 2.639 | vvw | 2.645 | w |
| 2.621 | 13 | 2.63 | 5 | – | – | 2.627 | vvw | 2.633 | vw | 2.627 | vw | 2.620 | vw | 2.624 | w |
| 2.614 | 4 | – | – | – | – | 2.605 | vvw | 2.613 | vw | 2.609 | vw | 2.601 | vvw | 2.607 | vw |
| 2.569 | 8 | – | – | – | – | – | – | 2.580 | vw | 2.572 | vw | 2.563 | vw | 2.569 | w |

TABLE B-3.5 continued :

| SULPHUR | | $CuFeS_2$ | | AgCl | | | | | | RESIDUES | | | | | |
|---|---|---|---|---|---|---|---|---|---|---|---|---|---|---|---|
| d Å | I | d Å | I | d Å | I | d Å | I | d Å | I | d Å | I | d Å | I | d Å | I |
| 2.501 | 7 | – | – | – | – | 2.502 | vw | 2.510 | vw | 2.502 | w | 2.498 | vw | 2.499 | w |
| – | – | – | – | – | – | – | – | – | – | – | – | 2.483 | vvw | 2.485 | vw |
| 2.424 | 13 | – | – | – | – | 2.428 | vw | 2.431 | vw | 2.430 | w | 2.421 | w | 2.425 | w |
| 2.404 | 2 | – | – | – | – | – | – | – | – | – | – | 2.403 | vw | 2.403 | vw |
| 2.375 | 4 | – | – | – | – | 2.377 | vw | 2.378 | vw | 2.375 | vw | 2.375 | vw | 2.377 | w |
| 2.366 | 4 | – | – | – | – | – | – | – | – | – | – | 2.365 | vw | 2.368 | w |
| – | – | – | – | – | – | 2.308 | vw | 2.313 | vw | 2.309 | vw | – | – | 2.305 | vw |
| 2.288 | 6 | – | – | – | – | 2.290 | vw | 2.294 | vw | 2.289 | w | 2.285 | w | 2.288 | w |
| 2.215 | 2 | – | – | – | – | – | – | – | – | – | – | – | – | 2.216 | vw |
| 2.146 | 4 | – | – | – | – | 2.129 | vvw | – | – | – | – | 2.142 | vw | 2.146 | vw |
| 2.112 | 10 | – | – | – | – | 2.116 | w | 2.121 | vw | 2.117 | w | 2.111 | vw | 2.115 | m |
| 2.098 | 2 | – | – | – | – | – | – | – | – | – | – | 2.094 | vw | 2.098 | vw |
| 2.057 | 1 | – | – | – | – | – | – | – | – | – | – | – | – | 2.059 | vw |
| 2.041 | 1 | – | – | – | – | – | – | – | – | – | – | – | – | 2.041 | vw |
| 2.003 | 2 | – | – | – | – | – | – | – | – | – | – | – | – | 2.005 | vw |
| 1.988 | 4 | – | – | – | – | – | – | – | – | – | – | 1.984 | vw | 1.989 | w |
| 1.957 | 2 | – | – | 1.962 | 50 | 1.948 | st | 1.967 | m | 1.966 | m | 1.958 | st | 1.958 | vw |
| – | – | – | – | – | – | – | – | – | – | – | – | – | – | 1.942 | sh |
| 1.926 | 1 | – | – | – | – | – | – | – | – | – | – | – | – | 1.925 | sh |
| 1.900 | 7 | – | – | – | – | 1.885 | m | 1.892 | sh | 1.905 | vvw | 1.899 | w | 1.903 | m |
| – | – | 1.865 | 40 | – | – | 1.870 | m | 1.875 | m | 1.871 | m | 1.868 | m | 1.870 | st |
| – | – | – | – | – | – | – | – | – | – | 1.866 | m | – | – | 1.863 | st |
| 1.856 | 1 | 1.854 | 80 | – | – | 1.856 | m | 1.860 | m | 1.858 | m | 1.852 | m | 1.854 | st |
| 1.823 | 4 | – | – | – | – | 1.827 | vvw | – | – | 1.826 | vvw | 1.820 | vw | 1.824 | w |
| 1.781 | 11 | – | – | – | – | 1.784 | w | 1.787 | vw | 1.782 | vw | 1.780 | vw | 1.781 | w |
| 1.754 | 7 | – | – | – | – | 1.757 | vw | 1.760 | vw | 1.758 | vw | 1.751 | vw | 1.756 | w |
| 1.725 | 8 | – | – | – | – | 1.725 | vw | 1.729 | vw | 1.726 | vw | 1.721 | vw | 1.724 | w |
| 1.698 | 7 | – | – | – | – | 1.699 | vw | 1.702 | vw | 1.701 | vw | 1.695 | vw | 1.698 | w |
| 1.665 | 2 | – | – | 1.673 | 15 | 1.674 | m | 1.678 | m | 1.675 | w | 1.670 | m | 1.665 | vw |
| 1.647 | 5 | – | – | – | – | 1.647 | vvw | 1.652 | vvw | 1.647 | vw | 1.643 | vw | 1.647 | w |
| 1.622 | 6 | – | – | – | – | 1.622 | vvw | 1.625 | vvw | 1.629 | w | 1.620 | vw | 1.622 | w |
| 1.607 | 6 | – | – | 1.602 | 15 | 1.602 | m | 1.605 | m | 1.603 | vw | 1.599 | m | 1.606 | w |

TABLE B-3.5 continued :

| SULPHUR | | $CuFeS_2$ | | AgCl | | | | | | RESIDUES | | | | | |
|---|---|---|---|---|---|---|---|---|---|---|---|---|---|---|---|
| d Å | I | d Å | I | d Å | I | d Å | I | d Å | I | d Å | I | d Å | I | d Å | I |
| 1.593 | 3 | 1.591 | 60 | – | – | 1.592 | m | 1.595 | m | 1.593 | m | 1.590 | m | 1.591 | st |
| – | – | 1.573 | 20 | – | – | 1.576 | m | 1.578 | m | 1.576 | w | 1.571 | w | 1.575 | m |
| 1.563 | 2 | – | – | – | – | – | – | – | – | – | – | – | – | 1.563 | vw |
| 1.542 | 1 | – | – | – | – | – | – | – | – | – | – | – | – | 1.543 | vw |
| 1.531 | 1 | – | – | – | – | – | – | – | – | – | – | – | – | 1.529 | vw |
| 1.515 | 1 | 1.518 | 20 | – | – | 1.518 | vw | 1.521 | vw | 1.519 | vvw | – | – | 1.518 | vw |
| 1.504 | 1 | – | – | – | – | – | – | – | – | – | – | – | – | 1.504 | vw |
| 1.475 | 2 | – | – | – | – | – | – | – | – | – | – | – | – | 1.473 | vw |
| 1.439 | 3 | – | – | – | – | – | – | – | – | – | – | 1.434 | vvw | 1.437 | sh |
| 1.424 | 3 | – | – | – | – | – | – | – | – | – | – | – | – | 1.421 | sh |
| 1.419 | 1 | – | – | – | – | – | – | – | – | – | – | 1.418 | vvw | 1.415 | sh |
| – | – | – | – | – | – | – | – | – | – | 1.402 | vw | 1.412 | vvw | – | – |
| 1.391 | 1 | – | – | 1.387 | 6 | 1.386 | m | 1.388 | w | 1.386 | vw | 1.384 | m | 1.390 | sh |

B-4 : Mixtures of Pure Minerals, X-ray diffraction data.

TABLE B-4.1 : X-ray data for the Bornite+Chalcopyrite+ Stromeyerite mixture after 34.74 wt% ofthe Copper had dissolved.

| d Å | I |
|---|---|
| 3.437 | vw |
| 3.372 | vw |
| 3.265, 3.235 | w |
| 3.081, 3.025 | st |
| Above band includes the lines: | |
| 3.076 | st |
| 3.037 | vst |
| 2.833 | w |
| 2.661 | vw |
| 2.644 | vw |
| 2.605 | w |
| 2.582 | w |
| 2.454 | w |
| 2.438 | w |
| 2.420 | w |
| 2.381 | m |
| 2.214 | w |
| 2.080 | w |
| 2.046 | vw |
| 1.963 | vw |
| 1.886, 1.854 | st |
| Above band includes the lines: | |
| 1.879 | st |
| 1.869 | st |
| 1.857 | st |
| 1.848 | vw |
| 1.594, 1.587, 1.575 | m, w |

TABLE B-4.3 continued:

| d Å | I |
|---|---|
| 1.967 | vw |
| 1.876 | w |
| 1.865 | st |
| 1.591 | w |

TABLE B-4.2 : X-ray data for the Bornite + Chalcopyrite mixture after 40.38 wt% of the Copper had dissolved.

| d Å | I |
|---|---|
| 4.723 | vvw |
| 3.857 | vw |
| 3.758 | vw |
| 3.448 | vw |
| 3.351 | vvw |
| 3.252, 3.222 | w |
| 3.064, 3.036 | st |
| Above band includes the line: | |
| 3.049 | st |
| 2.652, 2.633 | w |
| 1.873 | st |
| 1.861 | st |
| 1.598, 1.591 | w |
| 1.584 | w |
| 1.577 | w |

TABLE B-4.3 : X-ray data for the Bornite + Stromeyerite mixture after 46.66 wt% of the Copper had dissolved.

| d Å | I |
|---|---|
| 3.866 | vw |
| 3.580 | vw |
| 3.447 | w |
| 3.387 | vw |
| 3.347 | vw |
| 3.283 | vw |
| 3.253, 3.221 | w |
| 3.057, 3.035 | st |
| 2.840 | w |
| 2.673 | vw |
| 2.639 | w |
| 2.610 | w |
| 2.588 | vw |
| 2.442 | vw |
| 2.423 | vw |
| 2.386 | w |
| 2.217 | vw |
| 2.085 | w |

B-5 : Diffraction data from the A.S.T.M. X-ray Index File[207].

TABLE B-5.1

Mckinstryite[145]
$Cu_{0.8}Ag_{1.2}S$

| d Å | I |
|---|---|
| 6.97 | 5 |
| 4.20 | 5 |
| 4.02 | 10 |
| 3.91 | 10 |
| 3.69 | 5 |
| 3.51 | 60 |
| 3.39 | 10 |
| 3.06 | 60 |
| 2.945 | 5 |
| 2.913 | 5 |
| 2.862 | 60 |
| 2.797 | 10 |
| 2.763 | 5 |
| 2.688 | 5 |
| 2.606 | 100 |
| 2.567 | 40 |
| 2.524 | 10 |
| 2.505 | 10 |
| 2.472 | 5 |
| 2.436 | 5 |
| 2.407 | 40 |
| 2.333 | 5 |
| 2.307 | 30 |
| 2.250 | 10 |
| 2.188 | 30 |
| 2.167 | 20 |
| 2.137 | 5 |
| 2.088 | 20 |
| 2.070 | 70 |
| 2.009 | 10 |
| 1.948 | 50 |
| 1.888 | 20 |
| 1.874 | 5 |
| 1.844 | 10 |
| 1.827 | 5 |

TABLE B-5.2

Synthetic[133]
$Cu_{0.8}Ag_{1.2}S$

| d Å | I |
|---|---|
| 4.00 | 40 |
| 3.88 | 40 |
| 3.50 | 60 |
| 3.05 | 60 |
| 2.861 | 60 |
| 2.641 | 20 |
| 2.606 | 100 |
| 2.563 | 40 |
| 2.521 | 40 |
| 2.499 | 20 |
| 2.406 | 60 |
| 2.308 | 60 |
| 2.187 | 40 |
| 2.164 | 40 |
| 2.090 | 40 |
| 2.069 | 60 |
| 2.009 | 40 |
| 1.946 | 60 |

TABLE B-5.3

Synthetic Jalpaite[133]
$Ag_{1.55}Cu_{0.45}S$

| d Å | I |
|---|---|
| 6.93 | 40 |
| 4.32 | 60 |
| 3.671 | 40 |
| 3.564 | 40 |
| 3.479 | 40 |
| 2.803 | 100 |
| 2.753 | 100 |
| 2.483 | 60 |
| 2.431 | 100 |
| 2.353 | 100 |
| 2.325 | 40 |
| 2.268 | 40 |
| 2.165 | 40 |
| 2.120 | 60 |
| 2.011 | 40 |
| 1.930 | 20 |
| 1.865 | 20 |
| 1.743 | 40 |
| 1.714 | 20 |
| 1.677 | 20 |
| 1.586 | 20 |
| 1.567 | 20 |
| 1.489 | 40 |
| 1.471 | 20 |
| 1.442 | 40 |
| 1.414 | 40 |
| 1.395 | 40 |
| 1.376 | 20 |
| 1.327 | 40 |
| 1.285 | 20 |
| 1.188 | 20 |
| 1.146 | 20 |

TABLE B-5.4

Jalpaite[144]
$Ag_3CuS_2$

| d Å | I |
|---|---|
| 6.95 | 40 |
| 4.30 | 60 |
| 3.67 | 20 |
| 3.57 | 20 |
| 3.46 | 20 |
| 3.41 | 5 |
| 3.08 | 5 |
| 3.05 | 5 |
| 2.961 | 10 |
| 2.794 | 90 |
| 2.740 | 80 |
| 2.585 | 5 |
| 2.475 | 50 |
| 2.422 | 80 |
| 2.345 | 100 |
| 2.311 | 30 |
| 2.268 | 50 |
| 2.158 | 40 |
| 2.114 | 70 |
| 2.087 | 5 |
| 2.006 | 60 |
| 1.922 | 40 |
| 1.863 | 10 |
| 1.783 | 20 |
| 1.739 | 40 |
| 1.707 | 10 |
| 1.677 | 5 |
| 1.580 | 10 |
| 1.563 | 20 |
| 1.524 | 5 |
| 1.483 | 30 |
| 1.468 | 5 |
| 1.450 | 5 |
| 1.436 | 40 |
| 1.412 | 20 |
| 1.391 | 20 |
| 1.375 | 10 |
| 1.363 | 5 |
| 1.352 | 10 |
| 1.206 | 5 |
| 1.190 | 10 |
| 1.181 | 5 |

TABLE B-5.5

Silver sulphide
$Ag_2S$

| d Å | I |
|---|---|
| 3.96 | 10 |
| 3.571 | 6 |
| 3.437 | 35 |
| 3.383 | 20 |
| 3.080 | 60 |
| 2.836 | 70 |
| 2.664 | 45 |
| 2.605 | 100 |
| 2.583 | 70 |
| 2.456 | 70 |
| 2.440 | 80 |
| 2.421 | 60 |
| 2.383 | 75 |
| 2.213 | 45 |
| 2.093 | 16 |
| 2.083 | 45 |
| 2.072 | 16 |
| 2.047 | 16 |
| 1.995 | 16 |
| 1.963 | 20 |
| 1.935 | 4 |
| 1.918 | 4 |
| 1.903 | 14 |
| 1.866 | 16 |
| 1.816 | 4 |
| 1.798 | 4 |
| 1.733 | 12 |
| 1.718 | 20 |
| 1.691 | 6 |
| 1.610 | 4 |
| 1.587 | 14 |
| 1.579 | 10 |
| 1.554 | 8 |
| 1.540 | 8 |
| 1.513 | 12 |
| 1.483 | 10 |
| 1.470 | 10 |
| 1.459 | 14 |
| 1.379 | 6 |
| plus 5 lines to 1.305 | |

TABLE B-5.6

Silver chloride
AgCl

| d Å | I |
|---|---|
| 3.20 | 50 |
| 2.774 | 100 |
| 1.962 | 50 |
| 1.673 | 16 |
| 1.602 | 16 |
| 1.387 | 6 |
| 1.273 | 4 |
| 1.241 | 12 |
| 1.1326 | 8 |
| 1.0680 | 4 |
| 0.9810 | 2 |
| 0.9380 | 2 |
| 0.9248 | 4 |
| 0.8774 | 4 |
| 0.8462 | 2 |
| 0.8366 | 4 |

TABLE B-5.7

Covellite
CuS

| d Å | I |
|---|---|
| 8.18 | 8 |
| 3.285 | 14 |
| 3.220 | 30 |
| 3.048 | 65 |
| 2.813 | 100 |
| 2.724 | 55 |
| 2.317 | 10 |
| 2.097 | 6 |
| 2.043 | 8 |
| 1.902 | 25 |
| 1.896 | 75 |
| 1.735 | 35 |
| 1.634 | 4 |
| 1.609 | 8 |
| 1.572 | 16 |
| 1.556 | 35 |
| 1.463 | 6 |
| 1.390 | 6 |
| 1.354 | 8 |
| 1.343 | 6 |
| 1.280 | 10 |
| 1.227 | 8 |
| 1.210 | 10 |
| 1.0998 | 8 |
| 1.0946 | 10 |
| 1.0607 | 10 |
| 1.0155 | 8 |

TABLE B-5.8

Sodium Chloride
NaCl

| d Å | I |
|---|---|
| 3.258 | 13 |
| 2.821 | 100 |
| 1.994 | 55 |
| 1.701 | 2 |
| 1.628 | 15 |
| 1.410 | 6 |
| 1.294 | 1 |

| d Å | I |
|---|---|
| 1.261 | 11 |
| 1.1515 | 7 |
| 1.0855 | 1 |
| 0.9969 | 2 |
| 0.9533 | 1 |
| 0.9401 | 3 |
| 0.8917 | 4 |
| 0.8601 | 1 |
| 0.8503 | 3 |
| 0.8141 | 2 |

# APPENDIX C

## X-RAY POWDER PHOTOGRAPHS

## AND

## PHOTOMICROGRAPHS OF RESIDUES



MAGNIFICATIONS :

| | |
|---|---|
| C-2.1 to C-2.6 | x480 |
| C-2.7 to C-2.10 | x600 |
| C-2.11 to C-2.14 | x240 |
| C-2.15 | x160 |
| C-2.16 to C-2.22 | x480 |
| C-2.23 | x160 |

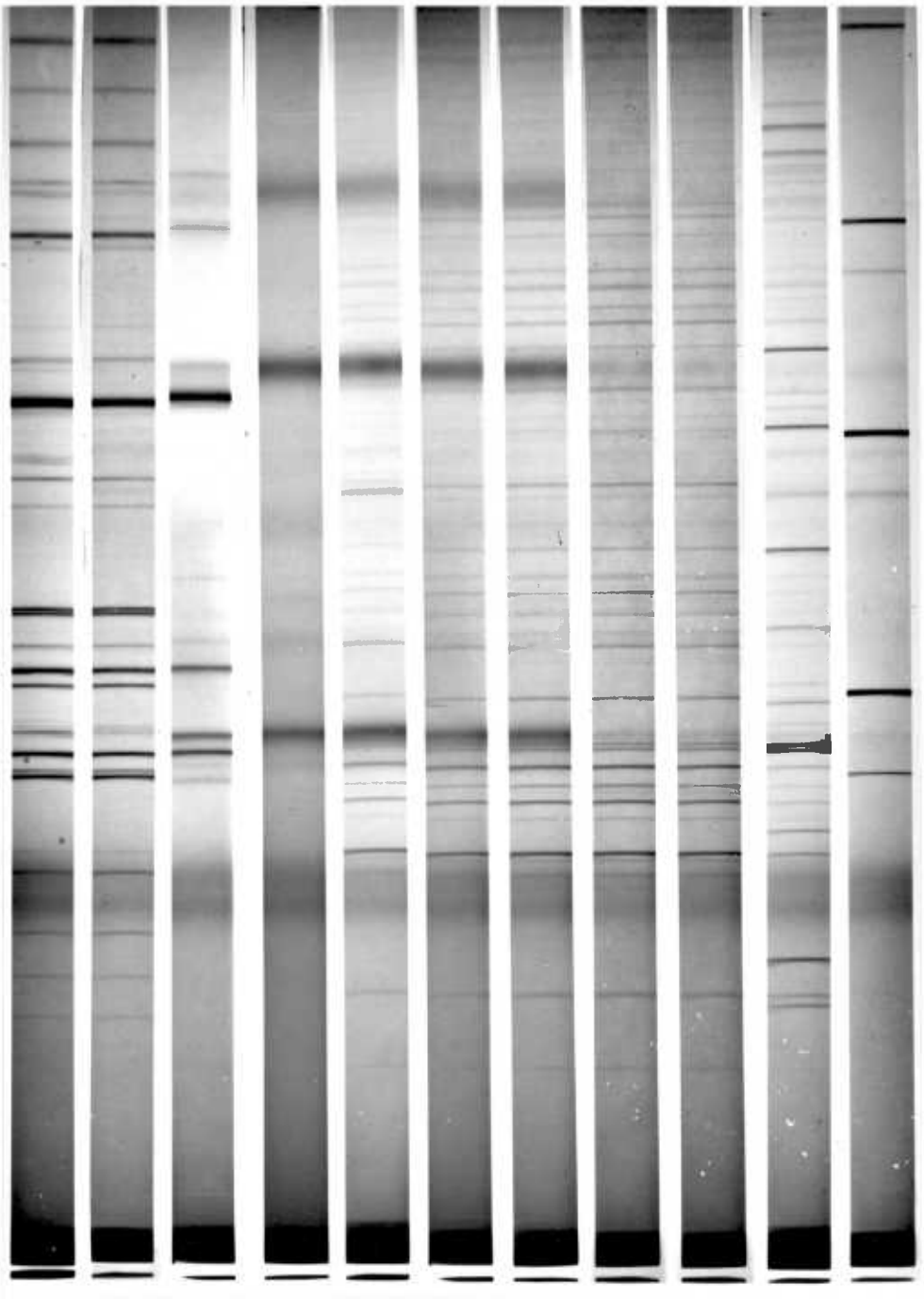


FIGURE C-1.1 : X-Ray Powder Photographs.

(a) Pure Bornite
(b) Silver-doped Bornite
(c) " " " residue, 20.1% Cu dissolved
(d) " " " " , 44.68% Cu, 0.20% Ag diss.
(e) " " " " , 64.29% Cu, 0.86% Ag diss.
(f) " " " " , 84.04% Cu, 1.76% Ag " .
(g) " " " " , 89.67% Cu, 4.97% Ag " .
(h) " " " " , 97.79% Cu, 1.20% Ag " .
(i) " " " " , 98.76% Cu, 2.16% Ag " .
(j) Jarosite
(k) NaCl (calibration standard).

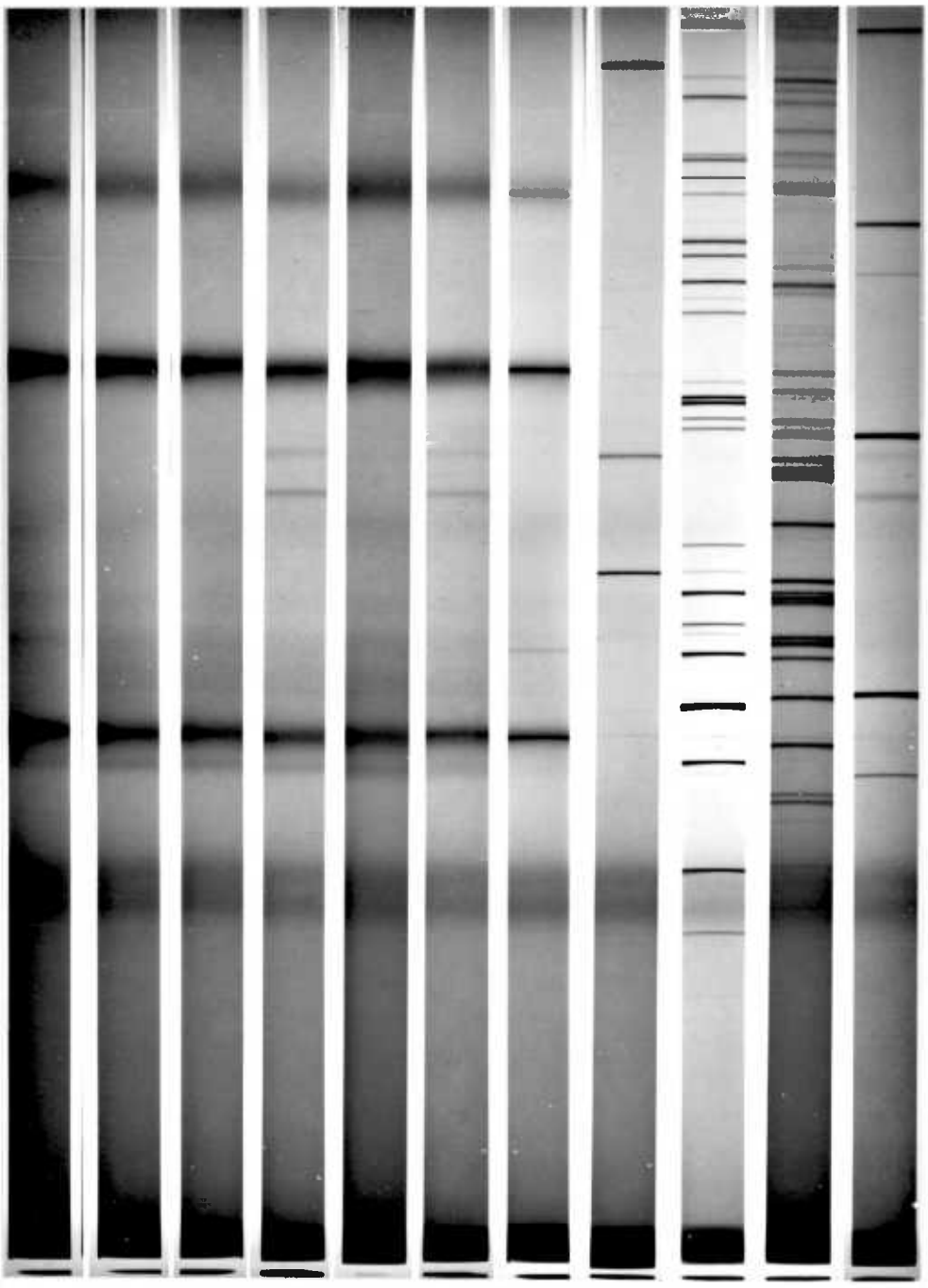

(a) (b) (c) (d) (e) (f) (g) (h) (i) (j) (k)

FIGURE C-1.2 : X-Ray Powder Photographs

(a)-(f) : Silver-doped bornite residues after removal of elemental Sulphur by $CS_2$.

(a) 44.68% Cu, 0.20% Ag dissolved
(b) 64.29% Cu, 0.86% Ag dissolved
(c) 84.04% Cu, 1.76% Ag dissolved
(d) 89.67% Cu, 4.97% Ag dissolved
(e) 97.79% Cu, 1.20% Ag dissolved
(f) 98.76% Cu, 2.16% Ag dissolved

(g) Pure Bornite, 43.7% Cu dissolved

(h) Silver

(i) Silver Sulphate, $Ag_2SO_4$

(j) Silver Sulphide, $Ag_2S$

(k) NaCl (calibration standard).

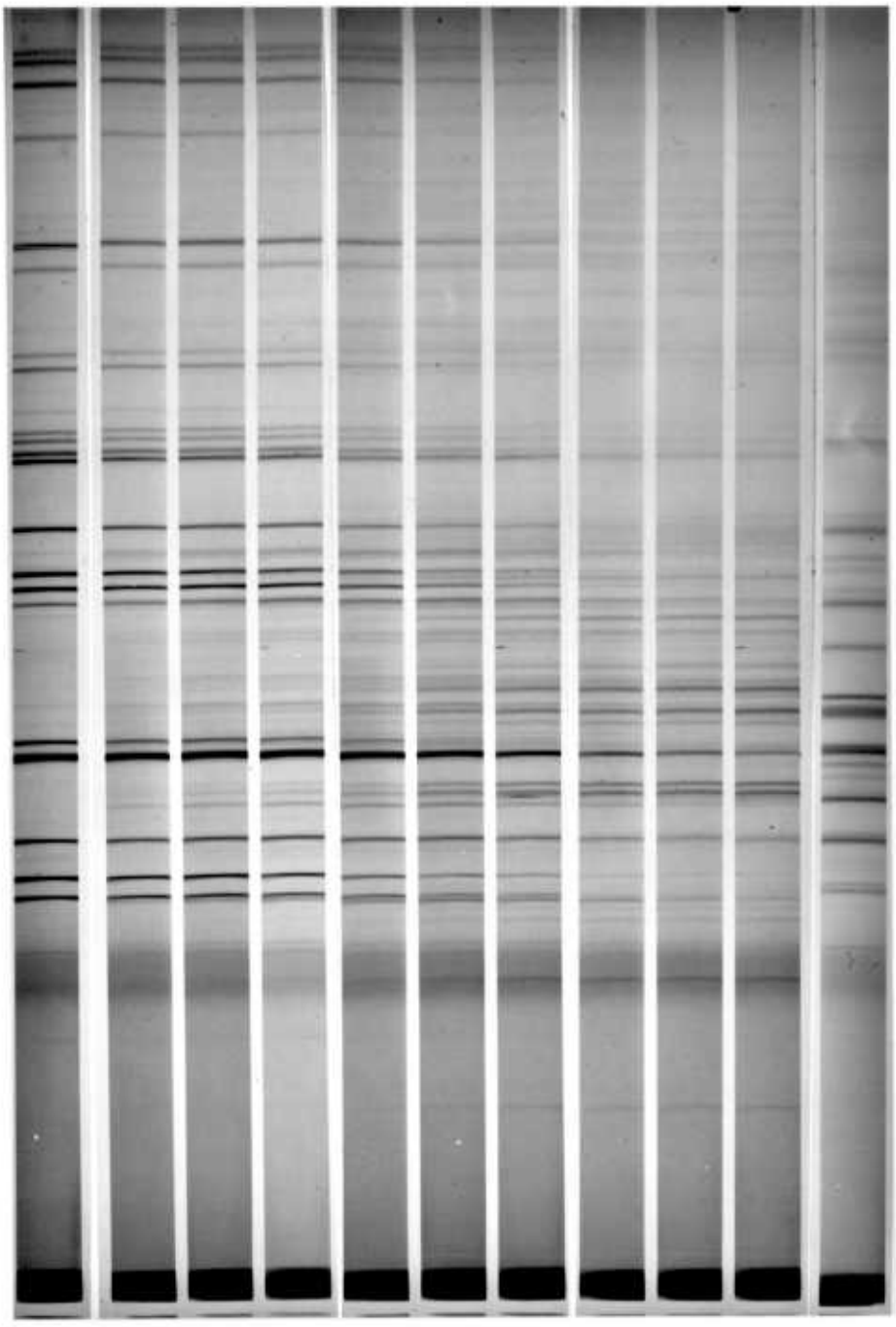

(a) (b) (c) (d) (e) (f) (g) (h) (i) (j) (k)

FIGURE C-1.3 : X-Ray Powder Photographs of Stromeyerite residues after leaching in ferric sulphate solutions.

(a) 0.00% Cu dissolved
(b) 5.44% " "
(c) 10.44% " "
(d) 12.17% " "
(e) 18.06% " "
(f) 26.15% " "
(g) 32.96% " "
(h) 38.16% " "
(i) 39.64% " "
(j) 41.72% " "
(k) 59.94% " "

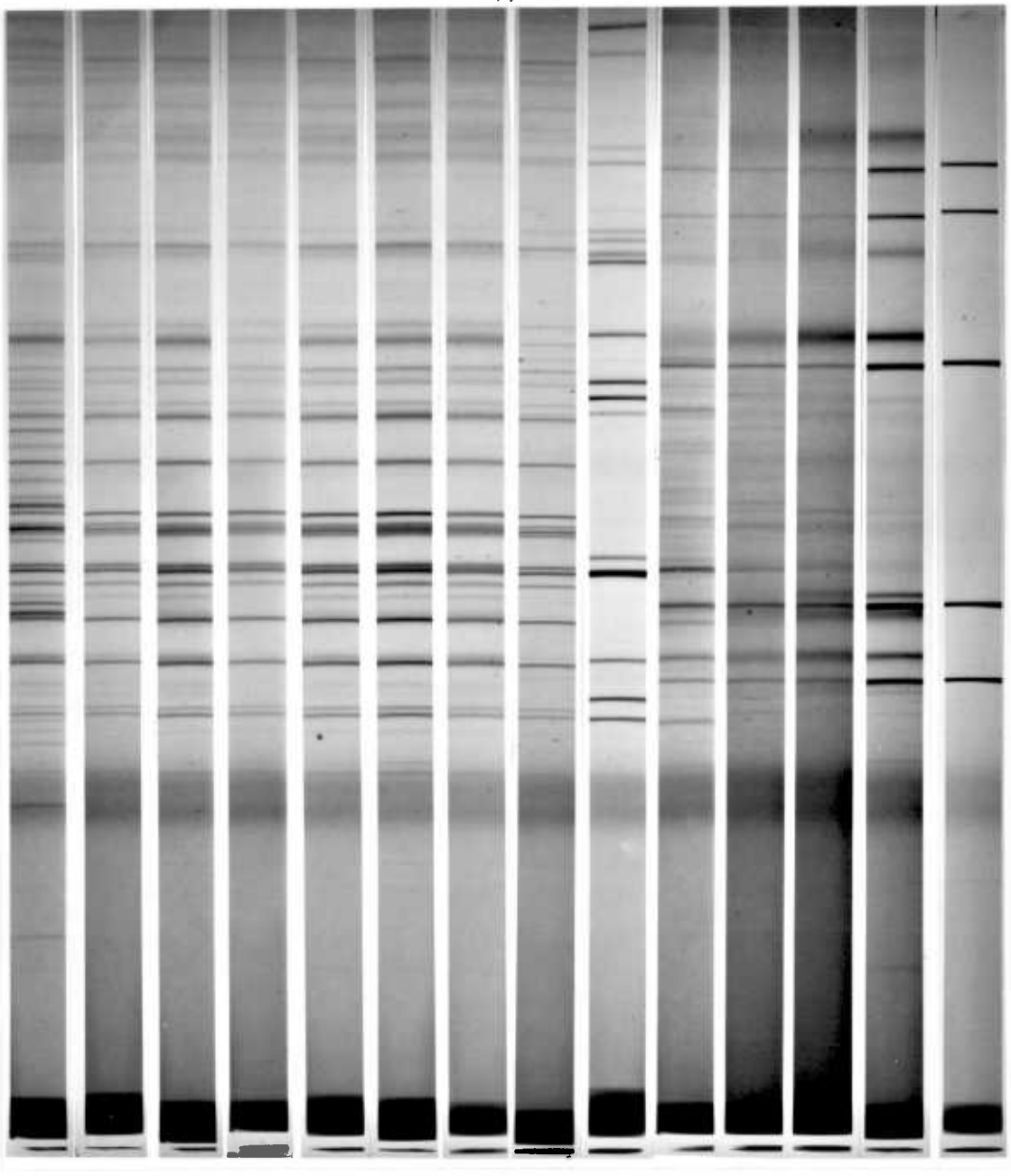

(a) (b) (c) (d) (e) (f) (g) (h) (i) (j) (k) (l) (m) (n)

FIGURE C-1.4 : X-Ray Powder Photographs

(a)-(f) : Stromeyerite residues after leaching in $Fe_2(SO_4)_3$.

(a) 47.37% Cu dissolved
(b) 50.60% " "
(c) 55.10% " "
(d) 59.94% " "
(e) 61.76% " "
(f) 77.58% " "

(g) Stromeyerite residue from $H_2O_2$ leaching(55.76% Cu diss.)

(h) Silver Sulphide, $Ag_2S$

(i) Unleached stromeyerite

(j)-(m) Stromeyerite residues from Chloride leaching

(j) 11.44% Cu, 18.92% Ag dissolved
(k) 20.25% Cu, 21.81% Ag "
(l) 23.64% Cu, 23.18% Ag "
(m) 25.17% Cu, 25.58% Ag "

(n) Silver Chloride, AgCl.

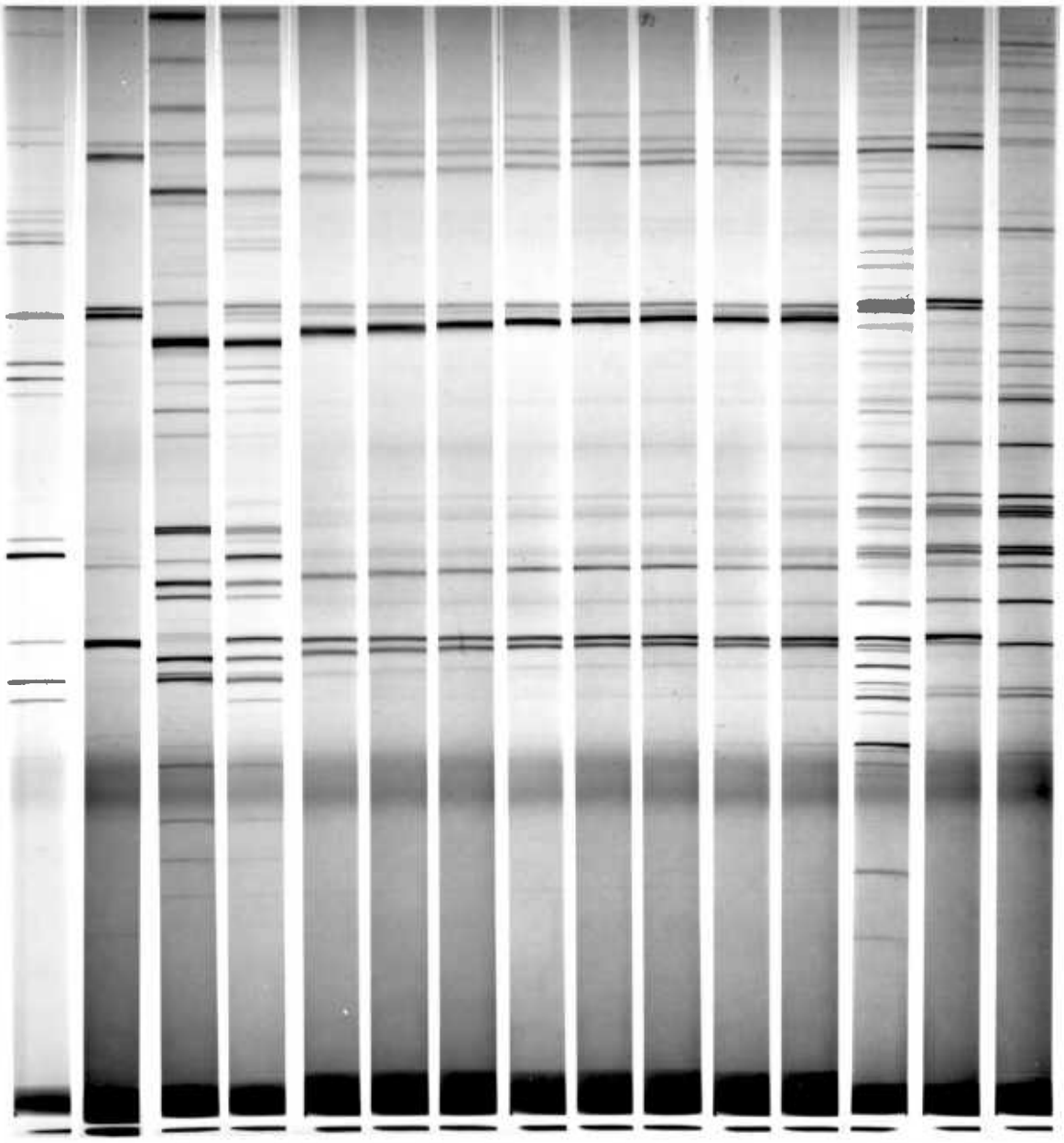

(a) (b) (c) (d) (e) (f) (g) (h) (i) (j) (k) (l) (m) (n) (o)

FIGURE C-1.5 : X-Ray Powder Photographs

(a) Stromeyerite, $Cu_{1.07}Ag_{0.93}S$

(b) Chalcopyrite, $CuFeS_2$

(c) Bornite, $Cu_5FeS_4$

(d) Mixed Sulphide Material

(e)-(m) : Mixed sulphide material residues

(e) 7.5% Cu dissolved
(f) 14.15% Cu "
(g) 23.30% " "
(h) 29.50% " "
(i) 39.45% " "
(j) 49.73% " "
(k) 61.70% " "
(l) 69.00% " "
(m) 93.00% " "

(n) Residue (m) after removal of elemental sulphur

(o) Silver Sulphide, $Ag_2S$

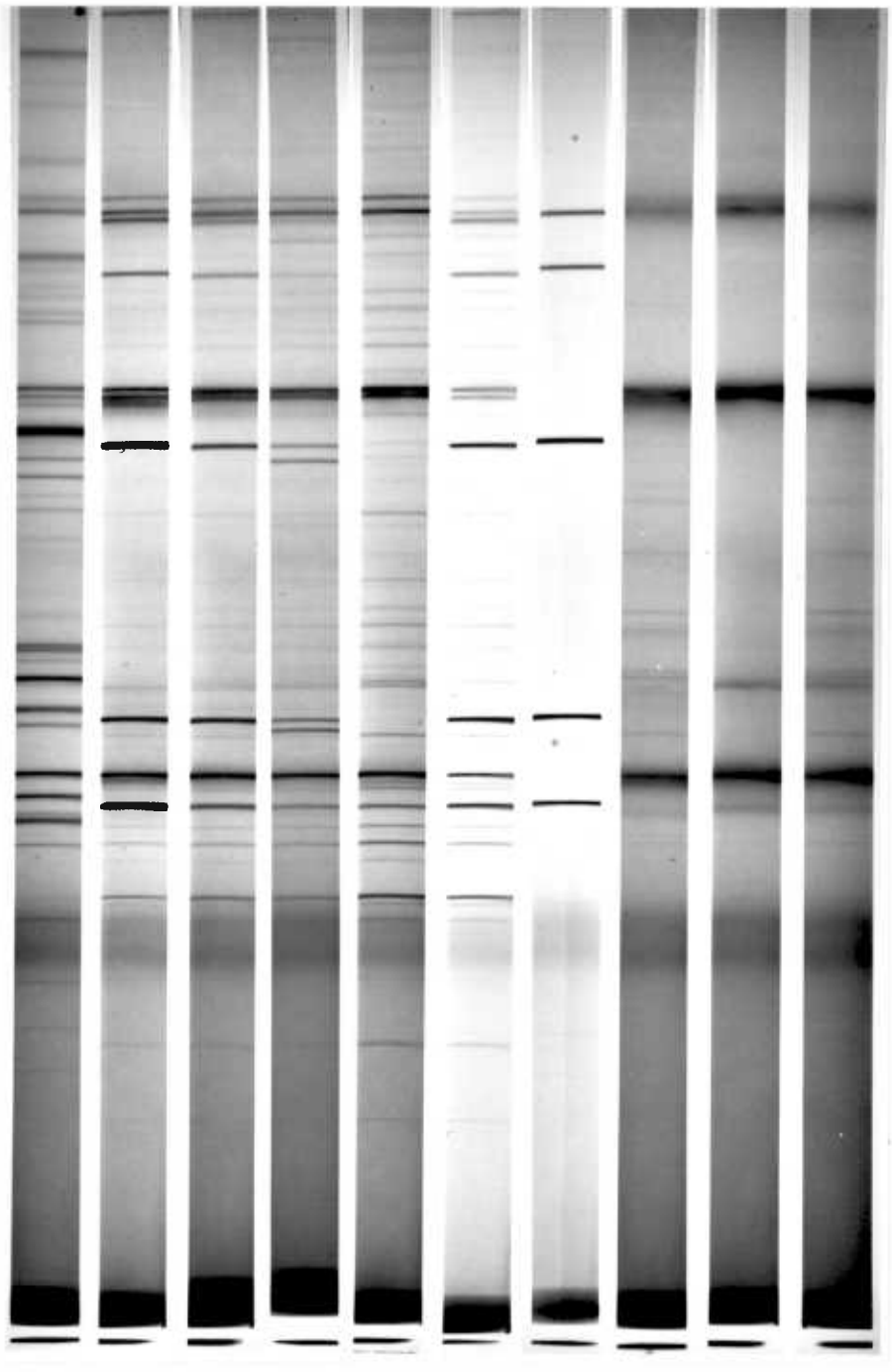


FIGURE C-1.6 : X-Ray Powder Photographs

(a) Mixed Sulphide Material

(b)-(f):Mixed sulphide material residues after leaching in chloride solutions.

(b) 56.41% Cu, 0.58% Ag dissolved
(c) 62.15% Cu, 15.55% Ag dissolved
(d) 67.13% Cu, 66.97% Ag dissolved
(e) 90.35% Cu, 76.84% Ag dissolved
(f) 95.33% Cu, 0.79% Ag dissolved

(g) Silver Chloride, AgCl

(h)-(j) : Mixtures of pure minerals, residues.

(h) Bornite + chalcopyrite + stromeyerite (34.47% Cu diss.)
(i) Bornite + chalcopyrite ( 40.38% Cu dissolved)
(j) Bornite + stromeyerite ( 46.66% Cu dissolved).

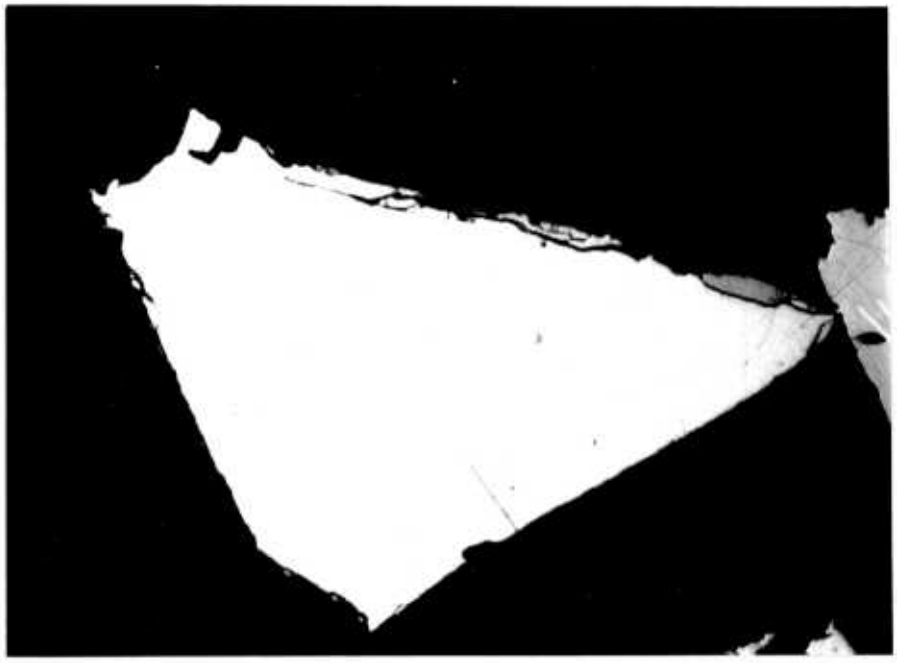

FIGURE C-2.1 : Silver-doped bornite leach residue (20.1 wt.% Cu dissolved). Particle still has well defined edges.

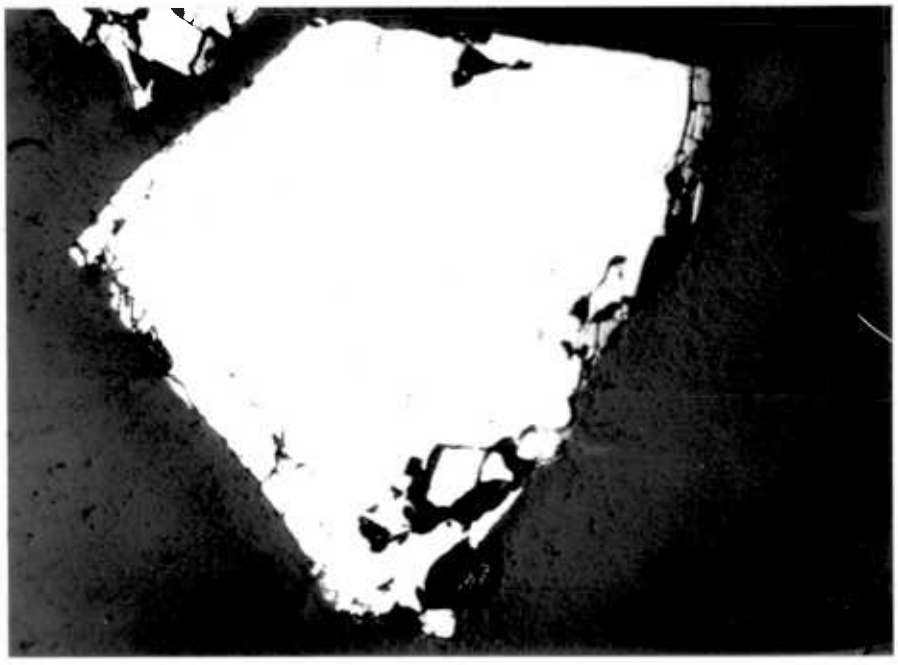

FIGURE C-2.2 : Silver-doped bornite residue (44.68 wt.% Cu dissolved). Attack at the edges has started.

FIGURE C-2.3 : Silver-doped bornite leach residue (64.29 wt.% Cu dissolved). Attack at the edges of the particle continues.

FIGURE C-2.4 : Silver-doped bornite leach residue (84.04 wt.% Cu dissolved), showing the hole left by the removal of the sulphur layer during polishing.

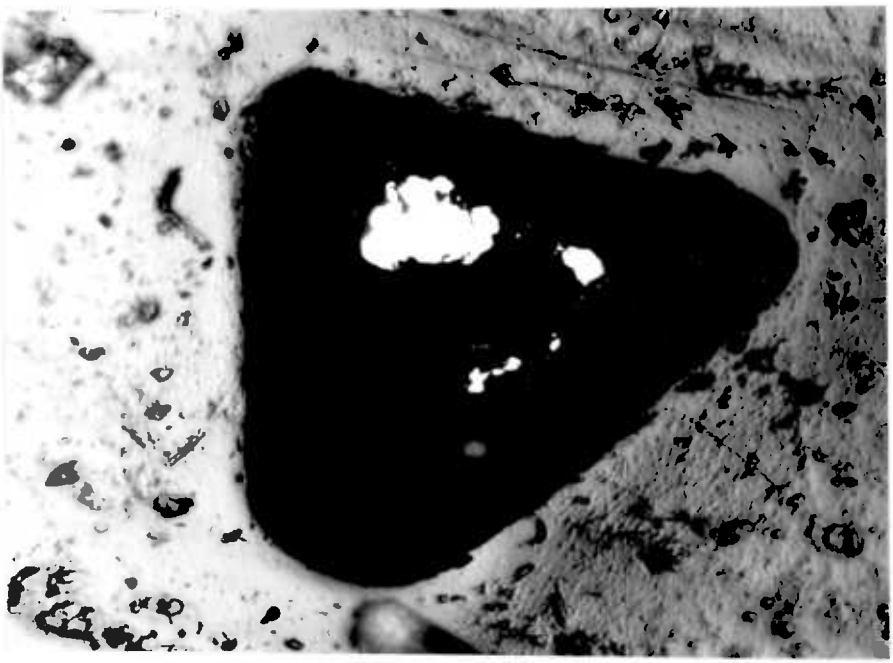

FIGURE C-2.5 : Silver-doped bornite residue (97.89 wt.% Cu dissolved). There is a residual amount of sulphide phase in the middle of a dark zone which consisted of elemental sulphur removed during polishing.

FIGURE C-2.6 : Stromeyerite leach residue (10.44% Cu dissolved). A blue phase has formed.

FIGURE C-2.7 : Stromeyerite leach residue (26.15% Cu dissolved), showing the increase in the amount of the blue phase as more Cu dissolved.

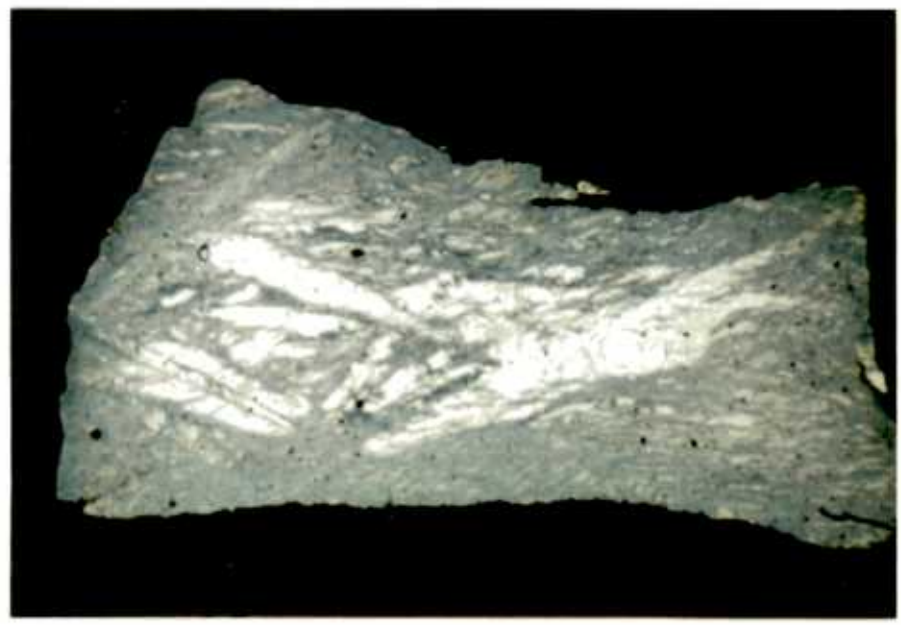

FIGURE C-2.8 : Stromeyerite leach residue (39.64% Cu dissolved).

FIGURE C-2.9 : Stromeyerite leach residue (50.06% Cu dissolved), showing the fine intergrowth of the blue phase and a light-coloured phase.

FIGURE C-2.10 : Stromeyerite leach residue (77.58% Cu dissolved), showing the attack at the edges of the particles.

FIGURE C-2.11 : Edge of a sample of Stromeyerite which had been in contact with a 0.1M $Fe^{3+}$ (pH 1) solution at 60°C for 4 hours, showing the formation of a blue and a light-coloured phase, and the dark spots formed due to the intense microscope light.

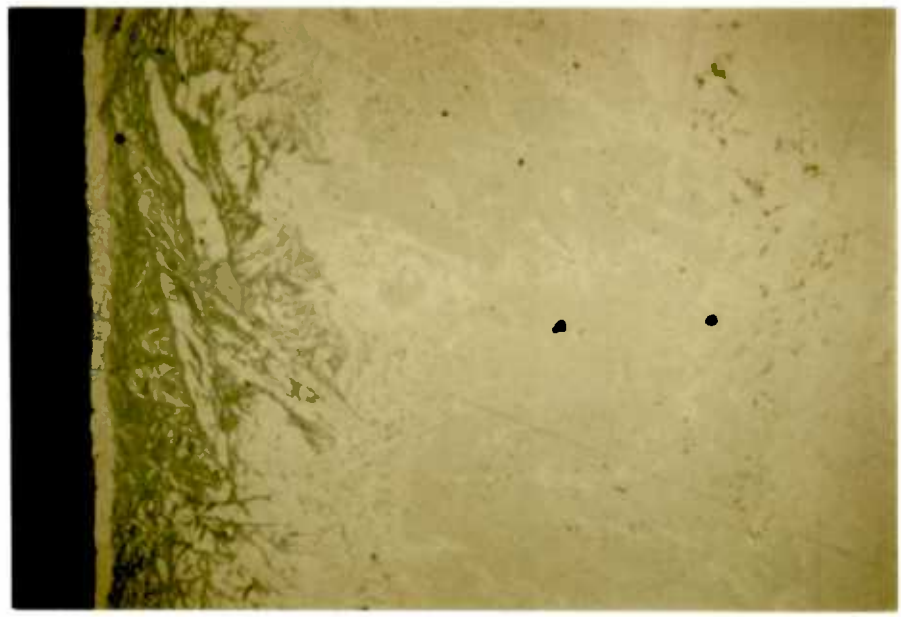

FIGURE C-2.12 : Edge of a sample of Stromeyerite after contact with a 0.1M $Fe^{3+}$ solution (pH 1) at 60°C for 24 hours, showing the formation of a light-coloured phase at the edge.

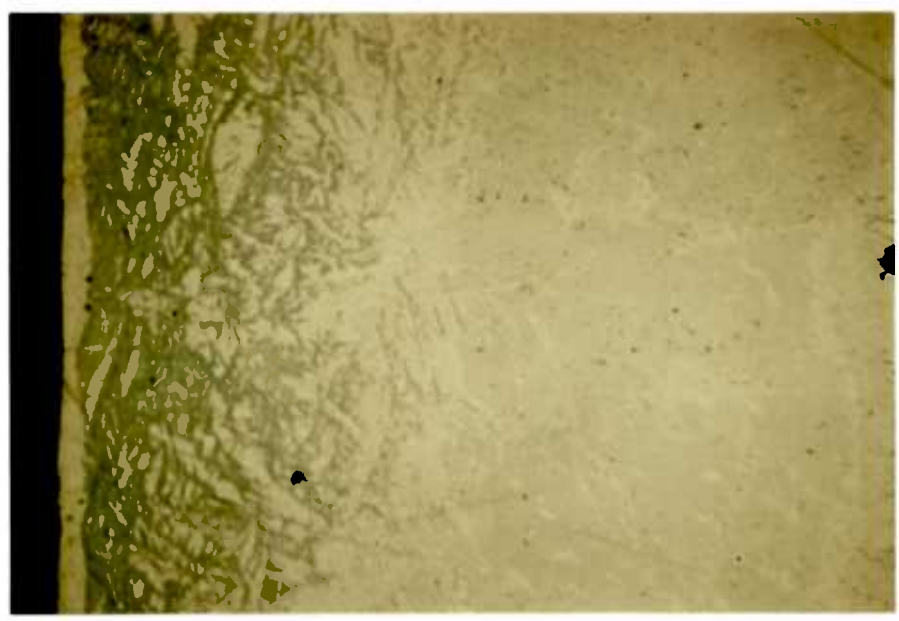

FIGURE C-2.13 : Edge of a sample of Stromeyerite after contact with a 0.1M $Fe^{3+}$ solution (pH 1) at 60°C for 48 hours.

FIGURE C-2.14 : Edge of a sample of Stromeyerite after contact with a 0.1M $Fe^{3+}$ solution (pH 1) at 60°C for 7 days.

FIGURE C-2.15 : Unleached sample of the Mixed Sulphide Material, showing the phases chalcopyrite (yellow), and stromeyerite (blue), in a bornite matrix.

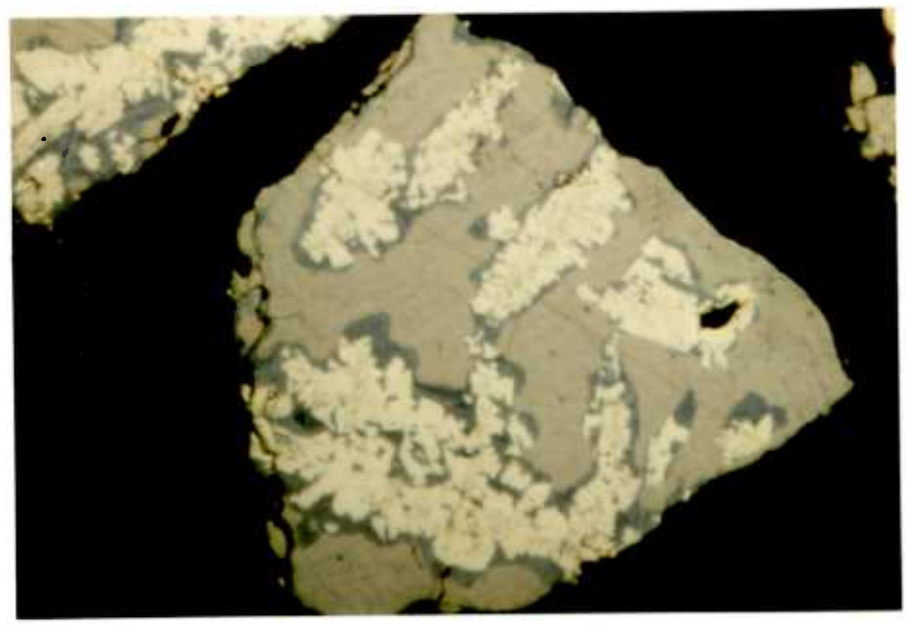

FIGURE C-2.16 : Mixed sulphide material leach residue (7-8% Cu dissolved), showing the formation of cracks and pits. The very fine intergrowth of stromeyerite (blue) in the bornite matrix is also visible.

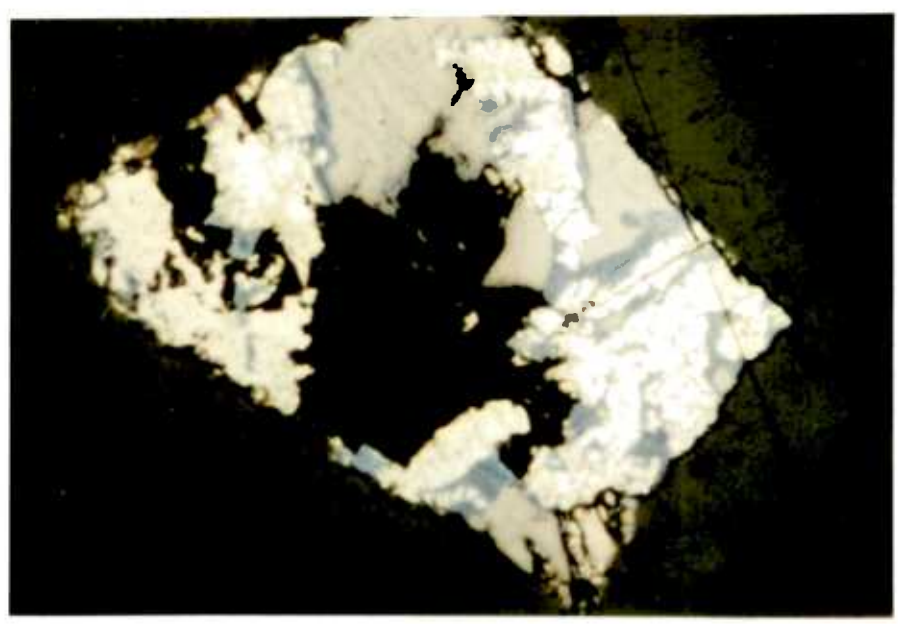

FIGURE C-2.17 : Mixed sulphide material leach residue (23.30% Cu dissolved), showing the attack on the bornite phase.

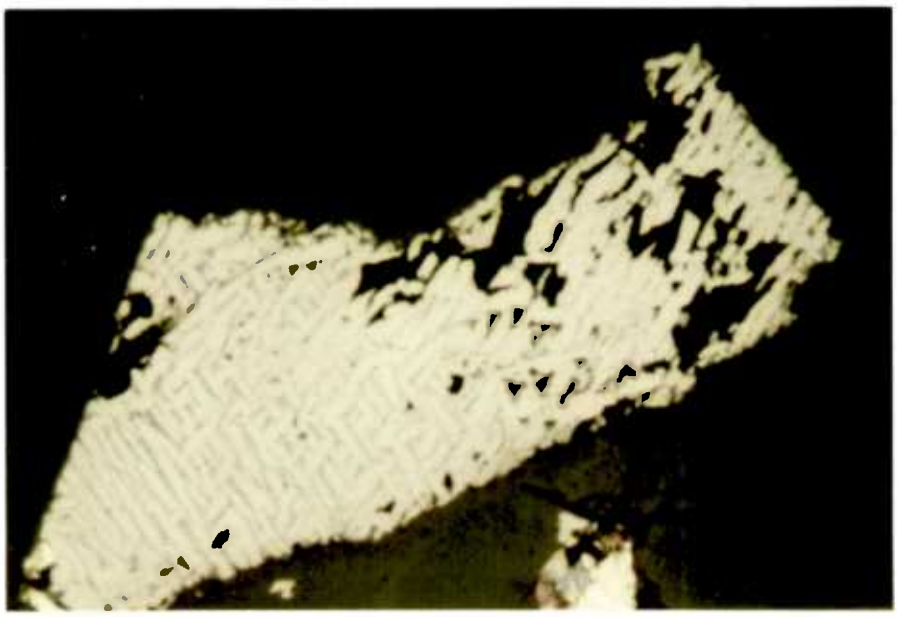

FIGURE C-2.18 : Mixed sulphide material leach residue (23.30% Cu dissolved), showing the apparently preferential dissolution along the stromeyerite intergrowth in the bornite matrix.

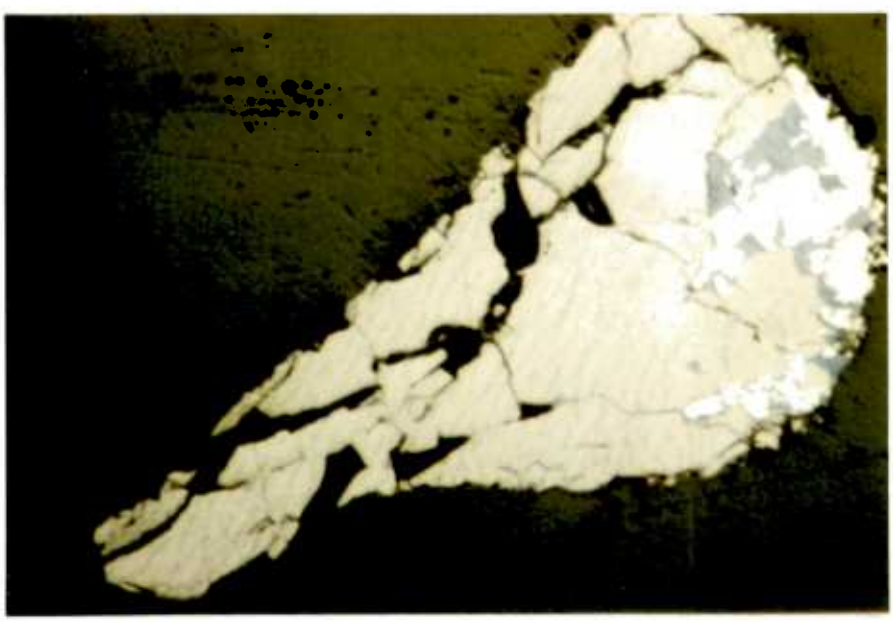

FIGURE C-2.19 : Mixed sulphide material leach residue showing the growth of the pits in the bornite as the stromeyerite (blue), and chalcopyrite (white) remain relatively unattacked.

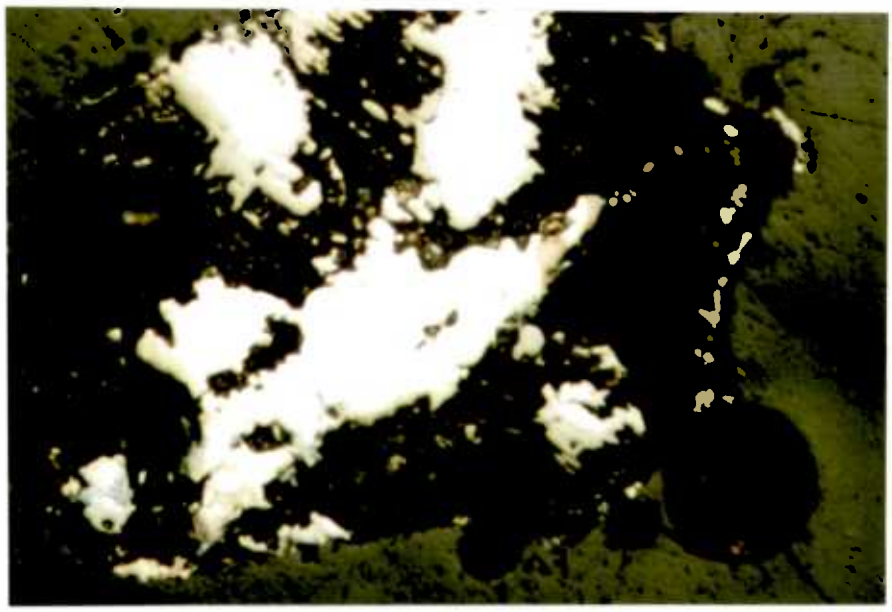

FIGURE C-2.20 : Mixed sulphide material leach residue (90% Cu dissolved), showing residual chalcopyrite (light-coloured), bornite (slightly darker) and stromeyerite (blue). The dark areas are holes left by sulphur removed during polishing.

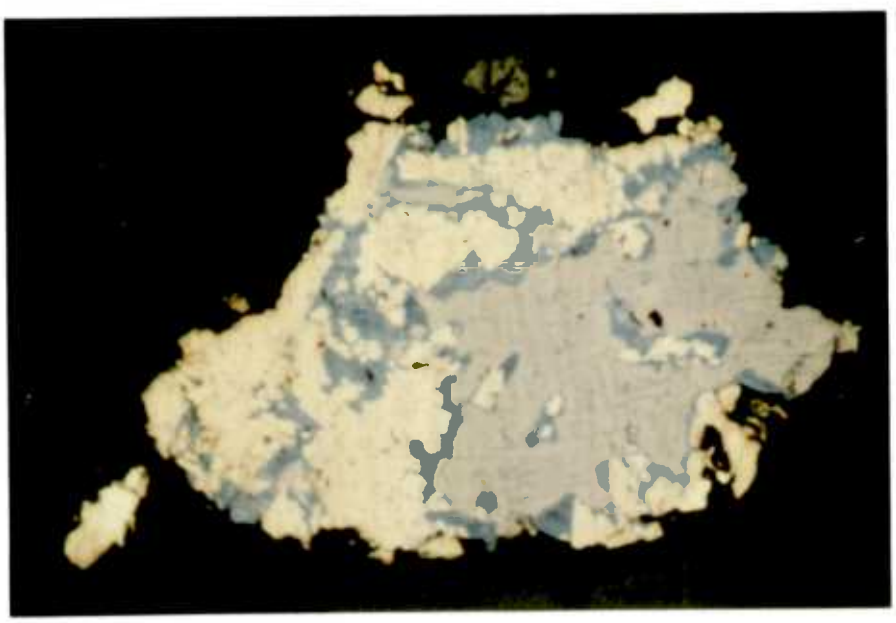

FIGURE C-2.21 : Mixed sulphide material leach residue after leaching in a Chloride solution, showing residual chalcopyrite (yellow), stromeyerite (blue), and bornite. The dark areas show that a layer has been removed during polishing.

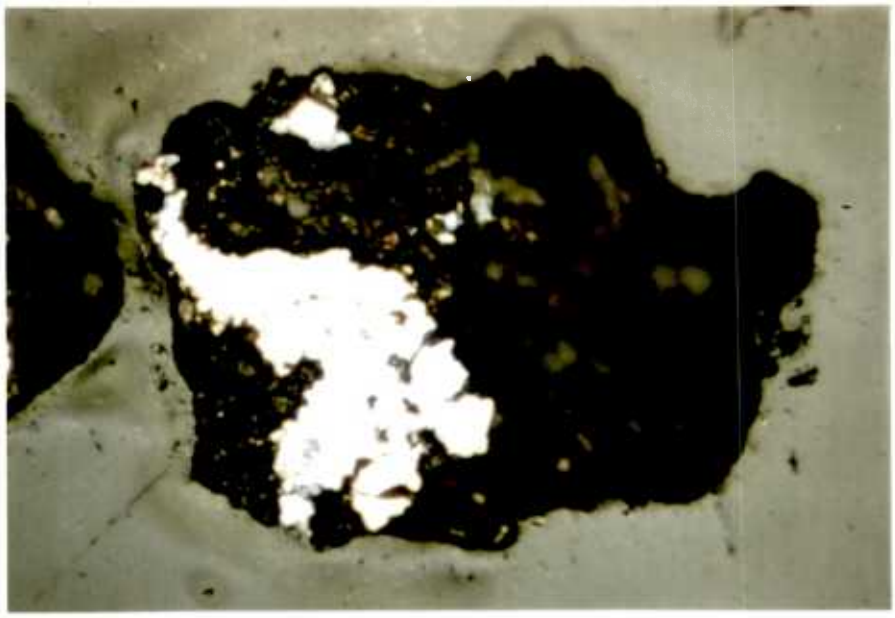

FIGURE C-2.22 : Mixed sulphide material leach residue after further leaching in a Chloride solution, showing that most of the residue (thought to be Sulphur + AgCl) has been removed during polishing. A small amount of undissolved chalcopyrite (white), bornite (slightly darker), and stromeyerite(blue).

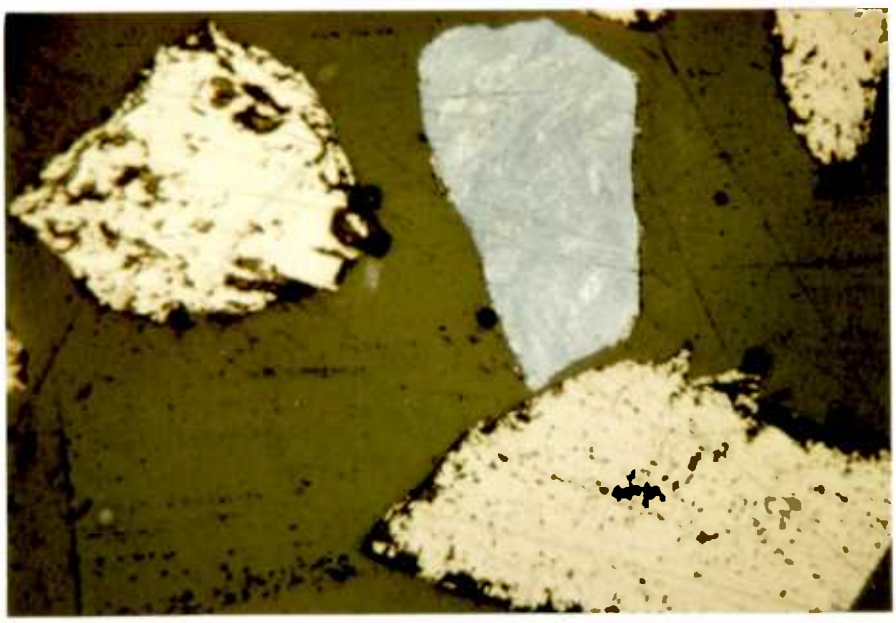

FIGURE C-2.23 : One particle of (from l. to r.) chalcopyrite, stromeyerite, and bornite from a mixture of separate partioles of the minerals after leaching in a 0.25M $Fe^{3+}$ (pH 1) solution at 60°C.

REFERENCES


1. Malouf, E.E. : Mining Eng., 24(8), 58-60 (1972).
2. Malouf, E.E. : 2nd International Symposium on Hydrometallurgy (Chicago, U.S.A.; Editors: D. Evans and R. Shoemaker) p.615, AIME, New York (1973).
3. Rosenbaum, J.B., and McKinney, W.A. : Symp. Eng. Nucl. Explos., Proc. 1970, 2, 877-87, USAEC : Oak Ridge,Tenn.
4. Harris, J.A. : Proc. Australas. Inst. Mining Metall., 230 , 81-92 (June 1969).
5. Bhappu, R.B., Johnson, P.H., Brierly, J.A., and Reynolds, D.H. : Trans. (Soc. Min. Engs.) AIME, 244 , 307-20 (1969).
6. Auck, Y.T., and Wadsworth, M.E. : 2nd International Symposium on Hydrometallurgy (Chicago, U.S.A.; Editors: D. Evans and R. Shoemaker), p.645, AIME,New York (1973).
7. Lewis, A.E., and Braun, R.L. : Trans. (Soc. Min. Engs.) AIME, 254 , 217-224 (Sept. 1973).
8. Prosser, A.P. : 9th Commonwealth Mining and Metallurgical Congress, Paper 20, Mineral Processing and Extractive Metallurgy Section (1969).
9. King, J.A. : Ph.D Thesis, Univ. of London, (1966).
10. Burkin, A.R. : Minerals Sci. Eng., 1 , 4-14 (1969).
11. Ugarte-Alvarez, F.J.G. : Ph.D. Thesis,Univ. of London,(1971).
12. Ferreira, R.C.H. : Ph.D. Thesis, Univ. of London, (1972).
13. Wright, J. : AMDEL Bulletin (Bulletin of the Australian Mineral developement Laboratories), No.12, (October, 1972).
14. Nichol, M.J., Needes, C.R.S., and Finkelstein, N.P. : Leaching and Reduction in Hydrometallurgy, London, Institute of Mining and Metallurgy,(1975). In press.
15. Boyle, R.W. : Geological Survey of Canada, Bulletin No.160 (1968)
16. Fleischer, M. : Econ. Geol., 50th Anniv. Vol., part 2, 970-1024 (1955).
17. Hawley, J.E., and Nichol, I. : Econ. Geol., 56(3), 467-487 (1961).
18. Dutrizac, J.E., and MacDonald, R.J.C. : Minerals Sci. Eng., 6(2) , 59-100 (April, 1974).
19. Burkin, A.R. : The Chemistry of Hydrometallurgical Processes, E. and F.N. Spon Ltd., London (1966).
20. De Alzugaray, J.B. : U.S. Patent 1,018,955 (1912).

21. David, A. : U.S. Patent 1,075,093 (1913).
22. Joseph, T.B. : Can. Patent 173,452 (1916).
23. Slater, H.B. : Can. Patent 165,980 (1915).
24. Reyes, R. : U.S. Patent 1,243,976 (1917).
25. Weber, F.W. : U.S. Patent 1,555,615 (1925).
26. Christensen,N.: U.S. Patent 1,485,909 (1924).
27. Larson, C. : Mining Sci. Press, 115 , 275-9 (1917).
28. Jones, D.W. : J. Soc. Chem. Ind., 38 , 365-71 (1919).
29. Cooke, H.C. : Jour. Geology, 21 , 1-28 (1913).
30. Head, R.E., and Miller, V. : Rept. Invest. U.S. Bur. Mines, No.2870 (1928).
31. Newton, R.F., Oldright, G.L., and Bradford, R.H. : Bull.16, Dept. Met. Research, Univ. of Utah, 16(4), 5-25 (1925).
32. Oldright, G.L. : Rept. Invest. U.S. Bur. Mines, No.2981 (1929).
33. Traill, R.J., McClelland, W.R., and Johnston, J.D. : Can. Dept. Mines, Mines Branch Rept.711, p.132-53 (1930).
34. Downie, CC. : Chemistry and Industry, 15 , 884 (1937).
35. Norsk Raffineringsverk : Brit. Patent 492,621 (1938).
36. Lee, H.E., and Muir, B.R. : U.S. Patent 2,197,272 (1940).
37. Salzberg, H., and King, C.V. : J. Electrochem. Soc., 97(9), 290-297 (1950).
38. King, C.V., and Lang, F.S. : J.Electrochem. Soc., 99(7), 295-300 (1952).
39. Salzberg, H.W., Knoetgen, H., and Molless, A.M. : J. Electrochem. Soc., 98(1), 31-35 (1951).
40. Kaiser, H. : Metalloberflaech-Angew. Electrchem., 2(1), 19-22 (1973).
41. Sato, M. : Econ. Geol., 55 , 1202-1231 (1960).
42. Azerbaeva, R.G., and Tseft, A.L. : Zh. Prikl. Khimii, 37(11), 367-71 (1964).
43. Tseft, A.L. , Ablanov, A.D., et al : Tr. Inst. Met. i Obogashch., Akad. Nauk. Kaz. SSR, 14 , 41-7 (1965).
44. Ablanov, A.D. : Vestn. Akad. Nauk. Kaz. SSR, 22(8), 3-8 (1966).
45. Sobol, S.I., Spiridonova, V.I, and Kurumchin, Kh.A. : Tsvet. Metall., 29(4), 44-9 (1956).
46. Kakovskii, I.A. : Tsvet. Metall., 43(12); Translation in Soviet Journ. of Non-ferrous Metals, 11(12), 20-23 (1970)
47. Potashnikov, Yu.M., Kakovskii, I.A., and Gubailovskii, V.V. : Izv. Ucheb. Zaved., Tsvet. Met., 12(6), 22-5 (1969).

48. Kakovskii, I.A., and Gubailovskii, V.V. : Dokl. Akad. Nauk. SSSR, 184(5), 1157-60 (1969).

49. Scheiner, B.J., Pool, D.L., and Lindstrom, R.E. : Rept. Invest. U.S. Bur. Mines, No.7660 (1972).

50. Scheiner, B.J., Pool, D.L., Sjoberg, J.J., and Lindstrom, R.E. : Rept. Invest. U.S. Bur. Mines, No.7736 (1973).

51. Dutko, J. : Czech. Patent 125,591 (1967).

52. Hoffmann, J.E., and Ernst, G.R. : Ger. Offen. 2,117,513 (1971).

53. Posel, J.G. : Ger. Offen. 2,307,297 (1973).

54. Gordy, J. : U.S. Patent 3,772,003 (1973).

55. Stenger, V.A., and Kramer, W.R. : U.S. Patent 3,647,261 (1972).

56. Stokes, H.N. : Econ. Geol., 1 , 644 (1906).

57. Noyes, A.A., and Brann, B.F. : J. Am. Chem. Soc., 34 , 1017-1027 (1912).

58. Tananaeff, N.A. : Zeit. f. Phys. Chem., 114 , 49-58 (1925).

59. Shaw, E.J., and Hyde, M.E. : J. Chem. Educ., 8 , 2065 (1931).

60. King, C.V. : J. Chem. Educ., 9 , 150 (1932).

61. Schumb, W., and Sweetser, S. : J.Am. Chem. Soc., 57 , 871-74 (1935).

62. Bray, W ., and Hershey, A . : J. Am. Chem. Soc., 56 , 1889 (1934).

63. Martel, A.E., and Sillen, L.G. : Stability Constants of Metal-ion Complexes, Special Publication No.17, The Chemical Society, London (1964); and also Supplement No.1, Special Publication No.25 (1971).

64. Bodlander, G., and Eberlein, W. : Z. Anorg. Chem., 39 , 197 (1904).

65. Hellwig, K. :Z. Anorg. Chem., 25 , 157 (1900).

66. Forbes, G.S. : J.Am. Chem. Soc., 33 , 1937 (1911).

67. Forbes, G.S., and Cole, H.I. : J. Am. Chem. Soc., 43 , 2492 (1921).

68. Pinkus, A., and Haugen, M. : Bull. Soc. Chim. Belges, 45 , 693 (1936).

69. Pinkus, A., and Timmermans, A.M. : Bull. Soc. Chim. Belges, 46 , 46 (1937).

70. Erber, W., and Schuhly, A. : J. Prakt. Chem., 158 , 176-185 (1941).

71. Garret, A.B., Noble, M.V., and Miller, S. : J. Chem. Educ., 19 , 485 (1942).

72. Barney, J., Angersinger, W., and Reynolds, C. : J. Am. Chem. Soc., 73 , 3785 (1951).

73. Jonte, J., and Martin, D. : J. Am. Chem. Soc., 74 , 2052 (1952).

74. Leden, I. : Svensk.Kem. Tidskr., 64 , 249-59 (1952).

75. Berne, E., and Leden, I. : Svensk. Kem. Tidskr., 65 , 88, (1953).

76. Leiser, K.H. : Z. Anorg. u. Allgem. Chem., 292 , 97-113 (1957).

77. Chateau, H., and Hervier, B. : J. Chim. Phys., 54 , 637 (1957).

78. Marcus, Y. : Bull. Rec. Counc. of Israel, A8 , 16-26 (1959).

79. Mironov, V.E. : Radiokhimiya, 4 , 707 (1962).

80. Rasse, D. : Bulletin de l'union des Physiciens, 65(530), 249-51 (1970).

81. Ciantelli, G. : La Ricerca Scientifica, 37(3), 203-10 (1967)

82. Jacques, S. : Helv. Chim. Acta, 29 , 1041 (1946).

83. Pinkus, A., Frederic, S., and Schepmans, R . : Bull. Soc. Chim. Belges, 47 , 304 (1938).

84. Leiser, K.H. : Z. Anorg. Chem., 304 , 296 (1960).

85. Dasher, J. : Can. Min. Metall. (CIM) Bull., 66(733), 48 (1973).

86. Roman, R.J., and Benner, B.R. : Minerals Sci. Eng., 5(1), 3-24 (1973).

87. Wadsworth, M.E. : Minerals Sci. Eng., 4(4), 36-47 (1973).

88. Peters, E., and Loewen, F. : Metall. Trans., 4(1), 5-14 (1973).

89. Subramanian, K.N., and Jennings, P.H. : Can. Met. Quarterly, 11(2), 387-400 (1972).

90. Brennet, P., Jafferali, S., Vanseveren, J., Vereecken, J., and Winand, R. : Metall. Trans., 5(1), 127-34 (1974).

91. Sullivan, J.D. : U.S. Bur. Mines, Tech. Paper 486 (1931).

92. Uchida, T., Matsumoto, H., Omori, S., and Murayama, A. : Hakko Kyokaishi (Japan), 25(4), 168-72 (1967).

93. Kopylov, G.A., and Orlov, A.I. : Izvest. Vysshikh Ucheb. Zaved. Tsvet. Met., 6 , 68 (1963).

94. Dutrizac, J.E., MacDonald, R.J.C., and Ingraham, T.R. : Metall. Trans., 1(1), 225 (1970).

95. Dutrizac, J.E., and MacDonald, R.J.C. : Proc. Australas. Inst. Min. Metall., 245 , 25-31 (March 1973).

96. Lowe, D.F. : Ph.D. Thesis, Univ. of Arizona, (1970). (See Diss. Abstr. Int. B 1970, 31(4), 2013-14.)

97. Groves, R.D., and Smith, P.B. : Rept. Invest. U.S. Bur. Mines, No.7801 (1973).

98. Paynter, J.C. : Jour. S. African Inst. Min. Met., 74(4), 158-170 (Nov.1973).

99. Corrans, I.J., Harris, B., and Ralph, B.J. : Jour. S. African Inst. Min. Met., 72(8), 221-30 (March 1973).

100. Kruesi, P.R., Allen, E.S., and Lake, J.L. : Can. Min. Metall. (CIM) Bull., 66(734), 81-87 (June 1973).

101. Jackson, K.J., and Strickland, J.D.H. : Trans. (Metall. Soc.) AIME, 212 , 373 (1958).

102. Klets, V.E., and Liopo, V.A. : Tr. Irkutsk. Politelch. Inst. No.27, 123-130 (1966).

103. Haver, F.P., and Wong, M.M. : J. Metals, 23(2), 25-9 (1971) (and also Rept. Invest. U.S. Bur Mines, No.7474 (1971))

104. Ermilov, V.V., Tkachenko, O.B., and Tseft, A.L. : Tr. Inst. Met. Obogashch, 30 , 3-14 (1969).

105. Dutrizac, J.E., MacDonald, R.J.C., and Ingraham, T.R. : Trans. (Metall. Soc. ) AIME, 245 , 955-59 (1969).

106. Dutrizac, J.E., and MacDonald, R.J.C. : Metall. Trans. 2(8), 2310 (1971).

107. Munoz-Ribadeneira, F.J., and Gomberg, H.J. : Nucl. Technol., 11 , 367-71 (1971).

108. Baur, J.P., Gibbs, H.L., and Wadsworth, M.E. : Rept. Invest. U.S. Bur. Mines, No.7823 (1974).

109. Prater, J.D., Queneau, P.B., and Hudson, T.J. : Trans. (Soc. Min. Engs.) AIME, 254 , 117-122 (June 1973).

110. Habashi, F. : Trans. (Soc. Min. Engs.) AIME, 254 , 224-8 (Sept. 1973).

111. Simkovich, G., and Wagner, J.B. : J. Electrochem. Soc., 110(6), 513-6 (1963).

112. Carlson, J.A., and Nikkola, D.E. : Metall. Trans., 5(4), 915-9 (April 1974).

113. Eadington, P., and Prosser, A.D. : Trans. Inst. Min. Metall. (Section C), 78 , C74-82 (1969).

114. Scott, T.R., and Dyson, N.F. : Trans. (Metall. Soc.) AIME, 242(9), 1815-1821 (1968).

115. Eadington, P. : Trans. Inst. Min. Metall. (Section C), 82 , C158-161 (Sept. 1973).

116. Gerlach, J., Pawleck, F., Rodel, R., Schade, G., and Weddige, H. : Erzmetall., 25(9), 448-53.

117. Warren, I.H., and Roach, G.I.D. : Trans. Inst. Min. Metall. (Section C), 80 , C152 .

118. Fox, R.W. : Phil. Trans. R. Soc. pt. 2, p.399 (1830).

119. Skey, W. : Trans. Proc. N.Z. Inst., 3 , 232-36 (1871).

120. Gottshalk, V.H., and Buehler, H.A. : Econ. Geol., 7 , 15-34 (1912).

121. Majima, H. : Can. Met. Q., 8(3), 269 (1969).

122. Dutrizac, J.E., MacDonald, R.J.C., and Ingraham, T.R. : Can. Met. Q., 10(1), 3-7 (1971).

123. Dutrizac, J.E., and MacDonald, R.J.C. : Can. Met. Q., 12(4), 409-20 (1973).

124. Kunieda, Y., Sawamoto, H., and Oki, T. : Nippon Kinzoku Gakkaishi, 35(7), 657-61 (1971).

125. Iwai, M. : Nippon Kinzoku Gakkaishi, 37(11), 1174-82 (1973).

126. Ramsdell, L.S.: Am. Mineral., 10 , 281-304 (1925).

127. Emmons, R.C., Stockwell, C.H., and Jones, R.H. : Am. Mineral., 11 , 326-8 (1926).

128. Schneiderhohn, H. : Am. Mineral., 12 , 210-11 (1922).

129. Palacios, J., and Salvia, R. : Anal. Soc. Espanola Fis. Quim., 29 , 269-279 (1931).

130. Ramsdell, L.S. : Am. Mineral., 28 , 401-425 (1943).

131. Kracek, F.C. : Trans. Am. Geophys. Union, 27 , 364-374 (1946).

132. Rahlfs, P. : Z. Physik. Chem., B31 , 157-94 (1936).

133. Djurle, S. : Acta Chem. Scand., 12 , 1427-1436 (1958).

134. Frueh, A.J. : Am. Mineral., 46 , 654 (1961).

135. Frueh, A.J. : Z. Krist., 110 , 136-144 (1958).

136. Bragg, L., and Claringbull, G.F. : The Crystalline State vol.IV , Crystal Structures of Minerals, G. Bell and Sons Ltd., London (1965).

137. Sadanaga, R., and Sueno, S. : Mineral. Journal (Japan), 5(2), 124-143 (1967).

138. Taylor, L.A. : Am. Mineral., 54 , 961-63 (1969).

139. Schwartz, G.M. : Econ. Geol. , 30 , 128-146 (1935).

140. Suhr, N. : Econ. Geol., 50 , 347-50 (1955).

141. Frueh, A.J.: Z. Krist., 106 , 299-307 (1955).

142. Frueh, A.J. : Phys. Chem. Solids, 11 , 334-5 (1959).

143. Skinner, B.J., Econ. Geol., 61 , 1-26 (1966).

144. Grybeck, D., and Finney, T.J. : Am. Mineral., 53 , 1530 (1968)
145. Skinner, B.J., Jambor, J.L., and Ross, M. : Econ. Geol., 61 , 1383-1389 (1966).
146. Robinson, B.W., and Morton, R.D. : Econ. Geol., 66 , 342-347 (1971).
147. Morimoto, N., and Kullerud, G. : Am. Mineral., 46 , 1270, (1961).
148. Morimoto, N. : Acta Crystall., 17(4), 351 (1964).
149. Manning, P.G. : Can. Mineral., 9(1), 85 (1967).
150. Pauling, L., and Brockway, L.O. : Z. Krist., 82 , 188 (1932).
151. Hall, S.R., and Stewart, J.M. : Acta Crystall., B29 , 579, (1973).
152. Aramu, F., and Bressani, T. : Nuovo. Cim., B51(2), 370-75 (1967).
153. Zuev, V.V. : Zap. Vses. Miner. Obschch., 96(6), 689-98, (1967).
154. Frueh, A.J. : Geochim. et Cosmochim. Acta, 6 , 78-89 (1954).
155. Rojkovic, I. : Geologicky Zbornick (Bratislava), 24(2), 325, (Nov. 1973).
156. Valvarde Diez, N. : Z. Phys. Chem., 62(1-4), 218-20 (1968).
157. Yund, R.A., and Kullerud, G. : J. Petrology, 7 , 454 (1966).
158. Barton, P.B., and Skinner, B.J. : Geochemistry of Hydrother-mal Ore Deposits, (Editor: H.L. Barnes); Holt, Rinehart and Winston, Inc., New York (1967).
159. Sillitoe, R.H., and Clark, N.H. : Am. Mineral., 54 , 1684 (1969).
160. Levy, C. : Fr. Rep. Mem. Bur. Rech. Geol. Minieres Bull., 54 , (1967).
161. Cabri, L.J. : Econ. Geol., 68 , 443-454 (1973).
162. Taylor, L.A. : Metall. Trans., 1 , 2523 (Sept. 1970).
163. Taylor, L.A. : Mineral. Deposita, 5 , 41-58 (1970).
164. Luder, V.E. : Metall. und Erz., 21 , 329-334 (1924).
165. Baker, E.H. : Trans. Inst. Min. Metall., 80 , C93 (1971).
166. Ramdohr, P. : The Ore Minerals and their Intergrowths, Pergamon Press, London (1969).
167. Edwards, A.B. : Textures of the Ore Minerals, Australasian Inst. Min. Metall., Melbourne (1960).
168. Douglas, C.B.E. : Trans. Inst. Min. Metall., 42 , 398-402 (1933).

169. Sengupta, J.G. : Minerals Sci. Eng., 5(3), 207-18 (1973).

170. Mallet, R.C. : Minerals Sci. Eng., 2(3), 28 (July 1970).

171. Belcher, R., Dagnall, R.M., and West, T.S., Talanta, 11 , 1257-1263 (1964).

172. Goodwin, E. : Atomic Absorption Newsletter (Perkin-Elmer Corporation), 9(4),95-6 (July-August 1970).

173. Vogel, A.I. : Quantitative Inorganic Analysis, 3rd Ed., Longmans, London (1961).

174. Stephens, J.D. : Minerals Sci. Eng., 3(1), 26-37 (1971).

175. Wittkop, R.W. : Minerals Sci. Eng., 3(1), 17 (1971).

176. Poole,D.M., and Martin, P.M. : Metall. Reviews, 14(133), 61 (1969).

177. Mason, P., Frost, M., and Reed, S. : B.M.-I.C.-N.P.L. computer programs for calculating corrections in quantitative X-ray microanalysis, Nat. Physical Lab., MS Report 2 (April, 1969).

178. De Wolff, P.M. : Acta Crystall., 1 , 207 (1948).

179. Klug, H.P., and Alexander, L.E. : X-Ray Diffraction Procedures for Polycrystalline and Amorphous Materials, 2nd Edition, New York, Wiley (1974).

180. Cabri, L.J. : Econ. Geol., 60 , 1569-1606 (1965).

181. Goldschmidt, V.M. : Geochemistry, (Edited by A. Muir), Oxford, Clarendon Press (1954).

182. Partho, E. : Crystal Chemistry of Tetrahedral Structures, Gordon and Breach, New York-London (1964).

183. Povarennykh, A.S. : Probl. Kristallokhim. Miner. Endogennogo Mineral. Obshchest., 77-95 (1967).

184. Indolev, L.N., Nevoysa, G.G., and Bryzgalov, I.A. : Dokl. Akad. Nauk. SSSR, 199(5), 1146-9 (1971); Translation in Doklady, 199 , 115 (1971).

185. Ottemann, J.,and Frenzel, G. : Neues Jahrb. Mineral., Monatsh, 1971(2), 80-9 (1971).

186. Prouvost, J. : Mineral. Soc. America, Special Paper No.1, p.144-148 (1963).

187. Berry, L.G. : Am. Mineral., 50 , 301-13 (1965).

188. Manning, P.G. : Can. Mineral., 8 , 567 (1966).

189. Manning, P.G. : Can. Mineral., 9 , 57 (1967).

190. Frenzel, G. : Jahrb. Mineral. Monatsh, 6 , 142 (1958); and Neues Jahrb. Mineral. Abh., 93 , 87 (1959).

191. Schafer, W.S., and Nitsche, R. : Mat. Res. Bull., 9 , 645-654 (1974).

192. Moh, G.H. : Neues Jahrb. Mineral., Abh., 94 , 1125-1146 (July 1960).

193. Gaudin, A.M., Fuerstenau, D.W., and Turkanis, M.M. : Trans.(Soc. Min. Engs.) AIME,208 , 65-69 (1957).

194. Techniques of Chemistry : (Edited by A. Weissberger and B.W. Rossiter), vol.1, Physical Methods of Chemistry, part 5, Determination of Thermodynamic and Surface Properties, p.257-308, Wiley-Interscience, New York (1971).

195. Handbook of Chemistry and Physics, 48th Ed., Weast, Cleveland : The Chemical Rubber Co., (1967-68).

196. May, A., Sjoberg, J.J., and Baglin, E.G. : Am. Mineral., 58(9-10), 936-41 (1973).

197. Fairchild, J.G. : Am. Mineral., 18 , 543-47 (1933).

198. Subramanian, K.N., and Kanduth, H. : Can. Min. Metall. (CIM) Bull., 66(734), 88-91 (June 1973).

199. Stephens, M.M. : Am. Mineral., 16 , 532-549 (1931).

200. Barth, H., Gans, W. and Knacke, O. :2nd International Symposium on Hydrometallurgy (Chicago, U.S.A.; Editors: D. Evans and R. Shoemaker), p.1081, AIME, New York (1973).

201. Dana, J.D., and Dana, E.S. : The System of Mineralogy, 7th Edition (Revised and Rewritten by C. Palache, H. Berman, and C. Frondel), Wiley, New York; Chapman and Hall, London (1941-1962).

202. Short,M.N. : Microscopic determination of the ore minerals, Washington, Govt. Printer (Bull. 825, U.S. Geol. Survey) (1931).

203. Clark, A.H., and Rojkovic, I. : Unpublished M.S. (1971) (see reference 204).

204. Bergstol, S., and Vokes, F.M. : Mineral. Deposita (Berl.), 9 , 325-337 (1974).

205. Yu, P., Hansen, C., and Wadsworth, M. : Metall. Trans., 4 , 2137-2144 (Sept. 1973).

206. Tuovinen, O.H., and Kelly, D.P. : Int. Met. Rev., 19 , (review 179), 21-31 (March 1974).

207. A.S.T.M. X-Ray Index Files :

(a) Bornite - File No.14-323.

(b) Sulphur (orthorhombic) - File No.8-247.

(c) Jarosite - File No.10-443.

(d) Silver Sulphide - File No.14-72.

(e) Stromeyerite - File No.12-156. (also ref. 133)

207. continued:

(f) α-Chalcopyrite - File No.9-423.

(g) Silver Chloride - File No.6-0480.

(h) Mckinstryite - File No.19-406, (also ref. 145).

(i) Synthetic $Ag_{1.2}Cu_{0.8}S$ - File No.12-152,(also ref. 133).

(j) Synthetic $Ag_{1.55}Cu_{0.45}S$ - File No.12-207, (also ref. 133).

(k) Jalpaite - $Ag_3CuS_2$ - File No.21-1336, (also ref. 144).

(l) Covellite - CuS - File No.6-0464.

(m) Sodium Chloride - File No.5-628.